

Departament de Ciències Experimentals i de la Salut
Facultat de Ciències de la Salut i de la Vida
Universitat Pompeu Fabra

Transcriptional activation induced by snail1 during epithelial-mesenchymal transition

Memòria presentada per na
Montserrat Porta de la Riva
per optar al Grau de Doctor

Treball realitzat sota la direcció del Dr. Josep Baulida i Estadella a la Unitat de Recerca en Biologia Cel·lular i Molecular de l'Institut Municipal d'Investigació Mèdica (IMIM-Hospital del Mar), dins el Programa de Recerca en Càncer

Tutor: Antonio García de Herreros Madueño

Barcelona, 2009

Josep Baulida i Estadella,
(director de la tesi)

Antonio García de Herreros Madueño,
(tutor de la tesi)

Montserrat Porta de la Riva,
(doctoranda)

IMIM
hospitaldelmar

 **UNIVERSITAT
POMPEU FABRA**

Als meus pares

A la meva germana

Al Jordi

És millor encendre un llum que maleir la foscor

Proverbi àrab

INDEX

FIGURE INDEX	v
TABLE INDEX	ix
NOTES TO THE READER	1
ABBREVIATIONS AND ACRONYMS INDEX	1
INTRODUCTION	3
I.1 Cancer: general overview	5
I.1.1 Epithelial cancers and epithelial to mesenchymal transition (EMT)	6
I.2 Epithelial-mesenchymal transition	7
I.2.1 Morphologic features and molecular markers of epithelial and mesenchymal cells	8
I.2.2 Physiological EMT	9
I.2.3 Pathological EMT	12
I.3 Molecular pathways involved in EMT	17
I.3.1 TGF-β/BMPs	17
I.3.2 Wnt/Frizzled	20
I.3.3 RTKs	21
I.3.4 Delta/Notch	22
I.3.5 Hedgehog/Patched	24
I.4 Key molecules in EMT	27
I.4.1 E-cadherin	27
I.4.2 The snail superfamily of transcription factors	28
I.4.2.1 snail1	29
I.4.2.2 snail2 (formerly slug)	32
I.4.3 The ZFH family of transcription factors	32
I.4.4 Basic helix-loop-helix (bHLH) family of transcription factors	33
I.4.4.1 E2A gene products	34
I.4.4.2 Twist	35
I.4.4.3 Id proteins	35
I.4.5 β-catenin	35
I.4.6 Nuclear factor-kappa B (NF-κB)	38

OBJECTIVES 43

RESULTS 45

R.1 Snail1 activates transcription of mesenchymal genes through an undescribed indirect mechanism independent of E-boxes47

- R.1.1** Snail1 increases the mRNA and protein levels of mesenchymal markers in EMT cell models.....47
- R.1.2** Snail1 promotes transcription from the *LEF1* and *FN1* promoters50
- R.1.3** *LEF1* promoter has a motif for snail1 binding, *FN1* promoter does not52
- R.1.4** Activation of *LEF1* and *FN1* transcription by snail1 requires motifs in their promoters different than E-boxes.....54
- R.1.5** Snail1 binds to *FN1* and *lef1* promoters through a different mechanism than to *CDH1* 55

R.2 Identification in *FN1* and *LEF1* of motives and transcription factors involved in snail1-induced transcriptional activation.....61

- R.2.1** Snail1 does not require TCF to activate *FN1* and *LEF1* transcription61
- R.2.2** β -catenin is not required for snail1 translocation to the nucleus66
- R.2.3** β -catenin binds to the *FN1* promoter in the presence of snail167
- R.2.4** The +451/+560 region in the *LEF1* promoter is required for its snail1-mediated activation69
- R.2.5** The -341/-323 region of the *FN1* promoter is required for snail1-induced transcriptional activation.....70
- R.2.6** The p300 binding motif in *FN1* and *LEF1* promoters is irrelevant for snail1-induced activation73
- R.2.7** Snail1 modulates protein interaction with the -341/-320 region of the *FN1* promoter75
- R.2.8** Neither snail1 nor β -catenin bind to the -341/-301 *FN1* promoter.....78
- R.2.9** Regions isolated as snaRE in *LEF1* and *FN1* promoters (+451/+560 for *LEF1* and -341/-320 for *FN1*) are not sufficient to mediate snail1-induced transcription80

R.3 NF- κ B cooperates with snail1 to activate transcription83

- R.3.1** Snail1 binds to the region -36/+265 of the *FN1* promoter83
- R.3.2** NF- κ B is involved in snail1-mediated activation of mesenchymal genes83
- R.3.3** p65/relA binds to the+35/+48 box in the *FN1* promoter.....88
- R.3.4** Snail1 binds to the same *FN1* promoter sequence as NF- κ B89
- R.3.5** NF- κ B binds to the *FN1* promoter *in vivo* in snail1 cells90

R.4 Snail1 modulates binding of the transcription factor CP2c (TFCP2c) to the *FN1* promoter93

R.4.1 Two motives are responsible for the formation of the EMSA complex.....	93
R.4.2 TFCP2c binds to the <i>FN1</i> promoter <i>in vivo</i>	93
R.4.3 TFCP2c function is required for snail1-induced activation of the <i>FN1</i> promoter	96
R.4.4 Snail1 induces nuclear accumulation of TFCP2c	100
R.4.5 TFCP2c is phosphorylated in snail1 expressing cells.....	103
DISCUSSION	105
D.1 Snail1 activates transcription of <i>FN1</i> and <i>LEF1</i> promoters through an undescribed mechanism independent of E-boxes	107
D.2 Snail1 requires β -catenin to accomplish activation from the <i>FN1</i> and <i>LEF1</i> promoters.....	115
D.3 NF- κ B is involved in the activation of <i>FN1</i> and <i>LEF1</i> promoters induced by snail1 ...	121
D.4 TFCP2c is required for the snail1-induced transcriptional activation of <i>FN1</i> promoter	129
D.5 Model	137
CONCLUSIONS	141
EXPERIMENTAL PROCEDURES	145
E.P.1 Cell culture.....	147
E.P. 2 DNA constructs.....	150
E.P.2.1 mmsnail1 constructs	150
E.P.2.2 VP16-TCF4/Rel-VP16.....	151
E.P.2.3 Luciferase reporter vector	152
E.P.2.4 TFCP2c constructs	157
E.P.2.5 pLKO	158
E.P.3 RNA stabilization	159
E.P.4 Reporter experiments.....	160
E.P.5 GST fusion protein purification.....	161
E.P.6 Biotinylated oligonucleotide pull-down assay (BOPA).....	163
E.P.7 Chromatin immunoprecipitation (ChIP)	167
E.P.8 Electrophoretic mobility shift assay (EMSA)	170
E.P.9 Transfection/infection	173
E.P.9.1 Transfection.....	173
E.P.9.2 Infection.....	173
E.P.10 Protein extraction and analysis.....	175
E.P.11 Computational tools.....	179

E.P.12 Immunofluorescence	180
E.P.13 RT-PCR.....	181
E.P.14 Cell electroporation (AMAXA)	182
REFERENCES	183
ANNEX	211
A.1 Vectors	213
A.2 <i>FN1</i> promoter	224
A.3 <i>LEF1</i> promoter.....	225
A.4 Article	226

FIGURE INDEX

INTRODUCTION

Figure I.1. Schematic representation of the model proposed by Hanahan and Weinberg of the set of functional capabilities acquired by most and maybe all cancers	5
Figure I.2. Main types of mechanisms involved in EMT induction	7
Figure I.3. Germ layers in embryo before and after gastrulation	9
Figure I.4. Formation and delamination of neural crest cells	10
Figure I.5. EMT in heart valve development and secondary palate formation	11
Figure I.6. Schematic illustration of the three mechanisms via which fibroblasts can originate during kidney injury	12
Figure I.7. EMT encompasses a wide range of metastatic phenotypes	13
Figure I.8. The metastable cell phenotype	14
Figure I.9. Cancer stem cells may be the result of either the transformation of normal stem cells or the induction of EMT in more differentiated cancer cells	15
Figure I.10. Multiple signaling pathways and effectors can contribute to EMT	17
Figure I.11. A schematic diagram of the TGF- β signaling pathway in which mechanisms potentially involved in TGF- β -mediated EMT are included	19
Figure I.12. Landscape of WNT signaling cascades	21
Figure I.13. In most cellular models EMT is induced by cooperation of overexpressed, constitutively active RTKs and TGF- β -R signaling	22
Figure I.14. The Notch pathway	23
Figure I.15. Hedgehog signaling pathway	24
Figure I.16. Schematic representation of the human E-cadherin promoter	27
Figure I.17. The snail superfamily of transcription factors	28
Figure I.18. Snail genes are a convergence point in EMT induction	29
Figure I.19. Schematic representation of snail1 in mammals	30
Figure I.20. Downstream targets of snail genes	31
Figure I.21. Schematic representation of the <i>ZFH</i> family members	32
Figure I.22. Multiple sequence alignment and classification of some representative members of the HLH family of transcription factors	34
Figure I.23. β -catenin is a protein that interacts with a wide variety of factors	36
Figure I.24. The migrating cancer stem (MCS) cell concept	38
Figure I.25. Schematic structure of NF- κ B and I κ B proteins	39
Figure I.26. Schematic overview of different NF- κ B activation pathways	40

Figure I.27. Representation of NF- κ B-dependent targets involved in different aspects of oncogenesis	41
---------------------------------------------------------------------------------------------------------------------------	-----------

RESULTS

Figure R.1. Phenotypic and molecular effects of the transfection of mmsnail1-HA in HT29 M6, RWP1 and SW480 cells	49
Figure R.2. The fragment -341/+265 of <i>FN1</i> promoter is sufficient to mediate <i>FN1</i> transcription in mesenchymal cells	50
Figure R.3. Snail1 increases the promoter activity of <i>LEF1</i> and <i>FN1</i>	51
Figure R.4. Snail1 does not stabilize LEF-1 and fibronectin mRNAs	52
Figure R.5. Schematic representation of the <i>FN1</i> and <i>LEF1</i> promoters cloned	52
Figure R.6. Snail1 cannot directly bind to E-box-lacking promoters.....	53
Figure R.7. The E-box at -527/+1389 <i>LEF1</i> promoter holds repressive function	54
Figure R.8. Snail1 binds indirectly to the <i>FN1</i> and <i>LEF1</i> promoters	56
Figure R.9. Snail1 binds to the <i>FN1</i> promoter <i>in vivo</i>	57
Figure R.10. Snail1-P2A fails to activate gene expression and to bind to the <i>FN1</i> promoter	59
Figure R.11. Mutation of the LEF/TCF box in the <i>FN1</i> promoter does not affect snail1-induced activation.....	61-62
Figure R.12. Mutation of the LEF/TCF box in the <i>LEF1</i> promoter does not affect snail1-induced activation	63
Figure R.13. Effect of downregulation of β -catenin and TCF4 signaling in snail1-mediated activation	65
Figure R.14. β -catenin knockdown does not have any effect in snail1 nuclear import. 67	
Figure R.15. β -catenin binds <i>in vivo</i> to the <i>FN1</i> promoter	69
Figure R.16. Deletion of the +451/+460 region of the <i>LEF1</i> causes insensitivity of the promoter to snail1	70
Figure R.17. The snaRE in the <i>FN1</i> promoter is delimited to -341/-192	71
Figure R.18. The snaRE in the <i>FN1</i> promoter is delimited to -341/-323	72
Figure R.19. The region +485/+490 of the <i>LEF1</i> promoter and -330/-324 of the <i>FN1</i> promoter have a little conserved p300 binding motif	73
Figure R.20. p300 motifs in +485/+490 of <i>LEF1</i> promoter and -330/-324 of <i>FN1</i> promoter are not involved in snail1-induced activation of such promoters	74
Figure R.21. Snail1 modulates complex formation in the region -339/-320 of the <i>FN1</i> promoter	76
Figure R.22. Snail1 presence is not enough to induce complex formation in -339/-320 <i>FN1</i> promoter	78

Figure R.23. Snail1 and β -catenin are not part of the complex induced by snail1 on -341/-301.....	79
Figure R.24. The regions isolated in the <i>FN1</i> promoter and the <i>LEF1</i> promoter as snaRE are not sufficient to mediate snail1-induced transcription	81
Figure R.25. Snail1-HA coprecipitates with the -36/+265 fragment of the <i>FN1</i> promoter	84
Figure R.26. Snail1 and NF- κ B cooperate to activate transcription.....	86-87
Figure R.27. Snail1 causes and E-cadherin prevents p65 association to the <i>FN1</i> promoter.....	89
Figure R.28. Snail1 is part of the complex formed by p65.....	90
Figure R.29. p65 binds to the <i>FN1</i> and <i>LEF1</i> promoters in the presence of snail1 and absence of E-cadherin	91-92
Figure R.30. Seven mutated probes were designed to compete the complex at -341/-320 in snail1 cells.....	93
Figure R.31. Two motives are responsible for the complex formed in the -341/-320 region of the <i>FN1</i> promoter	94
Figure R.32. TFCP2c is a good candidate for binding to the <i>FN1</i> promoter in the region -341/-301.....	95
Figure R.33. TFCP2c binds to the <i>FN1</i> promoter.....	96
Figure R.34. Expression of the dominant negative TFCP2c Q234L/K236E-myc causes decrease of fibronectin protein and mRNA levels in RWP1 and HT29 M6 snail1 clones.	98
Figure R.35. TFCPc interference causes decrease of fibronectin protein in HT29 M6 snail1 clones	99
Figure R.36. Snail1 induces different expression pattern of TFCP2c in several cell lines.....	100
Figure R.37. TFCP2c concentrates in the nucleus of HT29 M6 snail1 clones.....	101
Figure R.38. TFCP2c spliced variants have the same expression pattern in HT29 M6 clones	102
Figure R.39. Snail1 induces phosphorylation of TFCP2c	104

DISCUSSION

Figure D.1. Schematic representation of the <i>LEF1</i> 5' region.....	110
Figure D.2. Schematic representation of the human <i>FN1</i> promoter cloned used for this study and <i>Cis</i> elements identified.....	112
Figure D.3. Snail1 activates or represses its own promoter depending on cellular context	113
Figure D.4. Relationship between snail1 and β -catenin.....	116

Figure D.5. Effect of <i>sox7</i> and <i>sox9</i> in <i>snail1</i> mediated activation	118
Figure D.6. NF- κ B subcellular localization is regulated similarly to β -catenin	123
Figure D.7. Structural domains of human PARP-1	125
Figure D.8. Identified proteins in the mammalian LSF/GRH family	129
Figure D.9. Schematic representation of TFCP2c	130
Figure D.10. PI 3-kinase/Akt links APP with TFCP2c/LSF in anti-apoptotic signaling ..	134
Figure D.11. Our model of gene activation induced by <i>snail1</i>	138

EXPERIMENTAL PROCEDURES

Figure E.P.1. Inducible repression of β -catenin and Δ TCF4 in LS-174T clones	148
Figure E.P.2. The Prefibronectin sequence interferes with the <i>FN1</i> promoter activity	152
Figure E.P.3. The NF- κ B-box <i>FN1</i> promoter mutant is not sensitive to Rel-VP16 in reporter assays	154
Figure E.P.4. Loss of responsiveness to specific transcription factors of the different mutant promoters were confirmed in reporter assays.....	156

TABLE INDEX

INTRODUCTION

Table I.I. The TGF- β family and their representative activities	18
Table I.II. List of some target genes of Wnt/ β -catenin signaling	37

DISCUSSION

Table D.I. Summary of modulation of gene expression reported after snail1/2 expression	108
-----------------------------------------------------------------------------------------------------	------------

EXPERIMENTAL PROCEDURES

Table E.P.I. Cell lines used during the development of this study and some of their characteristics	147
Table E.P.II. Oligonucleotides used for mmsnail1 and mmsnail1-P2A	151
Table E.P.III. Sense and antisense primers used to amplify the specified <i>FN1</i> promoters	153
Table E.P.IV. Sense and antisense oligonucleotides used to amplify <i>FN1</i> promoter mutants	154
Table E.P.V. Sense and antisense oligonucleotides used to amplify <i>LEF1</i> promoter mutants	155
Table E.P.VI. Primers used to amplify the different TFCP2 constructs	158
Table E.P.VII. Pairs of primers used for quantitative RT-PCR after actinomycin D treatment	159
Table E.P.VIII. Sense and antisense primers used to amplify the probes for BOPA assays	163
Table E.P.IX. Sonication pulses in Branson DIGITAL Sonifier® UNIT Model S-450D sonicator	167
Table E.P.X. Antibodies used for ChIP analysis, their origin and assay dilution	167
Table E.P.XI. Primers used to analyze the promoters by quantitative PCR	168
Table E.P.XII. Number of cells seeded and days in plate to ensure formation of junctions before performing the assay	169
Table E.P.XIII. ³² P labelled probes used in EMSA experiments	170
Table E.P.XIV. Probes used to compete EMSA experiments	171
Table E.P.XV. Antibodies used in EMSA and their origin	171
Table E.P.XVI. Conditions in which cells were plated for transfection/infection	173
Table E.P.XVII. Conditions for PEI transfection	173
Table E.P.XVIII. Concentration medium according to cell flask	174

Table E.P.XIX. Proteins analyzed and details for western blot	176
Table E.P.XX. Reagents used to prepare polyacrylamide gels.....	178
Table E.P.XXI. Antibodies and conditions for immunofluorescence	180
Table E.P.XXII. Primers and conditions for RT-PCR analysis.....	181

NOTES TO THE READER

All exogenous snail1 used throughout this study is the murine homolog (mmsnail1)

GENES appear in upper italic case

Protein/protein appear in lower case

ABBREVIATIONS AND ACRONYMS INDEX

ACF: Aberrant Crypt Foci	FGF: Fibroblast Growth Factor
AMF: autocrine motility factor	FN1: Fibronectin
AMH: Anti-Müllerian hormone	FZD: Frizzled
AP1/2: adaptor protein complex 1 / 2	GDF: Growth differentiation factor
APC: Adenomatous Polyposis Coli	GFP: Green Fluorescent Protein
APP: Alzheimer's amyloid precursor protein	GRHL: Grainyhead like protein
Bcl2: B-cell lymphoma	GSK-3β: Glycogen Synthase Kinase-3 β
bHLH: basic Helix-Loop- Helix	GST: Gluthathione-S-Transferase
BMP: Bone Morphogenetic Protein	HA: Haemagglutinin
BOM: Brother of MGR protein	HDAC: Hystone Deacetylase
BOPA : Biotinnylated Oligonucleotide Pull-down Assay	HEK: Human Embryonic Kidney
bp: base pair	HGF: Hepatocyte Growth Factor
BSA: Bovine Serum Albumin	Hh: Hedgehog
βTRCP: β -transducin repeat-containing	HIV: Human Immunodeficiency Virus
cAMP: cyclic adenosine monophosphate	HNSCC: Head and Neck Squamous Cell Carcinoma
CBP: CREB Binding Protein	HPRT: Hypoxanthine Guanine Phosphoribosyl Transferase
CDH1: E-cadherin Gene	Id: Inhibitor of differentiation
Cdk: Cyclin-dependent kinase	IF: immunofluorescence
cDNA: complementary DNA	IFNγ: Interferon γ
cENS-1: chicken Embryonic Stem 1 gene	IGF: Insuline Growth Factor
ChIP: Chromatin IP	IgG: Immunoglobulin G
CK1: Casein Kinase 1	IκB: Inhibitor of nuclear factor Kappa B
CMV: Cytomegalovirus	IKK: I κ B kinase
COX-2: Cyclooxygenase-2	IL: Interleukin
CREB : cAMP responsive element binding protein	ILK: Integrin Linked Kinase
CSC: cancer stem cells	IP: Immunoprecipitation
CtBP: C-terminal Binding Protein	IRES: Internal Ribosome Entry Site
CXCL1: Chemokine (C-X-C motif) ligand 1	ISC: Intestinal Stem Cells
DFF: DNA fragmentation factor	ISH: <i>in situ</i> hibridization
DMEM: Dulbecco's Modified Eagle's Medium	KDa: KiloDalton
DMSO: Dimethyl sulfoxide	KO: Knock Out
DNA: Deoxyribonucleic acid	LAP: latency-associated peptide
dsDNA: double stranded DNA	LBP: leader-binding protein
DVL: Dishevelled	LEF1: lymphoid enhancer-binding factor 1
E-box: Ephrussi box- like motif	LOXL2: Lysyl Oxidase-Like 2
ECM: Extracellular Matrix	LPS: Lipopolysaccharide
EGF: Epidermal Growth Factor	LSF: Late simian virus 40 transcription factor
EGR: Epidermal Growth factor Receptor	LSF-ID: LSF-internally deleted.
Egr-1: early growth response protein 1	LTBP: latent TGF binding protein
EMSA: Electrophoretic Mobility Shift Assay	MAb: Monoclonal Antibody
EMT: Epithelial-to-Mesenchymal Transition	MAPK: Mitogen-Activated Protein Kinase
ERK: Extracellular-Regulated Kinase	MCS: migrating cancer stem cells
FACS: Fluorescent Activated Cell Sorting	MDCK: Madin Darby Canine Kidney
FAK: Focal Adhesion Kinase	MEF: mouse embryonic fibroblasts
FBS: Fetal Bovine Serum	MET: Mesenchymal-to-Epithelial Transition
	MGR: mammalian grainyhead
	MIS: Müllerian inhibiting substance

MMP: Matrix metalloproteinase
mRNA: Messenger RNA
Muc-1: Mucin 1
NES: Nuclear Export Signal
NF-kappaB: Nuclear Factor Kappa B
NLS: Nuclear Localization Signal
ODC : ornithine decarboxylase
OP1/2: Osteogenic Protein 1/2
PAK1: p21-activated kinase
PARP-1: Poly (ADP-ribose) polymerase-1
PBS: Phosphate Buffered Saline
PD98509: 2-amino-3-methoxyflavone
PDGF: platelet-derived growth factor
PI: Propidium Iodide
PI3K: Phosphoinositide-3 Kinase
PKC: protein kinase C
PLC: phospholipase C
PMA: Phorbol 12myristate 13-acetate.
PRC1/2: polycomb repressive complex 1/2
PRMT: protein arginine methyltransferase
Ptc: Patched
PTEN: phosphatase and tensin homolog
PTH(rPR): parathyroid hormone related peptide receptor
qRT-PCR: quantitative RT-PCR
Ras: retrovirus-associated DNA sequence
Rb: retinoblastoma
RHD: Rel Homology Domain
RhoB: Ras homolog gene family, member B
RNA: Ribonucleic acid
ROR2: receptor tyrosine kinase-like orphan receptor 2
RT-PCR: Reverse Transcriptase-Polymerase Chain Reaction.
RTK: Receptor Tyrosine Kinase
RYK: related to receptor tyrosine kinase
SAM: sterile alpha motif
SARA: Smad anchor for receptor activation
SCF: stem cell factor
SCS: stationary cancer stem cells
SD: Standard Deviation
SEF1: Serum amyloid A3 enhancer factor 1
shRNA: short hairpin RNA
SIP1: Smad Interacting Protein 1
siRNA: short interference RNA
SNAG: Sna/Gfi
snaRE: snail1 Responsive Element
SOM: Sister of MGR
SOX: Sry-related HMG box
Sp1: specificity protein 1
STS: staurosporine
SV40: Simian vacuolating virus 40
TBK1: TANK-binding kinase 1
TBP: TATA binding protein
TCF: T-cell factor
TFCP2c/d: Transcription factor CCAAT-binding protein 2 c/d
TFCP2L: Transcription factor CP2-like protein
TGFβ: Transforming Growth Factor beta
TNFα: Tumor Necrosis Factor alpha
TRITC: Tetramethyl Rhodamine Iso-Thiocyanate
TS: thymidylate synthase
TSS: Transcription Start Site
UBP1: Upstream region binding protein 1
UTR: Untranslated Region.
VASP: vasodilator-stimulated phosphoprotein
VDR: Vitamin D Receptor
VEGF: Vascular endothelial growth factor
WB: Western Blot
Wg: Wingless
WRE: Wnt Responsive Element
XR11: *Xenopus* Bcl-xL homolog
ZEB1/2: Zinc finger E-box binding homeobox 1/2
Zfh-1/2: Zinc-finger homeodomain-1/2

INTRODUCTION

I.1 CANCER: GENERAL OVERVIEW

The multiplication of cells is a process carefully regulated in response to specific needs of the body: in a young animal cell multiplication exceeds cell death to increase the animal size, while in an adult the processes of cell birth and death are balanced to produce a steady state. Very occasionally, the controls that regulate cell multiplication break down causing cells to grow and divide in an unregulated fashion, without regard to the body's need for further cells of its type [1]. The result of mutations affecting critical genes that regulate cell proliferation and survival in somatic cells may be cause of more than 100 diseases grouped in what has been called cancer [2].

Abnormal mass of tissue, or tumours, of different subtypes can be found within specific organs. Initially, the mutations responsible for these diseases were thought to promote malignancy in a straightforward manner, either through inactivation of "tumour suppressor" genes or activation of "oncogenes", which directly modulate cell birth or death. Some more years of study, however, have shown that susceptibility genes that work through less direct mechanisms also play important roles [3]. Although the paths that cells take on their way to becoming malignant are highly variable, it has been suggested that there are six essential alterations in cell physiology shared by most, if not all, types of human tumours (**Figure I.1**). They are self-sufficiency in growth signals, insensitivity to antigrowth signals, evasion of programmed cell death, limitless replicative potential, sustained angiogenesis and tissue invasion and metastasis (or colonization of new and distant tissues). Each of these physiologic changes represents the successful breaching of an anticancer defense mechanism hardwired into cells and tissues [4].

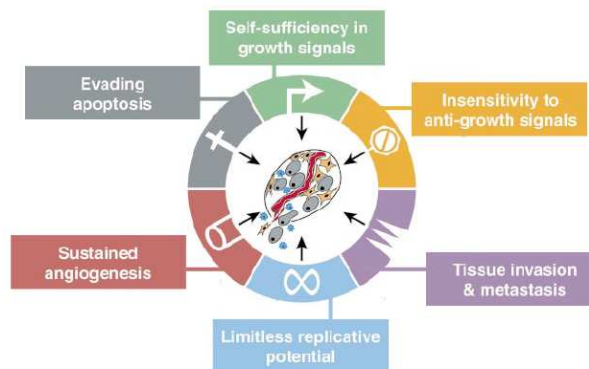


Figure I.1. Schematic representation of the model proposed by Hanahan and Weinberg of the set of functional capabilities acquired by most and maybe all cancers (adapted from [4]).

I.1.1 Epithelial cancers and epithelial to mesenchymal transition (EMT)

An invasive malignant tumour derived from epithelial tissue that tends to metastasize to other areas of the body is called carcinoma. Carcinomas are by far the most prevalent form of cancer, with over 90% of all human malignancies derived from epithelial cells, and represents one of the prime causes of human mortality [5, 6]. Well-differentiated epithelial cells possess extensive junctional networks that physically separate the plasma membrane into apical and basolateral domains, promote adhesion, and facilitate intercellular communication, thus restricting motility, preserving tissue integrity, and permitting individual cells to function as a cohesive unit [7].

During the progression of carcinoma, advanced tumour cells frequently exhibit a downregulation of epithelial markers and a deficit of intercellular junctions, resulting in a loss of epithelial polarity and reduced intercellular adhesion. The loss of epithelial features is often accompanied by increased cell motility and expression of mesenchymal genes. This process, referred to as epithelial to mesenchymal transition (EMT), can promote hallmark features of carcinoma, including loss of contact inhibition, altered growth control, and enhanced invasiveness [8]. Molecular and morphologic features indicative of EMT correlate with poor histologic differentiation, destruction of tissue integrity and metastasis, being considered a crucial event in late stage tumorigenesis [5, 6].

I.2 EPITHELIAL-MESENCHYMAL TRANSITION

While epithelial and mesenchymal cell types have long been recognized, the conversion of epithelial cells into mesenchymal cells was only defined as a distinct cellular program in 1980s by Greenburg and Hay. They were the first to use the term Epithelial-Mesenchymal Transition as conclusion of a series of experiments where they observed that differentiated epithelial cells could be transformed into mesenchymal cells. Subsequent cell-biological and molecular studies resulted in EMT being loosely defined by three major changes in the cellular phenotype [9, 10]: (1) morphological changes from a cobblestone-like monolayer of epithelial cells with an apical-basal polarity to dispersed, spindle shaped mesenchymal cells with migratory protrusions, (2) changes of differentiation markers from cell-cell junction proteins and cytokeratin intermediate filaments to vimentin filaments and fibronectin, and (3) the functional changes associated with the conversion of stationary cells to motile cells with capacity of invading through the extracellular matrix (**Figure I.2**).

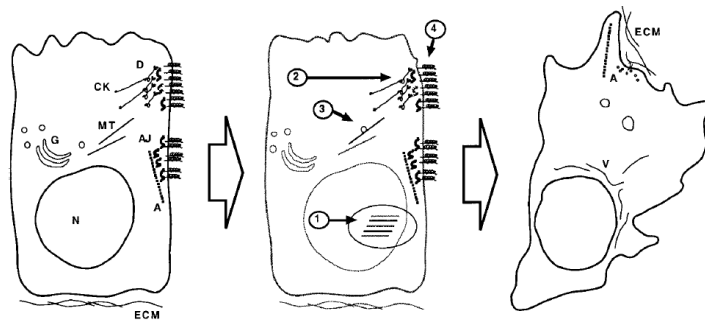


Figure I.2. Main types of mechanisms involved in EMT induction [11]. An epithelial cell (left) undergoes EMT and expresses a mesenchymal-like phenotype (right). The center panel outlines the putative general mechanisms involved: (1) transcriptional downregulation of cell-cell adhesion structures, (2) postranslation regulation: destabilization of cell-cell adhesion structures, (3) downregulation of maintenance pathways, (4) active degradation of cell-cell adhesion components: active cell-cell dissociation. A, actin; AJ, adherens junction; CK, cytokeratins; D, desmosome; ECM, extracellular matrix; G, Golgi; MT, Microtubules; N, nucleus; V, vinculin.

Although all three changes are not invariably observed during all EMTs, acquisition of the ability to migrate and invade ECM as single cells is considered a functional hallmark of the EMT program [12]. Indeed, Edme and collaborators suggest that EMT is always associated with cell scattering, which is defined by two events that seem to appear simultaneously: (1) cell-cell dissociation, as a consequence of the rupture of intercellular complexes and (2) cell movement, resulting from rearrangements of the cytoskeleton and formation of new cell-substratum contacts [13].

The process of EMT was originally identified during specific stages of embryonic development in which epithelial cells migrate and colonize different embryonic territories [14, 15], however, it has also been described to be crucial in transient pathological situations such as wound healing, inflammation and cancer [16-18]. Tumorigenesis-associated EMT includes, though, additional critical features, which dramatically increase the malignancy of these cells towards local tumour infiltration and metastasis [6].

1.2.1 Morphologic features and molecular markers of epithelial and mesenchymal cells

Epithelial and mesenchymal cells represent distinct lineages, each with a unique gene expression profile that gives specific attributes to each cell type. E-cadherin is a transmembrane protein and the best characterized molecular marker expressed in epithelial cells. It regulates the establishment of the adherens junctions, which form a continuous belt below the apical surface. The extracellular domain of E-Cadherin mediates calcium-dependent homotypic interactions with adjacent cells while the intracellular domain connects with the actin cytoskeleton indirectly via catenins. Early contacts between two cells are also mediated by E-cadherin molecules, which cluster into small complexes expanding afterwards to form stable adherens junctions and promote the formation of desmosomes below them [19, 20]. Tight junctions are situated just above the adherens junctions, at the apical side of the lateral membrane. Claudins and occludins are the transmembrane proteins typical of this type of junctions which are essential for plasma membrane polarity. Together with the adherens junctions, tight junctions seal intercellular spaces between cells and form permeability barriers.

In contrast to well-differentiated epithelial cells, mesenchymal cells form irregular structures and rarely establish direct contacts with neighboring mesenchymal cells. Professor Elizabeth Hay, who has done the most thorough analysis of EMT, proposed four functional criteria based on morphology and invasive motility, to define a mesenchymal cell [21]: it must have (1) elongated morphology with (2) front-back end asymmetry that facilitates motility and locomotion [10], (3) filopodia, formed at the leading edge and enriched with integrin receptors that interact with the extracellular matrix and matrix metalloproteinases (MMP) that digest basement membranes [22] and (4) invasive motility. Intermediate filaments, such as vimentin, cytoskeletal proteins, β -filamin, α -actin, and extracellular matrix components, such as fibronectin and collagen precursors, are also increased in mesenchymal cells [23].

I.2.2 Physiological EMT

Several EMT processes take place at different moments during embryonic development. The formation of the mesoderm, or third germ layer, from the primitive ectoderm is initiated during gastrulation and represents the earliest example of EMT in embryogenesis. In the two weeks embryo (**Figure 1.3.A,B**), only formed by the epiblast (the layer of the blastula that gives rise to the ectoderm after gastrulation) and the hypoblast (the endoderm after gastrulation), takes place the first event in mesoderm formation: the invagination of epithelial cells. This step is characterized by drastic but small changes in a population of epithelial cells that range from narrowing of apical compartment and redistribution of organelles to bulging of basal compartments. Once cells are ready to ingress, the basal membrane breaches locally and cells lose their cell-cell adhesion, remaining attached to the neighboring cells only by disperse focal contacts. The completion of the EMT program during gastrulation occurs when these cells migrate along the narrow extracellular space underneath the ectoderm (**Figure 1.3.A,B**) [12]. Ingression of these cells results in formation of the mesoderm and replacement of some of the hypoblast cells to produce the definitive endoderm.

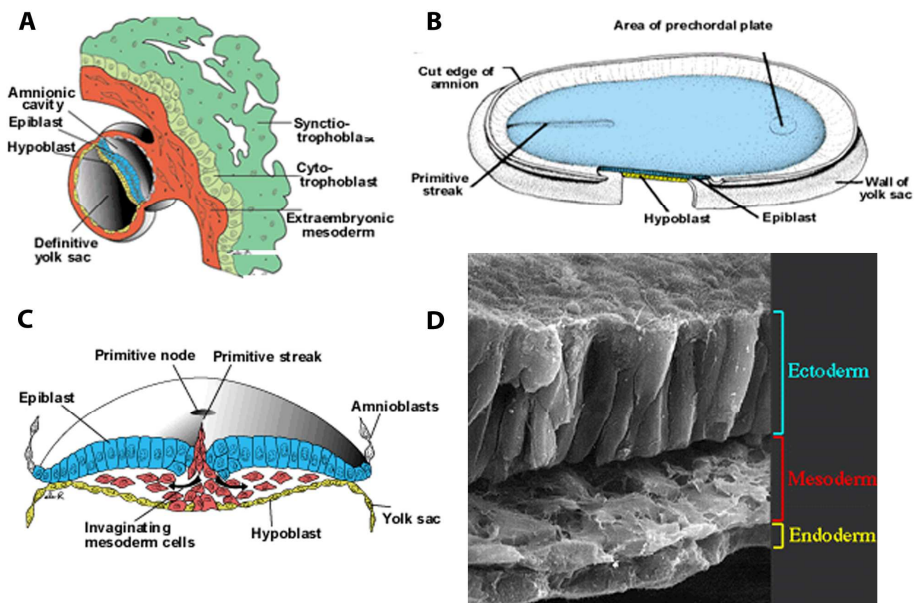


Figure 1.3. Germ layers in embryo before and after gastrulation [24]. **A.** Late in the second week of human gestation, the embryo has two cell layers, the epiblast and the hypoblast, and is surrounded by the amnionic cavity and the yolk sac. **B.** Dorsal view of the two week embryo; the epiblast and the hypoblast are indicated. **C.** Cross-section of the embryo where epiblast cells are seen to converge at the midline and ingress at the primitive streak. **D.** Electron microscopy micrograph of a cut through the embryo illustrates the three germ layers: ectoderm (formerly referred to as epiblast), mesoderm and endoderm.

Another example of EMT is provided by neural crest development (also portrayed as a second gastrulation event in vertebrates [25]). The neural crest (sometimes referred to as fourth germ layer) develops at the boundary between the neural plate and the epidermal ectoderm, from a small portion of the dorsal neural tube, being both the epidermis and neural plate capable of giving rise to neural crest cells [24-26]. The emergence of neural crest begins with the presence of a distinct population of cells with rounded and pleiomorphic shapes, which contrast with those of the polarized neural tube that form nearby (**Figure I.4.A**) [12]. The presumptive neural crest cells proceed to lose cell-cell adhesion while becoming excluded from the neural epithelium [27] and actively invade through the basal lamina to migrate away from the neural tube (**Figure I.4.B**) and finally differentiate into bone, smooth muscle, peripheral neurons, glia and melanocytes [28-30].

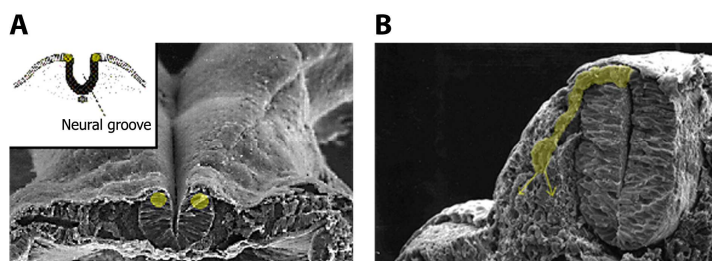


Figure I.4. Formation and delamination of neural crest cells [24]. **A.** The cells at the tips of the neural folds, lying between the neural tube and the overlying epidermis, become the neural crest cells. **B.** Following the closure of the trunk neural folds, the neural crest cells leave the dorsal aspect of the neural tube.

Cardiac valve formation and secondary palate formation are two more processes quite well studied involving EMT. In cardiac valve formation, the myocardial cells secrete a large amount of ECM, displacing the endocardium away from the myocardium and creating endocardial cushions. These cushions are filled by epithelial cells from the endocardial cell layer which undergo EMT (**Figure I.5.A** [31, 32]). On the other hand, development of the secondary palate requires fusion of the palatal shelves at the midline which is accomplished by approach of the two shelves from opposite sides of the developing oral cavity. Epithelial cells that cover the tip of each shelf intercalate to form the medial seam, undergoing EMT soon after fusion and integrating into the mesenchymal compartment of the palate (**Figure I.5.B**) [31, 33].

While mesoderm formation and neural crest development represent two processes in which the resulting cells maintain oligopotentiality, heart valve development and secondary palate formation occur in relatively well-differentiated epithelial cells that are destined to become defined mesenchymal cell types. The latter two processes

support the hypothesis that EMT may also be induced under certain physiological or pathological conditions in adult tissues [12].

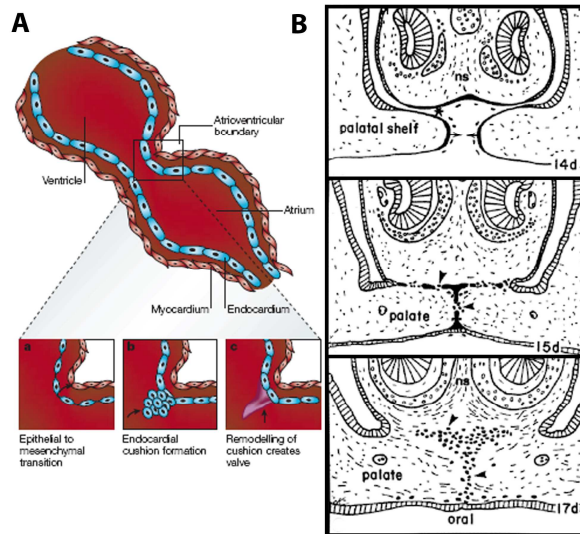


Figure 1.5. EMT in heart valve development and secondary palate formation. A. Along the anterioposterior axis of the developing vertebrate heart endocardial cells undergo an EMT and migrate into the extracellular matrix between the myocardium and the endocardium (cardiac jelly) to later give rise to valvular structures [32]. **B.** Drawings showing the successive stages in the fusion of the secondary palatal shelves in the mouse [33]. The fused basal layers form midline palatal and horizontal palate nasal seams, which break up into epithelial islands that transform into mesenchymal cells (arrowheads, 15d). The result is mesenchymal confluence across the palate midline and between nasal septum (ns, 17d) and dorsal plate. The location of the epithelium-derived mesenchymal cells is shown in black (arrowheads, 17d).

Wound healing is another example of EMT, in this case, in adult tissues. While the repair of the dermis is required of the recruitment of fibroblasts to the wound site, coverage of the wound at the epidermis level is achieved by hyperproliferation of keratinocytes at the wound edge, which suffer a process reminiscent of EMT. Keratinocytes move forwards between the injured dermis and the fibrin clot by rearranging their actin cytoskeleton and extending lamellipodia. They also lose both cell-cell contacts and attachment to the basement membrane. In addition, keratinocytes at the front alter the expression of integrin receptors to allow attachment to new substrates and degrade connective tissue. However, a full EMT does not occur as keratinocytes at the wound edge still retain some intercellular junctions; furthermore, they continue to express epidermal keratins (though not vimentin) [34].

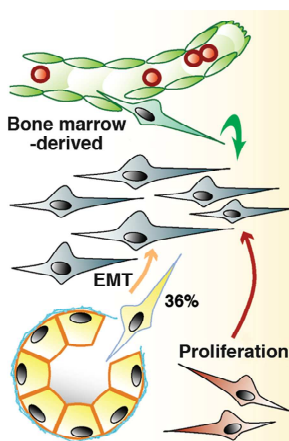
This example also illustrates that the EMT program does not always represent an irreversible process since, in several cases, the converted mesenchymal cells can revert

to an epithelial cell state by passing through a Mesenchymal-Epithelial Transition (MET), as it happens in the formation of the nephron epithelium in the developing kidney [35]. Together, EMT and MET processes demonstrate substantial cell plasticity and suggest that interconversion between epithelial and mesenchymal cell states may also occur under certain pathological conditions [6, 12, 18].

I.2.3 Pathological EMT

As mentioned above, wound healing also involves the activation of fibroblasts, which are recruited to the wound site. Fibroblasts produce great amounts of ECM and some of them even transdifferentiate to contractile, myofibroblasts that aid in wound contraction at the dermis level. When epithelial injury involves blood loss it leads to platelet activation, the production of several growth factors and an acute inflammatory response. Under normal circumstances, the epithelial barrier is repaired and the inflammatory response resolves. However, in fibrotic disease, the fibroblast response continues, resulting in unresolved wound healing [36].

Although most of the fibroblasts that accumulate at sites of inflammation derive from the bone marrow, some others are the result of epithelial cells at injury site that suffer EMT [37, 38]. Great evidence exists for EMT associated with progressive kidney diseases and probably is also true for lung and liver diseases. Fibroblasts are not particularly abundant in normal kidneys, but when there is tissue damage many inflammatory cells incite EMT using cytokines and growth factors. About 36% of new fibroblasts come from local EMT, between 14-15% from the bone marrow and the rest from local proliferation (**Figure I.6** [37, 39]). In pulmonary fibrosis a similar process takes place, and it has been described that alveolar epithelial cells are induced to undergo EMT [40, 41].



Though there is evidence that EMT also triggers dissemination of single carcinoma cells from the site of the primary tumours to distant sites, it took a long time for EMT to be recognized as a potential mechanism for carcinoma progression. Nowadays it is almost universally accepted by molecular biologists that EMT mediates this pathological step, nonetheless, there is still some controversy, particularly among pathologists, mainly because EMT, as a consequence of the great diversity of cellular organization observed in human tumours, cannot be followed in time and space [42, 43], but also from the observation that metastases appear histologically similar to the primary tumour [43]. The histological similarity between the secondary metastasis and the primary tumour, however, can also be interpreted as a reversible EMT (a transient activation of the EMT program) some carcinoma cells undergo during tumour metastasis [42]. According to this model, carcinoma cells would activate the EMT program to achieve invasion and dissemination to different organs yet, once they have reached those organs, these mesenchymal cells may revert via a MET to an epithelial identity and regain proliferative ability as growths in distant organ sites (**Figure I.7**).

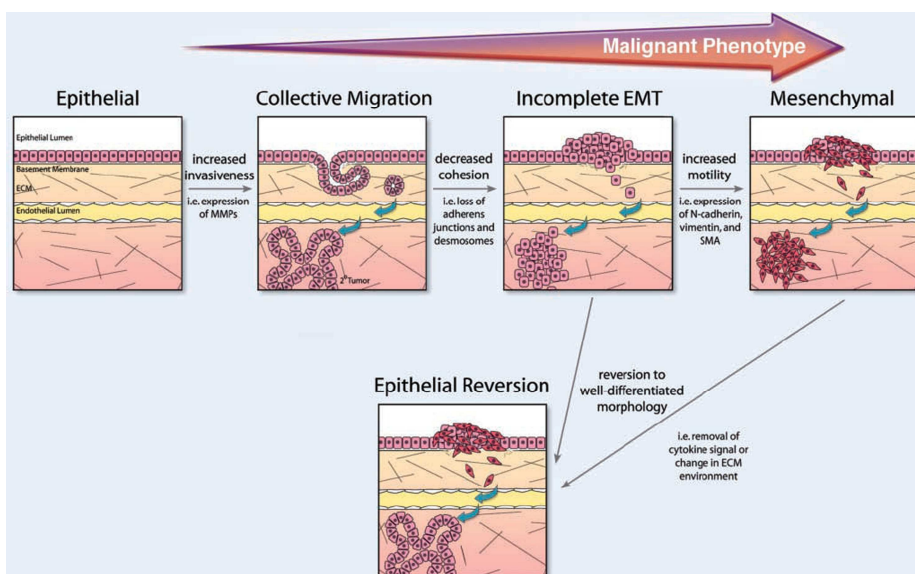


Figure I.7. EMT encompasses a wide range of metastatic phenotypes [5]. During the progression of invasive and metastatic carcinoma, normal epithelial cells can adopt increased invasiveness yet retain well-differentiated morphology and cohesiveness. These cells can invade surrounding tissue and metastasize by collective migration. Loss of intercellular cohesion via incomplete EMT would increase metastatic potential, as would a full conversion to a mesenchymal phenotype. Following invasion or distal metastasis, cells that have undergone progressive steps of epithelial to malignant transition can also revert to a well-differentiated epithelial phenotype.

Figure I.6. Schematic illustration of the three mechanisms via which fibroblasts can originate during kidney injury (adapted from [37]).

The hypothesis that cancer cells may pass through a partial EMT program rather than complete one is supported by the fact that they do express both epithelial and mesenchymal markers, which is consistent with the stem-like profile reported by several authors in colon carcinoma cells at the invasive front. This ability of cells to express attributes of both phenotypes was referred to by Savagner as “metastable phenotype” (Figure I.8) [28].

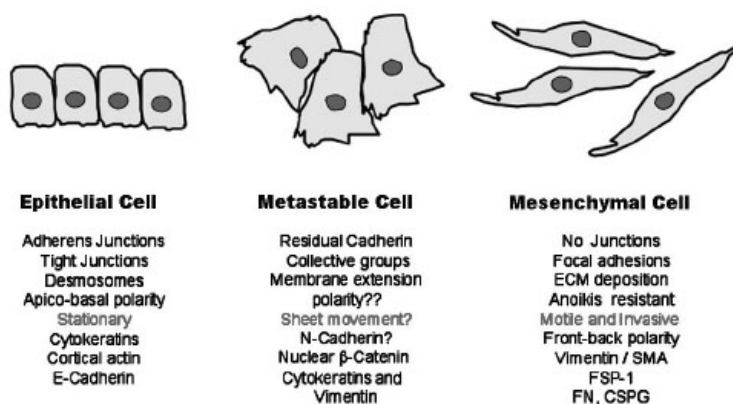


Figure I.8. The metastable cell phenotype [28]. An epithelial (left) and a mesenchymal (right) cell and between them the hybrid metastable cell.

Consistent with the “metastable phenotype” hypothesis, evidence of self-renewing, stem-like cells within tumours and other types of cancer has recently been reported. These newly defined cells, which have been called cancer stem cells (CSCs) [44], have been described in the hematopoietic system [45] and in several solid tumours originating from the breast [46, 47], colon [48, 49] and brain [50]. The induction of EMT in more differentiated cancer cells seems to generate CSC-like cells with increased ability to self-renew and initiate new tumours at least in colon and breast cancer [47]. Some studies also suggest that cancer stem cells can be divided into two types: the stationary (SCS) and the migrating (MCS) [51]. SCS cells are still embedded in the epithelial tissue, already active in benign precursor lesions, such as adenomas, and persist in differentiated areas throughout all the steps of tumour progression; however the SCS cells cannot disseminate. On the contrary, migrating stem cells are located predominantly at the tumour–host interface and are derived from SCS-cells through the acquisition of a transient EMT in addition to stemness. As a consequence, MCS can disseminate, and disseminating cancer cells that retain stem-cell functionality can form metastatic colonies. These links between EMT and stem cells indicate that the EMT process may facilitate the generation of cancer cells with the mesenchymal traits

needed for dissemination as well as the self-renewal properties needed for initiation of secondary tumours (**Figure I.9**).

The CSC hypothesis suggests that neoplastic clones are maintained exclusively by a rare fraction of cells with stem cell properties, true measures of which are the capacity of self-renewal and the exact recapitulation of the original tumour [44]. Because normal stem cells and cancer cells share the ability to self-renew, it seems reasonable that newly arising cancer cells appropriate the machinery for self-renewing normally expressed in stem cells. In fact, many observations suggest analogies between normal stem cells and tumorigenic cells: 1) both normal stem cells and tumorigenic cells have extensive proliferative potential and the ability to give rise to new (normal or abnormal) tissues; 2) both tumours and normal tissues are composed of heterogeneous combinations of cells, with different phenotypic characteristics and different proliferative potentials [52-55]; 3) due to the clonal origin of most tumours [56, 57]. Tumorigenic cancer cells must give rise to phenotypically diverse progeny, including cancer cells with indefinite proliferative potential, and cancer cells with limited or no proliferative potential. All these statements support the hypothesis that tumorigenic cancer cells undergo processes analogous to the self-renewal and differentiation of normal stem cells.

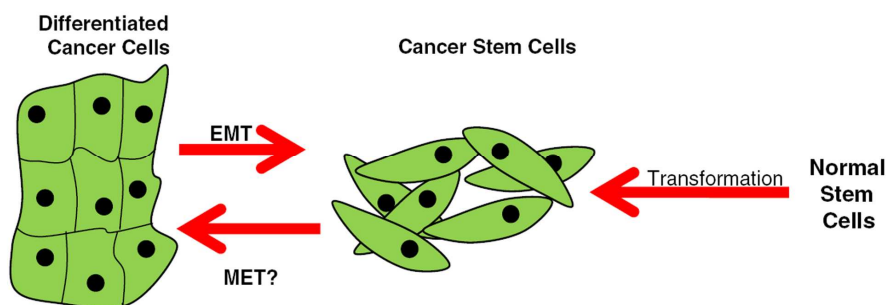
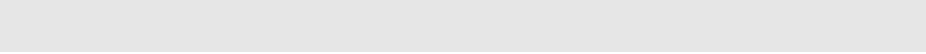


Figure I.9. Cancer stem cells may be the result of either the transformation of normal stem cells or the induction of EMT in more differentiated cancer cells [58].

An important note is that the subpopulation of CSCs has been demonstrated to be more resistant to contemporary cancer therapies than is the major population of more differentiated cancer cells, at least for breast cancer [59]. It is thought that the CSCs that remain in residual tumours after treatment are the major contributor to the relapse of cancer. Similarly, cells that have undergone EMT and exhibit stem cell properties have been shown to be more resistant to numerous cancer therapies [60], thus indicating direct evidence for an association between the EMT phenotype, CSC

and therapeutic resistance [58]. Jones and colleagues [61] refer to this concept as the “dandelion hypothesis,” in that you need to remove the roots (the resistant cells) to prevent the regrowth of the dandelion (the tumour).



I.3 MOLECULAR PATHWAYS INVOLVED IN EMT

Together, the study of cancer genetics and developmental biology has revealed that several developmentally important genes and pathways that induce EMT are activated in tumour models and promote EMT in the context of tumour progression. These pathways (TGF- β /BMPs, Wnt/Frizzled, Tyrosine Kinase Receptors (RTKs), Delta/Notch and Hedgehog/Patched) form an increasingly complex network, as they interact at multiple levels and regulate different cellular processes, so when their expression pattern is altered, the consequences can be fatal for the normal regulation of cell behavior and homeostasis (**Figure I.10**) [62, 63].

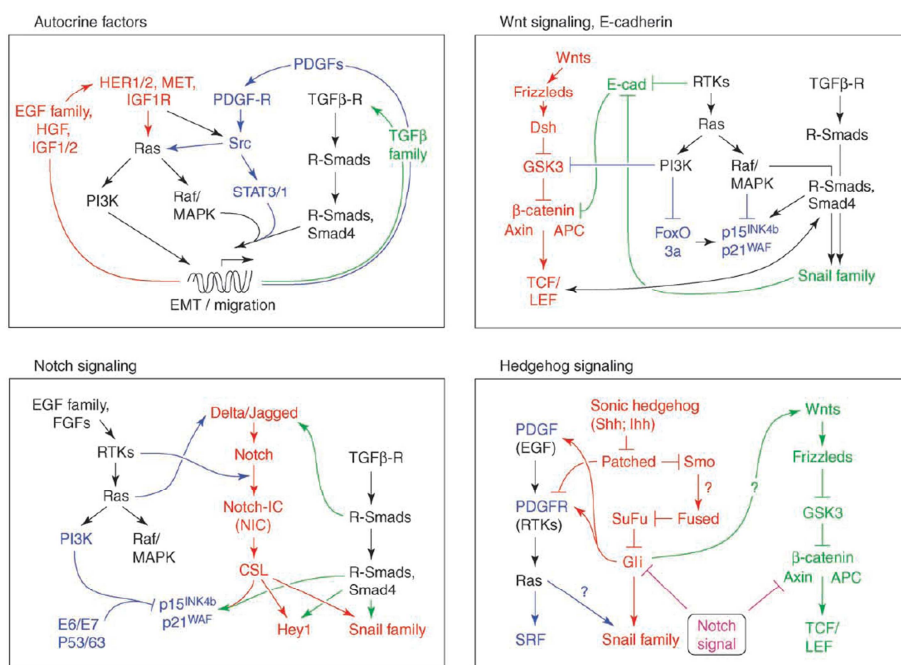


Figure I.10. Multiple signaling pathways and effectors can contribute to EMT (adapted from [62]). Upper, left panel, autocrine growth factor loops contributing to EMT (TGF- β (green), RTKs and their ligands (red)). Upper, right panel, signal integration of Wnt/ β -catenin signaling (red) with the downstream effectors of Ras (blue) and TGF β (green). Lower, left panel, Notch signaling (red) cooperates with TGF- β and/or oncogenes to induce EMT. Lower, right panel, signal integration of Hedgehog signaling (red) with RTK (blue) and Wnt/ β -catenin signaling (green).

I.3.1 TGF- β /BMPs

Expressed in complex temporal and tissue specific patterns, Transforming Growth Factor β (TGF- β) and related factors are a family of cytokines that play a prominent role

in the development, homeostasis and repair of virtually all tissues in organisms. The TGF- β family members regulate cellular processes such as cell proliferation, lineage determination, differentiation, motility, adhesion and death [64]. The TGF- β family members, which can be divided into several subfamilies according to bioactive domains sequence comparison (**Table I.1**), are also multifunctional agonists whose effects depend on the responsiveness state of the target cell as much as on the factors themselves [64]. Indeed, the components of the TGF- β signaling pathways are not unique and many of the molecules that function downstream of the ligand-receptor interaction are linked by several shared components [21], phenomenon that illustrates the complex network of the pathway.

Subfamily	Members	Representative activities
BMP2	BMP2 BMP4	Gastrulation, neurogenesis, chondrogenesis, interdigital apoptosis
BMP5	BMP5 BMP6/Vgr1, BMP7/OP1 BMP8/OP2	Along with BMPs 2 and 4, this subfamily participates in the development of nearly all organisms, many roles in neurogenesis
GDF5	GDF5/CDMP1 GDF/CDMP2 GDF7	Chondrogenesis in developing limbs
Vg1	GDF1 GDF3/Vgr2	Axial mesoderm induction in frog and fish.
BMP3	BMP3/osteogenin GDF10	Osteogenic differentiation, endochondral bone formation, monocyte chemotaxis
Intermediate members	Nodal Dorsalin GDF8 GDF9	Axial mesoderm induction, left/right asymmetry Regulation of cell differentiation within the neural tube Inhibition of skeletal muscle growth
Activin	Activin β a Activin β B Activin β C Activin β E	Pituitary follicle-stimulating hormone (FSH) production, erythroid cell differentiation
TGF-β	TGF- β 1 TGF- β 2 TGF- β 3	Cell cycle arrest in epithelial and hematopoietic cells, control of mesenchymal cell proliferation and differentiation, wound healing, extracellular matrix production, immunosuppression
Distant members	MIS/AMH, Inhibin α GDNF	Mullerian duct regression Inhibition of FSH production and other actions of activin Dopaminergic neuron survival, kidney development

Table I.1. The TGF- β family and their representative activities (adapted from [64]).

TGF- β and related factors use mechanisms to signal to the nucleus based on membrane bound receptors with a cytoplasmic serine/threonine kinase domain [65]. Based on structural and functional properties, the TFG- β receptor family is divided into two subfamilies: type I and type II receptors. Type I receptors have a higher level of sequence similarity than type II, particularly in the kinase domain [64]. The bioactive,

dimeric form of the TGF- β receptor can activate two different signaling pathways: Smad-dependent or Smad-independent (Figure I.11).

Extensive studies in various developmental EMT systems provide convincing evidence that TGF- β signaling is a primary inducer of EMT (some authors even refer to it as “master switch” [66]). The precise signaling pathways activated by individual family members, yet, may differ during various EMT events [12, 67, 68]. There is substantial evidence, although almost entirely *in vitro*, for TGF- β activation of Smad-independent signaling in some aspects of EMT. However, the distinction between Smad-dependent and independent mechanisms can be difficult as there may be significant cross-talk between these pathways with non-Smad proteins modulating Smad activity and vice versa [66]. In some cases, stimulation of several signaling pathways such as Wnt or Notch provides the context for induction and specification of EMT within a particular tissue, with Smads representing the dominant pathway, which is, in some instances, necessary but not sufficient for induction of full EMT [69, 70].

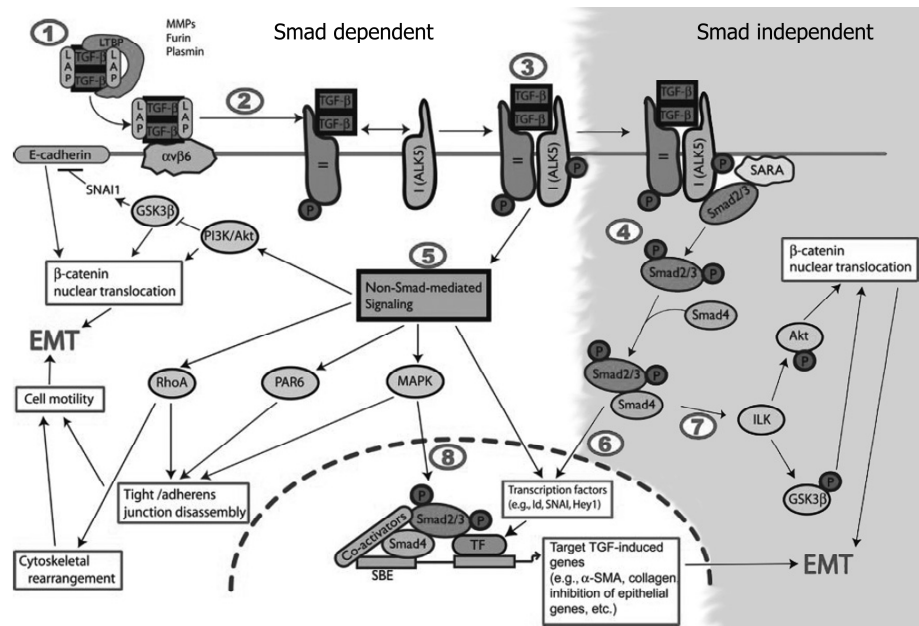


Figure I.11. A schematic diagram of the TGF- β signaling pathway in which mechanisms potentially involved in TGF- β -mediated EMT are included (adapted from [66]). (1) Most of the TGF- β is present in the extracellular matrix, kept inactive by the latency-associated peptide (LAP), and bound by the latent TGF binding protein (LTBP). (2) LAP-associated TGF presented to TGF receptors. (3) TGF- β dimers associate with the type II TGF- β receptor that recruits and phosphorylates type I receptor. The activated receptor initiates a signaling pathway, resulting in both transcriptional and nongenomic signaling. (4, 6) In Smad dependent pathway activated type I receptor phosphorylates receptor associated Smads (Smad2/3), allowing their release from cytoplasmic anchoring proteins such as SARA (Smad anchor for receptor) (continues)

(continues) activation). Phosphorylated Smad2/3 form dimers or trimers with Smad4 and translocate to the nucleus where they can either directly recognize target genes with several copies of the Smad cognate sequence (-CAGAC-) or incorporate additional DNA-binding cofactors that recognize nearby sequences, causing activation of target genes as well as inhibition of epithelial genes throughout. (7) Smad-mediated signaling can also activate nongenomic signaling molecules, such as ILK, which leads to Akt and GSK3 β phosphorylation and β -catenin nuclear translocation, contributing to EMT. (5) Non-Smad-mediated pathways include PI3K/Akt, RhoA, PAR6, and MAPK and lead to cellular changes including tight/adherens junction disassembly, cytoskeletal rearrangements, E-cadherin downregulation, β -catenin nuclear translocation and EMT. (8) Finally, non-Smad-mediated signalling pathways can interact with Smad-mediated genomic signaling through modulation and activation of transcription factors [66, 71].

1.3.2 Wnt/Frizzled

Wnt genes encode a large family (close to 100 Wnt genes have been isolated from different species) of secreted, cysteine-rich proteins that play key roles as intercellular molecules in development as well as in adult tissues [72]. The processes in which Wnt signals are involved are as diverse as segmentation, central nervous system patterning, control of asymmetric cell division, regulation of cell proliferation, differentiation, migration and fate specification among others [72-74]. The transduction of Wnt signals between cells proceeds in a complex series of events including post-translational modification and secretion of Wnts, binding to transmembrane receptors, activation of cytoplasmic effectors and, finally, transcriptional regulation of target genes [72].

Wnt signals can be transduced to two pathways: the canonical, mainly involved in cell determination, and the non-canonical, for control of cell movement and tissue polarity (**Figure I.12**). The canonical Wnt/ β -catenin pathway has a particularly tight link with EMT as β -catenin is an essential component of adherens junctions, providing the link between E-Cadherin and α -catenin and modulating cell-cell adhesion, proliferation and cell migration. In the absence of Wnt signaling, free cytoplasmic β -catenin is complexed with Axin (a scaffolding protein), adenomatous polyposis coli (APC) and GSK3 β among others (β -catenin degradation complex), phosphorylated, and polyubiquitinated by β TRCP1 or β TRCP2 complex for proteasome mediated degradation. However, β -catenin levels are increased and its transcriptional function *via* TCF/LEF enhanced if E-cadherin is degraded or transcriptionally repressed. In fact, several types of cancer are associated with mutations in β -catenin, for the most part resulting in stabilization of cytoplasmic β -catenin and its association with LEF/TCF in the nucleus which suggests an inappropriate Wnt signaling in tumours*. Mutations in

* Information regarding β -catenin and its involvement in tumor progression is detailed in **I.4.5**.

the modulator of β -catenin stability APC, also translated into increased β -catenin activity, are even more frequent in tumours [75, 76]. There is also evidence that Wnt acting through the non-canonical pathway can promote tumour progression, although the mechanism is still unknown [77].

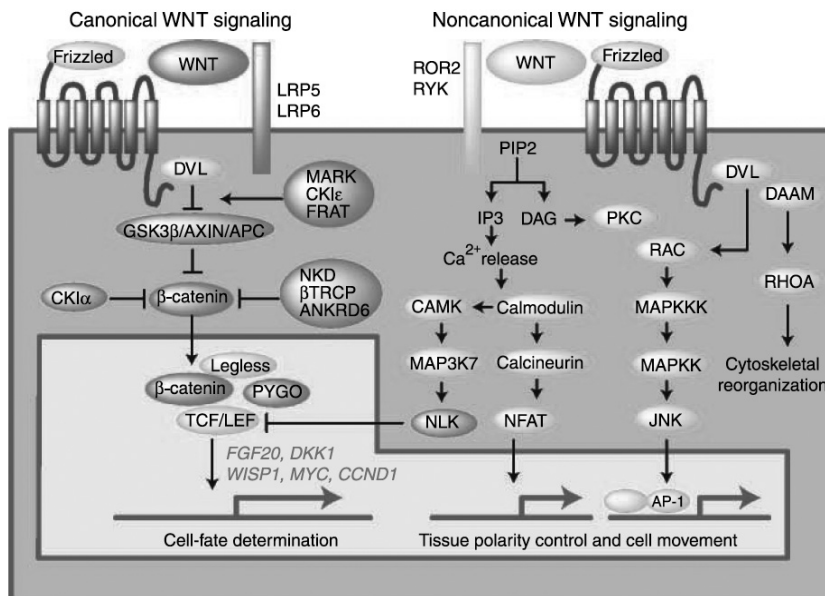


Figure 1.12. Landscape of WNT signaling cascades [78]. Canonical Wnt signals (left) are transduced through the Frizzled (FZD) receptor family, the LRP5/6 coreceptor and Dishevelled (DVL) disrupting the activity of the degradation complex of β -catenin and increasing the cytoplasmic pool of the protein, which can interact with members of the LEF-1/TCF family of transcription factors in the nucleus. The non-canonical pathway (right) is also transduced by Frizzled but ROR2 and RYK are the cofactors responsible for DVL activation [74, 79, 80]. Small G-proteins and c-jun NH₂-terminal kinase are the DVL dependent effectors of this pathway [81, 82]. Wnt signals are context-dependent transduced to both pathways based on the expression profile of Wnt, SFRP, WIF, DKK, Frizzled receptors, coreceptors and the activity of intracellular Wnt signaling regulators [78].

1.3.3 RTKs

One of the first cell surface receptors identified as capable of stimulating epithelial scattering was the Met receptor tyrosine kinase. Upon autophosphorylation of two closely spaced tyrosines in the cytoplasmic domain, Met recruits a vast array of adaptor (Gab1, Cbl...) and effector (PI3K, Src, PLC γ ...) proteins, the overall effect of which is the amplification and transduction of the signal [42].

In addition to Met, several other tyrosine kinase receptors, including Fibroblast Growth Factor (FGF), Insulin-like Growth Factor (IGF), ERBB family, Epidermal Growth Factor (EGF) family members, and more recently PDGF, also play critical roles in

regulating EMT/like morphogenetic events *in vivo* and *in vitro* [28]: FGFR1 is involved in EMT and morphogenesis of mesoderm at the primitive streak; activation of ErbB2-ErbB3 is required for the EMT program during the mouse cardiac valve formation; in mice, ablation of HGF or Met genes results in the complete absence of all muscle groups derived from long-range migrating progenitors [12].

The transduction of signals of several growth factors such as HGF, TGF- α , EGF or FGFs through their RTKs has Ras as central effector. In order to achieve both proliferation and scattering, the constitutive activation of RTKs and their downstream signaling effectors, Mitogen Activated Kinase (MAPK) and phosphoinositide 3-kinase (PI3K) are needed (**Figure I.13**), providing hyperplastic/pre-malignant lesions. In most cases, however, the pre-malignant state does not involve loss of phenotypical epithelial features and cytokines such as TGF- β are needed to induce and maintain EMT in cooperation with activated Ras [6], which is mutated in 30% of human cancers.

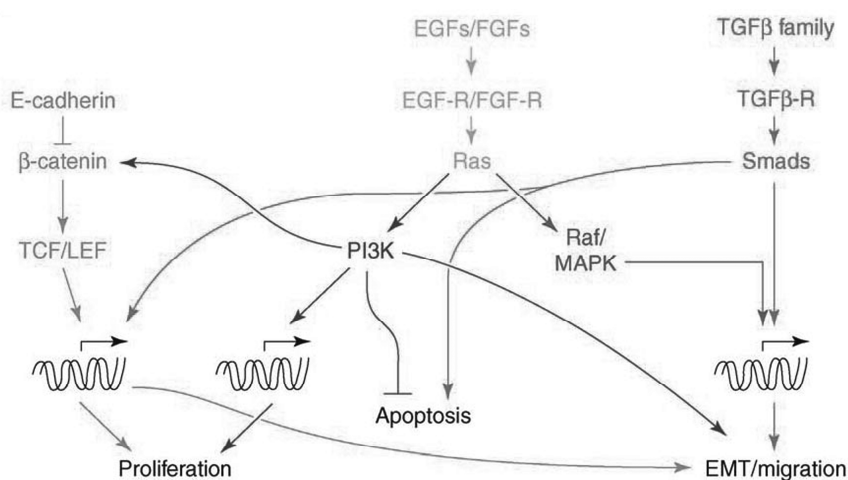


Figure I.13. In most cellular models EMT is induced by cooperation of overexpressed, constitutively active RTKs and TGF- β -R signaling [62]. While EMT is mainly driven by a hyperactive Raf/MAPK pathway plus TGF- β signaling, protection from TGF- β -mediated cell cycle arrest and apoptosis is caused by a hyperactive PI3K pathway. Both downregulation of E-cadherin and PI3K signaling can activate Wnt/ β -catenin signaling, which can also cooperate with TGF- β /Smad signaling to cause dedifferentiation and cell motility.

I.3.4 Delta/Notch

Notch is an ancient cell signaling system involved in the regulation of cell fate specification, stem cell maintenance and initiation of differentiation in embryonic and in postnatal tissues [83]. Both Notch receptors (Notch1-4) and ligands (Delta1, Delta3, Delta4 and Jagged1-2 in mammals) are bound to the plasmatic membrane and

activated by receptor-ligand interaction between two neighboring cells (**Figure I.14**). In the last decade, deregulation of either Notch ligands, receptors, modulators or targets has been described in a growing number of solid tumours and leukemias.

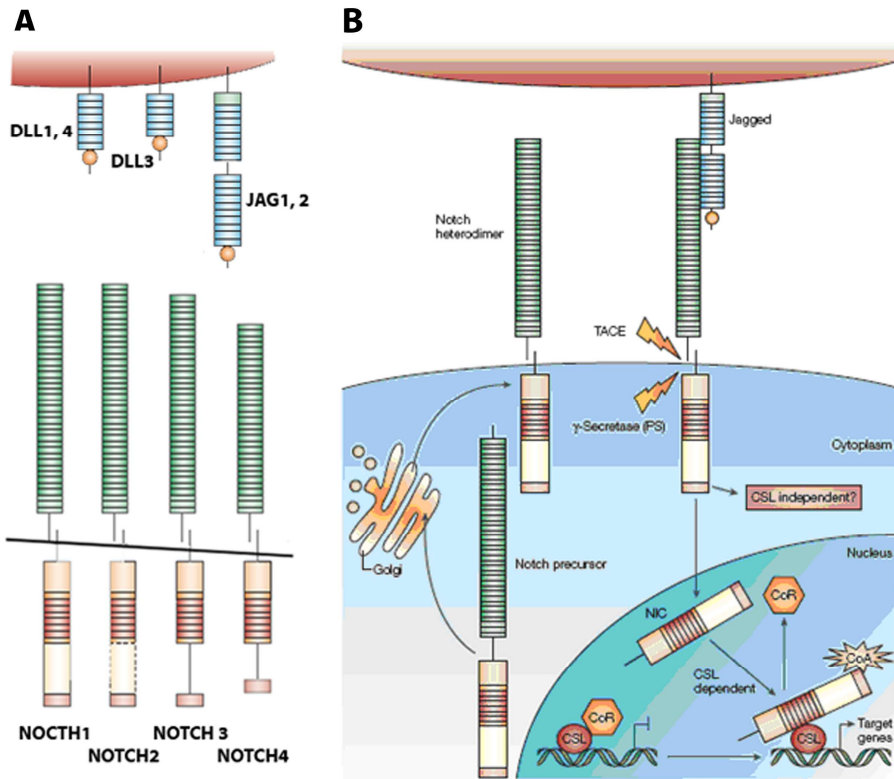


Figure I.14. The Notch pathway (adapted from [84]). **A.** Notch ligands (upper panel) have an amino-terminal structure called DSL followed by EGF-like repeats. Jagged1 and 2 also have a cysteine-rich domain following the EGF-like repeats. Notch proteins (lower panel) are presented as heterodimers. The ectodomain contains epidermal-growth-factor (EGF)-like repeats, a cysteine-rich Notch/Lin12 domain (LN), followed by a transmembrane RAM domain, six ankyrin repeats, two nuclear localization signals (NLS), the transactivation domain and a PEST sequence. NOTCH1 and 2 also contain a transactivation domain in the cytoplasmic part. **B.** Notch proteins are synthesized as precursors that are processed by a furin-like convertase before being transported to the cell surface. Interaction with their ligands leads to a cascade of proteolytic cleavages which liberate the cytoplasmic Notch domain (NIC). NIC enters the nucleus and binds to the transcription factor CSL, which leads to transcriptional activation of downstream target genes. Genetic evidence points to the existence of a CSL-independent pathway, which is poorly characterized at present.

In tumour development Notch has been observed in two different faces; one as a promoter and the other as a suppressor of tumorigenesis. Notch shown face is dependent on the cellular context and the crosstalk with other signal-transduction pathways. Notch itself is not a very efficient oncogene; it needs to cooperate with oncoproteins that can override the G1–S checkpoint in order to cause cancer [84]. As a

tumour suppressor, Notch1 function might be involved in mechanisms concerning cell cycle arrest and differentiation since conditional inactivation of Notch1 has been described to lead to tumour formation in mouse skin [84, 85]. Growing evidence also suggests a fundamental role for Notch in promoting EMT both in development [86-89] and in tumour progression, although Notch may need to cooperate with other signaling pathways in this process. Despite the fact that the expression of components of the Notch pathway are increased in several tumours (such as pancreatic [69], lung, breast, prostate, colorectal, uterus and ovarian cancer [90]), a study of the expression states of Notch pathway elements and potential target genes in metastatic versus non-metastatic tumours has not yet been carried [87].

1.3.5 Hedgehog/Patched

The case of the Hedgehog (Hh)/Patched (Ptc) pathway is another example that the study of signaling pathways in the development of the embryo can lead to important insights into disease programs. The Hh signaling pathway (**Figure I.15**) was first identified in a large *Drosophila* screen for genes that were required for patterning the early embryo [91]. Hh signaling can initiate cell growth, cell division, lineage specification and can also function as a survival factor.

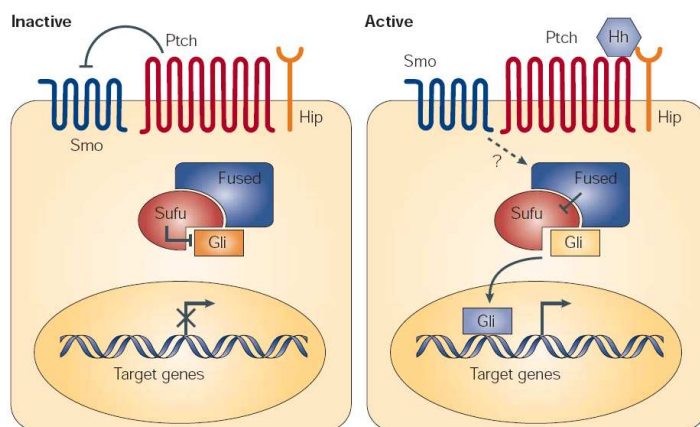
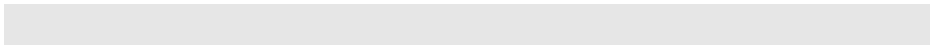


Figure I.15. Hedgehog signaling pathway [91]. In the absence of ligand, the Hh signaling pathway is inactive (left). In this case, the transmembrane protein receptor Patched (Ptc) inhibits the activity of Smoothened (Smo), a seven transmembrane protein. The transcription factor Gli, a downstream component of Hh signaling, is prevented from entering the nucleus through interactions with cytoplasmic proteins, including Fused and Suppressor of Fused (Sufu). As a consequence, transcriptional activation of Hh target genes is repressed. Activation of the pathway (right) is initiated through binding of any of the ligands to Ptc. The Hh ligands (in vertebrates Sonic (Shh), Desert (Dhh) and Indian (Ihh), and Hedgehog in *Drosophila*) are secreted proteins that undergo several post-translational modifications to gain full activity [92]. Ligand binding results in de-repression of Smo, thereby activating a cascade that leads to the translocation of the active form of the transcription factor Gli to the nucleus.

Mutations in the components of the Hh pathway are associated with both embryonic development defects and tumour progression [93]. The ability of the Hh pathway to regulate cell differentiation and renewal makes it essential for numerous processes during organ development and maintenance of organ function, but also means that altered pattern of expression of this pathway can result in uncontrolled cell proliferation. Deregulation of the Hh signaling pathway, however, only seems to cause tumours in a subset of adult cell types, usually arising from populations of adult stem cells that require Hh signaling for their proliferation and maintenance [91]. In the pancreas, for example, Hh signaling components are undetectable in a normal ductal epithelium, but are strongly expressed in pancreatic precursors and invasive lesions [94].

Increased Hh signaling has been linked to tumours in the brain, skin, muscle, lungs, gastrointestinal tract and pancreas [94-96]. Several studies show that specific inhibition of this pathway blocks tumour growth, indicating that active Hh signaling is not only a key contributor to cancer formation, but also to tumour maintenance and survival [94, 96, 97]. Hedgehog signaling activation indirectly leads to EMT through FGF, Notch, TGF- β signaling cascades and miRNA regulatory networks [98].



I.4 KEY MOLECULES IN EMT

I.4.1 E-cadherin

E-cadherin is the prototypic type I cadherin that mediates homophilic intercellular interactions by forming adhesive bonds between one or several immunoglobulin domains in their extracellular region and connecting to actin microfilaments indirectly through α -catenin and β -catenin in the cytoplasm [99-101]. E-cadherin contacts modulate the epithelial phenotype and decrease of its levels has several important consequences that are of direct relevance to EMT to the extent that functional loss of E-cadherin in an epithelial cell has been considered a hallmark of EMT. When E-cadherin levels become limiting, E-cadherin-mediated sequestering of β -catenin in the cytoplasm is abolished, activating transcriptional regulation through LEF/TCFs [102]. Although E-cadherin is considered a repressor of the mesenchymal phenotype and disruption of contacts allows activation of several signaling pathways that induce the molecular and phenotypical changes observed during EMT (MAPK [103], RhoA [104], ILK [105] and NF- κ B [106, 107] among others), loss of E-cadherin is not enough to activate the mesenchymal gene program, indicating that additional signals are required [108].

During tumour progression E-cadherin can be functionally inactivated by different mechanisms including somatic mutation (which, together with previous mutation of one allele, leads to loss of heterozygosity) and downregulation of gene expression through promoter methylation and/or transcriptional repression [109]. The best-studied transcriptional modulation during EMT is that involving the E-cadherin (*CDH1*) gene promoter [12]. Studies carried out on the *CDH1* gene have identified E-box elements (short six-base sequences –CACCTG- or –CAGGTG-) in its promoter (see **Figure I.16**) responsible for its transcriptional repression in non-E-cadherin-expressing mesenchymal cells [110, 111]. These E-box elements are known to be directly bound by several transcription factors downstream of the different pathways promoting EMT previously described (**I.3**). Those transcription factors will be further explained in subsequent sections.

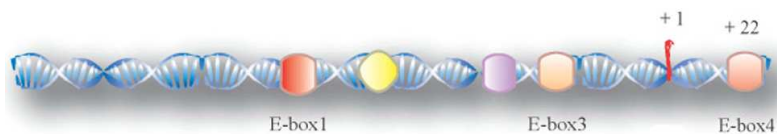


Figure I.16. Schematic representation of the human E-cadherin promoter [109]. The three E-boxes are indicated. E-box2 does not appear because it is not conserved with mouse E-cadherin promoter, organism where E-cadherin promoter was first characterized [112]. E-box3 and E-box4 are also named E-box2 and E-box3 respectively [113].

I.4.2 The snail superfamily of transcription factors

SNAIL genes encode transcription factors of the Zinc finger type. Based on phylogenetic relationships, the snail superfamily can be subdivided into two related but independent groups: the snail and the scratch families. At the same time, the vertebrate snail genes seem to be subdivided into two subfamilies (Figure I.17.A): snail (snail1) and slug (snail2). A third member of the snail family has been described in vertebrates (mouse, human and fish [78, 114, 115]), previously named smuc and recently renamed snail3, which is highly divergent to the other members of the family outside the Zinc finger domain. All members of the snail superfamily share a similar organization, with a quite divergent amino-terminal region and a highly conserved carboxi-terminal region, which contains from four to six Zinc fingers. Zn fingers are of the C₂H₂ type [116] and function as sequence-specific DNA binding motifs [117].

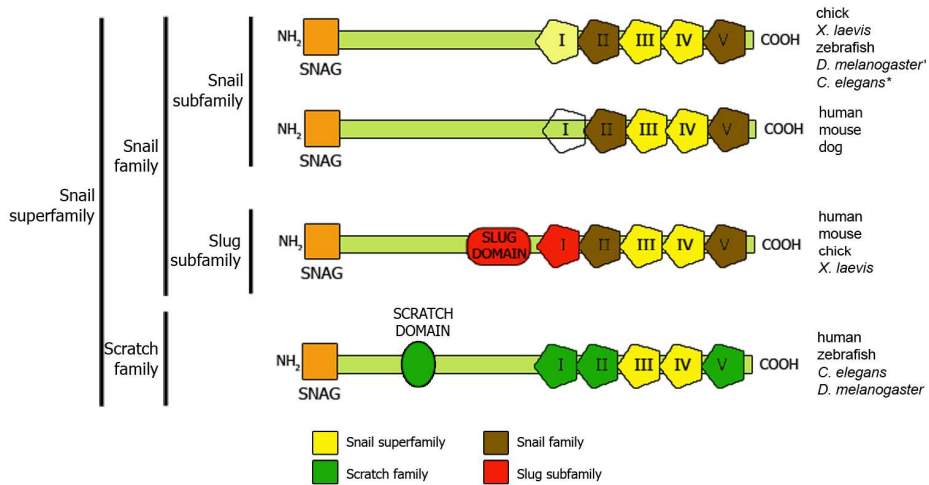


Figure I.17. The snail superfamily of transcription factors (adapted from [118]). Specific domains found in the snail superfamily (dark yellow), the scratch (green) and snail (brown) families, and the slug subfamily (red). The third and fourth zinc fingers are conserved in all proteins while the SNAG (Sna/Gfi) domain is conserved in all vertebrate members (*in *D.melanogaster* and *C.elegans* there is a CtBP interacting domain in its place). The second and fifth Zinc fingers constitute shared motifs for either the snail or the scratch families. Diagnostic domains of the scratch family are the scratch domain and the first finger. The presence of a slug domain and the first zinc finger are characteristic of the slug subfamily. Mammal snail1 protein has lost the first Zinc finger.

The snail and scratch families have been described to have originated after the duplication of an ancestral gene between 1000–500 million years ago. Subsequent independent duplications in protostomes and deuterostomes seem to have led to the present situation [118]. Snail genes are expressed in all EMT processes in which they have been studied independently of the signaling pathway that originates the

transition [119]. **Figure 1.18** shows a summary of different cellular contexts that promote EMT and snail family gene expression.

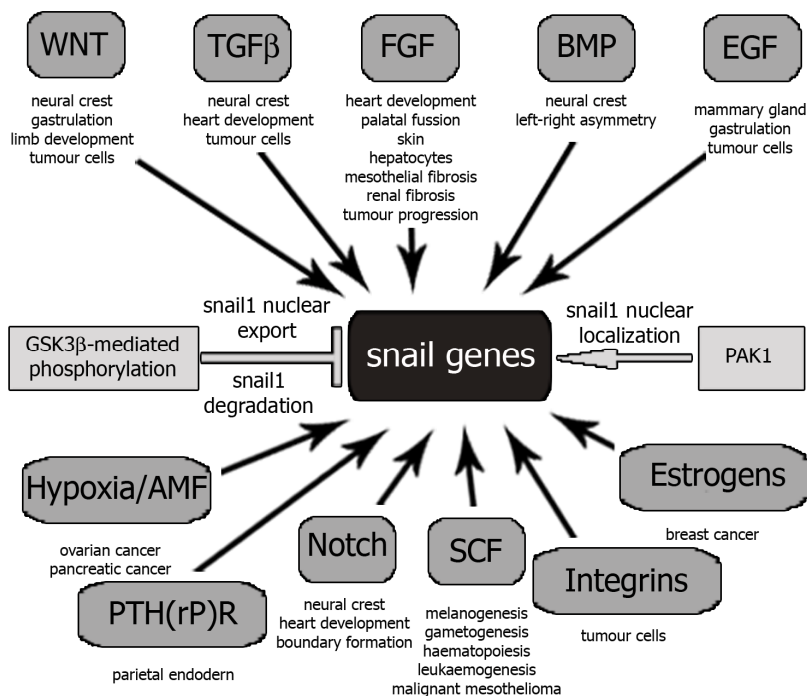


Figure 1.18. Snail genes are a convergence point in EMT induction (adapted from [119]). Below each extracellular signal are the tissues and processes in which they have been studied. In addition to being tightly regulated at the transcriptional level, snail activity is also regulated by its subcellular localization, which is governed by at least two kinases: GSK3β [120] and PAK1 [121]. AMF, autocrine motility factor; EGF, epidermal growth factor; FGF, fibroblast growth factor; PAK1, p21-activated kinase; PTH(rP)R, parathyroid hormone related peptide receptor; SCF, stem cell factor.

1.4.2.1 Snail1

Snail1 is the most well-characterized homolog of the family. Snail1 is sufficient to induce EMTs in tissue culture, thus, transfection of snail1 into epithelial cell lines is associated with downregulation of E-cadherin expression and EMT [113, 122]. In the same sense, forced EMT in cultured cells correlates with induction of the snail1 transcriptional factor [123-125]. Studies in *Drosophila* show that snail mutant embryos display a gastrulation-defective phenotype that has been associated with impaired downregulation of E-cadherin and imperfect EMT [126]. In chick, embryos treated with antisense oligonucleotides directed against snail2, the functional homologue of snail1 in chick development [127], show improper mesoderm formation related to defects in cell migration at EMT compartments [128].

Snail1 is a 264 residue protein composed of two well differentiated domains (Figure I.19) that interact with each other: the amino-terminal (residues 1-151) and the carboxi-terminal (151-264). Two important features have been described in the amino region: the SNAG (Sna/Gfi) subdomain, required for repression [113], and a serine rich sequence which has been described to contain two phosphorylation motifs. GSK3 β binds to and phosphorylates snail1 at these two consensus motifs to dually regulate the function of this protein. Phosphorylation of the first motif regulates its β Trcp-mediated ubiquitination (what connects snail1 with the WNT pathway I.3.2), and phosphorylation of the second motif controls its subcellular localization [129, 130]. Oxidation of the protein in residues K98 and K137 by lysyl oxidase-like 2 enzyme (LOXL2) has been described to be required for the function and stability of the protein [131], which would mask GSK3 β phosphorylation motifs [132]. The carboxi-terminal part of the protein is not only responsible for DNA binding through its four Zinc fingers, but can also be phosphorylated by PAK1 kinase, which retains the protein in the nucleus [121].

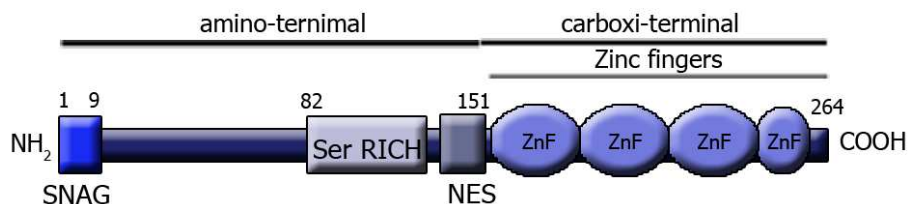


Figure I.19. Schematic representation of snail1 in mammals (adapted from [130]). Amino-terminal region comprises residues 1-151 and contains a SNAG domain, needed for repression [113], a serine rich domain, involved in protein regulation and localization [120, 130], and a nuclear export signal [130]. The carboxi-terminal region contains four Zinc fingers, the last of which does not match the C₂H₂ consensus and has been demonstrated to be involved in protein folding [130].

E-boxes of the type E2 (-CACCTG-), identical to those found in the *CDH1* promoter, have been described to be the specific DNA binding motif for snail1 [117]. The same box can be bound by transcription factors of the basic helix-loop-helix family (bHLH, see I.4.3), thus competing with the snail family of transcription factors for binding [114]. Several studies have demonstrated that snail1 blocks the expression of E-cadherin by binding to the E-boxes in its promoter [113, 122]. Furthermore, recent studies show that snail1 overexpression correlates with deacetylation of histones 3 and 4 (H3/4). The same study also describes that snail1 interacts with histone deacetylase 1 and 2 (HDAC1/2) through the Sin3A corepressor [133], a step probably required for a further recruitment of the polycomb repressive complex 2 (PRC2) to the promoter by snail1 and posterior trimethylation of lysine 27 on H3 [134].

As a general rule, E-cadherin and snail1 expression are opposite in cancerous cell lines [113, 122, 135, 136]; when snail1 is eliminated, levels of expression of E-cadherin are partially recovered and the mesenchymal phenotype is reversed to a more epithelial one in most cell lines [113, 137]. Snail1 repression, however, does not exclusively affect E-cadherin transcription but also other epithelium-specific genes such as Muc1, Vitamin D receptor, cytokeratin 18, occludin, desmoplakin, claudins and others [113, 122, 138-140]. In fact, knockout mouse embryos for snail1 die at gastrulation due to their incapability to undergo a complete EMT. They display a mesoderm formed though cells still express epithelial markers and exhibit epithelial morphology [141].

Although the snail1 repression mechanism is quite well described and snail family members are known to induce the expression of genes characteristic of mesenchymal cells, nothing has been described so far about the activation mechanism of snail1. Genes activated by snail1 are diverse and include extracellular matrix proteins like fibronectin [122, 138], matrix metalloproteases (MMPs) [136] and cytoskeleton proteins such as vimentin [122] that together with regulatory proteins like RhoB [142] and COX-2 [143] or transcription factors like LEF-1 [138] or ZEB1 [138] force changes in cell shape and gain of motility and invasive properties. Snail1 is also involved in the survival context, downregulating caspases and p53, among others [144-148], and increasing the activity of PI3K and ERK [147] (see **Figure I.20** for details).

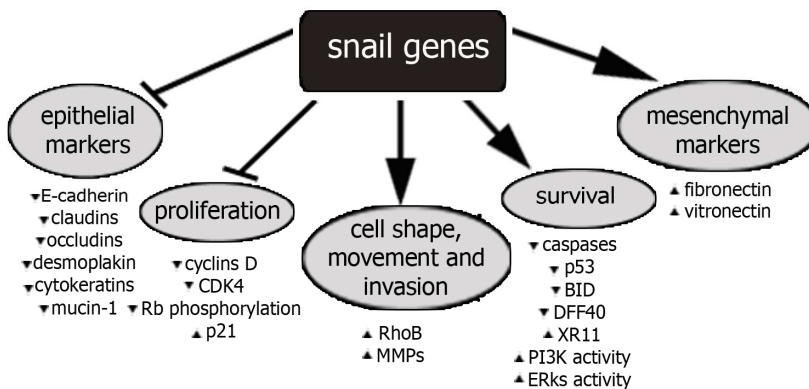


Figure I.20. Downstream targets of snail genes (adapted from [119]). Snail gene expression induces the loss of epithelial markers and the gain of mesenchymal markers, as well as inducing changes in cell shape and morphology and the acquisition of motility and invasive properties. The snail genes also regulate cell proliferation and cell death. BID, Bcl-interacting death agonist; CDK, cyclin-dependent kinase; DFF, DNA fragmentation factor; ERKs, extracellular signal regulated kinases; MMPs, metalloproteinases; PI3K, phosphoinositide 3-kinase; p21, cyclin-dependent kinase inhibitor; p53, tumour suppressor; Rb, retinoblastoma; XR11, *Xenopus* Bcl-xL homolog.

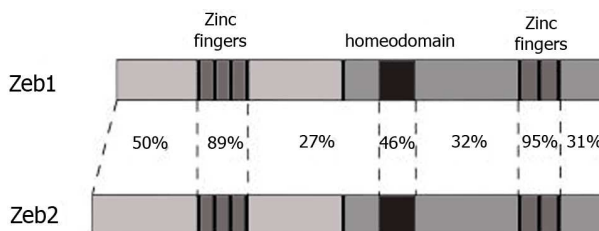
1.4.2.2 *Snail2* (formerly *Slug*)

As member of the snail family, *snail2* is also involved in EMT in vertebrates [149]. Both *snail1* and *snail2* are present in all vertebrate species, though *snail1* carries out the function developed by *snail2* in amphibian and avian [118, 150]: while *snail2* is induced during chick gastrulation and *Xenopus* neural crest formation, *snail1* is expressed in the mouse primitive streak and neural crest precursors [122]. Studies performed in cultured cells also show repression of E-cadherin [151], downregulation of claudins and occludins [144], disruption of desmosomes, cytokeratin rearrangement [152] and resistance to programmed cell death [153] upon *snail2* forced expression.

1.4.3 The *ZFH* family of transcription factors

Members of the *ZFH* family were first identified in *Drosophila* [154, 155] and consist of two groups of Zinc fingers of the C₂H₂ and C₃H type at amino and carboxi regions and an internal homeodomain. While the homeodomain seems to be involved in protein interaction [156, 157], ZEB factors interact with DNA through the simultaneous binding of the two zinc-finger domains to high-affinity binding sites composed of two E-box sequences (although the finger located in the carboxi region (CTZF) has been described to better bind DNA [156]). The ZEB family of transcription factors contains two members (*zeb1*/TCF8/ δ EF1/*zfh-1* and *zeb2*/ZFXH1B/*Sip1*/*zfh-2*) encoded by independent genes (*ZFHX1A* and *ZFHX1B*, respectively, see **Figure I.21**).

ZEB factors are expressed during development in the central nervous system, heart, skeletal muscle and haematopoietic cells. In these tissues, a functional deficiency in one of these factors can be partially compensated by the other, indicative of a common role for both factors [158]. However, the *ZEB2* knockout mouse is embryonic lethal with specific defects in neural crest migration that cannot be compensated by *ZEB1* [159]. Major differences are found in the expression pattern of both factors in lymphocytes, with a predominant expression of *ZEB1* in the thymus during T-lymphocyte development and of *ZEB2* in spleen B cells [158].



Snail1 induces the expression of the zeb1 transcriptional factor [138, 160], which also binds to E-cadherin promoter E-boxes [161, 162]. High levels of zeb1 are detected in cells with a mesenchymal phenotype and are also observed after snail1-induced EMT. On the basis of these data, and the sustained expression of zeb1 after snail1 down-regulation, it has been suggested that zeb1 might work by extending the repression of E-cadherin initiated by snail1 [138]. Overexpression of zeb2 also induces E-cadherin down-regulation and EMT [163, 164]. However, zeb2 transcripts are not generally increased after EMT and do not always correlate with the mesenchymal phenotype [123, 138]. In an article recently published by our group, we demonstrate that zeb2 protein is up-regulated in response to snail1 expression. However, unlike zeb1, the effect of snail1 on zeb2 expression depends on alternative processing of zeb2 mRNA rather than on increased mRNA levels [165].

1.4.4 Basic helix-loop-helix (bHLH) family of transcription factors

The basic common structure for all helix loop helix (HLH) family members involves two parallel amphipathic α -helices joined by a loop required for dimerization. This structure can be found alone or accompanied by a basic domain. Additional regulatory domains can be found in some family members, such as a leucine zipper domain (MYC) or a PAS domain (bHLH-PAS). bHLH proteins bind to DNA using a consensus E-box site (-CANNTG-) as homo- or heterodimers [166]. In some cases, bHLH proteins can act as transcriptional inducers or repressors by the recruitment of histone acetyl transferase (HAT) proteins (such as p300 or the SAGA complex), or corepressors (such as groucho or Sin3A [167]).

The HLH family members have been classified into seven families according to their tissue distribution, dimerization capacities and DNA-binding specificities (**Figure 1.22**). With regards to epithelial-mesenchymal transition (EMT), the most representative members belong to class I, II and V. Class I HLH proteins, also known as E-proteins, are encoded by *TCF3/E2A* (E12 and E47 isoforms, generated by alternative splicing [168]), *TCF4* (E2-2A and E2-2B isoforms) and *TCF12* (α/β isoforms). They are widely expressed and act as homodimers or heterodimers with class II proteins [167, 169-171]. Class II factors are tissue-specific bHLH proteins that always act as heterodimers with class I factors, among which *TWIST1* and *TWIST2* can be found. Class

Figure 1.21. Schematic representation of the ZFH family members (adapted from [158]). Shown is the scheme of the structure of human *ZEB-1* and *ZEB-2* genes. Percentage indicates identity at the amino acid level.

V HLHs, known as Id (Inhibitor of differentiation) proteins (Id1–4), lack the basic domain and so act as class I and class II dominant-negative factors because of their high heterodimerization affinity with class I bHLHs. bHLH heterodimers are involved in cell lineage determination and the control of cell proliferation, whereas Id proteins are key regulators of a wide range of developmental and cellular processes, including cell-cycle regulation, proliferation and angiogenesis [167, 172-174].

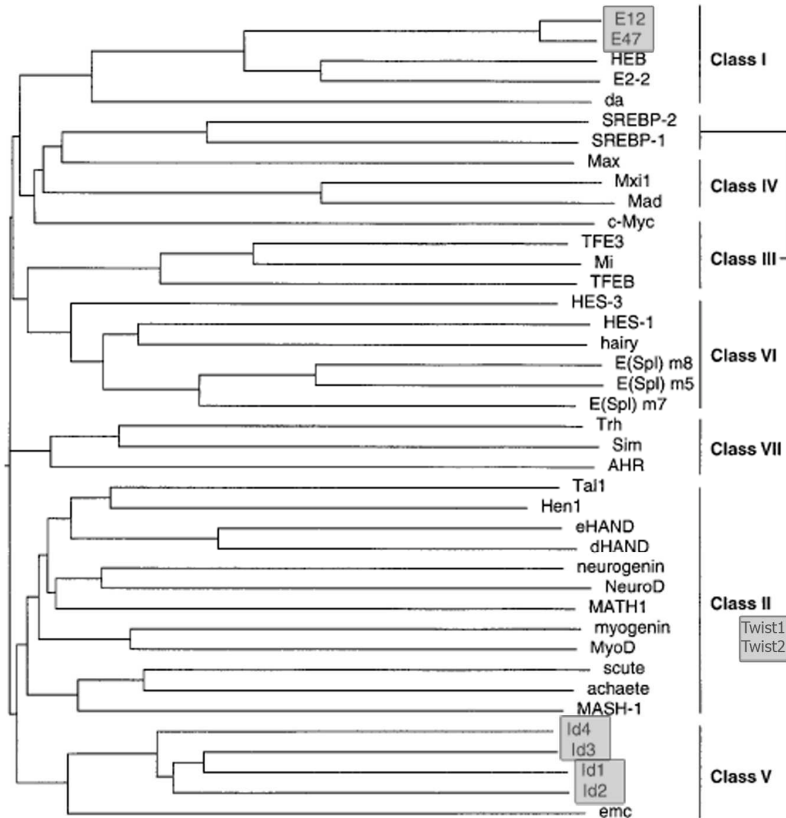


Figure 1.22. Multiple sequence alignment and classification of some representative members of the HLH family of transcription factors (adapted from [167]). Shown is a dendrogram created by aligning the sequences of the indicated HLH proteins by the Clustal W algorithm [175]. Note that twist1 and twist2 are not included in the alignment and are added next to the name of the group to which they belong.

1.4.4.1 E2A gene products

While the majority of studies regarding *E2A* gene products focus on their central role in lymphoid cell differentiation, a number of studies in recent years have suggested that *E2A* gene products may be of relevance in EMT [176]. Exposure of epithelial cells to TGF-β resulted in upregulation of *E2A* gene products and a

concomitant downregulation of Id proteins [177]. Ectopic expression of E47 in the absence of any other stimulus in MDCK cells (Madin-Darby canine kidney epithelial) caused EMT by direct involvement of the E-boxes present in the *CDH1* promoter [178], an effect also demonstrated in HK-2 cells (human proximal tubular epithelial) [179]. Overexpression of the *E2A* gene products was sufficient to significantly reduce E-cadherin expression and induce α -SMA (α -smooth muscle actin) expression in HK-2 cells [179].

1.4.4.2 Twist

The class II HLH protein twist was originally identified as a factor required for proper gastrulation and mesoderm formation in *Drosophila melanogaster* [180]. A number of reports have demonstrated that twist has the ability to inhibit the differentiation of multiple cell types, including muscle and neurons [167]. Ectopic expression of twist results in loss of E-cadherin-mediated cell-cell adhesion, activation of mesenchymal markers, and induction of cell motility, suggesting that twist contributes to metastasis by promoting EMT [181]. Activation of mesenchymal markers, contrarily to what has been described for snail family members, appears to be independent of E-cadherin expression, since ectopic expression of E-cadherin could not revert the EMT phenotype in twist-expressing cells [181].

1.4.4.3 Id proteins

The *Id1* to *Id4* gene products are closely related in their HLH regions and show similar affinities for the various E-proteins, though they differ in their expression patterns [167]. Ids serve as downstream targets of known oncogenic pathways. However, the characterization of Id expression in human tumours and mouse models of cancer requires more careful analysis. Ids can contribute to tumorigenesis by inhibiting cell differentiation, stimulating proliferation and facilitating tumour neoangiogenesis. Id overexpression might mimic the activity of other oncogenes or the loss of tumour suppressor activity. [172].

1.4.5 β -catenin

β -catenin is a modular protein first discovered as a link between cadherins and the cytoskeleton [182] (**Figure 1.23.A**), though later it was described to be an effector of the Wnt signaling pathway [183-186]. It belongs to the *Armadillo* superfamily [187] and is composed by a central armadillo region formed by twelve repetitive motifs that conform a rigid scaffold [188] and two flexible tails, one at the amino-terminal region

and another at the carboxi-terminal region [189]. The amino-terminal domain harbours the binding site for α -catenin [190] as well as GSK3 β [184], while the carboxi-terminal, consequently named *transactivation domain*, interacts with transcription factors (TBP [191], SOX [192, 193], SMAD4 [194]). The armadillo domain binds other partners as cadherins, or members of the TCF/LEF family of transcription factors in overlapping sites [189], though the amino and carboxi tails have been described to interact with the armadillo region to prevent such binding [195-197] (see **Figure I.23.B**).

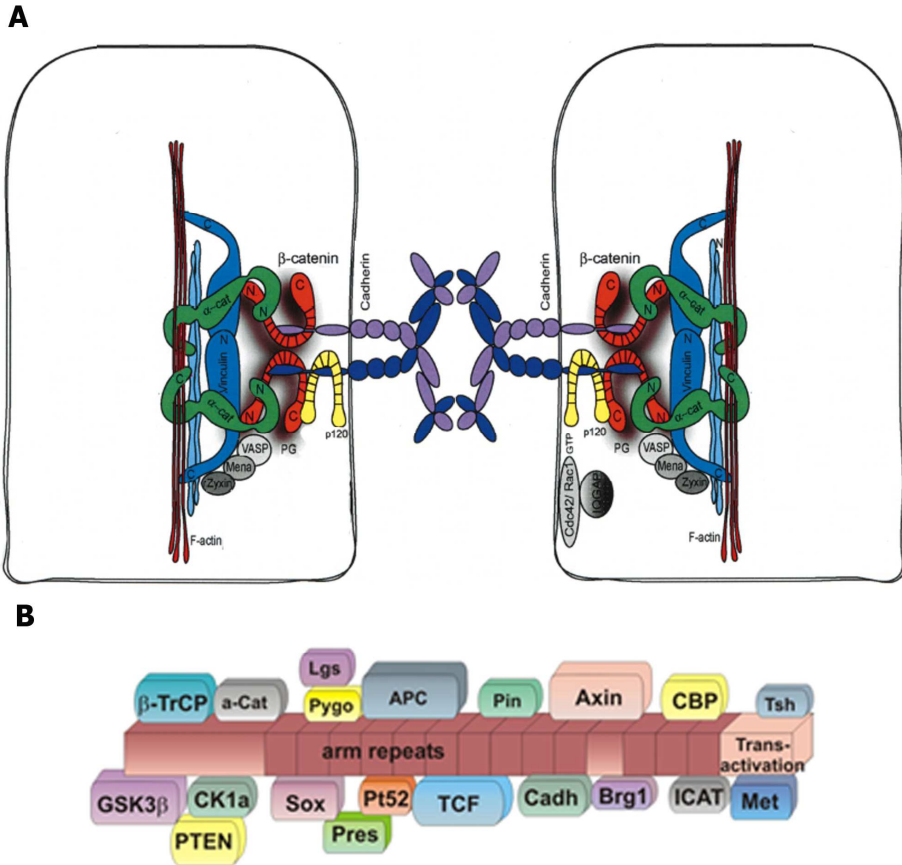


Figure I.23. β -catenin is a protein that interacts with a wide variety of factors. A. Simplified model of an adherens junction which highlights some of the main protein–protein interactions found in this structure. p120ctn, adherens junction protein p120; VASP, vasodilator-stimulated phosphoprotein (adapted from [198]). **B.** Approximate regions of binding in β -catenin (adapted from [199]).

As mentioned in **I.3.2**, β -catenin levels are tightly controlled by a regulated degradation pathway. β -catenin can act as a coactivator of DNA-binding transcription factors such as LEF/TCFs or SOX and activate a variety of target genes (**Table I.2**). In fact,

β -catenin relocalization (from the membrane to the nucleus) is a characteristic of EMT [200, 201] and several signals described to induce such transition cause nuclear β -catenin import [202-204].

Gene	Function	Up/downregulated	Organism/system
c-Myc	proliferation	up	human colon cancer [205]
TCF1	differentiation	up	human colon cancer [206]
c-jun	proliferation/ differentiation	up	human colon cancer [207]
VEGF	proliferation	up	human colon cancer [208]
SOX9	proliferation/ differentiation	up down	intestine [209] mesenchyme [210-212]
BMP4	differentiation	up	human colon cancer [213]
Axina-2	feedback β -catenin/snail1	up	human colon cancer [214-216]
EphB/ephrinB	cell-cell interactions	up/down	human colon cancer [217]
LEF1	differentiation	up	human colon cancer [218, 219]
MMP-7	tissue remodeling	up	human colon cancer [220, 221]
Snail1	EMT	up	ES/EB [222]
Fibronectin	cell adhesion and migration	up	ES/EB [222] xenopus [223]
Id2	negatively regulates cell differentiation	up	human colon cancer [224, 225]

Table I.II. List of some target genes of Wnt/ β -catenin signaling (adapted from [226]).

Based on studies in different tissues, a correlation has been established between β -catenin expression and stemness [227]. A good example are the studies showing that intestinal crypts are monoclonal due to the fact that each crypt is derived from its own intestinal stem cells (ISC, [228-231]). Cells undergoing mutation either in APC or β -catenin become independent of the physiological signals controlling β -catenin/TCF activity and so they continue to behave as crypt progenitor cells (or stationary cancer stem cells) in the surface epithelium, giving rise to aberrant crypt foci (ACFs, [227]). Activation of the EMT program in tumoral cells might have a higher β -catenin activation threshold that can be overcome either by further mutations (genetic progression) or unusual signals from the environment at the invasive front (dynamic progression), resulting in migrating cancer stem cells. Such changes can lead to higher levels of nuclear β -catenin [51], consistent with the observation of β -catenin nuclear

accumulation in dedifferentiated tumour cells at the invasive front and scattered in the adjacent stromal compartment [232, 233]. **Figure 1.24** depicts all the mentioned situations.

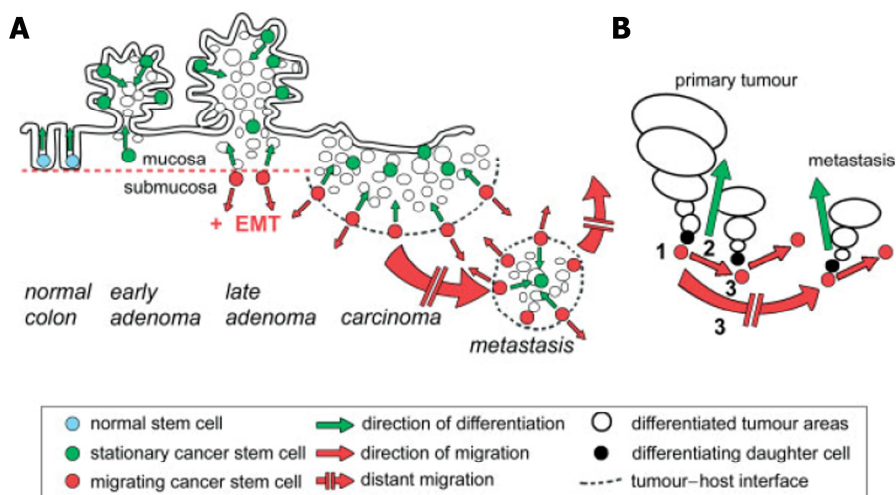


Figure 1.24. The migrating cancer stem (MCS) cell concept [234]. **A.** Normal stem cells (expressing nuclear β -catenin) are located at the crypt base of normal colon mucosa. Stationary cancer stem (SCS) cells are embedded in benign adenomas and might still be detectable in differentiated central areas of carcinomas and metastases. A crucial step towards malignancy is the induction of an EMT in tumour cells, including SCS cells, which now become mobile, migrating cancer stem cells (MCS) cells. **B.** Detailed view on MCS cells in carcinomas and metastases. (1) MCS cells divide asymmetrically; one daughter cell starts proliferation and differentiation. (2) The remaining MCS cell either migrates a short distance before new asymmetrical division, thereby adding mass to the primary tumour (3), or eventually starts long-range dissemination through the blood or lymphatic vessels.

β -catenin altered expression has also been associated with carcinoma of the uterine endometrium [235], tumorigenesis of the mammary gland [236] and prostate cancer [237] among others. In fact, the dynamic changes in the non-random distribution of β -catenin and EMT of tumour cells at the invasive front can be, at least partially, explained by interactions with tumour environment. A micro-ecosystem exists at the invasive front of tumours where the stromal cells interact with parenchymal cells by producing extracellular matrix and secreting cytokines that can promote cell invasion [77].

1.4.6 Nuclear Factor-kappa B (NF- κ B)

The NF- κ B proteins are a small group of closely related transcription factors, which in mammals consists of five members: Rel (also known as c-Rel), RelA (also known as

p65 and NF- κ B3), RelB, NF- κ B1 (also known as p50) and NF- κ B2 (also known as p52) [238]. All five proteins have a Rel homology domain (RHD), which serves for dimerization, DNA binding and principal regulatory domain. RHD contains a nuclear-localization sequence (NLS), which is rendered inactive through binding of specific NF- κ B inhibitors, known as the I κ B proteins, and mediates retention of the proteins in the cytoplasm [239]. p50 and p52 are initially translated as larger precursors, p105 and p100 respectively, which are fused through its C terminus to an auto-inhibitory I κ B-like domain, already dimerizing with the different Rel proteins and trapping them in the cytoplasm. Usually, p105 undergoes constitutive (non-regulated) processing to p50, causing the release of dimers containing the p50 subunit, which translocate to the nucleus unless met by another I κ B protein [238]. p100, found in the cytoplasm mostly dimerized with RelB, is subjected to regulated, signal-dependent processing that results in the preferential release of p52–RelB dimers [240] (see **Figure I.25**).

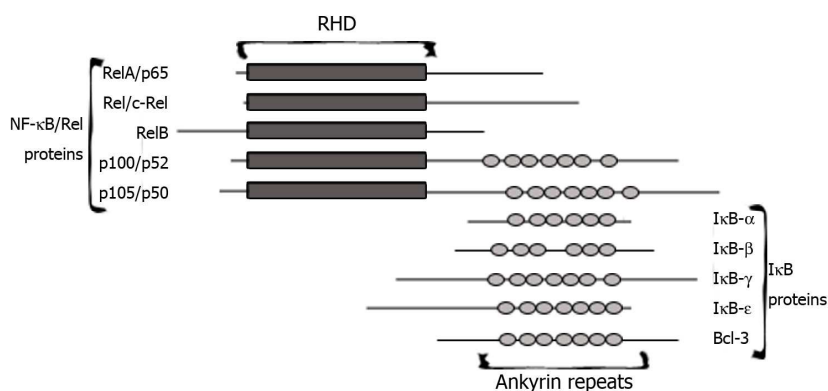


Figure I.25. Schematic structure of NF- κ B and I κ B proteins (adapted from [238]). The NF- κ B proteins are related to each other by the presence of the Rel homology domain (RHD) whereas I κ B proteins share six to seven ankyrin repeats (AR). The ARs of the inhibitors dock onto the RHDs of the NF- κ B proteins and cause their cytoplasmic retention. In the case of the p105 and p100 precursors, these interactions can occur intramolecularly or with the RHD of the partner to which the precursor is bound to.

As a general activation mechanism, I κ B is phosphorylated by I κ B kinases (IKKs), subsequently ubiquitinated, and then degraded by a proteasome complex. Degradation of I κ B leads to the release of NF- κ B and translocation into the nucleus, where it binds to the promoter region of various genes, including cytokines such as tumour necrosis factor- α (TNF- α) [241], or interleukin 1 β (IL-1 β) [242], COX-2 [243], inducible NO-synthase (iNOS) [244] and matrix metalloproteinases (MMPs) [245-248], thereby activating their transcription [249]. The activation of NF- κ B can be induced by various pathways (**Figure I.26**). The classical, canonical pathway is induced by TNF- α

[241, 250-252] and IL-1 β [253] and is crucial for the activation of innate immunity and inflammation as well as inhibition of apoptosis. An alternative noncanonical pathway, involved in B-cell activation, lymphoid organogenesis, and humoral immunity, is activated by different stimuli that finally activate p100/RelB [254-256]. Other NF- κ B pathways are induced by DNA damage [257] or by phorbol 12-myristate 13-acetate (PMA) [258, 259], lipopolysaccharide (LPS) [247] and cytokines, although the mechanism of this last pathway is not fully understood.

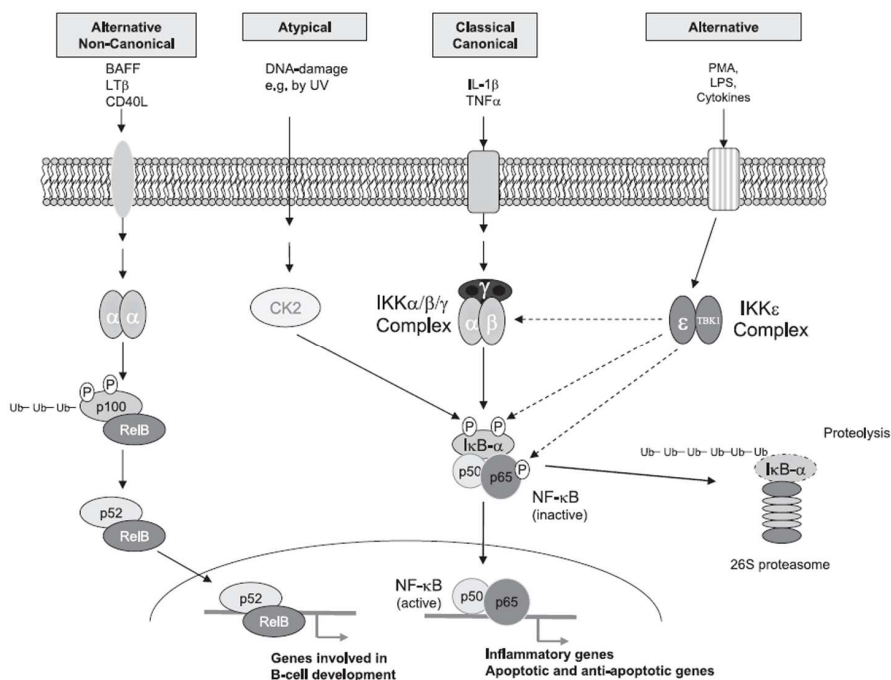


Figure I.26. Schematic overview of different NF- κ B activation pathways [249]. The noncanonical pathway is activated by binding of the CD40 ligand [255], B-cell activating factor (BAFF) [254], or lymphotoxin β (LT β) [256] to their respective receptors, leading to activation of IKK α , which induces the processing of p100 releasing p52, which can translocate as a heterodimer with RelB into the nucleus and bind to the promoter of genes frequently involved in B-cell development. The atypical pathway, which is triggered by DNA damage activates casein kinase 2 (CK2) and leads to phosphorylation and subsequent I κ B α degradation *via* an IKK-independent pathway [260]. The classical canonical NF- κ B activating pathway can be induced by inflammatory stimuli [241, 253] and is crucially dependent upon activation of the classical IKK α,β,γ complex, which leads to the phosphorylation, ubiquitination (Ub, ubiquitin) and degradation of I κ B α *via* the proteasome. The heterodimer p50-p65 is then released and migrates to the nucleus, where it binds to specific κ B sites and activates a variety of NF- κ B target genes. A novel alternative pathway is represented by an IKK complex consisting of IKK ϵ /IKK ι and most likely the TANK-binding kinase 1 (TBK1). This complex is activated by different stimuli, such as phorbol esters (PMA) or LPS, and may lead to phosphorylation of several targets in the NF- κ B activation pathway leading to NF- κ B activation [261, 262]. However, this activation pathway is not yet fully elucidated, which is indicated by the dashed arrows.

Although NF- κ B target genes have been most intensely studied for their involvement in immunity and inflammation, this transcription factor also regulates cell proliferation and migration, apoptosis, angiogenesis and EMT (see **Figure I.27** for targets details). Therefore, it is not surprising that NF- κ B has been shown to be constitutively activated in several types of cancers. Recent evidence (basically on EMT and evasion of apoptosis) has accumulated from a large variety of human malignancies indicating a role for NF- κ B in promoting oncogenic conversion and in facilitating later stage tumour properties such as metastasis [263-268]. All this information suggests that NF- κ B can function as a link between inflammation and cancer. Supporting this hypothesis, cancer can be defined as “a wound that never heals”, what that states the everyday clearer link between cancer and inflammation [269].

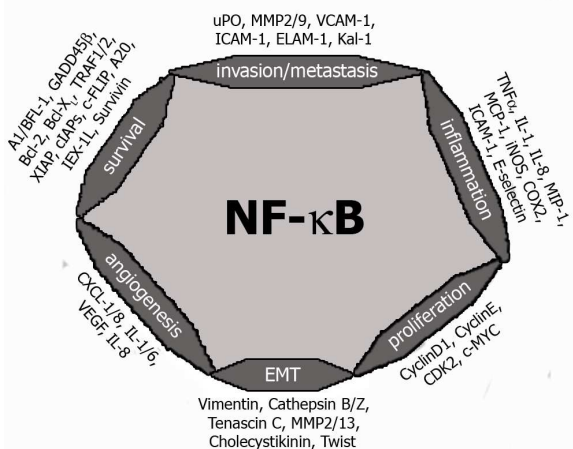


Figure I.27. Representation of NF- κ B-dependent targets involved in different aspects of oncogenesis (adapted from [263]).

Multiple lines of evidence exist indicating that factors involved in EMT are regulated either directly or indirectly by NF- κ B [267]. A very clear example is twist, whose homolog in *Drosophila* is already a direct transcriptional target of the NF- κ B protein Dorsal [270]. Several observations support an important role for NF- κ B in regulation of *SNAIL1* gene transcription as well: (1) GSK3 β inhibition stimulates the transcription of the human gene encoding snail1 via NF- κ B signaling [271], (2) a region is localized in the human *SNAIL1* promoter for stimulation of snail1 expression by ectopic co-expression of NF- κ B p65 [123] and (3) NF- κ B was identified as the upstream regulator of snail1 expression during EMT of human mammary epithelial MCF10A cells

overexpressing a constitutively active Type I insulin-like growth factor receptor (IGF-IR) [272]. To study sustaining NF- κ B mediated regulation of *snail1* transcription, demonstrates that the induction of *snail1* mRNA levels during EMT can be reversed by inhibition of NF- κ B signaling [267].

NF- κ B activation has also been associated with the induction of *ZEB1* and *ZEB2* expression in MCF-10A cells, which, when stably expressing the NF- κ B subunit p65, displayed elevated levels of expression of *ZEB1* and *ZEB2* compared to the parental MCF-10A line. Moreover, in transient transfection assays, p65 increased *ZEB1* promoter activity. Induction of *ZEB1* and *ZEB2* by NF- κ B was also observed following treatment of MCF-10A cells with IL-1 α or TNF- α [265]. Thus, *ZEB1* and *ZEB2* may serve as key mediators of p65 NF- κ B signaling during EMT.

Recent studies also link NF- κ B to β -catenin, which may interact with p50/p65 in an indirect manner independently of I κ B- α . Although the interaction does not involve changes in the protein level, β -catenin binding disrupts the ability of NF- κ B to bind DNA [273]. Moreover, two different approaches point at GSK3 β as key regulator of NF- κ B transcriptional activity [274], and one of them also indicates APC and β -catenin involvement in the process [129]. Further evidence of the relationship between NF- κ B and β -catenin is provided by the observation that IKK α increases β -catenin-dependent transcriptional activity while IKK β decreases it. More interestingly, IKK α and IKK β have been described to interact with and phosphorylate β -catenin using both *in vitro* and *in vivo* assays, suggesting that differential interactions of β -catenin with IKK α and IKK β may in part be responsible for regulating β -catenin protein levels and cellular localization and integrating signaling events between the NF- κ B and Wnt pathways [275].

OBJECTIVES

The general objective of this thesis was to describe new molecular regulatory mechanisms by which snail1 transcription factor sustains mesenchymal phenotype. To that aim we focused on:

- i) The characterization of the mechanism by which snail1 induces transcriptional activation of *FN1* and *LEF1*: DNA binding, recruitment of other factors, comparison with the repression mechanism
- ii) The study of how other transcription factors are involved in such activation and their relationship with E-cadherin expression and repression
- iii) The delimitation of sequences in the promoters required for snail1-induced transcriptional activation

RESULTS

R.1 SNAIL1 ACTIVATES TRANSCRIPTION OF MESENCHYMAL GENES THROUGH AN UNDESCRIBED INDIRECT MECHANISM INDEPENDENT OF E-BOXES

R.1.1 Snail1 increases the mRNA and protein levels of mesenchymal markers in EMT cell models

As mentioned in the introduction, snail1 expression is sufficient to cause a complete EMT in cultured cells (reviewed in [119]). Three cell lines are most frequently used in this work, which are HT29 M6 (colon adenocarcinoma), RWP1 (liver metastasis of ductal pancreatic adenocarcinoma) and SW480 (colon adenocarcinoma). **Figure R.1** summarizes the phenotypic and molecular features of these cells and the changes induced by stable expression of *mmsnail1*[†]. Other cell lines are used in our lab and, as consequence, some of them have been included in some experiments either to increase the number of models under some situations (NIH3T3) or because they offer the possibility of a better approach in a specific context (LS174T).



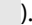
Figure R.1.A states the morphological changes induced by snail1 ectopic expression. In panels 1 and 2 there are pictures of HT29 M6 cells, which look small and round, forming compact colonies in the absence of snail1 (picture 1). However, upon snail1 transfection, these cells acquire a spindle shape, resembling fibroblasts; colony formation is lost and cells grow in a scattered fashion, dispersing throughout the plate (picture 2). The second column (pictures 3 and 4) shows pictures of RWP1 cells, which already express low levels of snail1. Nevertheless, when stably transfected with snail1 these cells are less compactly arranged and look more elongated.

SW480 cells (pictures 5-8) already present elongated shape in the absence of exogenous snail1 (compare panels 5 and 6) as consequence of the carcinoma stage these cells derive from. SW480 control cells already express snail1 (higher levels than RWP1 cells) and, at subconfluence, present an incomplete epithelial phenotype with low E-cadherin contacts and partial apico-basal polarization. Nevertheless, increase of cell confluence causes mature cell-cell contacts and epithelial phenotype. Snail1 ectopic expression causes a modest change in the phenotype at low confluence and prevents colony formation at high cell density. For SW480 cells two more clones stably expressing E-cadherin were introduced. The addition of E-cadherin under the control of an exogenous promoter diminishes the experimental variability due to confluence state because it provokes epithelial colony formation already at low confluence. It can

[†] See note on page 1

also be observed that the effect of E-cadherin overcomes the snail1 effect, noticeable by the reversion of the disperse growing to compact colonies in snail1/ E-cadherin cells[‡].

The changes in the phenotype induced by snail1 are accompanied by alterations in the gene expression profile. EMT induction and upregulation of mesenchymal genes in the three cell lines was confirmed by quantitative (**Figure R.1.B**) and semiquantitative (**Figure R.1.C**) mRNA analyses. In all three cell lines, ectopic snail1 expression causes downregulation of E-cadherin (**Figure R.1.B**, left graph), what is used as positive control for the EMT process. Upon snail1 stable expression fibronectin levels are increased between 1.8 and 5.5-fold depending of the cell line, being SW480 (control vs snail1) the cell line where less increase is detected (**Figure R.1.B**, middle graph). LEF-1, which is not expressed in differentiated colon epithelial tissue, is not detected in HT29 M6 control cells, though it is in SW480 control cells. Upon snail1-HA expression, LEF-1 expression is induced in HT29 M6 while the amount in RWP1 and SW480 cells (control vs snail1) increases until they nearly double it (**Figure R.1.B**, right graph).

Note that SW480 cells display less E-cadherin levels in control cells than HT29 M6, stating the different carcinoma stage between these two cell lines. Higher fibronectin and LEF-1 levels are also observed in SW480 cells (**Figure R.1.B**, ). However, forced E-cadherin expression reverses the activation of fibronectin and LEF-1 in SW480 until mRNA levels are hardly detectable for fibronectin and not detected at all for LEF-1 (**Figure R.1.B**, middle and right panels, respectively ). Even exogenous snail1-HA expression cannot activate both mesenchymal genes if E-cadherin expression is forced (**Figure R.1.B**, middle and right panels, .

Protein of total cell extracts was also analyzed (**Figure R.1.D**). Western blot was performed with antibodies against fibronectin, E-cadherin, LEF-1, HA (tagging snail1) and pyruvate kinase, as loading control. Increase in fibronectin and LEF-1 [276][§] protein upon snail1 expression is observed in all cell lines except when E-cadherin is expressed ectopically (SW480-E-cadherin, SW480-snail1/E-cadherin). The analysis displayed here confirms snail1 as inducer of the EMT process in HT29 M6, RWP1 and SW480 cells because its forced expression correlates with downregulation of endogenous E-cadherin and verifies that fibronectin and LEF-1 mRNA and protein levels are increased as consequence of such process. In addition, we observe that ectopic E-cadherin prevents the changes associated with EMT.

[‡] These cell clones were kindly provided by Dr. Alberto Muñoz (Instituto de Investigaciones Biomédicas "Alberto Sols," Consejo Superior de Investigaciones Científicas–Universidad Autónoma de Madrid, Madrid, Spain)

[§] Note the two bands appearing for LEF-1, which are probably due to alternative splicing

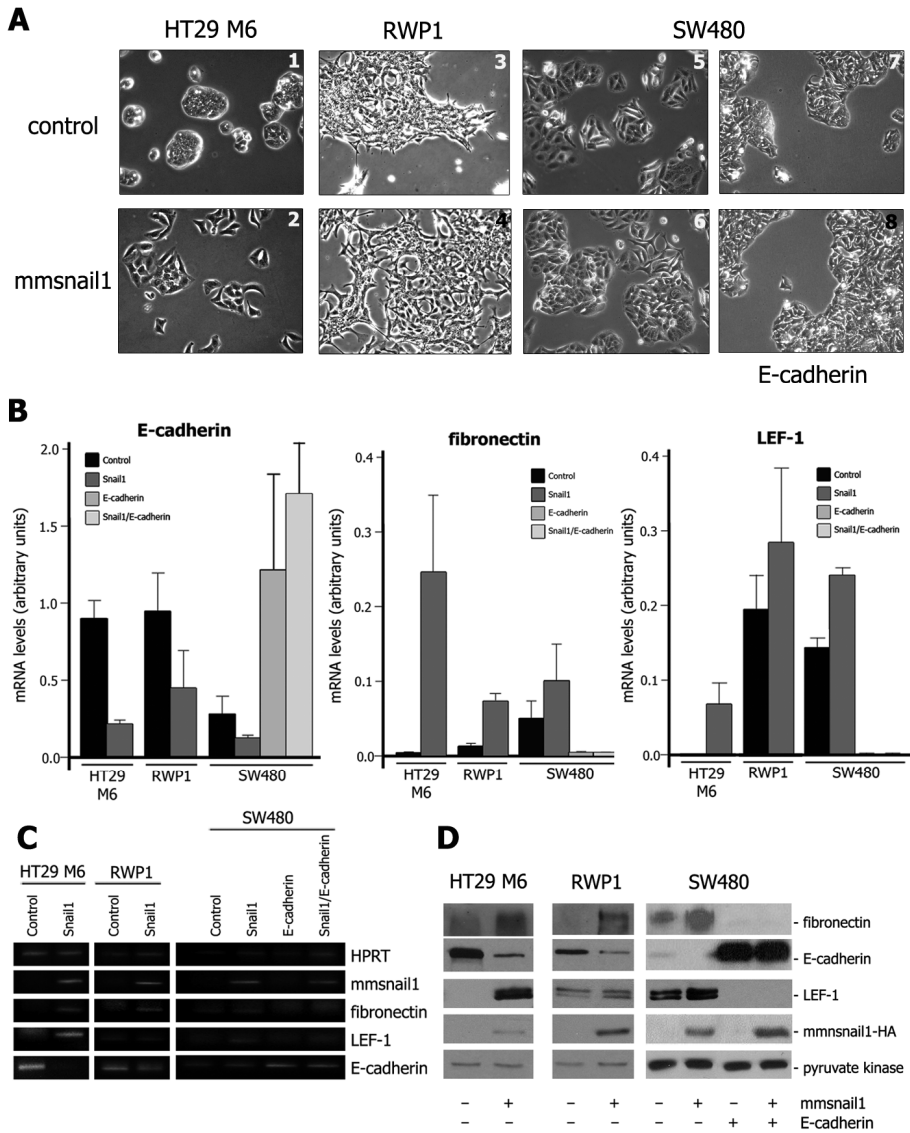


Figure R.1. Phenotypic and molecular effects of the transfection of mmsnail1-HA in HT29 M6, RWP1 and SW480 cells. **A.** Pictures of HT29 M6, RWP1 and SW480 stable clones for mmsnail1-HA (2, 4, 6) and their corresponding control cells (1, 3, 5). Pictures of E-cadherin clones in SW480 cells are also included (7 and 8). Magnification is of 440 times. **B.** qRT-PCR (E.P.13) to check the approximate numeric difference in the mRNA levels of the different markers between control and snail1 cells (also E-cadherin cells in the case of SW480 cells). Pumilio was used as internal control. Error bars correspond to the mean +/- standard deviation of a minimum of three independent analyses. **C.** Semiquantitative RT-PCR of mmsnail1-HA, fibronectin, LEF-1 and E-cadherin in the clones previously displayed. HPRT levels were used as control. Pictures displayed are representative of, at least, three independent detections. **D.** Protein levels of total cell extracts obtained with SDS lysis buffer (see E.P.10). 5 μ g of protein were loaded to detect fibronectin (270 kDa), E-cadherin (120 kDa) and pyruvate kinase (66 kDa), used as loading control; 40 μ g to detect LEF-1 (55 kDa) and snail1-HA (35 kDa). Pictures displayed are representative of, at least, three independent determinations.

R.1.2 Snail1 promotes transcription from the *LEF1* and *FN1* promoters

Because snail1 has been described as a transcriptional factor, we first analyzed whether it could act at such level to increase fibronectin and LEF-1 mRNA and protein quantities. A fragment corresponding to the *LEF1* promoter had already been cloned in our lab and is described in [130], though in this thesis it has been renamed -527/+1389 taking as reference the most frequent Transcription Start Site (TSS1) [218]. To delimitate the *FN1* promoter we cloned three fragments corresponding to sequences -867/+265, -606/+265 and -341/+265 (with respect to the TSS) in a luciferase vector and assessed their activity in epithelial (HT29 M6, RWP1 and SW480) and mesenchymal (NIH3T3) cells. We observed that the three constructions presented comparable activity (**Figure R.2**). The detected activity of the three *FN1* promoters in mesenchymal NIH3T3 fibroblasts was between two and three-fold higher than in epithelial cells (HT29 M6, RWP1 and SW480**), indicating that the sequence -341/+265 of the promoter contained the requirements for expression in mesenchymal cells.

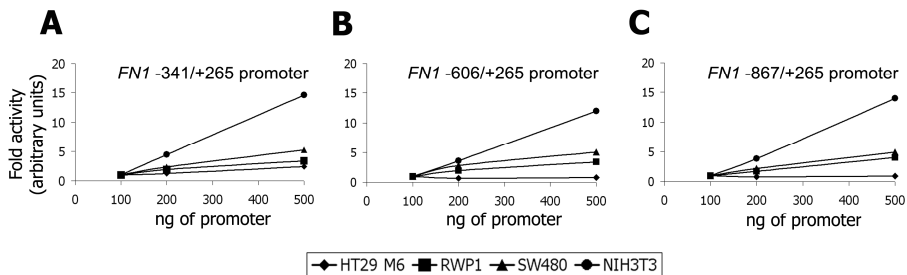


Figure R.2. The fragment -341/+265 of *FN1* promoter is sufficient to mediate *FN1* transcription in mesenchymal cells. Reporter assays were performed with HT29 M6, RWP1, SW480, and NIH3T3 cells, transfected either with 100 ng, 200 ng or 500 ng of pGL3* containing -341/+265 (A), -606/+265 (B) or -867/+265 (C) *FN1* promoter fragments. Luciferase activity was measured and compared to that of 100 ng of promoter (represented as 1).

Once *FN1* and *LEF1* promoters had been successfully delimited in the context of the study, we decided to check if transcription of both *LEF1* and *FN1* promoters was increased by snail1 *via* reporter assays. *FN1* and *LEF1* promoters (-341/+265 for *FN1* and -527/+1389 for *LEF1*) cloned in pGL3*^{††} were transfected into several stable snail1 cell lines as well as in the adequate control clone. **Figure R.3.A** shows the transcriptional activity of *LEF1* promoter in SW480-snail1 cells when compared to control cells (value

** Note that for the three sequences tested the activity of the promoter was higher according to the sequence SW480>RWP1>HT29 M6, in accordance to the levels of mRNA shown in **Figure R.1.B** (control cells)

†† This vector is marked with an asterisk because it carries a mutation as described in **E.P.2**.

taken as 1). Whereas the empty pGL3* vector was not activated in snail1 cells (data not shown), *LEF1* promoter activity increased up to four-fold. The same experiment was performed for *FN1* and similar results were obtained in SW480 cells (up to three-fold) and also in HT29 M6 cells (up to six-fold, **Figure R.3.B**). A dose-response experiment was also carried out in RWP1 wild type cells by cotransfecting the promoters and increasing amounts of a vector containing the cDNA of snail1. Activation of both promoters by snail1 was between two and two and a half-fold when compared to cells transfected with empty vector (value taken as 1, **Figure R.3.C**).

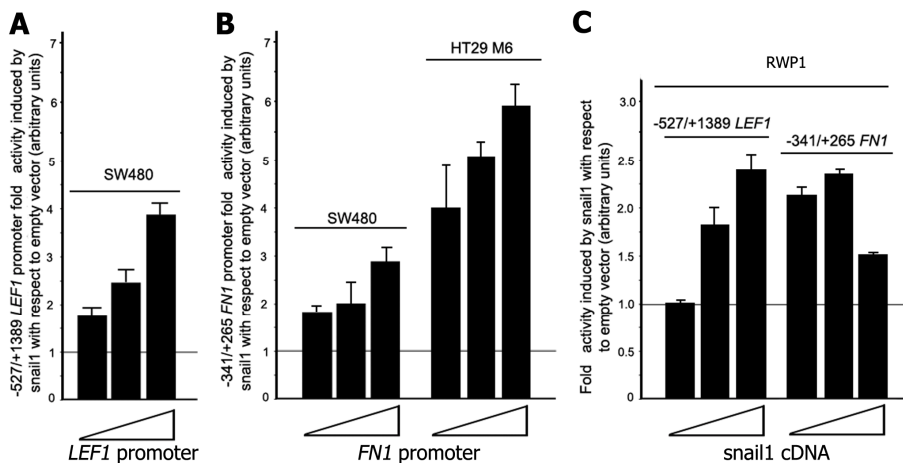


Figure R.3. Snail1 increases the promoter activity of *LEF1* and *FN1*. Stable SW480 (**A** and **B**) or HT29 M6 (**B**) transfectants for snail1-HA and control cells were transfected with 100 ng, 250 ng or 500 ng of -527/+1389 *LEF1* promoter (**A**) or -341/+265 *FN1* promoter (**B**). The activity of the promoters was examined in reporter assays and compared to that of control cells (values taken as 1 and represented by horizontal lines). **C**. Snail1 activates *FN1* and *LEF1* promoters in a dose-dependent manner. The activity of the *FN1* (100 ng) and *LEF1* (250 ng) promoters was determined in RWP1 wild type cells by transient cotransfection with pcDNA3-snail1-HA at different concentrations (1 ng, 5 ng and 10 ng). Promoter activity was referred to that of the promoters when cotransfected with empty pcDNA3, taken as 1 (represented by the horizontal line). In all cases values presented are the mean +/- standard deviation of, at least, three independent experiments performed in triplicate.

We also analyzed whether RNA stabilization was involved in mRNA increase of both LEF-1 and fibronectin. To that aim, cells stably transfected with snail1-HA or the empty vector were treated with actinomycin D, a drug that interferes the transcriptional machinery (see **E.P.3**). In **Figure R.4** the representation of the mRNA amount for both LEF-1 and fibronectin (left and right respectively) after several hours of treatment with actinomycin D is shown. No changes were observed in the degradation rate of mRNA when comparing control and snail1 cells. These results, thus, discard a role for snail1 in stabilization of mRNA as the means to increase fibronectin and LEF-1 levels.

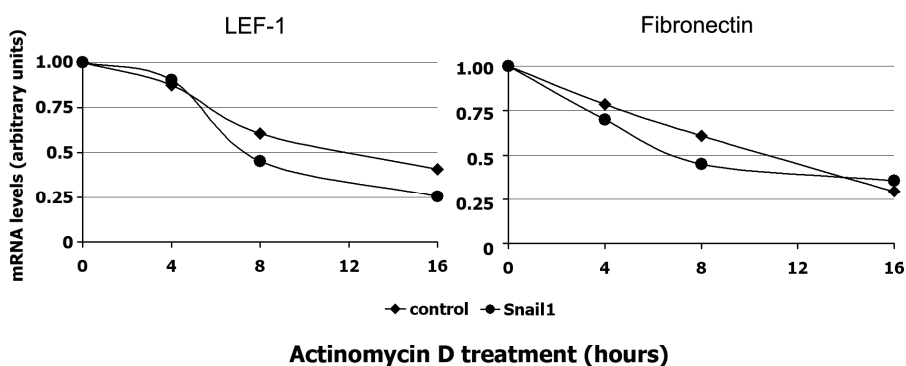


Figure R.4. Snail1 does not stabilize LEF-1 and fibronectin mRNAs^{}.** LS174T cells (see E.P.1 for further details), previously shown to display *FN1* and *LEF1* gene activation upon snail1 expression [277, 278], were treated with actinomycin D at 5 $\mu\text{g/ml}$ concentration for several hours prior to RNA extraction. qRT-PCR was performed with specific oligonucleotides (see E.P.3) to amplify LEF-1 (left) or fibronectin (right) mRNAs. For the representation, levels of mRNA at time 0 were taken as reference. HPRT was used as internal control.

R.1.3 *LEF1* promoter has a motif for snail1 binding, *FN1* promoter does not

As mentioned in the introduction (1.4.2.1), the only transcriptional mechanism described for snail1 required the presence in the promoters of short (six base pairs) consensus sequences called E-boxes (concretely, 5'-CACCTG-3' or 5'-CAGGTG-3'). With the aim of testing if E-boxes were, the same as for *CDH1*, mediating the transcriptional effect of snail1, we scanned the *FN1* and *LEF1* promoters searching for the presence of E-boxes. One E-box was found in *LEF1* placed between +191 and +196, whilst none was located in the *FN1* promoter cloned (Figure R.5). The absence of E-boxes in *FN1* suggested us that snail1 could activate transcription through an E-box-independent mechanism.

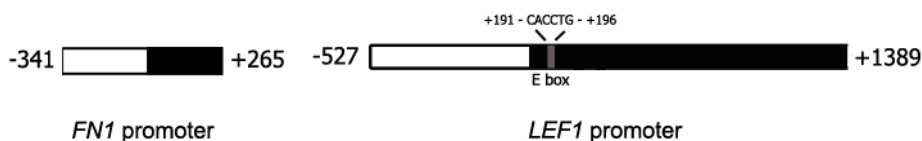


Figure R.5. Schematic representation of the *FN1* and *LEF1* promoters cloned. Black indicates regions downstream TSS. The *FN1* promoter contains no E-boxes (left) while the *LEF1* promoter cloned contains one (in grey) at +191/+196 (right).

In order to test whether snail1 was able to directly bind to DNA through sequences other than E-boxes, we performed biotinylated oligonucleotide pull-down assays

^{**} Experiment performed by Francisco Sánchez-Aguilera

(BOPA) with recombinant GST-snail1-HA protein. We used as bait the -341/+265 *FN1* promoter to immunoprecipitate snail1 and as positive control for snail1-DNA binding a fragment of the *CDH1* promoter (sequence -92/-64) carrying E-box 1. All DNAs were tagged at the 5' end with biotin (see **E.P.6**). **Figure R.6.A** shows that the amount of snail1 pulled-down by the -341/+265 *FN1* promoter (lane 3) was the same observed in the control pull-down where no DNA was loaded (lane 2), indicating the absence of specific binding for the -341/+265 *FN1* promoter. The positive control with the *CDH1* promoter, on the other hand, interacted greatly with recombinant snail1-HA (lane 4).

We then compared the binding capacity of snail1 to the wild type -527/+1389 *LEF1* and to a version of the promoter with the E-box mutated (with a double mutation previously described to prevent snail1 binding: -AACCTA-, **Figure R.6.B**). When we performed BOPA experiments with the -527/+1389 *LEF1* promoters (wild type and E-box mutant)⁵⁵ we observed that only the wild type successfully pulled-down snail1-HA (**Figure R.6.C**, lane 3) while the mutant for the E-box barely interacted with the transcription factor (**Figure R.6.C**, lane 4). These results indicate that snail1 cannot directly bind to the -341/+265 *FN1* promoter and that, probably, the only sequence it directly binds in the -527/+1389 *LEF1* promoter is the E-box at position +191/+196.

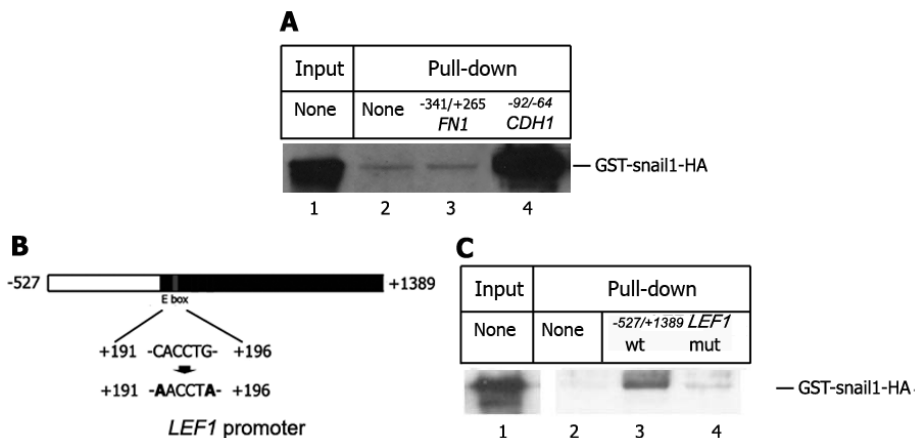


Figure R.6. Snail1 cannot directly bind to E-box-lacked promoters. **A.** *In vitro* BOPA with the -341/+265 *FN1* promoter. Biotinylated DNA was incubated with purified GST-snail1-HA recombinant protein and pulled down with streptavidin-combined beads (NEB). Precipitated snail1-HA was analyzed by western blot with rat antibody against HA (Roche). As negative control, protein was incubated with binding buffer but no DNA. A probe containing E-box 1 from the *CDH1* promoter (-92/-64) was used as a positive control. 10 % of the recombinant protein used for the assay was loaded as input (see **E.P.6**). Lanes: 1, input; 2, negative control; 3, -341/+265 *FN1* promoter; 4, -92/-64 *CDH1* promoter (positive binding control). The (continues)

⁵⁵ Performed by Cristina Agustí and collected in her PhD thesis entitled *Mecanisme d'activació de Fibronectina i LEF1 per Snail1 durant la transició epiteli-mesènquima*

(continues) picture is representative of a series of three experiments performed independently. **B.** Schematic representation of the *LEF1* promoter where the E-box is indicated. Mutations introduced are shown in bold. Black matches sequence downstream the TSS. **C.** *In vitro* BOPA with the -527/+1389 *LEF1* promoter. Simultaneously in the group, An experiment similar to the one shown in **A** was carried out with wild type and E-box mutated -527/+1389 *LEF1* promoter (see **E.P.6**). Both biotinylated DNAs as well as a negative control, without DNA, were incubated with recombinant GST-snail1-HA and pulled down with streptavidin-combined beads. The recombinant protein precipitated with the DNAs was analyzed by western blot with rat antibody against HA (Roche). Lanes: 1, input; 2, negative control; 3, wild type -527/+1389 *LEF1* promoter; 4, E-box mutant -527/+1389 *LEF1* promoter.

R.1.4 Activation of *LEF1* and *FN1* transcription by snail1 requires motifs in their promoters different than E-boxes

To test whether the E-box present in the -527/+1389 *LEF1* promoter was required for snail1-mediated activation, we performed reporter assays using either the wild type or the E-box mutant -527/+1389 *LEF1* promoter. First, RWP1 cells were transfected with both promoters separately; second, the two promoters were cotransfected with snail1-HA. In basal conditions, the E-box mutant displayed two/three-fold higher activity than the wild type promoter (**Figure R.7.A**) suggesting that the E-box repressed rather than activated transcription. Upon cotransfection with snail1, we detected an increase in promoter activation of 2.5-fold for the wild type and over 6-fold for the E-box mutant, being the E-box mutant activated by snail1 between twice and three times more than the wild type promoter (**Figure R.7.B**). These results imply that snail1 induces activation of *LEF1* transcription independently of the E-box, like in the case of *FN1*, and suggest that snail1, or another E-box-binding-repressor, also represses *LEF1* transcription through direct binding to the E-box at position +191/+196.

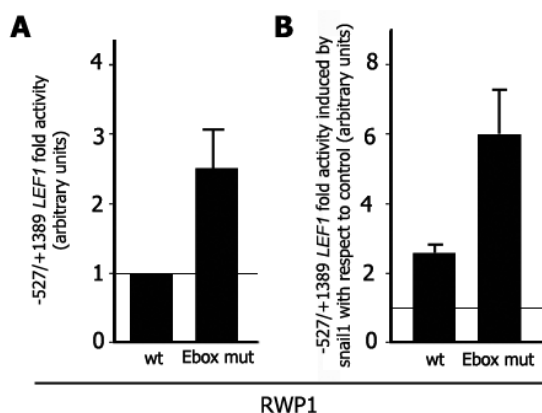


Figure R.7. The E-box at -527/+1389 *LEF1* promoter holds repressive function. A. The E-box mutant of the -527/+1389 *LEF1* promoter displays higher baseline activity than the wild type promoter. Reporter assays were performed transfecting 100 ng of the two *LEF1* (continues)

R.1.5 Snail1 binds to *FN1* and *LEF1* promoters through a different mechanism than to *CDH1*

After discarding direct binding of snail1 to the *FN1* promoter and the participation of the E-box in *LEF1* promoter in the activation mechanism, we decided to check if snail1 was able to bind to these promoters indirectly. We performed BOPA experiments with extracts of cells expressing snail1, which, in addition to snail1, would also supply other proteins, if required, to mediate snail1 binding to the DNA.

The positive control for snail1-DNA binding consisted of a fragment of the *CDH1* promoter carrying E-box 1 (sequence -92/-64) while for the negative control the E-box in the same fragment was mutated as previously described (--AACCTA-, **Figure R.8.A**, lanes 3 and 4 respectively). The -341/+265 *FN1* promoter was observed to be capable of pulling-down snail1-HA from nuclear extracts of SW480-snail1-HA cells (**Figure R.8.A**, compare lanes 2 and 4). Snail1 binding was also observed to *LEF1* promoters, both the wild type and the E-box mutant, in an equivalent experiment (**Figure R.8.B**, lanes 3 and 4 respectively).

The observation that snail1 supplied in cell extracts but not purified could bind to the *FN1* and E-box mutant *LEF1* promoters indicate that snail1 is capable of binding to *FN1* and *LEF1* promoters indirectly, through some other cellular protein or proteins and independently of E-boxes. In the case of the *LEF1* promoter, the slight decrease in the binding of snail1 between the wild type and the E-box mutant observed in **Figure R.8.B** (lanes 3 and 4) could be due to the lack of direct binding through the E-box in the mutant, what would be in accordance with the hypothesis of the existence of two balanced mechanisms. Such mechanisms would probably consist on repression by snail1 direct binding to the E-box and activation through indirect binding to another region of the promoter.

(continues) promoters (E-box mutant and wild type) into RWP1 wild type cells. Luciferase activity is referred to that of the wild type promoter, taken as 1 (horizontal line). **B**. The E-box mutant -527/+1389 *LEF1* promoter is activated by snail1. Luciferase activity was measured after cotransfection of 100 ng of the promoters with 5 ng of either pcDNA3-snail1-HA or pcDNA3 (empty vector). Values are referred to the activity of the promoters when cotransfected with pcDNA3, taken as 1 (represented as a horizontal line). The results shown (**A** and **B**) are the average +/- standard deviation of, at least, three independent experiments performed in triplicate.

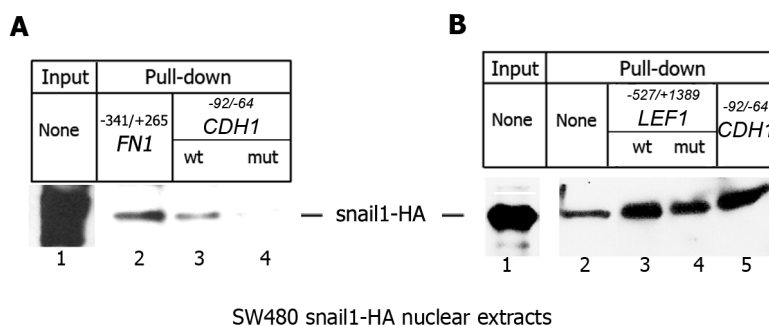


Figure R.8. Snail1 binds indirectly to the *FN1* and *LEF1* promoters. **A.** Snail1 binds to the -341/+265 *FN1* promoter when supplied with cell extracts. BOPA experiment was performed incubating the -341/+265 *FN1* promoter with the nuclear fraction of SW480-snail1-HA cell extracts. DNA was pulled down with streptavidin-combined beads (NEB) and samples analyzed by western blot with rabbit antibody against HA (Sigma). A probe containing E-box 1 from the *CDH1* promoter (-92/-64) was used as a positive control. The same *CDH1* promoter probe in which the E-box was mutated (see **E.P.6**) was used as negative control. 10 % of preincubated sample (see **E.P.6**) was stored and loaded as input. Lanes: 1, input; 2, -341/+265 *FN1* promoter; 3, wild type -92/-64 *CDH1* promoter; 4, E-box mutant -92/-64 *CDH1* promoter. **B.** Snail1 binds to the -527/+1389 *LEF1* when supplied with cell extracts independently of the E-box. Biotinylated *LEF1* promoters (wt and E-box mutant) were incubated with nuclear cell extracts of SW480-snail1-HA cells, pulled down with streptavidin-conjugated beads and protein analyzed by western blot with rabbit antibody against HA (Sigma). As negative control, protein was incubated with binding buffer but no DNA (see **E.P.6**). A probe containing E-box 1 from the *CDH1* promoter (-92/-64) was used as a positive control. 10 % of preincubated sample (see **E.P.6**) was stored and loaded as input. Lanes: 1: input; 2: negative control; 3, wild type -527/+1389 *LEF1* promoter; 4, E-box mutant -527/+1389 *LEF1* promoter; 5, wild type -92/-64 *CDH1* promoter. The pictures (**A** and **B**) are representative of a series of three experiments performed independently.

Although BOPA experiments indicated that snail1 could bind to E-box-lacked promoters, we wanted to use a more physiological approach to confirm binding *in vivo*. Chromatin immunoprecipitation (ChIP) assays were performed transfecting RWP1 control and snail1 cells with -341/+265 *FN1* promoter. Nuclear enriched extracts (see **E.P.7**) were immunoprecipitated either with unspecific mouse antibody or specific rat antibody against HA (Roche). We amplified the DNA precipitated with snail1-HA with specific oligonucleotides for exogenous *FN1* promoter or for an irrelevant DNA (see **E.P.7**). When we analyzed the results we compared the levels of exogenous *FN1* promoter to the levels of irrelevant DNA, this last showing little difference in the levels between control and snail1 cells. Finally, the ratio exogenous *FN1* promoter/irrelevant DNA was compared between control and snail1 cells. Results showed that the immunoprecipate of snail1 cells contained five-fold more -341/+265 *FN1* promoter than control cells (**Figure R.9.A**).

The result in RWP1 for exogenous *FN1* promoter was validated for the endogenous promoter in HT29 M6 snail1-HA cells, where we observed about five-fold more *FN1* promoter immunoprecipitated in snail1 than in control cells (**Figure R.9.B**). Similarly to

HT29 M6 cells, we checked endogenous *FN1* immunoprecipitating with snail1 in SW480 clones. Differently than in the previous cases, though, we used an antibody against snail1, which would precipitate endogenous snail1 (in addition to the exogenous). Although we detected slightly higher *FN1* promoter levels immunoprecipitated in snail1 cells, we also recovered *FN1* DNA from control cells, probably reflecting the fact that SW480 already express endogenous snail1. In addition, we observed that stable expression of E-cadherin, either alone or together with snail1, decreased the binding of snail1 to the *FN1* promoter (**Figure R.9.C**), illustrating a dominant inhibitory effect of E-cadherin on snail1 binding (similarly to what we observed for fibronectin expression, **Figure R.1.B, C, D**). In conclusion, the results of ChIP assays performed with the three different cell lines confirmed that snail1 binds to *FN1* promoter *in vivo*.

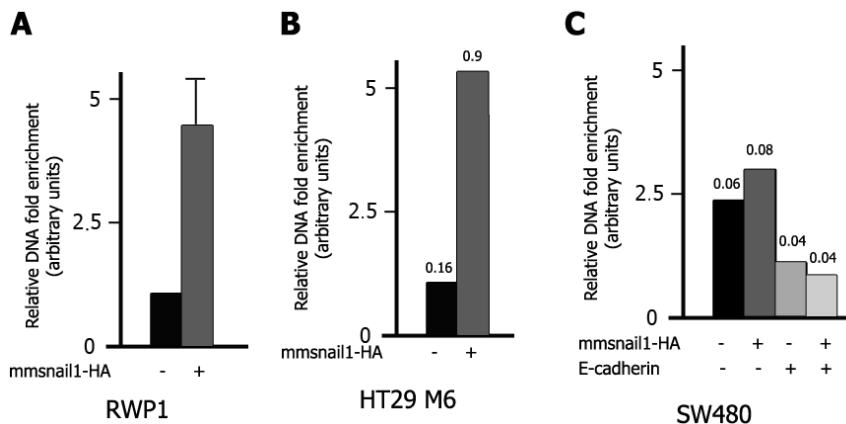


Figure R.9. Snail1 binds to the *FN1* promoter *in vivo*. **A.** ChIP analysis was performed transfecting pGL3*-341/+265 *FN1* promoter into RWP1-snail1-HA and control cells as described in **E.P.7**. Snail1-HA was immunoprecipitated from RWP1 nuclear-enriched extracts using a rat antibody against HA (Roche) and exogenous *FN1* promoter amplified using specific oligonucleotides. At the same time, a DNA corresponding to a fragment of the polymerase II (pol II) promoter, irrelevant to our study, was amplified (see **E.P.7**). The levels of *FN1* promoter were standardized with the levels of the fragment of pol II (which displayed no difference between control and snail1 cells). The ratio *FN1*/pol II promoter of snail1 cells was compared to that of control cells (represented as 1 in the graph). Error bars correspond to standard deviation of six experiments performed independently. **B.** Snail1-HA was immunoprecipitated from nuclear-enriched HT29 M6 cell extracts with rabbit antibody against HA (Sigma) and endogenous *FN1* promoter amplified using specific primers for the region +200 bp. At the same time, a region corresponding to -2kb of the *FN1* promoter, irrelevant to our study and which did not change between control and snail1 cells, was amplified (see **E.P.7**). As before, the ratio *FN1* promoter/irrelevant DNA was compared between control and snail1 cells and represented in the graph. Numbers on bars indicate the percentage of input immunoprecipitated (for the -2kb region it was of between 0.02 and 0.08). **C.** In the case of SW480 clones the antibody used was from mouse and against snail1, obtained after purification of a hybridoma in our laboratory. Endogenous *FN1* promoter coimmunoprecipitated with snail1 was amplified as described in **E.P.7**. Representation corresponds to an analysis performed as in **B**. Numbers on bars match the percentage of input immunoprecipitated which was around 0.009 in all cases for an unspecific antibody. The experiment displayed is representative of a series of three.

According to the results obtained so far, snail1 requires a different mechanism for repressing and activating genes. For the first mechanism, E-boxes and direct binding to the DNA are necessary [113, 122]; for the second, none of them are needed, but indirect binding to an undefined sequence. To further compare the activation and repression mechanisms, we decided to study the involvement of the SNAG domain in activation, which had been previously described to be required to achieve repression [113, 134]. We took profit of a mutant for snail1 that had already been generated in the laboratory, named P2A (proline number two mutated to alanine), which had been reported to be unable to repress *CDH1* expression [113]. A schematic representation of the snail1-P2A mutant is shown in **Figure R.10.A** where the mutated residue is indicated.

To check the effect of the snail1-P2A mutant on transcriptional activation of the *FN1* and *LEF1* promoters we transfected the -341/+265 *FN1*, the -527/+1389 *LEF1* or the -178/+92 *CDH1* promoters in RWP1 stable transfectants for snail1-HA, snail1-P2A-HA, as well as control cells. Reporter analyses in **Figure R.10.B** show that *FN1* and *LEF1* promoters were activated about two-fold by snail1 and *CDH1* promoter repressed four times in the same cells. However, we observed no effect on the promoters (activation for *LEF1* and *FN1* or repression in the case of *CDH1*) when we compared the activity between RWP1 cells stably expressing snail1-P2A and control cells.

Western blot analysis of total cell extracts from the clones revealed that, even though the clones stably expressing snail1-P2A-HA expressed more exogenous protein than snail1-HA clones (**Figure R.10.C**, third panel), the levels of E-cadherin and fibronectin were similar to those detected in control cells. These observations indicated that, contrarily to what was appreciated in snail1-HA clones, no downregulation of E-cadherin and no upregulation of LEF-1 and fibronectin was taking place upon snail1-P2A expression (**Figure R.10.C**). When we examined fibronectin and LEF-1 mRNA levels, we also observed little difference between control and snail1-P2A-HA cells (**Figure R.10.D**). Our results, thus, pointed at the requirement of the integrity of the SNAG domain in the snail1 transcriptional activation mechanism of *FN1* and *LEF1* gene expression.

Since we had discarded direct binding of snail1 to the *FN1* and *LEF1* promoters, we confirmed that the mechanisms for snail1 binding to promoters to activate and repress were different. Previous studies had demonstrated that snail1-P2A, since it carries an intact DNA binding domain, still retains its DNA binding capacity and can bind to *CDH1* promoter [113, 134]. With the aim to study if the DNA binding domain was also enough for binding to the *FN1* promoter, we performed ChIP assays and compared the

binding capacity of snail1-P2A to both the *CDH1* promoter, which we used as positive control, and the *FN1* promoter. Nuclear-enriched RWP1 stable cells extracts were immunoprecipitated with rat antibody against HA (to precipitate both wt snail1-HA and snail1-P2A-HA). Results (represented as previously: ratio *FN1* (or *CDH1*) DNA/irrelevant DNA and referred to binding in control cells) showed that, while snail1-P2A had the capacity of binding to the *CDH1* promoter (Figure R.10.E, right panel, ■), it was unable to bind to the *FN1* promoter (Figure R.10.E, left panel, ■). Wild type snail1-HA was confirmed to bind to both promoters (Figure R.10.E, ■).

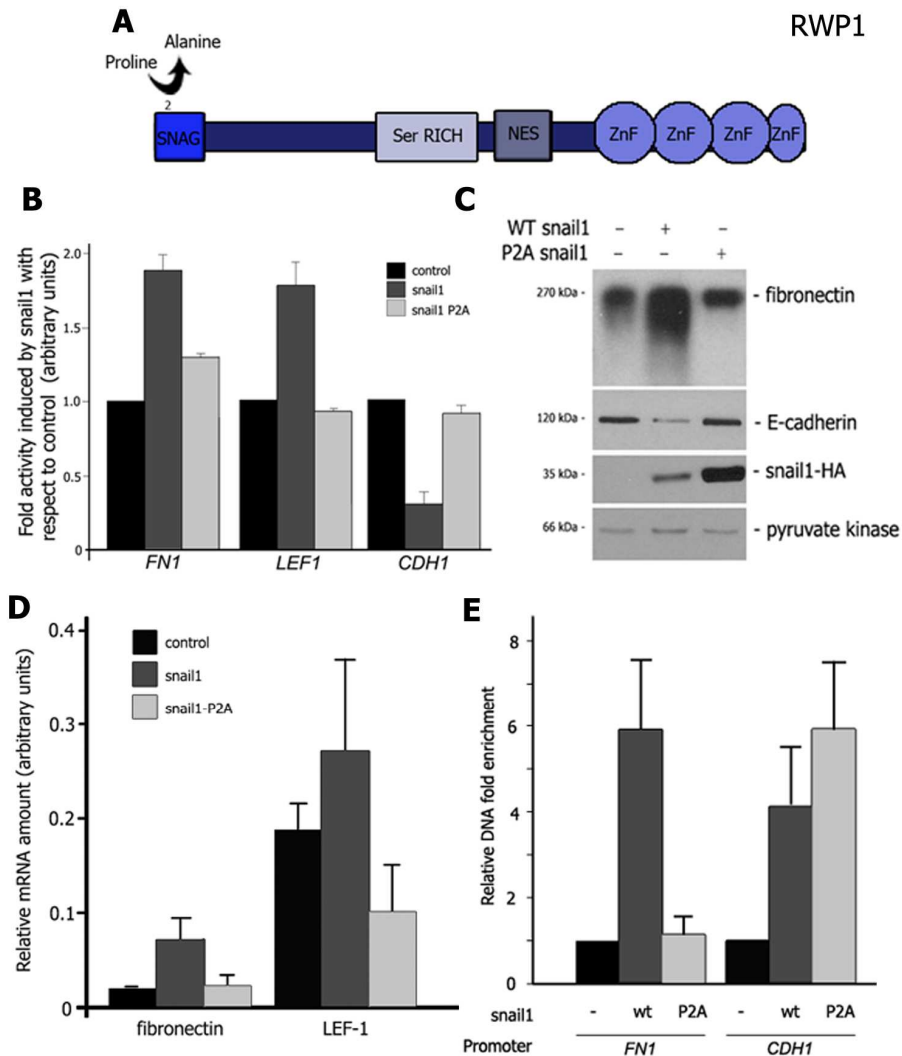


Figure R.10. Snail1-P2A fails to activate gene expression and to bind to the *FN1* promoter. **A.** Schematic representation of snail1 where the mutation of Proline 2 to Alanine is displayed. **B.** Reporter assays were performed with RWP1 cells stably transfected with wild type snail1, snail1-P2A or empty vector and cotransfected with 100 ng of *FN1* (-341/+265), *LEF1* (continues)

(continues) (-527/+1389) or *CDH1* (-178/+92) promoter. Values presented are the mean +/- standard deviation of, at least, three independent experiments performed in triplicate. **C.** Lysis of the indicated RWP1 clones was carried out with total extraction buffer (SDS 1%), protein loaded in polyacrylamide gels and analysed by western blot with specific antibodies (**E.P.10**). Pyruvate kinase was used as loading control. Picture displayed is representative of a series of, at least, three independent determinations. **D.** qRT-PCR was performed with RNA from RWP1 clones as described in **E.P.13**. Values are corrected according to levels of Pumilio mRNA, used as internal control. Bars correspond to average +/- standard deviation of three experiments performed independently. **E.** CHIP assays were performed with chromatin from stable RWP1 snail1-HA or snail1-P2A-HA transfectants and antibody against HA (Roche) to immunoprecipitate. Results are related to the amplification of irrelevant DNA corresponding to the -2 Kb region of *FN1* (**E.P.7**) and referred to the binding in control cells (taken as 1).

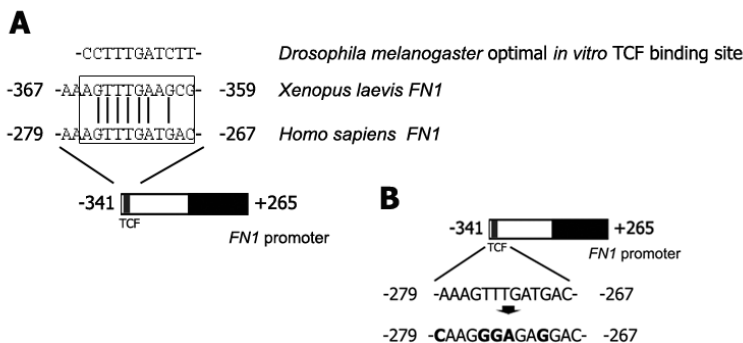
All these data suggest that the SNAG domain plays different roles during snail1-mediated transcriptional activation and repression. For repression, DNA binding is achieved through the Zn finger domain while the SNAG domain recruits corepressors to the promoter. For activation it seems that snail1 requires the SNAG domain to indirectly bind DNA, probably by mediating the interaction of snail1 with a DNA binding partner. In addition, we should also consider the possibility that the requirement of the integrity of the SNAG domain in transcriptional activation induced by snail1 could be due to the need of prior repression of some genes (maybe E-cadherin) and consequent cellular/molecular changes. These possibilities will be further studied in subsequent chapters.

R.2 IDENTIFICATION IN *FN1* AND *LEF1* OF MOTIVES AND TRANSCRIPTION FACTORS INVOLVED IN SNAIL1-INDUCED TRANSCRIPTIONAL ACTIVATION

R.2.1 Snail1 does not require TCF to activate *FN1* and *LEF1* transcription

The β -catenin/TCF complex was studied as a putative mediator of snail1 binding to the promoters because of its well-characterized involvement in EMT and also because the release of β -catenin from the junctional complex is a direct consequence of snail1 effect on E-cadherin expression [202, 204]. Sequences of the *FN1* and *LEF1* promoters were scanned looking for LEF/TCF binding motifs. Although no functional LEF/TCF box had been described in human *FN1* promoter, one had been in the *Xenopus laevis FN1* promoter [223]. After sequence alignment between both genes, we located the TCF/LEF box in the human promoter, which was quite similar to the consensus, at -277/-267 (**Figure R.11.A**).

To study the relevance of this box in the mechanism of snail1 transcriptional activation, we proceeded to mutate it (see **E.P.2**, **Figure R.11.B**) and performed several reporter assays. We first compared the transcriptional activity in reporter experiments of the LEF/TCF box mutant and wild type -341/+265 *FN1* promoters in basal conditions by transfecting them into RWP1 cells. Next, in order to compare the responsiveness of the promoters (wild type and TCF-box mutant) to snail1, we cotransfected them with either RSVneo-snail1-HA or empty RSVneo, also in RWP1 cells. Results showed that, although the mutation affected the basal activity of the *FN1* promoter, decreasing it about fifty per cent (**Figure R.11.C**), it did not affect snail1-mediated activation (**Figure R.11.D**) indicating, thus, that the LEF/TCF-like box located at -277/-267 in the *FN1* promoter was not mediating snail1 activation.



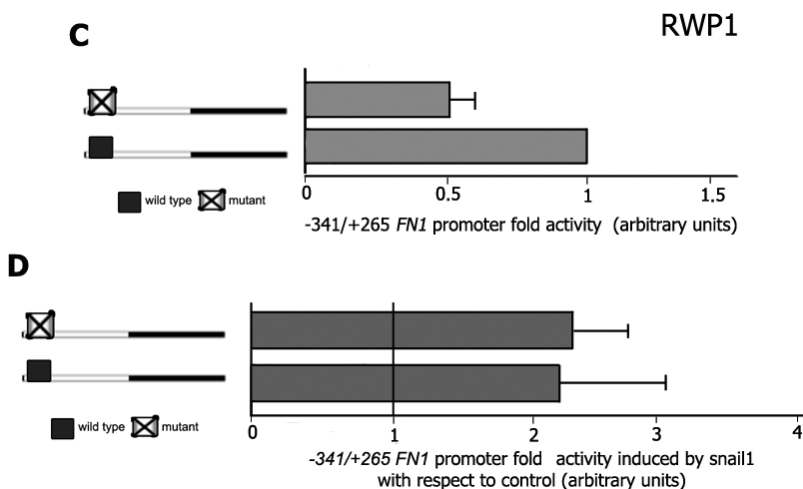


Figure R.11. Mutation of the LEF/TCF box in the *FN1* promoter does not affect snail1-induced activation. Black matches downstream of the TSS. **A.** Alignment of optimal *in vitro* binding site for *Drosophila melanogaster* TCF [279], LEF/TCF box in *Xenopus laevis* *FN1* promoter and LEF/TCF box in *Homo sapiens* *FN1* promoter. **B.** Mutations introduced to the LEF/TCF box of the human *FN1* promoter (bold). **C.** Reporter assay in which activity of the LEF/TCF box mutant *FN1* promoter was compared to that of wild type promoter after transfecting RWP1 cells with 100 ng of each promoter. Values are referred to the activity of the wild type promoter, taken as 1. **D.** Snail1-induced transcriptional activation of wild type and LEF/TCF box mutant *FN1* promoter. 150 ng of RSVneo-snail1 or empty vector were cotransfected with 100 ng of promoter in RWP1 cells and luciferase activity measured. Values are referred to the activation of each promoter when cotransfected with empty RSVneo vector, taken as 1 (represented with the vertical line). Values presented (**C** and **D**) are the mean +/- standard deviation of, at least, three independent experiments performed in triplicate.

We next scanned the sequence of the *LEF1* promoter for LEF/TCF boxes and located two, at +330/+340 (box 1) and +406/+416 (box 2, **Figure R.12.A**), which had already been described [218]. The same mutations used for *FN1* were introduced in both LEF/TCF boxes of the *LEF1* promoter to generate three mutant promoters: one for box 1, one for box 2 and a third mutant with both boxes mutated (**Figure R.12.B**). After confirming that mutations conferred resistance to TCF induced transcriptional activation (see **E.P.2**), we transfected all promoters into RWP1 wild type cells to analyze both their activity in the absence of snail1 and their responsiveness to the transcription factor. Analysis of basal expression demonstrated that only the promoter with box 1 mutated presented lower activity than the wild type promoter (around 0.3, **Figure R.12.C**). When assessed upon cotransfection with snail1, we observed that all promoters carrying mutations (even the one with mutated box 1) were activated similarly to the wild type -527/+1389 *LEF1* promoter: between two and three-fold (**Figure R.12.D**). These results suggest that, for *LEF1*, like in the case of *FN1*, LEF/TCF boxes are not involved in snail1-induced promoter activation.

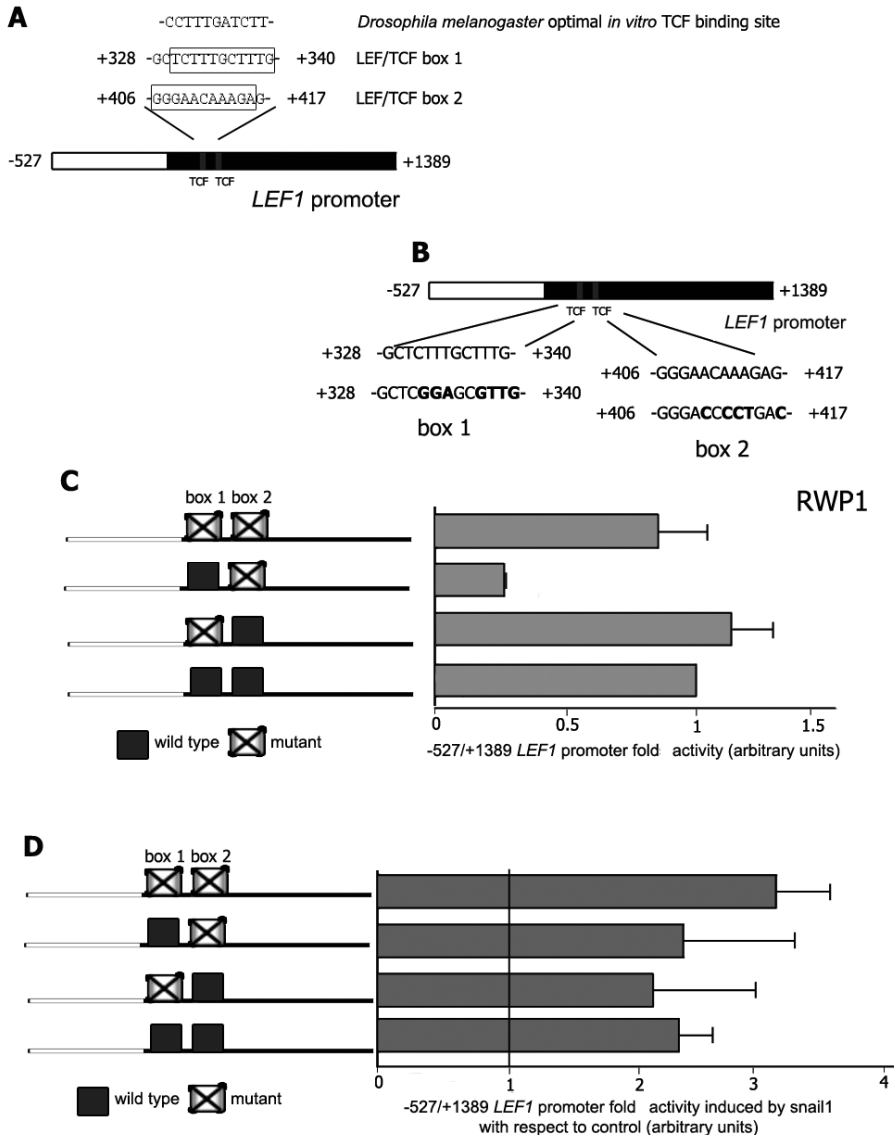


Figure R.12. Mutation of the LEF/TCF box in the *LEF1* promoter does not affect snail1-induced activation. Black indicates sequence downstream of the TSS. **A.** Alignment of optimal *in vitro* binding site for *Drosophila melanogaster* TCF [279] and the two LEF/TCF boxes located in *LEF1* promoter. Note that box 2 is antisense. **B.** Mutations introduced to the LEF/TCF boxes in *LEF1* promoter (bold). **C.** Results of reporter experiments in which the activity of the three LEF/TCF mutant promoters (box 1, box 2 and boxes 1 & 2) is compared to that of wild type promoter (activity represented as 1) after transfecting RWP1 cells with 100 ng of each promoter. **D.** Snail1-induced activity of wild type and mutant promoters measured in reporter assays. 150 ng of RSVneo-snail1 or empty vector were cotransfected with 100 ng of promoter and luciferase activity determined. Values are referred to the activity of each promoter when cotransfected with RSVneo empty vector, taken as 1 (represented by a vertical line). In all cases results are the average \pm standard deviation of, at least, three independent experiments performed in triplicate.

Even though our results indicated that LEF/TCF boxes were not involved in snail1-mediated activation of *FN1* and *LEF1* promoters, simultaneous results from the group^{***} pointed at β -catenin as a transcriptional cofactor in such mechanism, yet in a LEF/TCF-independent fashion. For these experiments we used three LS174T cell clones kindly provided by Dr. Hans Clevers: one of the clones was stably transfected with a doxycycline-inducible dominant negative form of TCF4 (Δ TCF4) [227], another with a doxycycline-inducible siRNA for β -catenin and the third with the backbone plasmid [280]. To increase the mRNA levels of fibronectin, which were hardly detectable in these clones, we stably transfected them with a vector containing snail1-HA cDNA (see **E.P.1** for characterization of these clones) generating three new clones from the ones obtained from Clevers' laboratory.

With these clones, we studied the effect that both β -catenin and TCF had on *LEF1* and *FN1* expression. We studied a total of six snail1 clones (two of them also carrying inducible β -catenin siRNA, two with inducible Δ TCF4 and two as control with backbone vector) and compared the expression of the two mesenchymal markers in cells treated with doxycycline or with its carrier (DMSO). We also analyzed the expression of c-myc, a well-characterized target of the β -catenin/TCF pathway as control. Results obtained are displayed in **Figure R.13.B**. The left column shows the relative mRNA levels of fibronectin (upper row), LEF-1 (middle row) and c-myc (lower row) in two different snail1 clones where β -catenin expression was knocked down. Values were referred to the relative mRNA levels in cells treated with DMSO (in which no knock-down was induced), which were taken as 1 (represented by a dotted line). In all cases, β -catenin knock-down caused decrease of the mRNA levels of about 70-90 %, indicating that it was involved in the snail1-induced transcriptional activation of these genes. **Figure R.13.B** middle panel shows the results obtained for inducible Δ TCF4 (also compared to the results obtained in cells treated with DMSO, dotted line). In this case, fibronectin expression was barely affected (upper row), while LEF-1 suffered a modest decrease of 30-40 % (middle row). Levels of c-myc, on the other hand, decreased between 60 and 70 %, indicating that Δ TCF4 was properly interfering TCF4 signaling. The last column (right) displays two more snail1 clones, in this case obtained on cells previously expressing the backbone plasmid and treated with DMSO. For the three genes, little unspecific interference (0-20%) was observed by the addition of doxycycline.

^{***} Performed by Francisco Sánchez-Aguilera, Ferran Pons and Cristina Agustí and collected in the PhD thesis entitled *Mecanisme d'activació de Fibronectina i LEF1 per Snail1 durant la transició epitel·li-mesènquima*, by Cristina Agustí

Taken together, the results shown suggest a β -catenin-dependent/TCF-independent mechanism for *FN1* transcription in snail1 cells, while for *LEF1* both TCF-dependent and independent mechanisms appear to be mediating activation. We also performed reporter assays in RWP1 cells, which confirm the existence of a TCF independent mechanism. In **Figure R.13.C**, cells were cotransfected either with the *LEF1* or the *FN1* promoters, snail1-HA or empty vector, and either Δ TCF4 or APC, a member of the β -catenin destruction complex. β -catenin knockdown by APC negatively affected *LEF1* and *FN1* activation by snail1, while Δ TCF4 did not vary the promoter activity of any of them, data that support the conclusions previously raised.

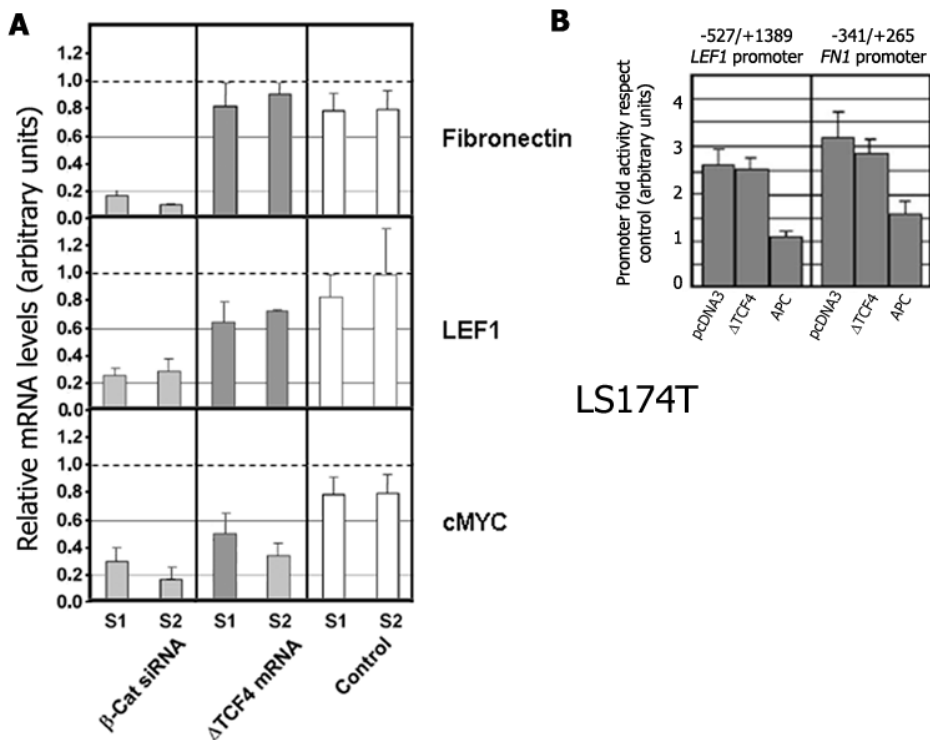


Figure R.13. Effect of downregulation of β -catenin and TCF4 signaling in snail1-mediated activation. **A.** Relative mRNA levels of fibronectin, LEF-1 and myc extracted from six snail1-HA clones (named S1 and S2 in all cases) was analyzed by qRT-PCR. Two clones also express the inducible siRNA of β -catenin (left), two the inducible Δ TCF4 (middle) and two were transfected with control vector (right). Relative mRNA levels of cells treated with DMSO are represented as 1 (dotted line). HPRT, with similar levels for all cells, was used as internal control. **B.** Promoter activity was assessed in reporter assays after cotransfection of RWP1 wild type cells with *LEF1* (left) or *FN1* (right) promoters, snail1-HA and either Δ TCF or APC or empty vector. Values represent the activity in cells transfected with snail1 with respect to the activity in cells transfected with the empty vector.

R.2.2 β -catenin is not required for snail1 translocation to the nucleus

The fact that TCFs were not involved in snail1-mediated activation of the *FN1* and *LEF1* promoters made us think of other roles rather than the transcriptional for β -catenin involvement in such mechanism. Since β -catenin was known to act as importin [281], and observations from the group indicated that snail1 and β -catenin could interact *in vitro*⁺⁺⁺, we decided to assess if β -catenin was involved in snail1 nuclear import.

We used for this experiment LS174T cells stably transfected with the doxycycline inducible siRNA for β -catenin. We electroporated these cells with a vector containing the cDNA of a fusion protein composed of green fluorescent protein (GFP) and snail1-HA (see **E.P.14**), which previous articles had demonstrated to mimic endogenous snail1 localization (mainly nuclear) [130]. As a result of the low electroporation efficiency of these cells, we could not include more than two positive cells for GFP-snail1 in each field; therefore, we included quadruplicates of each condition in **Figure R.14.A-D** (displayed in two columns of four panels). As a control for nuclear staining we incubated cells with propidium iodide (**Figure R.14.A-D** left column, blue).

First we treated cells either with doxycycline (causing β -catenin knock-down, **Figure R.14.B**) or DMSO (**Figure R.14.A**) for 24 hours. We checked β -catenin levels by immunofluorescence and observed that protein was slightly decreased, mainly in the nucleus (compare **Figure R.14.A** and **B**, right column, red). We noticed no changes regarding GFP-snail1 subcellular localization, which, despite being detected throughout the cell, was more intensely found in the nucleus (compare **Figure R.14.A** and **B**, left column, green/blue).

We next tried to further decrease β -catenin protein by treating cells with doxycycline (**Figure R.14.D**) or DMSO (**Figure R.14.C**), for 48 hours. We observed that total protein levels were lower, but still some β -catenin could be detected, mainly in the junctions (**Figure R.14.C.D** right column, red). However, we discerned no differences in the distribution of GFP-snail1 between cells expressing β -catenin and the siRNA against it (**Figure R.14.C.D**, green), suggesting that β -catenin does not play a role in the nuclear entrance of snail1.

⁺⁺⁺ By a series of experiments performed independently by Cristina Agustí and Patricia Villagrasa.

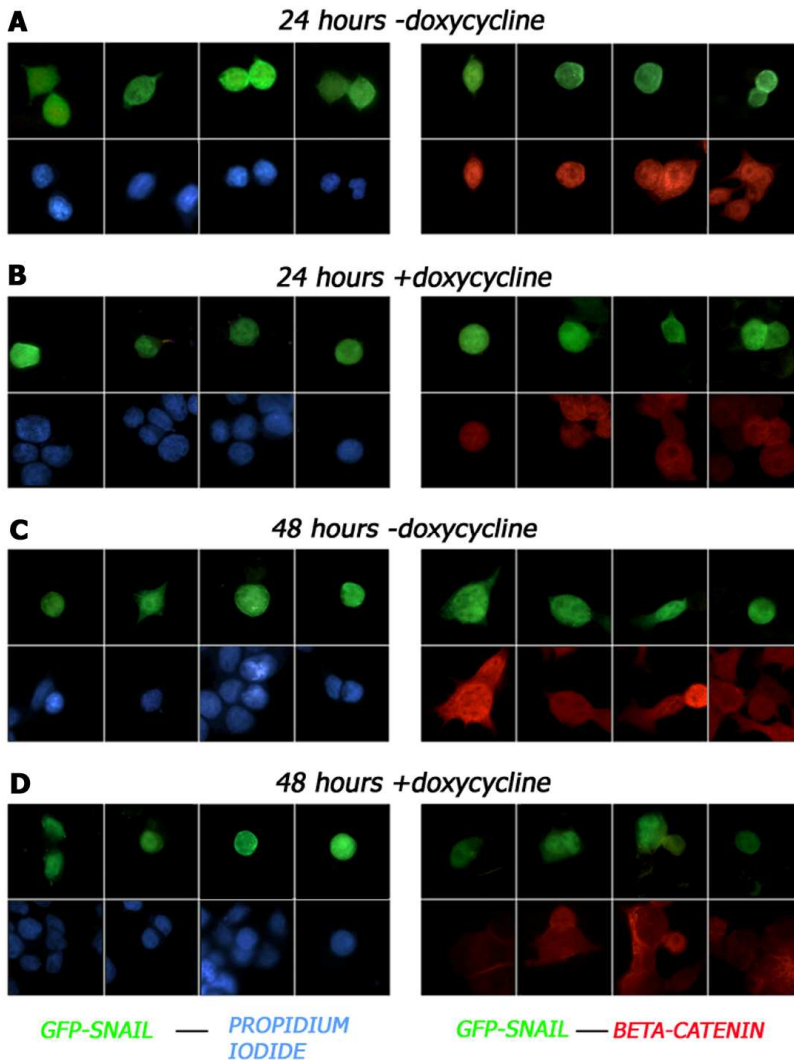


Figure R.14. β -catenin knockdown does not have any effect in snail1 nuclear import. LS174T cells stably transfected with doxycycline-inducible siRNA for β -catenin were electroporated with GFP-snail1-HA (see E.P.14). For the left half nuclei are dyed with propidium iodide (changed to blue) while in the right half immunofluorescence was performed with a monoclonal mouse antibody for β -catenin from BD Transduction Laboratories and secondary antibody TRITC combined against mouse antibody. In all panels green matches snail1. In the upper panels cells were treated 24 hours either with DMSO (A) or doxycycline (B); in the lower panels cells were treated with DMSO (C) or doxycycline (D) for 48 hours. Doxycycline was used at 1 μ g/ml.

R.2.3 β -catenin binds to the *FN1* promoter in the presence of snail1

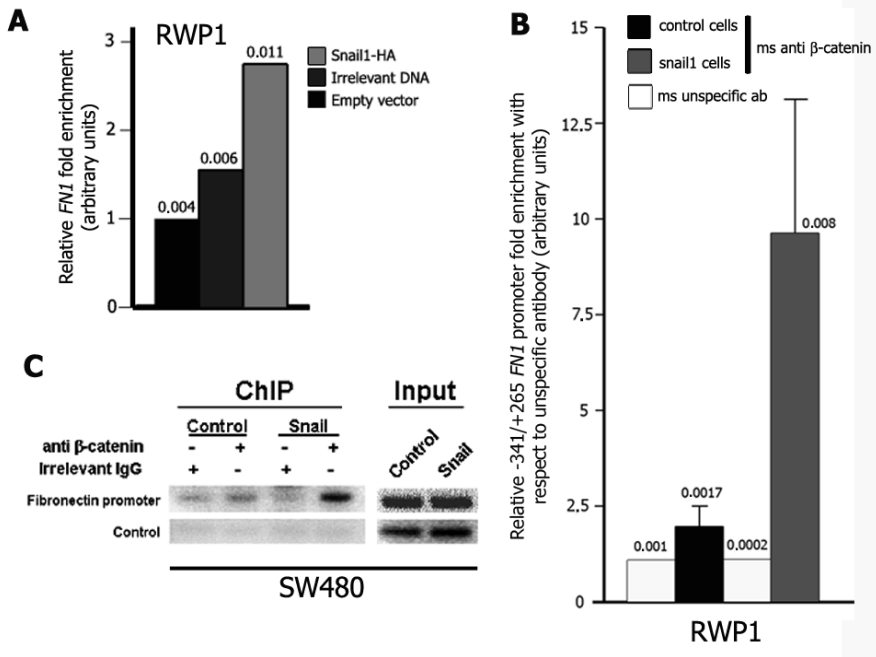
We next decided to assess if, even though TCFs were not involved in snail1-induced transcriptional activation of *FN1* and *LEF1* promoters, β -catenin was binding to

the *FN1* promoter. We performed ChIP assays in two cell lines: RWP1 and SW480. We transiently transfected RWP1 wild type cells with a vector containing snail1-HA cDNA, an irrelevant cDNA-HA tagged or the empty vector. After immunoprecipitation of β -catenin with a specific mouse antibody (BD Transduction Laboratories) and purification of the DNA coprecipitated, PCR was performed to quantify the endogenous *FN1* promoter. As shown in **Figure R.15.A**, the amount of *FN1* promoter precipitated with β -catenin was enriched between two and three-fold in the presence of snail1 when compared to empty vector (corresponding to 0.011 % of input). We obtained similar results in RWP1 snail1-HA clones transfected with a vector containing the -341/+265 fragment of the *FN1* promoter. In this experiment, the immunoprecipitation of β -catenin in snail1 cells was highly enriched in -341/+265 *FN1* promoter when compared to an irrelevant mouse antibody (9-fold), while in control cells it was only slightly enriched (2-fold, **Figure R.15.B**).

For SW480 cells we used the stable clone for snail1 and control cells to perform ChIP assays and we analyzed the results by semiquantitative PCR. Again, it was observed that β -catenin bound to the *FN1* promoter in control and snail1 cells, though more immunoprecipitated DNA was detected in presence of snail1-HA (**Figure R.15.C**). No *FN1* amplification was observed when using an irrelevant mouse antibody or oligonucleotides to amplify an irrelevant DNA corresponding to a sequence in the polymerase II promoter (**Figure R.15.C**, IgG and control respectively). Thus, all ChIP results indicate that snail1 expression induces a low but reproducible β -catenin interaction with the *FN1* promoter, suggesting a transcriptional role for the protein in snail1-induced transcriptional activation.

Figure R.15. β -catenin binds *in vivo* to the *FN1* promoter. **A.** ChIP analysis with RWP1 cells transiently transfected with snail1-HA, irrelevant cDNA-HA or empty vector. Cells were lysed and the extracts immunoprecipitated with mouse antibody against β -catenin (BD Transduction Laboratories). *FN1* promoter was amplified by qPCR (see **E.P.7**). The number on each bar corresponds to the percentage of input immunoprecipitated in each case. This experiment is representative of a series of two. **B.** ChIP experiment performed in RWP1 stable clones for snail1. Control and snail1 cells were transfected with the -341/+265 *FN1* promoter and lysates immunoprecipitated either with unspecific mouse antibody or with mouse antibody against β -catenin (BD Transduction Laboratories). *FN1* promoter was amplified with specific oligonucleotides for the exogenous DNA (see **E.P.7**) and results compared to the binding with unspecific antibody. Numbers on bars correspond to the percentage of input immunoprecipitated in each case. Values presented are the mean +/- standard deviation of three independent experiments performed in triplicate. **C.** ChIP performed with anti- β -catenin antibody in SW480 stable transfectants for snail1 and control cells. Nuclear-enriched lysates were incubated with mouse β -catenin antibody (BD Transduction Laboratories) and endogenous *FN1* promoter amplified from the purified DNA with specific primers (continues)

(continues) (E.P.7). Semiquantitative analysis was performed. Amplification of polymerase II (Poll) promoter was used as negative control^{***}.



R.2.4 The +451/+560 region in the *LEF1* promoter is required for its snail1-mediated activation

We had demonstrated that β -catenin was necessary for snail1-induced transcriptional activation of the *FN1* and *LEF1* promoters even though LEF/TCF did not seem to be involved in such mechanism. Engelhard and collaborators had isolated a 110 bp sequence in the *LEF1* promoter (+451/+560) that was necessary to induce transcription upon Wnt stimulation; such sequence required β -catenin to be active, but not LEF/TCFs [218, 282]. Due to the similarities in both mechanisms, we decided to study if the WNT responsive element in the region +451/+560 of the *LEF1* promoter (WRE from now on) was required for snail1-induced activation of the *LEF1* promoter.

We constructed a mutant internally deleted for the WRE (as described in E.P.2) and transfected it into RWP1 wild type cells. In **Figure R.16.A** the activity of the mutant in the absence of snail1 is represented, which decreased more than 50 % compared to the full-length promoter (represented as 1). We next assessed the responsiveness of

^{***} Experiment kindly performed by Dr. Sandra Peiró

the WRE-deleted mutant to *snail1* and we observed that it could not be activated by *snail1*, displaying the same activity than the control with empty luciferase vector (represented as the reference value 1 in **Figure R.16.B**). These results, thus, suggest that *snail1* can activate transcription of *LEF1* promoter in a LEF/TCF-independent/ β -catenin-dependent manner probably through the region +451/+560. Nevertheless, since the mutation decreased the basal activity to 30% its normal rate, we cannot discard that by deleting the WRE we removed an element necessary for promoter activity.

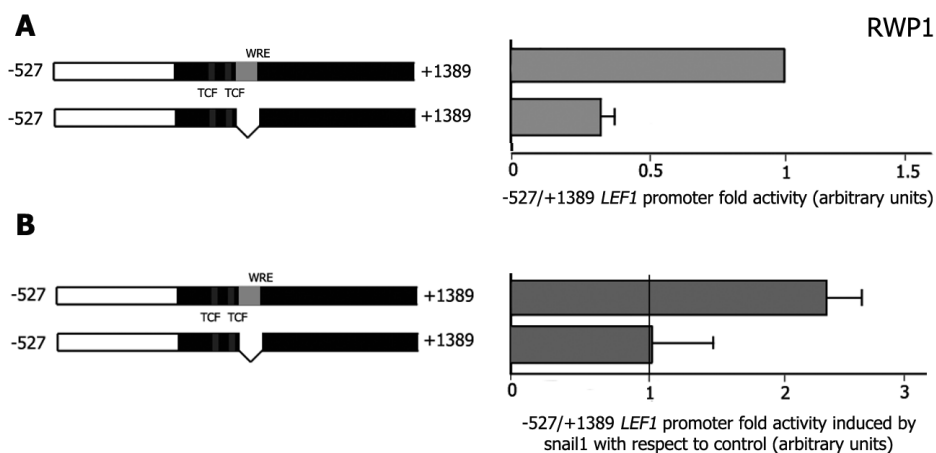


Figure R.16. Deletion of the +451/+460 region of the *LEF1* causes insensitivity of the promoter to *snail1*. Black matches regions downstream of the TSS. **A.** Basal activity in reporter assays of the WRE-deleted mutant compared to wild type promoter after transfecting RWP1 cells with 100 ng of each promoter. Activity of the wild type promoter is taken as the reference value of 1. **B.** *Snail1*-induced activity of wild type and deleted promoter. 150 ng of RSVneo-*snail1* or empty vector were cotransfected with 100 ng of promoter. Values are referred to the activation of each promoter when cotransfected with RSVneo empty vector (represented as 1, vertical line). Presented values are the mean \pm standard deviation of six independent experiments performed in triplicate.

R.2.5 The -341/-323 region of the *FN1* promoter is required for *snail1*-induced transcriptional activation

Contrarily to the *LEF1* promoter, no sequence mediating transcription in a β -catenin-dependent/TCF-independent fashion had been described in *FN1*. As a consequence we decided to truncate the -341/+265 *FN1* promoter to delimitate the *snail1*-responsive elements (snaRE from now on) in it. We constructed three shortened promoters by PCR amplification (see **E.P.2**): -192/+265, -36/+265 and -341/+72 and studied both their activity in the absence of *snail1* and their responsiveness to *snail1* in RWP1 cells.

When we studied the basal activity of the deleted promoters compared to the full-length *FN1* promoter (activity represented as 1) we observed that two repressor regions appeared to be contained in the -341/+265 *FN1* promoter. One of such regions was located at 5', since deletion of bases -341/-193 increased by ten-fold the activity of the promoter. The other repressor region was placed between bases +72 and +265, since the -341/+72 promoter had a basal activity of around 75-fold the basal activity of the full-length promoter (**Figure R.17.B**). Upon *snail1* cotransfection with the three promoters, we observed that the only promoter activated by *snail1* was the -341/+72 (**Figure R.17.C**).

With these results we can discard the +72/+265 region of the *FN1* promoter (as well as the probable repressor binding there) as required for the activation mediated by *snail1*. In addition, we can conclude that the sequence located between -341 and -192 is required for *snail1*-mediated activation of the *FN1* promoter. However, data obtained with the experiments of activity in absence of *snail1* also raise the possibility that, to enhance transcription, *snail1* needs to displace a repressor from -341 to -192.

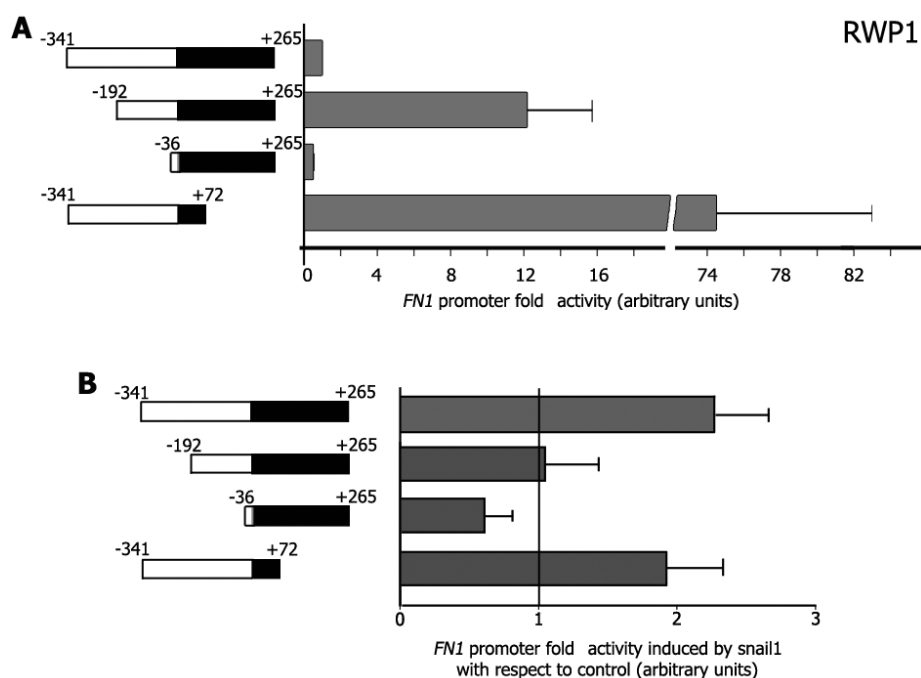


Figure R.17. The *snARE* in the *FN1* promoter is delimited to -341/-192. Black matches regions downstream of the TSS. **A.** Basal activity measured in reporter assays of 100 ng of several *FN1* promoters transfected into wild type RWP1 cells compared to -341/+265 *FN1* promoter (and represented as 1). **B.** *Snail1* induced transcriptional activity of wild type and shortened promoters. RWP1 wild type cells were cotransfected with 100 ng of promoter and either 5 ng of pcDNA3-*snail1*-HA or empty vector. Luciferase activity was measured (continues)

(continues) and activity upon snail1 cotransfection was related to that of the promoters when cotransfected with empty pcDNA3 (represented as 1, vertical line). Results displayed are the mean of five independent experiments performed in triplicate +/- standard deviation.

We next tried to narrow a little more the snaRE in the *FN1* promoter, which we had delimited to be between -341 and -192. We designed new primers to amplify three more fragments of the *FN1* promoter which were: -322/+265, -308/+265 and -278/+265. As before, we transfected them into wild type RWP1 and checked their basal and snail1-induced activity. We observed that their activation in the absence of snail1 was higher than that of the full-length promoter in all cases (between eighteen and thirty-fold, **Figure R.18.A**), what delimited a putative repressor in the region -341/-323. To our surprise, none of the deleted promoters retained the responsiveness to snail1 (**Figure R.18.B**), narrowing the snaRE to the region -341/-323. These results indicate that the same region in the *FN1* promoter required for snail1-induced activation, which is 18 bp long, binds a repressor complex.

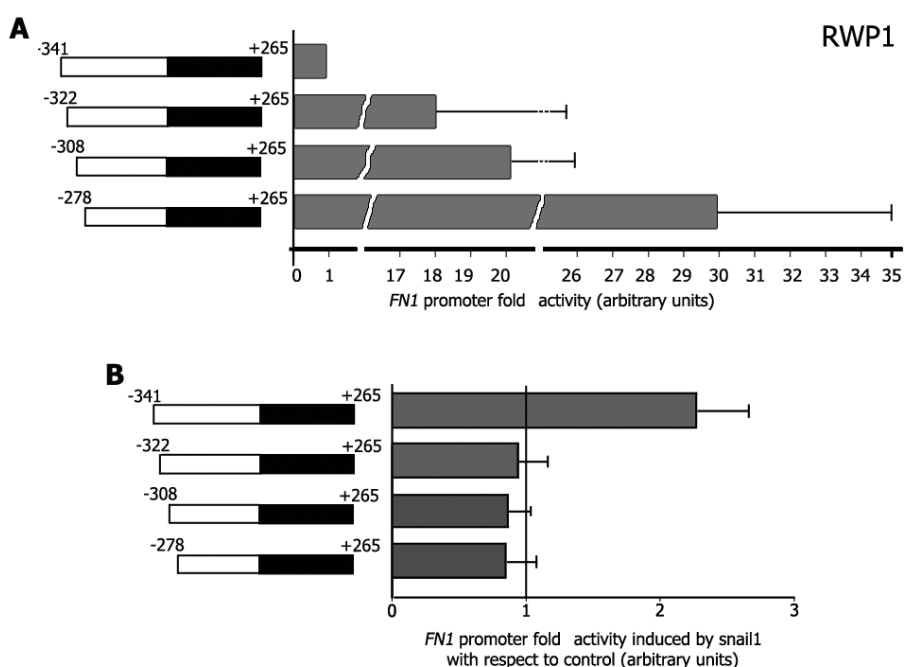


Figure R.18. The snaRE in the *FN1* promoter is delimited to -341/-323. Black indicates regions downstream of the TSS. **A.** Basal activity measured in reporter assays performed with wild type RWP1 cells and 100 ng of the -322/+265, -308/+265 and -278/+265 *FN1* promoters. Activity is compared to that of the -341/+265 *FN1* promoter, represented as 1. **B.** Snail1 induced transcriptional activity of wild type and shortened promoters. Reporter experiments were performed with RWP1 wild type cells. Cotransfection was carried out with 100 ng of each promoter, separately, and either 5 ng of pcDNA3-snail1-HA or empty vector. Values have been related to activity of the promoters when cotransfected with empty pcDNA3 (taken as 1, vertical line). Results displayed in all cases are the mean of four independent experiments performed in triplicate +/- standard deviation.

R.2.6 The p300 binding motif in *FN1* and *LEF1* promoters is irrelevant for snail1-induced activation

Provided that one region required for snail1 activation had been isolated in each promoter (+451/+560 in *LEF1* and -341/-323 in *FN1*), and considering the possibility of a common mechanism to activate transcription, we analyzed these sequences with specific programs that recognize transcription factors binding motifs (see **E.P.11**). One transcription factor was found to have the ability of binding both regions: p300. p300 (and CBP, a highly similar protein) is a global transcriptional coactivator involved in the regulation of several DNA-binding transcriptional factors [283]. Although p300 has been traditionally described as a histone acetyltransferase [283-287], it has also been demonstrated to bind DNA [288, 289]. We aligned a putative consensus motif for p300 with the regions in *FN1* and *LEF1* promoters predicted to bind such transcription factor (**Figure R.19.A**).

To analyze the putative relevance of the p300 binding sequence, we checked the conservation of the motif by aligning *LEF1* and *FN1* promoters with their respective homologues in other species. For *LEF1* no apparent conservation was found for the p300 motif (**Figure R.19.B**). In the case of *FN1* only the first base was strongly conserved (**Figure R.19.C**). Despite the fact that alignments pointed at the p300 sequence as a non-conserved sequence (what probably meant that it was not relevant), the little information regarding p300 DNA binding motif added to the quite variable sequences for p300 binding described in [289] prompted us to investigate if this protein had a role in snail1-mediated activation of *FN1* and *LEF1* promoters.

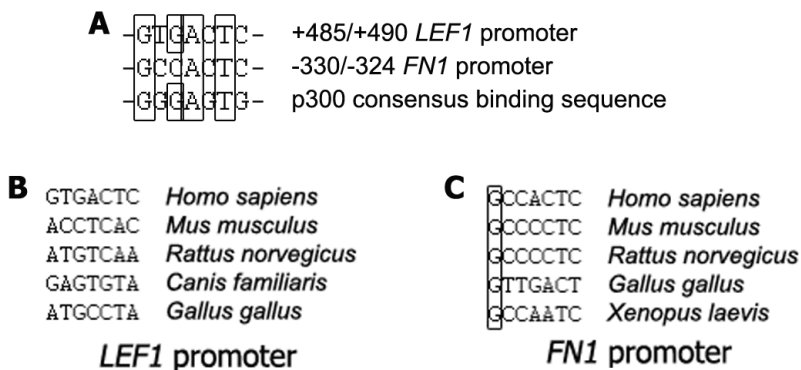


Figure R.19. The region +485/+490 of the *LEF1* promoter and -330/-324 of the *FN1* promoter have a little conserved p300 binding motif. **A.** Alignment of both p300 boxes with a putative consensus motif for p300 [289]. Bases equal to the consensus are boxed. **B.** Alignment of *LEF1* promoter with its homologues in other species. **C.** Alignment of *FN1* promoter with its homologues in other species. Equal bases are boxed.

To investigate the involvement of p300 in snail1-mediated activation, we proceeded to the mutation of the boxes (**Figure R.20.A**) and assayed the basal activity of the mutants (compared to that of the wild type promoters) as well as their responsiveness to snail1 using reporter experiments in RWP1 cells. **Figure R.20.B** shows the effect of the mutation in absence of snail1. The mutation of the p300 box in *FN1* promoter caused a decrease of about 60 % compared to wild type promoter (upper bars), while for *LEF1* it was only of around 30 % (lower bars). When we cotransfected the promoters with snail1 we observed no difference in *FN1* (**Figure R.20.C**, upper bars) or *LEF1* (**Figure R.20.C**, lower bars) between the activity of the p300-mutated box and wild type promoters compared to the activity when cotransfected with empty vector (represented as 1, vertical line). The results were conclusive: although the mutation had some effect in basal activity of the promoters, the p300 binding site was not involved in snail1-induced activation of *LEF1* and *FN1* promoters.

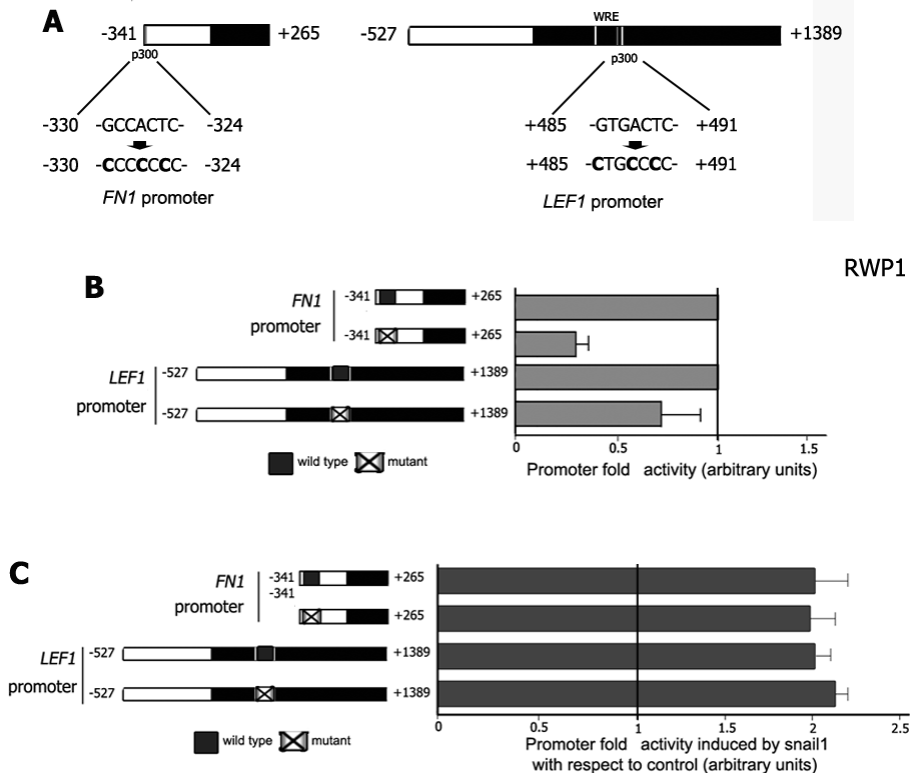


Figure R.20. p300 motifs in +485/+490 of *LEF1* promoter and -330/-324 of *FN1* promoter are not involved in snail1-induced activation of such promoters. Black indicates sequence downstream of the TSS. **A.** Mutations introduced to p300 boxes (bold) in each one of the two promoters. **B.** Activity in RWP1 wild type cells of 250 ng of mutant promoters (*FN1* and *LEF1*) was examined in reporter experiments and compared to wild type promoters (*FN1* and *LEF1*, respectively, represented as 1, vertical line) in the absence of snail1. Equivalent (continues)

R.2.7 Snail1 modulates protein interaction with the -341/-320 region of the *FN1* promoter

We decided to further confirm the importance of the -341/-323 region of the *FN1* promoter in snail1-induced activation by analyzing whether this sequence had the capacity to bind protein complexes in such conditions. We performed electrophoretic mobility shift assays (EMSA) with nuclear extracts of cells stably transfected either with snail1-HA or with the backbone vector (pcDNA3) and a ³²P-labelled probe containing the region -341/-301 of the *FN1* promoter (**Figure R.21.A**).

We observed the formation of two complexes when the probe was incubated with extracts of control cells (**Figure R.21.B**, black arrowheads, lane 2 and also in lanes 5 and 8). The upper of these two complexes did not appear when the probe was incubated with extracts containing snail1, while a faint signal could be detected for the lower band (**Figure R.21.B**, black arrowhead, lane 3 and also in lane 9). We also observed the formation of a new complex when the probe was incubated with nuclear extracts of snail1 clones (**Figure R.21.B**, arrow, lane 3). When we added fifty fold cold probe to the mix with nuclear extracts of control cells, we observed that both complexes were competed, although the lower not completely (**Figure R.21.B**, compare lanes 5 and 6), what indicated specificity, at least of the upper complex. Competition was also observed when we added fifty-fold cold probe to compete with the complex formed with snail1 extracts (**Figure R.21.B**, compare lanes 9 and 10), stating the specificity of the band.

We next wanted to narrow, if possible, where, in this 40 bp (-341/-301), the snail1-induced complex was binding. To that aim we divided the probe into two halves: the first consisting of nucleotides -339/-320, where we had previously delimited the snaRE by reporter assays, and the second containing the region -322/-309 (**Figure R.21.A**). We incubated both probes, separately, with extracts either of RWP1 control cells or RWP1 cells stably expressing snail1.

We detected complexes in the probe -339/-320 (**Figure R.21.C**, left panel); however, we did not observe the formation of any complex in the -322/-309 probe (**Figure R.21.C**,

(continues) results were obtained with 100 ng of promoter (data not shown). **C.** Reporter assay in which the snail1-induced activity of 250 ng of wild type and mutant promoters is represented. 5 ng of pcDNA3-snail1-HA or empty vector were cotransfected with the different promoters. Values are referred to the activity upon cotransfection of the promoters with empty pcDNA3 (taken as 1, vertical line). Equivalent results were obtained with 100 ng of promoter (data not shown). Results displayed in all cases are the mean of, at least, three independent experiments performed in triplicate +/- standard deviation.

right panel). The pattern of complexes appearing in the -339/-320 probe when incubated with nuclear extracts of control cells was different than in the longer -341/-301 probe since only one of the two complexes observed in extracts of control cells was detected (**Figure R.21.C**, black arrowhead, lane 2). On the other hand a complex was observed to be produced in the extracts of snail1 cells (**Figure R.21.C**, arrow, lane 3).

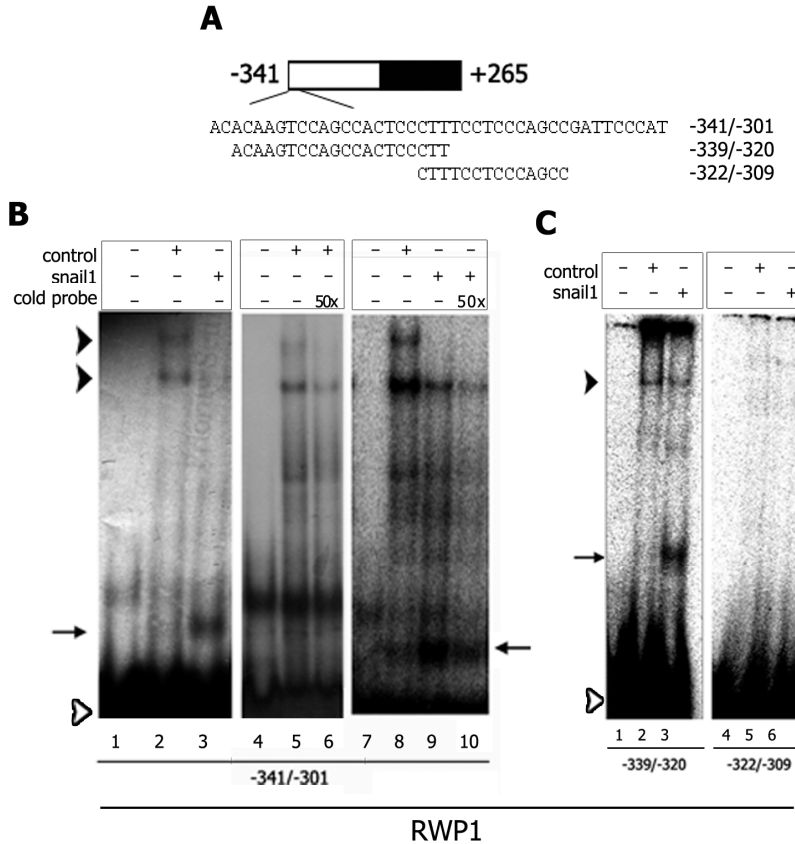


Figure R.21. Snail1 modulates complex formation in the region -339/-320 of the *FN1* promoter. **A.** The three probes used of the *FN1* promoter sequence used for the assay. **B.** EMSA was performed with the -341/-301 region of the *FN1* promoter as described in **E.P.8**. Black arrowheads indicate complexes forming in extracts of control cells (lanes 2, 5, 6 and 8), arrow indicates the complex formed in extracts of snail1 stable clones (lanes 3, 9 and 10), white arrowhead indicates the migration of the free probe. Competition was performed in lanes 6 (control cells) and 10 (snail1 cells) with fifty-fold cold probe. Lanes 1, 4 and 7 correspond to probe alone. The pictures displayed are representative of, at least, three independent experiments. **C.** EMSA was performed either with the -339/-320 region of the *FN1* promoter (left panel) or the -322/-309 region (right panel) as described in **E.P.8**. Black arrowhead indicates the complex formed in extracts of control cells (lane 2), arrow indicates the complex formed in extracts of snail1 stable clones (lane 3). White arrowhead indicates the migration of the free probe. Lanes: 1 and 4, probe only; 2 and 5, probe + control cells nuclear extracts; 3 and 6, probe + snail1 cells nuclear extracts. The pictures displayed are representative of, at least, three independent experiments.

These data suggest that a repressor complex binds to the -339/-320 region of the *FN1* promoter in control cells, consistent with previous observations in reporter assays. This repressor complex may be released/displaced upon *snail1* expression, causing the formation of another complex, which would be involved in transcriptional activation.

From previous BOPA experiments we had concluded that, though *snail1* was capable of binding to the -341/+265 *FN1* promoter (see **Figure R.8**), it could not do so in a direct manner (see **Figure R.6**). In addition, we had confirmed binding of *snail1* to the *FN1* promoter in several cell lines (by ChIP experiments *in vivo*, see **Figure R.9**). The presence of the shift observed in EMSA experiments in the region -339/-320, which we had identified as *snaRE* in such promoter by reporter assays (**Figure R.18**), made us wonder if *snail1* was binding there.

We carried out new EMSA assays in which we incubated the -339/-320 *FN1* probe with purified GST-*snail1*-HA and nuclear extracts of RWP1 control cells (which did not have *snail1*) as a source for possible *snail1* partners. We expected to see a retarded complex if *snail1* was binding to the probe through a bridge protein already present in the extracts of control cells. As negative controls for *snail1* binding, we incubated on one hand, GST or GST-*snail1*-HA directly with the -339/-320 *FN1* probe and, on the other, GST with nuclear extracts of RWP1 control cells.

We observed no complex formation in any of the lanes corresponding to the negative controls, neither when the probe was incubated with GST or GST-*snail1*-HA (**Figure R.22**, lanes 2-3 and 4-5 respectively) nor when we incubated extracts of control cells with recombinant GST protein (**Figure R.22**, lanes 7-8). No complex could either be appreciated when we incubated nuclear RWP1 control cells extracts with recombinant GST-*snail1*. The detection of a complex in the positive control (performed by incubating the *FN1* probe with nuclear extracts of RWP1 *snail1* stable transfectants, **Figure R.22**, lane 11) made us conclude that *snail1* cannot bind to the -339/-320 by binding to a nuclear protein of RWP1 control cells. These results, thus, discard a simple model in which *snail1* interacts with a protein to bind to this region, suggesting an event (maybe protein activation, redistribution, stabilization or others) prior to transcriptional activation, which would assist *snail1*-induced activation of the *FN1* promoter.

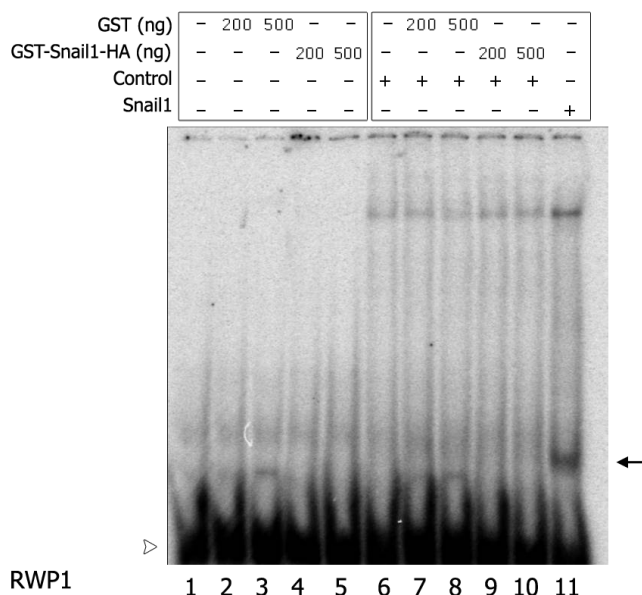


Figure R.22. Snail1 presence is not enough to induce complex formation in -339/-320 *FN1* promoter. EMSA experiment was performed with the -339/-320 *FN1* probe as detailed in **E.P.8**. Lane 1 corresponds to probe alone. For the left half of the image (lanes 2-5) the indicated amount of recombinant GST (lanes 2, 3) or GST-snail1-HA (lanes 4, 5) were incubated with probe alone. For the right half nuclear extracts of RWP1 control cells were also added to the reaction mix (lane 6 for only extracts, lanes 7 and 8 for extracts + GST, 9 and 10 for extracts + GST-snail1-HA). As positive control, nuclear extracts of snail1-HA RWP1 stable transfectants were used on the same probe. Arrow indicates the complex formed in snail1 cells. White arrowhead indicates the migration of the free probe. The image is representative of two independent experiments.

R.2.8 Neither snail1 nor β -catenin bind to the -341/-301 *FN1* promoter

We next wanted to study if snail1 was taking part of the complex appearing in the EMSA experiments by using a specific antibody against snail1 (see **E.P.8**). We performed new EMSA experiments and incubated the -341/-301 *FN1* probe either with mouse unspecific antibody, as control, or mouse specific antibody against snail1 prior to the addition of the nuclear extracts. No changes could be appreciated in the formation of the complex neither when unspecific antibody was used nor when the mix was incubated with specific antibody against snail1 (**Figure R.23**, lanes 7-8 and 5-6 respectively). We obtained the same result when we used rat antibody against HA (Roche, data not shown). These results suggest that snail1 is not binding to the -341/-301 region of the *FN1* promoter.

Several observations in the previous experiments had pointed at β -catenin as necessary to mediate snail1-induced transcriptional activation: (1) β -catenin knock-

down prevents snail1 transcriptional activation of the *FN1* and *LEF1* promoters (**Figure R.13**); (2) β -catenin binds to the *FN1* promoter upon snail1 expression (**Figure R.15**). In addition, we had several signs indicating that an event prior to snail1-induced transcriptional activation was required to succeed in such process (**Figures R.10** and **R.22**). Since snail1 mobilizes β -catenin from the junctions by repressing E-cadherin, we figured out that an increase of the pool of β -catenin could be the previous requirement for snail1-induced transcriptional activation.

Given that β -catenin seemed to be a good candidate of being involved in the complex formed in the -339/-320 region of the *FN1* promoter, we repeated EMSA assays attempting to detect the presence of the protein with specific mouse antibody against β -catenin (BD Transduction Laboratories). Results, displayed in **Figure R.23**, lanes 10 and 11, showed no changes in the shift of the complex. With these observations we concluded that β -catenin, the same as snail1, was not part of the complex forming in the -339/-320 *FN1* promoter.

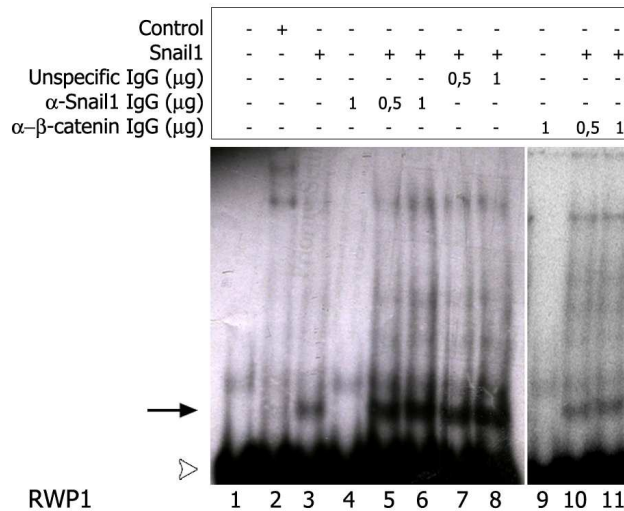


Figure R.23. Snail1 and β -catenin are not part of the complex induced by snail1 on -341/-301. EMSA was repeated with the -341/-301 *FN1* probe as before (**E.P.8**). Lane 1 corresponds to probe alone; lane 2 to probe incubated with nuclear extracts of control cells; lane 3 to probe incubated with nuclear extracts of snail1 cells. The indicated amount of non-specific mouse antibody (lanes 7 and 8), mouse specific antibody for snail1 (lanes 4-6) or mouse specific antibody against β -catenin (lanes 9-11) were added to the reaction after a 20-minute incubation of RWP1-snail1-HA nuclear extracts and the *FN1* -341/-301 probe. Same results were obtained when the incubation of the antibodies with the probe was performed before the addition of the nuclear extracts. For lanes 4 and 9, specific mouse antibody against snail1 or β -catenin, respectively, were incubated with the probe. White arrowhead indicates the migration of the free probe. Arrow indicates the specific complex formed in RWP1-snail1-HA extracts. The pictures displayed are representative of, at least, three independent experiments.

R.2.9 Regions isolated as snaRE in *LEF1* and *FN1* promoters (+451/+560 for *LEF1* and -341/-320 for *FN1*) are not sufficient to mediate snail1-induced transcription

The absence of β -catenin and snail1 binding to the region we had delimited as snaRE indicate that other regions than the -339/-320 in the *FN1* promoter are required for binding snail1 and β -catenin and, therefore, the region named as snaRE is probably not sufficient to mediate snail1 activation. We decided to check if this region conferred snail1 response when placed in *cis* with a minimal promoter insensitive to snail1. To that aim we cloned the region -341/-185^{§§§} of the *FN1* promoter in a pGL3* vector containing the minimal promoter of Thymidine Kinase (*TK*, see **E.P.2**) and analyzed the activity of the fused promoters in reporter assays performed with RWP1 cells. We expected to detect luciferase activity if the subcloned *FN1* promoter fragment was carrying all the requirements to mediate the activation by snail1.

Figure R.24.A shows that the activity of the -341/-185 region of *FN1* promoter was not modified by increasing amounts of snail1 (in comparison to increasing amounts of empty vector, taken as the reference value of 1). These observations indicate that, even though this region is required for snail1-induced transcriptional activation of the *FN1* promoter, another region in the promoter is required to fulfil such process. Since we had already discarded the region +72/+265 of the *FN1* promoter as required for snail1-induced transcriptional activation (**Figure R.17**), we can conclude that the additional region in the *FN1* promoter needed to mediate this phenomenon is placed between -210 and +72.

We also performed this experiment with the WRE of the *LEF1* promoter (+451/+560), isolated as the snaRE in this promoter, to examine if such region was sufficient to activate transcription upon snail1 stimulation. Similarly to what we observed for *FN1*, only background activation seemed to be detected upon snail1 cotransfection in RWP1 cells when compared to cotransfection with empty vector, which we defined as the reference value 1 (**Figure R.24.B**). With these results we conclude that, although the region +451/+560 of the *LEF1* promoter is required for the snail1-induced transcriptional activation, it is not enough to successfully mediate this process.

^{§§§} Note that this region is longer than the previously delimited snaRE. The reason is mainly practical because we had already cloned this promoter and decided to test it before trying to clone another fragment.

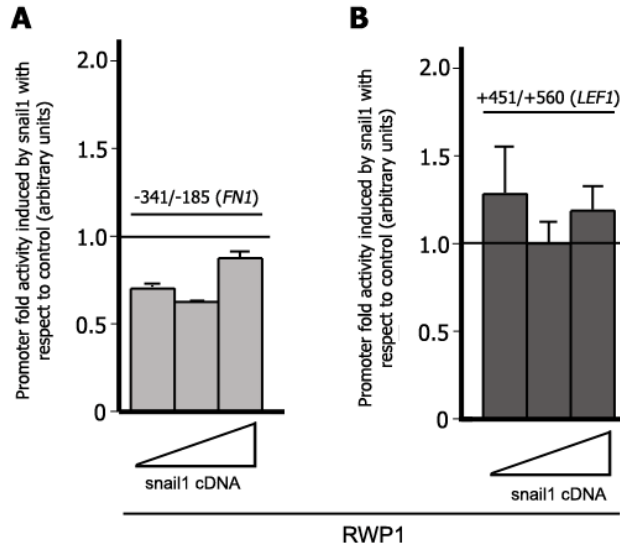


Figure R.24. The regions isolated in the *FN1* promoter and the *LEF1* promoter as *snaRE* are not sufficient to mediate *snail1*-induced transcription. **A.** The promoter activity of the -341/-185 *FN1* fragment cloned in pGL3**TK* was assessed by reporter assays in RWP1 cells. Activity of 100 ng of promoter upon cotransfection with increasing amounts of RSVneo-*snail1*-HA (100 ng, 150 ng and 200 ng) was referred to the activity of the promoter cotransfected with the same amounts of empty vector, taken as 1 (horizontal line). **B.** The promoter activity of the +451/+560 *LEF1* fragment cloned in pGL3**TK* was assessed by reporter assays in RWP1 cells. Activity of 100 ng of promoter upon cotransfection with increasing amounts of pcDNA3-*snail1*-HA (1 ng, 5 ng and 10 ng) was referred to the activity of the promoter cotransfected with the same amounts of empty vector, taken as 1 (horizontal line). Results displayed are the average +/- standard deviation of, at least, three independent experiments.

R.3 NF- κ B COOPERATES WITH SNAIL1 TO ACTIVATE TRANSCRIPTION

So far we have described a mechanism for snail1-induced transcriptional activation that requires snail1 binding to the DNA in an indirect fashion. The data presented in the previous chapters also point at a β -catenin-dependent/TCF-independent system to mediate such activation; however, we do not know if β -catenin and snail1 form a complex to induce transcription. In the previous sections we also delimited one snail1 responsive element in each the -527/+1389 *LEF1* promoter and -341/+265 *FN1* promoter. We have also demonstrated that for both promoters, regions other than the delimited as snaRE are required for snail1-induced activation. Furthermore, in the case of *FN1* we have also described that neither snail1 nor β -catenin appear to bind to the snaRE we delimited. In this chapter we focus in this unknown region of the *FN1* promoter that binds snail1 in an indirect way and we try to decipher the mechanism required for such binding and consequent promoter transcriptional activation.

R.3.1 Snail1 binds to the region -36/+265 of the *FN1* promoter

With the aim to have a better idea of the region to which snail1 was binding in the *FN1* promoter, we decided to perform BOPA assays with two fragments of the *FN1* promoter with exclusive sequences. We amplified by PCR (with sense oligonucleotides labelled with biotin) the two halves of the -341/+265 promoter: -341/-37 and -36/+265 (**Figure R.26.A**) and used them as probes for the assays.

Consistent with the previously performed BOPA assays (**Figure R.8**), we extracted protein from SW480-snail1-HA cells and incubated them either with the -341/+265, the -341/-37 or the -36/+265 *FN1* probes; we analyzed pulled-down snail1-HA by western blot with rat specific antibody against HA (Roche). As positive control for snail1-pull-down we used the same fragment of the *CDH1* promoter containing E-box 1 we had used before (-92/-64). As we had previously described, we observed that snail1 precipitated with the -341/+265 *FN1* promoter (**Figure R.26.B** lane 3). When we examined the two halves of the promoter, we observed that the fragment -341/-37 precipitated a small amount of snail1 (**Figure R.26.B** lane 4), however, this amount was comparable to the levels of snail1 precipitated in the negative control, performed without DNA (**Figure R.26.B** lane 2).

On the other hand, we detected great amount of snail1-HA pulled-down with the fragment -36/+265 of the *FN1* promoter (**Figure R.26.B** lane 5). When we compared the quantity of DNA used of each promoter by loading equal amounts (see **E.P.6**) in a DNA electrophoresis gel, we observed that we used much more DNA of the fragment -341/-37, to which we detected no binding (**Figure R.26.C**). With these results, we concluded that snail1 binding occurs in the region -36/+265 of the *FN1* promoter. In addition, this data confirms the EMSA results that indicate that the -341/-323 region, delimited as snaRE, is not responsible for snail1 binding to the *FN1* promoter.

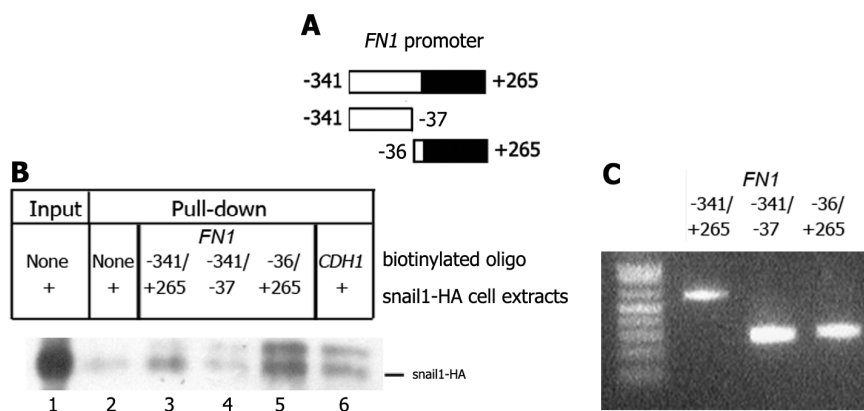


Figure R.25. Snail1-HA coprecipitates with the -36/+265 fragment of the *FN1* promoter. **A.** Schematic representation of the three probes used for this experiment. Black indicates regions downstream the TSS **B.** BOPA experiment in which the -341/+265, -341/-37 or -36/+265 fragments of the *FN1* promoter were incubated with total SW480-snail1-HA cell extracts (**E.P.6**). DNAs were pulled down with streptavidin-combined magnetic beads (NEB), samples loaded in a polyacrylamide gel and analyzed by western blot with rat antibody against HA (Roche, **E.P.10**). A probe containing E-box 1 from the *CDH1* promoter (-92/-64) was used as a positive control. 10 % of preincubated sample was stored and loaded as input. The picture is representative of a series of three independent experiments. **C.** Equal amounts (determined using a spectrophotometer) of DNA of the three probes were loaded in an agarose gel and stained with ethidium bromide.

R.3.2 NF- κ B is involved in snail1-mediated activation of mesenchymal genes

Since we had previously discarded the region +72/+265 of the *FN1* promoter as required for snail1-induced transcriptional activation (see **R.4**), we scanned the sequence between -36 and +72 searching for motives susceptible of transcription factor binding (see **E.P. 11**). The finding of an NF- κ B box located at +35/+48 caught our attention because of the previously described link between NF- κ B and transcriptional activation of mesenchymal genes in some EMT processes (see **I.4.6**). There was also evidence in a previous article of an NF- κ B box in the *FN1* promoter involved in its transcription under certain stimuli [290]. However, this box was located at -41, and

since we had observed that snail1 binding was taking place downstream -36, we considered that the box at -41 was not relevant for the mechanism of our investigation. Even though no exact motif had been identified, there were other evidences linking NF- κ B with activation of *FN1* transcription [291, 292] as well as other mesenchymal genes such as MMPs [245-248], ZEB1 [265] and even *SNAIL1* [123]. All this evidence prompted us to investigate if NF- κ B signaling was participating in snail1-induced transcriptional activation.

Before analyzing the relevance of the +35/+48 box, we studied if snail1 had the ability to activate NF- κ B transcription. To that aim we performed reporter assays to examine the luciferase activity of an NF- κ B reporter construct, called *NF3*, which contains three consensus binding sequences for NF- κ B upstream the luciferase gene (see **E.P.2**). We transfected RWP1 stable transfectants for snail1-HA, snail1-P2A-HA or control cells with *NF3* and we used *FN1* and *LEF1* promoters as positive controls for snail1-induced transcription. We observed the same pattern upon snail1 expression for the three genes, which were activated between 1.8 and 2.5-fold in snail1 stable transfectants while they were not induced in snail1-P2A transfectants (**Figure R.26.A**). When we examined *NF3* activity in SW480 clones, we also detected an increase of *NF3* activity when comparing snail1 transfectants with control cells (**Figure R.26.B**). Interestingly, *NF3* activity was severely reduced when adherens junctions formation was forced, in SW480 E-cadherin clones, similarly to what we had observed for *FN1* and *LEF1* promoters**** and consistent with the lower amount of protein and mRNA detected in E-cadherin clones for fibronectin and LEF-1 when compared to control cells (see **Figure R.1**). With these evidences, we concluded that snail1 had the ability to enhance transcription from an NF- κ B specific reporter construct, supporting a possible collaboration of these two pathways.

We next decided to investigate whether the *FN1* and *LEF1* promoters were sensitive to NF- κ B activity. We used a chimeric cDNA which had been previously described to activate NF- κ B sensitive promoters [123]. This construct combined the cDNA of the rel binding domain (responsible for DNA binding of the NF- κ B family members, see **I.4.6**) with the transactivation domain of the herpes simplex virus protein VP16, cloned into pcDNA3 (see **E.P.2**). We cotransfected *FN1* and *LEF1* promoters with increasing amounts of Rel-VP16 into SW480 wild type cells and

**** In a series of experiments performed by Cristina Agustí and collected in her PhD thesis entitled *Mecanisme d'activació de Fibronectina i LEF1 per Snail1 durant la transició epiteli-mesènquima*.

observed that both promoters responded in a dose-dependent manner to the addition of the fusion protein (**Figure R.26.C**). These data pointed at NF- κ B as a plausible factor in snail1-induced transcriptional activation of *FN1* and *LEF1* promoters.

To assess the involvement of the NF- κ B sequence in the *FN1* promoter in the activation mechanism induced by snail1, we mutated it (see **E.P.2**) to check whether the lack of NF- κ B binding affected snail1 transcriptional activity (**Figure R.26.D**). Since we confirmed that the mutations introduced conferred resistance to NF- κ B signaling to the promoter (see **E.P.2**), we transfected both -341/+265 *FN1* promoters (wild type and NF- κ B mutant) into HT29 M6 clones (control and snail1-HA) and studied their activity. We observed that the activity of the mutated promoter in the absence of snail1 was higher than the wild type, about forty-fold (**Figure R.26E**), suggesting that this sequence is involved in repressing basal *FN1* transcription in epithelial cells. When we studied the activation of both promoters in snail1 stable transfectants compared to control cells, we observed that the mutant was only partially activated (over 50 %, **Figure R.26.F**). Even though with these last results we could not discard that the lack of activation induced by snail1 observed in the mutant was due to saturation of its activation in non-snail1 conditions, all the data gathered strongly suggest that NF- κ B, through the +35/+48 box, is a possible candidate to collaborate in the snail1-induced transcriptional activation of the *FN1* promoter.

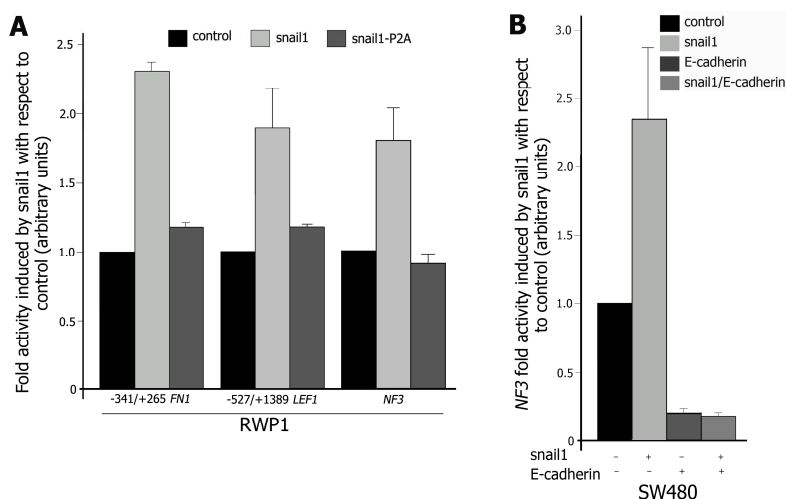
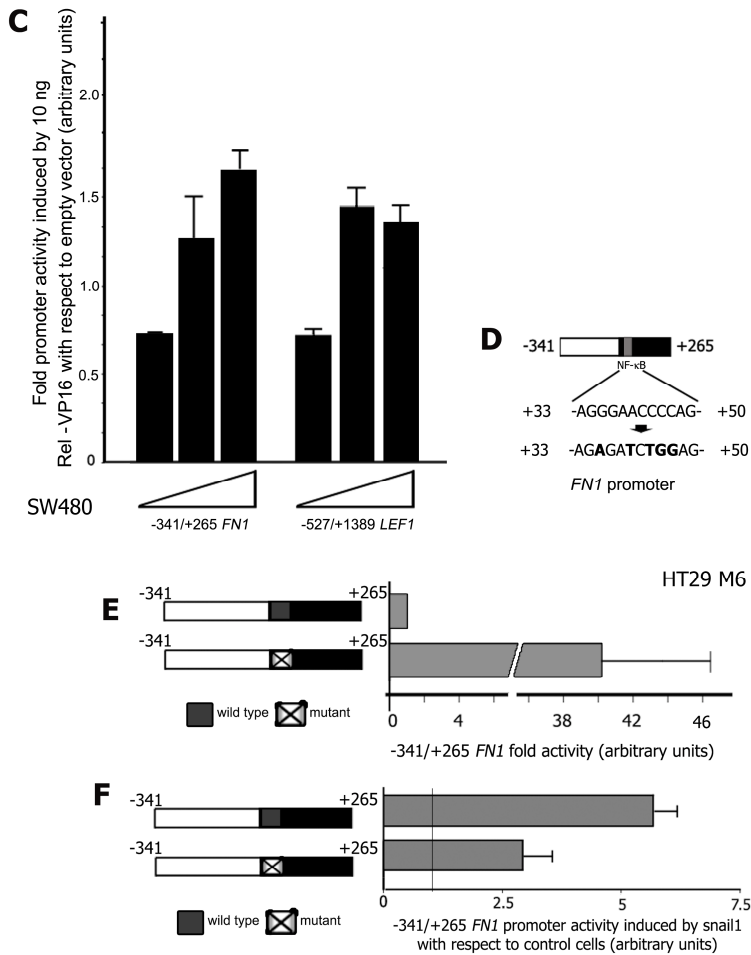


Figure R.26. Snail1 and NF- κ B cooperate to activate transcription. **A.** *NF3* is activated by snail1 in reporter assays. 100 ng of *NF3*, -341/+265 *FN1* or -527/+1389 *LEF1* promoters were transiently transfected into RWP1 control, snail1-HA or snail1-P2A-HA stable transfectants. *FN1* and *LEF1* promoters were used as positive controls. Values are referred to the activity of the promoters in control cells. Results displayed are the average \pm standard deviation of three independent experiments performed in triplicate. **B.** Snail1 and E-cadherin (continues)



(continues) modulate NF- κ B transcriptional activity. The activity of an *NF3* was determined by reporter assays in SW480 cells stably transfected with snail1-HA, E-cadherin or both as well as control cells. Values are referred to the activity of the promoters in control cells. Results displayed are the mean \pm standard deviation of three independent experiments performed in triplicate. **C.** *FN1* and *LEF1* promoters are activated by VP16-Rel. SW480 cells were cotransfected with several amounts of the *FN1* and *LEF1* promoters (100 ng, 250 ng or 500 ng) and 10 ng of VP16-Rel in reporter experiments. Values are referred to the activity of the promoters upon cotransfection with empty pcDNA3. Results are the mean \pm standard deviation of a series of two independent experiments performed in triplicate. Equivalent results were obtained when cotransfecting 25 ng of VP16-Rel (data not shown). **D.** Schematic representation of the *FN1* promoter where localization of the NF- κ B box is indicated (around +40 bp). Mutations introduced are also displayed (bold). **E.** The NF- κ B mutant *FN1* promoter displays forty-fold activity in the absence of snail1 compared to the wild type *FN1* promoter as measured by reporter assays. 500 ng of each promoter were transfected into HT29 M6 control cells and luciferase activity analysed. These results are the mean \pm standard deviation of a series of two independent experiments performed in triplicate. **F.** Snail1 activates transcription of the wild type *FN1* promoter two-fold compared to the NF- κ B box mutant promoter. 500 ng of each promoter were transfected into HT29 M6 stable clones for snail1 as well as control cells and their activity measured in reporter experiments. Values are referred to the activity of the promoters in control cells (taken as 1, vertical line). Results displayed are the mean \pm standard deviation of a series of two independent experiments performed in triplicate.

R.3.3 p65/RelA binds to the +35/+48 box in the *FN1* promoter

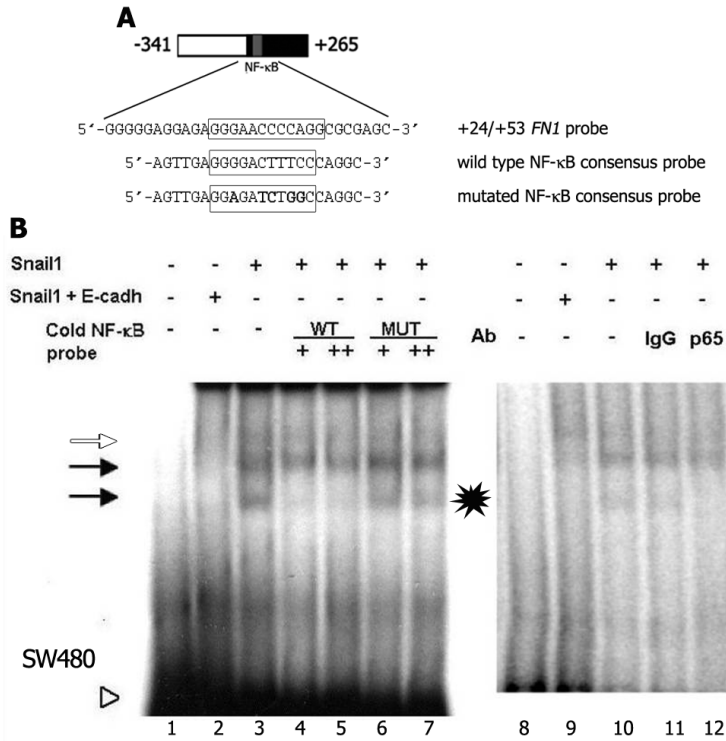
With the aim to confirm that NF- κ B was binding to the +35/+48 box in the *FN1* promoter in the presence of snail1, we performed EMSA experiments with SW480-snail1-HA and SW480-snail1-HA/E-cadherin cells nuclear extracts and the region +24/+53 of the *FN1* promoter as probe (see **Figure R.27.A**). We detected two major retarded bands generated by incubation of the *FN1* probe with nuclear extracts of SW480-snail1-HA cells (**Figure R.27.B**, arrows, lanes 3 and 10), but none of these two bands was observed in SW480-snail1-HA/E-cadherin cells (**Figure R.27.B**, upper arrow, lanes 2 and 9). A third band much less intense was detected in the different EMSA experiments performed and is indicated with a white arrow.

When we added to the reaction mix 50 or 100-fold excess of a cold probe containing a consensus box for NF- κ B (see **E.P.8**, **Figure R.27.A**) we observed competition with the faster migrating band (**Figure R.27.B**, lower arrow, lanes 4 and 5). However, when the probe used for competing had the consensus NF- κ B box mutated (**Figure R.27.A**), no competition was detected (**Figure R.27.B**, lower arrow, lanes 6 and 7). These observations pointed at NF- κ B as a likely factor to be part of the complex. When we added a specific antibody against p65/RelA to the reaction, we confirmed the presence of this member of the NF- κ B family in the faster retarded complex: in lane 11 and 12 of **Figure R.27.B** it can be observed that an irrelevant rabbit antibody did not have any effect on the fastest migrating band developed in snail1-HA cells, while a specific antibody for p65/RelA (Santa Cruz) prevented the formation of the complex. Since the upper band was not competed with the wild type NF- κ B probe or with the specific p65 antibody, we concluded that it did not correspond to the p65 complex.

These experiments confirm that p65/RelA binds to the *FN1* promoter through interaction with the consensus box at +35/+48 in snail1 cells. The observation that such complex is not formed with lysates extracted from snail1/E-cadherin cells suggests that E-cadherin prevents the formation of such complex.

Figure R.27. Snail1 causes and E-cadherin prevents p65 association to the *FN1* promoter. A. Schematic representation of the -341/+265 *FN1* promoter and the three probes used for the EMSA experiments where the NF- κ B motif is boxed; mutations introduced appear in bold. Black corresponds to regions downstream the TSS. **B.** Gel shift assays were performed as detailed in **E.P.8** with a probe corresponding to region +24/+53 of the *FN1* promoter, which contains an NF- κ B binding element (+35/+48). Nuclear extracts from SW480 cells stably transfected with snail1-HA (lanes 3-7, 10-12) or both snail1-HA and E-cadherin (lanes 2 and 9) were used. In the left panel, binding of the radioactive probe was competed with a 50- or 100-fold excess of non-radioactive probe containing a consensus binding element for NF- κ B (lanes 4-7), either wild-type (WT) or mutated (MUT). For the right panel, binding reaction was carried out (continues)

(continues) either with an irrelevant rabbit IgG (lane 11) or a specific rabbit antibody for p65 (Santa Cruz, lane 12). The arrows show the bands detected in this assay (white arrow indicates the faint signal of one band); the asterisk marks the specific band; the arrowhead indicates the migration of the free probe. Lanes 1 and 8 correspond to probe alone. These results are representative of four (right) or five (left) experiments.



R.3.4 Snail1 binds to the same *FN1* promoter sequence as NF-κB

Foreseeing a collaboration between snail1 and NF-κB we next decided to study if NF-κB was the DNA binding protein responsible for snail1 interaction with the *FN1* promoter. With that intention, we performed EMSA assays again with the +24/+53 *FN1* probe and tested the presence of snail1 in the complexes observed by adding a specific antibody to the reaction. In this case we used nuclear extracts from the four SW480 clones (control, snail1, E-cadherin and snail1/E-cadherin). We detected the three complexes previously indicated (**Figure R.27.B**) with snail1 extracts. These complexes were not observed or only slightly formed in E-cadherin cell extracts (**Figure R.28**, lanes 4 and 5). We attributed the more intensely detection of the higher complex (white arrow) in this experiment to the fact that the gel was better resolved and more exposed than the one in **Figure R.27**.

When we added to the reaction of snail1 extracts a specific antibody against snail1 we observed that the lower band disappeared, and also that the others suffered shifting, specially the middle band (**Figure R.28**, asterisk, lane 6). These phenomena were not observed when the antibody used was an irrelevant mouse one (**Figure R.28**, asterisk, lane 7). These results indicate that snail1 takes part in the complex formed by NF- κ B on the *FN1* promoter upon snail1-induced transcriptional activation and suggest the presence of another protein, represented by the middle complex, that may also mediate snail1 binding to this region.

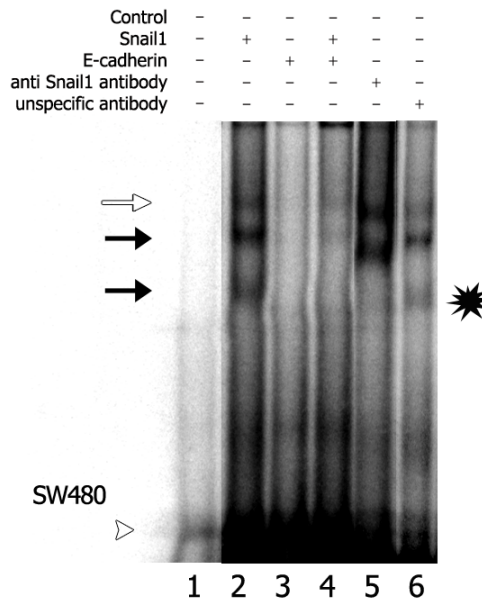


Figure R.28. Snail1 is part of the complex formed by p65. Gel shift assays were performed similarly as before with the addition of specific antibody against snail1. Nuclear extracts from SW480 cells stably transfected with snail1 (lane 2), E-cadherin (lane 3) or both snail1 and E-cadherin (lane 4) were used. For lanes 5 and 6 binding reaction was carried out either with an irrelevant mouse IgG (lane 5) or a specific mouse antibody for snail1 (lane 6). The arrows indicate the retarded bands observed (white arrow indicates the band only slightly observed in the previous experiment), while the asterisk shows the specific band detected with this assay; the arrowhead indicates the migration of the free probe. These results are representative of three experiments performed.

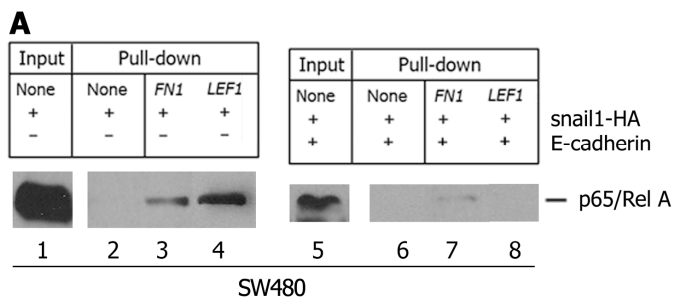
R.3.5 NF- κ B binds to the *FN1* promoter *in vivo* in snail1 cells

We next wanted to study if snail1 could induce *in vivo* p65/NF- κ B binding to the promoters. To that aim we analyzed by BOPA assays the ability of p65 to bind to the *FN1* and *LEF1* promoters in SW480-snail1 and SW480-snail1/E-cadherin cells. We observed that both *FN1* and *LEF1* promoters precipitated p65/RelA when incubated

with snail1-HA extracts (**Figure R.29.A**, left panel). However, only a faint signal was observed for *FN1* when incubated with extracts of SW480-snail1/E-cadherin cells (**Figure R.29.A**, left panel), in which *FN1* and *LEF1* expression is low (**Figure R.1**).

When we compared the input we observed that the amount of p65/RelA in the nuclear extract of SW480-snail1-HA was greater than in SW480-snail1-HA/E-cadherin (compare lanes 1 and 5 in **Figure R.29.A**). We performed an extract fractionation of all SW480 clones^{****} and we confirmed that the nuclear fractions of the E-cadherin clones had much less detectable p65/RelA than control and snail1 cells (**Figure R.29.B**), indicating that E-cadherin has a role in the subcellular distribution of p65/RelA.

Although the BOPA results had demonstrated that p65/RelA had the ability to bind to the -341/+265 *FN1* promoter, we wanted to confirm such binding in a more physiological system. We performed ChIP assays in all four SW480 clones because it would again illustrate if the sole presence of snail1 was enough to enhance p65/RelA binding to the *FN1* promoter or if E-cadherin prevented it. We incubated nuclear enriched extracts of the SW480 clones with specific rabbit antibody against p65/RelA (Santa Cruz) and amplified the *FN1* promoter precipitated with p65. The results shown in **Figure R.29.C** confirm what we had already observed in the BOPA assays: p65/RelA was capable of binding the *FN1* promoter in presence of snail1, but E-cadherin prevented such binding. Quantification of the *FN1* promoter precipitated indicated that snail1 extracts were enriched about thirty-fold in such DNA compared to E-cadherin cells (data not shown). This observation is somehow in accordance to what we had described in **R.1**, when we observed that E-cadherin forced expression in SW480 cells correlated with less fibronectin when compared to control or snail1 cells (**Figure R.1**).



^{****} In collaboration with Dr. M. Duñach's group, experiment performed by Dr. Guiomar Solanas

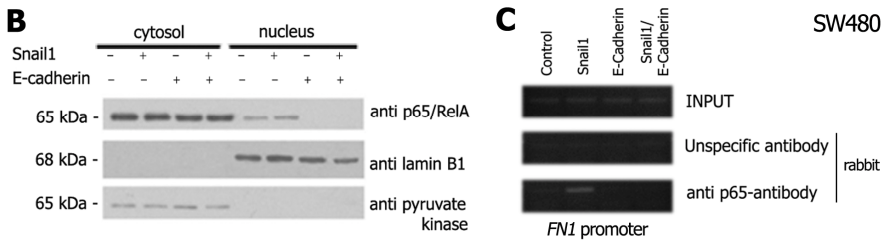


Figure R.29. p65 binds to the *FN1* and *LEF1* promoters in the presence of *snail1* and absence of E-cadherin. **A.** BOPA experiments were performed with nuclear extracts of SW480-*snail1*-HA or SW480-*snail1*-HA/E-cadherin cells and biotin-tagged DNA of each promoter (see **E.P.6**). DNA was precipitated with streptavidin-combined magnetic bead (NEB) and samples analyzed by western blot with rabbit specific antibody against p65/RelA (Santa Cruz). As negative control, protein was incubated with binding buffer but no DNA. 10 % of sample was preincubated (see **E.P.6**) and loaded as input. The pictures displayed are representative of a series of, at least, two independent experiments. **B.** E-cadherin prevents NF- κ B nuclear localization. Cell fractionation of SW480 cells was performed and the levels of p65/RelA analysed by western blot. Lamin B1 was used as nuclear marker, while pyruvate kinase was used as marker for the cytosolic fraction. **C.** Semiquantitative analysis of a ChIP performed with SW480 clones is shown. Nuclear-enriched extracts of the SW480 clones were incubated with rabbit anti-p65/RelA antibody (Santa Cruz) and washed as described in **E.P.7**. Equivalent results were obtained in RWP1 clones with endogenous and exogenous/transfected *FN1* promoter (data not shown). The picture displayed corresponds to one representative experiment out of three.

All the data gathered in this chapter strongly suggest that both NF- κ B and *snail1* form a complex on *FN1* promoter to achieve transcriptional activation and that this complex is disrupted by the presence of E-cadherin. In addition, the observations presented here are complimented by other experiments performed either in our laboratory^{****} or in collaboration with Dr. Mireia Duñach's group (UAB), which further support a collaborative role between NF- κ B and *snail1*. This relationship will be discussed later (**D.3**).

**** By Jelena Stanisavljevic

R.4 SNAIL1 MODULATES BINDING OF THE TRANSCRIPTION FACTOR CP2c (TCP2c) TO THE *FN1* PROMOTER

While trying to isolate the *snaRE* element in the -341/+265 *FN1* promoter, we narrowed a region that was required for *snail1*-induced transcriptional activation, located at -341/-323. In the present chapter, we focus on the transcription factor that could be binding to this sequence upon *snail1* induction, describing a new role for a protein that had not been previously related to EMT.

R.4.1 Two motives are responsible for the formation of the EMSA complex

With the objective to delimitate the DNA binding motif of the complex appearing in EMSA experiments with the -341/-320 *FN1* promoter probe, we designed a set of seven oligonucleotides of the same region of the promoter. Each of these seven probes carried three mutated bases (except for probe #7, which had four), which were mutated consecutively to cover all the -341/-320 region (**Figure R.30**). We pretended to use each of these seven oligonucleotides in EMSA assays to compete the complex we had previously observed in this promoter region in *snail1* cells (**Figures R.21, R.22, R.23**).

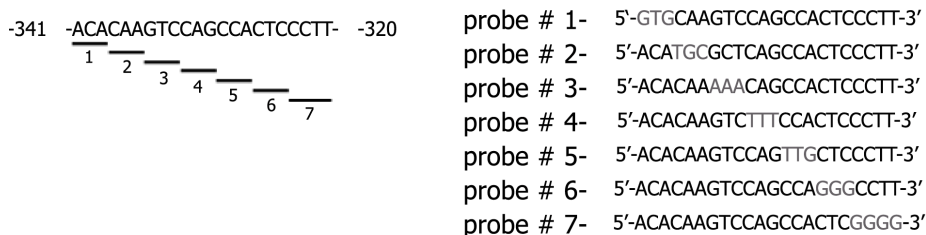


Figure R.30. Seven mutated probes were designed to compete the complex at -341/-320 in *snail1* cells. Original -341/-320 *FN1* promoter probe (left) with the indication of the triplets mutated (grey) and the number assigned to each new probe. On the right, the seven mutated probes designed (grey indicates the mutated triplets in each case). Each oligonucleotide (#1-7) was annealed with an antisense oligonucleotide to be used as cold dsDNA competitor.

We performed EMSA assays incubating the seven mutated double stranded oligonucleotides (fifty-fold, separately and unlabelled) with nuclear extracts of RWP1 *snail1* cells and ^{32}P labelled wild type -341/-301 probe (since we had observed stronger complex signal when using this probe than the -341/-320, see **Figure R.21.B-C**). We expected that, if a mutation was introduced to the motif required for the formation of the complex, no competition would take place. This result would indicate, at least, part of the DNA motif to which the complex was binding. We observed a subtle band

indicating little competition when we used the probe with the first three bases mutated (Figure R.31, lane 4, grey asterisk). This band seemed to be less competed with probes 4 and 6 (Figure R.31, lanes 7 and 9, black asterisks). The other probes appeared to compete the same as the wild type (Figure R.31, compare lane 3 with lanes 5, 6, 8 and 10). Although not very convincingly, these results provided us with six bases (-332/-330 and -326/-324) that could be involved in the formation of the complex.

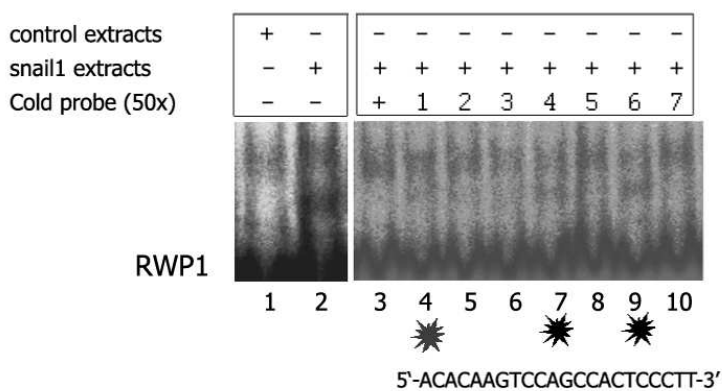


Figure R.31. Two motives are responsible for the complex formed in the -341/-320 region of the *FN1* promoter. EMSA with ^{32}P labelled -341/-301 *FN1* probe and 50X cold probe competition. In lane 2 appears the complex forming when incubating nuclear cell extracts of RWP1 snail1 cells; that complex does not appear in control cells (lane 1). For the first competed sample (lane 3) cold wild type -341/-320 probe was used, the rest were competed with the indicated mutated probe (lanes 4-10). The asterisks indicate the lanes where less (grey and black) competition was detected. Below the EMSA, the -341/-320 *FN1* promoter sequence is shown where the bases mutated in the probes that seem to have less ability to compete are underlined. The picture displayed is representative of a series of three.

R.4.2 TFCP2c binds to the *FN1* promoter *in vivo*

To have an idea if there was any protein with the ability to bind to the two delimited regions (and thus, to belong to the complex observed in the EMSA assays), we searched in the Transfac database (see E.P.11) for factors that recognized the -332/-324 region of the *FN1* promoter. We found out that the bases located at -333/-330 and at -326/-323 matched the consensus motif of a transcription factor named TFCP2c/LSF/LBP-1c, which belongs to the Grainyhead family of transcription factors and binds to spaced motives (Figure R.32.A, for review see [293]). When we searched for TFCP2c motives in the longer -341/-301 *FN1* promoter probe, we observed that a third motif was contained there (in Figure R.32.A the -341/-311 fragment of this probe is shown). The existence of this third box (located between -317 and -314) may explain why we observed the complex forming on this probe more intensely than in the

with the ones obtained in the EMSA experiments, indicated that TFCP2c was a transcription factor likely to be involved in snail1-induced transcriptional activation.

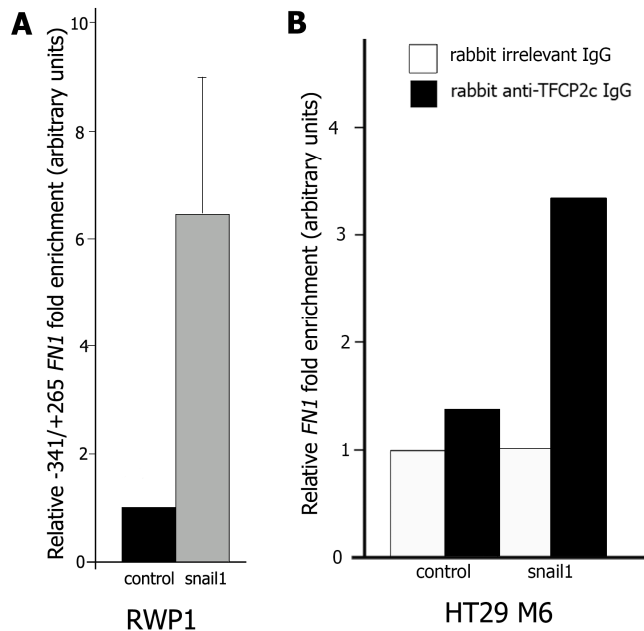


Figure R.33. TFCP2c binds to the *FN1* promoter. **A.** RWP1 cells stably expressing snail1 and control cells were transfected with the -341/+265 *FN1* promoter and lysates, nucleus enriched, incubated with rabbit specific antibody against TFCP2c (Abcam). Exogenous *FN1* promoter was amplified with specific primers and the levels of -341/+265 *FN1* promoter referred to the levels of an irrelevant DNA (see **E.P.7**). The graph represents the fold enrichment of the ratio *FN1*/irrelevant DNA in snail1 cells compared to control cells. The results displayed are the mean +/- standard deviation of four independent experiments. **B.** HT29 M6 clones were lysed and nuclear-enriched extracts incubated with rabbit either irrelevant or specific TFCP2c antibody (Abcam). Endogenous *FN1* promoter was amplified with specific primers amplifying to the region -375/-320. Levels of *FN1* promoter precipitated with specific antibody (■) were referred to the amount of *FN1* promoter precipitated with unspecific antibody (□), represented as 1). Results displayed are representative of a series of three equivalent experiments (performed with different amplicons and/or referred to irrelevant DNA) performed in triplicate.

R.4.3 TFCP2c function is required for snail1-induced activation of the *FN1* promoter

We next decided to study if the alteration of TFCP2c function affected fibronectin mRNA and protein levels. TFCP2c is a protein found as dimers in solution, yet it has been described to bind DNA either as a dimer or as a tetramer. With the aim of interfering TFCP2c DNA binding and subsequent transcriptional activation, we constructed a mutant that had not only been described to be unable to bind DNA but also to act as a dominant negative by inhibiting the DNA binding of wild type TFCP2c

when used at equimolar concentration (**Figure R.34.A**) [294]. We cloned the TFCP2c mutant, named TFCP2c Q234L/K236E, into a retroviral vector (pBABE, see **E.P.2**).

We infected RWP1 and HT29 M6 clones (control and snail1) with pBABE-TFCP2c Q234L/K236E-myc and lysed them after 48 hours of expression (see **E.P.9**). We analysed fibronectin protein levels (and TFCP2c Q234L/K236E-myc as infection control) in total cell extracts by western blot. We detected slight differences in fibronectin protein levels of RWP1 control cells infected with the dominant negative form of TFCP2c (**Figure R.34.B**, lanes 1 and 2). However, the quantity of fibronectin we observed in snail1 cells was much less if they had been infected with TFCP2c Q234L/K236E-myc (**Figure R.34.B**, compare lanes 3 and 4), indicating that TFCP2c was required for the increase of fibronectin protein in snail1 cells. The hypothesis that TFCP2c had a role specifically in snail1-induced transcriptional activation was reinforced by the fact that control cells expressed higher levels of the dominant negative form of TFCP2c than snail1 cells (**Figure R.34.B**, compare lanes 2 and 4).

When we analyzed fibronectin protein levels in HT29 M6 cells we observed similar effects than in RWP1 cells. In this case, though, no fibronectin protein was detected in control cells (**Figure R.34.B**, compare lanes 5 and 6). The effect in HT29 M6 snail1 clones, however, was stronger than in RWP1 cells: the levels of fibronectin in snail1 cells infected with TFCP2c Q234L/K236E-myc were hardly detectable compared to cells infected with the empty vector (**Figure R.34.B**, lanes 7 and 8).

To further confirm the effects of TFCP2c Q234L/K236E-myc on *FN1* gene expression we analyzed the mRNA levels of the fibronectin in the snail1 clones of both RWP1 and HT29 M6 cells. The examination of the RT-PCR results showed that in RWP1 snail1 cells the expression of the dominant negative form of TFCP2c decreased about 50 % fibronectin mRNA when compared to cells infected with empty vector. In the case of HT29 M6 snail1 clones, the decrease of the fibronectin mRNA levels in cells infected with pBABE-TFCP2c Q234L/K236E-myc was around 60 % (**Figure R.34.C**, left panel). We also confirmed the increased levels of TFCP2c mRNA in cells infected with the dominant negative form, which expressed around three-fold more TFCP2c than cells infected with the empty vector (**Figure R.34.C**, right panel)^{§§§§}.

^{§§§§} Note that the oligonucleotides used for PCR analysis did not discriminate between the wild type and the mutant form.

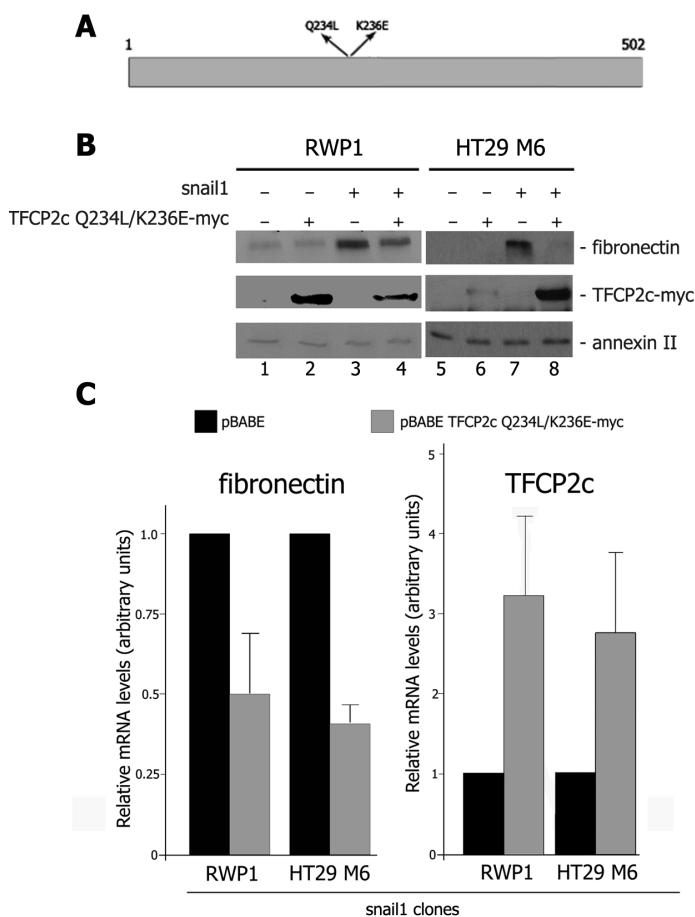


Figure R.34. Expression of the dominant negative TFCP2c Q234L/K236E-myc causes decrease of fibronectin protein and mRNA levels in RWP1 and HT29 M6 snail1 clones. A. Schematic representation of TFCP2c where the mutations introduced are indicated. **B.C.** RWP1 and HT29 M6 control and snail1 cells were infected either with empty pBABE or pBABE-TFCP2c Q234L/K236E-myc and lysed 48 hours after second infection (**E.P.9**). **B.** Lysis was carried out with total extraction buffer (SDS 1%), protein loaded in a polyacrylamide gel (**E.P.10**, 5 μ g for fibronectin and annexin, 20 μ g for TFCP2c-myc) and analysed by western blot with specific antibodies. Annexin was used as loading control. Picture displayed is representative of a series of, at least, three independent experiments. **C.** qRT-PCR of the levels of fibronectin (left) and TFCP2c (right) in the snail1 clones of RWP1 and HT29 M6 cells after infection with empty pBABE or pBABE-TFCP2c Q234L/K236E-myc. Primers used for the analysis of TFCP2c amplify both endogenous TFCP2c and exogenous TFCP2c Q234L/K236E-myc. Pumilio was used as internal control. Values are referred to mRNA levels of snail1 cells infected with empty vector. Values presented are the mean \pm standard deviation of two (RWP1) or three (HT29 M6) experiments.

These results promisingly pointed at TFCP2c as a requirement for snail1-induced upregulation of fibronectin. However, TFCP2c Q234L/K236E-myc had been hypothesised to have the ability of interfering the transcriptional activity of other members of the TFCP2 family [293]. Although ChIP assays were performed with an antibody specific for TFCP2c and raised no doubt concerning other members of the

family, we decided to make another functional approach by specifically interfering TFCP2c expression with the use of shRNAs.

We infected RWP1 and HT29 M6 cell clones with either a mix containing five shRNAs for TFCP2c (SIGMA MISSION) or an irrelevant shRNA, and analyzed both TFCP2c and fibronectin levels 48 hours after infection. Although the experiment was carried out in several conditions and with different models (data not shown), we could only modestly decrease the protein levels of TFCP2c in HT29 M6 cells. In accordance with the results obtained with the dominant negative of TFCP2c, we detected less fibronectin protein in snail1 cells treated with the specific shRNAs for TFCP2c (**Figure R.35**). These results, thus, provide further evidence that TFCP2c specifically is involved in snail1-induced increment of fibronectin during EMT.

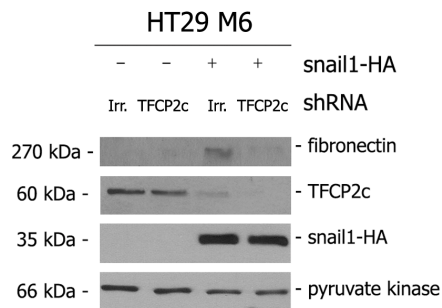


Figure R.35. TFCPc interference causes decrease of fibronectin protein in HT29 M6 snail1 clones. HT29 M6 cells were infected either with irrelevant shRNA or a mix containing five specific shRNAs for TFCP2c and lysed 48 hours after infection (**E.P.9**). Lysis was carried out with total extraction buffer (SDS 1 %), protein loaded in a polyacrylamide gel and analysed by western blot with specific antibodies (**E.P.10**). Pyruvate kinase was used as loading control. Picture displayed is representative of a series of two. Irr: irrelevant.

Strikingly, in the previous experiments we observed less expression of TFCP2c protein and mRNA (data not shown) in HT29 M6 snail1 cells than in control cells. In order to investigate such expression, we decided to perform a closer analysis of the protein and mRNA levels of TFCP2c in HT29 M6, RWP1 and SW480 cells.

Figure R.36 (A and B) shows the observations we made with protein and mRNA. In HT29 M6 total cell extracts we detected, as before, less TFCP2c protein in snail1 clones than in control cells. For RWP1, TFCP2c levels were similar between both clones, while we observed slightly more TFCP2c in SW480 control and snail1 clones than in E-cadherin cells. (**FigureR.36.A**). The analysis of the mRNA levels of the three cell lines confirmed what we had observed for protein: (remarkably) less in HT29 M6 snail1 than

control, similar amounts between both RWP1 clones and slightly more in control and snail1 vs E-cadherin clones in SW480 (**Figure R.36.B**).

These observations suggested us that TFCP2c could be target of a dual regulation, probably by snail1, depending of the epithelial/mesenchymal gene expression equilibrium and similarly to that observed for *LEF1* promoter (see **R.2**). This aspect will be further discussed in **D.4**.

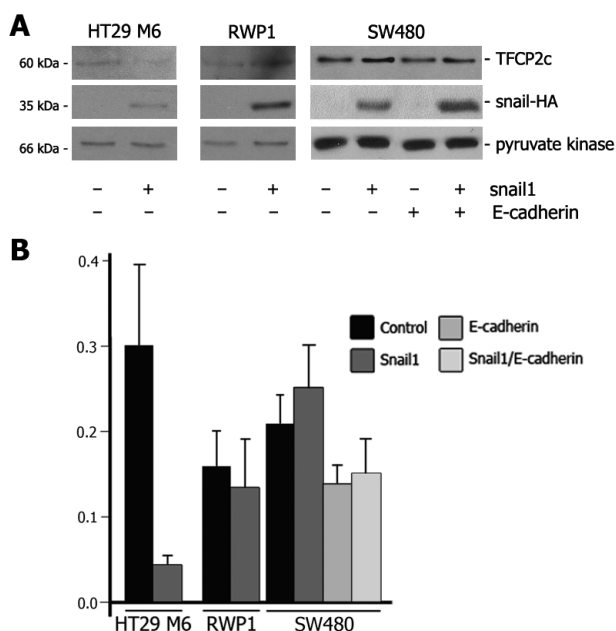


Figure R.36. Snail1 induces different expression pattern of TFCP2c in several cell lines. A. Analysis of total TFCP2c protein levels in HT29 M6, RWP1 and SW480 cell clones. Lysis was carried out with total extraction buffer (SDS 1 %), protein loaded in a polyacrylamide gel and analysed by western blot with specific antibodies (**E.P.10**). Pyruvate kinase was used as loading control. Picture displayed is representative of, at least, three different extractions. **B.** qRT-PCR of TFCP2c mRNA levels in HT29 M6, RWP1 or SW480 clones. Pumilio was used as internal control. Values presented are the mean +/- standard deviation of, at least, three different extractions.

R.4.4 Snail1 induces nuclear accumulation of TFCP2c

In order to study the mechanism by which snail1 could modify the activity of TFCP2c to activate *FN1* gene expression we decided to examine whether in our model this transcription factor was already in the nucleus or if it was accumulated there upon snail1 expression. We performed immunofluorescence on HT29 M6 cells using specific rabbit antibody against TFCP2c (Abcam) and incubated the samples with secondary alexa-488 antibody. When we analyzed the samples we observed that in HT29 M6

control cells TFCP2c was ubiquitously localized (**Figure R.37.A**, left column), though in some cases we detected more protein in the perinuclear region (arrow). On the contrary, more TFCP2c was detected in the nuclei than in the cytosol of HT29 M6 snail1 cells (**Figure R.37.A**, right column). In all cases the nucleus were visualized with propidium iodide.

We also detected differences when we carried out cell-fractionated protein extraction. We observed TFCP2c only in the cytosol of HT29 M6 control cells, while no TFCP2c was detected in this compartment in snail1 clones (**Figure R.37.B**, left panel). On the other hand, in the nuclear fractions we detected a little less TFCP2c in control cells than in snail1 cells, what indicated an increase in the nucleus/cytosol ratio in snail1 cells vs control cells. Since the migration pattern seemed to be different in snail1 and control cells, we decided to highly resolve the gel in further experiments to better analyze TFCP2c migration (**R.4.6**).

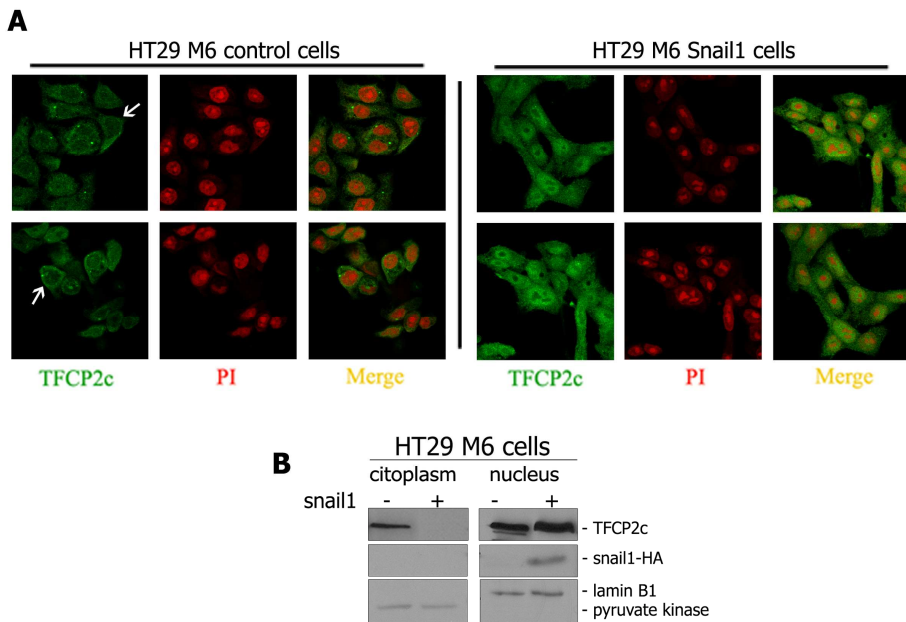


Figure R.37. TFCP2c concentrates in the nucleus of HT29 M6 snail1 clones. A. Immunofluorescence performed on HT29 M6 control (left) and snail1 (right) cells to detect TFCP2c. HT29 M6 clones were grown on glass coverslips for 48 hours prior to fixation. Cells were incubated with primary rabbit antibody against TFCP2c (Abcam) and secondary Alexa-488 antibody (left panels). Propidium iodide was used to stain the nucleus (middle panels). **B.** Protein analysis of fractionated HT29 M6 cell extracts. Cytosolic and nuclear fractions were extracted as described in **E.P.10**, loaded in a polyacrylamide gel and analyzed by western blot with specific antibodies (**E.P.10**). Pyruvate kinase and lamin B1 were used as loading control for cytosol and nucleus respectively. Results displayed are representative of three independent extractions.

A spliced variant of TFCP2c (named TFCP2d/LSF-ID) that resides primarily in the cytoplasm has also been discovered (**Figure R.38.A**) [295]. This spliced variant does not have the DNA binding domain, but still retains the ability to dimerize, similarly to the TFCP2c Q234L/K236E form, with the difference that this shorter variant only acts as a dominant negative when is much more abundant than the wild type form (about ten-fold) [293]. To study the possibility that the ratio TFCP2d/c was higher in HT29 M6 control cells, we specifically amplified TFCP2d mRNA (see **E.P.13**) and compared the quantity of this spliced and the full-length forms in HT29 M6 control and snail1 cells.

Semiquantitative analysis showed that control cells expressed more TFCP2c and TFCP2d than snail1 cells (**Figure R.38.B**). The results of the quantitative mRNA analysis, yet, indicated that the ratio between both forms was similar in the two clones (**Figure R.38.C**), indicating that nuclear accumulation of TFCP2c in snail1 cells is not due to differential splicing of TFCP2 mRNA. In addition, the different expression of the *TFCP2* gene in HT29 M6 control and snail1 cells was confirmed.

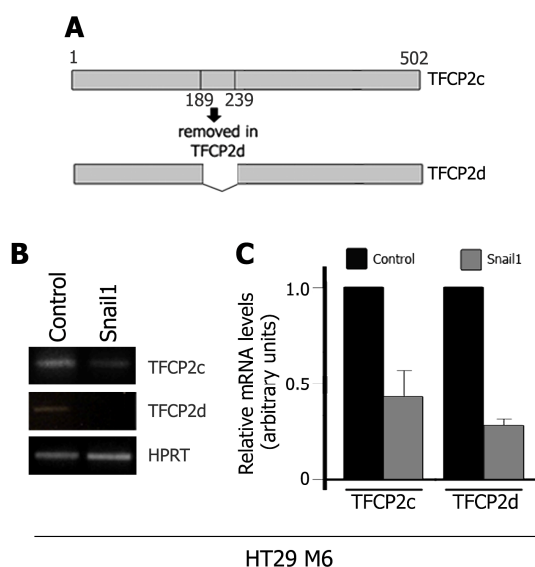


Figure R.38. TFCP2c spliced variants have the same expression pattern in HT29 M6 clones. **A.** Schematic representation of TFCP2c and indication of the region missing in TFCP2d, corresponding to residues 189-239. **B.** Semiquantitative mRNA analysis with specific oligonucleotides (**E.P.13**) to amplify either TFCP2c or TFCP2d in HT29 M6 control and snail1 cells. HPRT was used as loading control. Picture displayed is representative of three determinations. **C.** qmRNA analysis with specific oligonucleotides (**E.P.13**) to amplify either TFCP2c or TFCP2d in HT29 M6 control and snail1 cells. Pumilio was used as internal control. Relative amount of TFCP2c/d in snail1 cells was compared to that control cells (referred to as 1). Error bars correspond to average +/- standard deviation of a minimum of three independent analyses.

R.4.5 TFCP2c in phosphorylated in snail1 expressing cells

Previous articles had described that TFCP2c could resolve as three different migrating bands when analyzed by western blot. These three bands have been attributed to diverse phosphorylation states of the transcription factor. The phosphorylation of TFCP2c has also been related to an increase in DNA binding and transcriptional activity [296, 297]. We had observed both that TFCP2c increased its DNA binding activity and displayed a slightly different migrating pattern in HT29 M6 snail1 cells compared to control cells. We next decided to examine more in detail the migrating pattern of TFCP2c upon snail1 expression.

We proceeded to extract the nuclear fractions of HT29 M6, RWP1 and SW480 cell clones and loaded them in 7.5 % polyacrylamide Protein Xi gels (Biorad, **E.P.10**) in order to better resolve TFCP2c migration and check molecular weight changes in the presence of snail1. We came across different patterns in snail1 vs control cells. We observed the most striking differences in SW480 cells, in which we compared snail1 clones with E-cadherin clones. In E-cadherin clones a thick band was markedly detected, which appeared to really contain two bands. In addition, a weak band was noticed a little more retarded than the former. In snail1 clones the most abundant form of TFCP2c was the retarded one, while only a shadow of the other bands was distinguished (**Figure R.39.A**, left panel). For HT29 M6 the differences were also seen, although not so evident. The most retarded band was more intensely detected in HT29 M6 snail1 cells, while the two faster were better observed in control cells (**Figure R.39.A**, middle panel). In RWP1, on the other hand, we distinguished only very subtle differences (**Figure R.39.A**, right panel).

Two residues on TFCP2c have been recently described to be subjected to phosphorylation: serine 291 and serine 309 [296, 298]. We decided to test if these residues were phosphorylated in the retarded forms of TFCP2c we observed upon snail1 expression. Again we extracted nuclear protein, in this case only of HT29 M6 cell clones, and loaded them in the same type of gels as before (7.5 % polyacrylamide Protein Xi, **E.P.10**). We incubated the membranes with specific antibodies for total TFCP2c, phospho-residue S291 or phospho-residue S309 in TFCP2c (courtesy of U. Hansen, see **E.P.10**). We observed that the total levels of TFCP2c were lower in snail1 with respect to control cells. However, the levels of phospho-TFCP2c were only increased when compared to the total levels in snail1 cells, in a remarkable manner for S291-phospho antibody (**Figure R.39.B**).

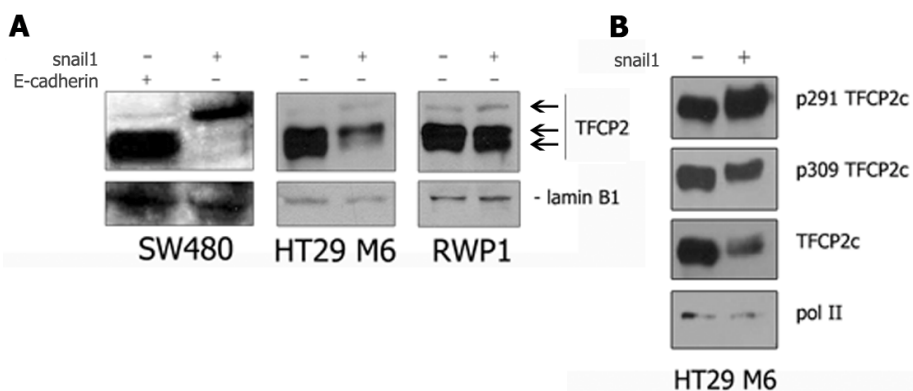


Figure R.39 Snail1 induces phosphorylation of TFCP2c. **A.** Nuclear extracts from SW480, HT29 M6 and RWP1 cells were loaded in a polyacrylamide gel and transferred to a nitrocellulose membrane (E.P.10). Western blot was performed with specific antibody against TFCP2c (Abcam). Lamin B1 was used as loading control. **B.** Membranes were prepared as in **A** and western blot with specific non-commercial antibodies was performed in Ulla Hansen's lab, Boston USA. Phospho-antibodies also detect, though with lower affinity, the non-phosphorylated form of TFCP2c (personal communication from Dr. U. Hansen)

All the results shown in this chapter point at TFCP2c as a clear candidate to be involved in snail1-induced transcriptional activation of the *FN1* promoter. The data presented here also point at a mechanism that requires both nuclear localization and phosphorylation for TFCP2c to achieve transcriptional activation. However, with the studies carried out so far, we find it hard to determine which of the two processes takes place first. On the other hand, it would be interesting to analyze what the kinase responsible for such phosphorylation is. All these possibilities will be further discussed in **D.4**.

DISCUSSION

D.1 SNAIL1 ACTIVATES TRANSCRIPTION OF *FN1* AND *LEF1* PROMOTERS THROUGH AN UNDESCRIBED MECHANISM INDEPENDENT OF E-BOXES

SNAIL genes codify for transcription factors classically described as repressors. They have been demonstrated to directly repress genes such as epithelial markers [113, 122, 138], pro-apoptotic factors [144, 146, 148], cell cycle regulators [147] and hormone receptors [140] by binding to E-boxes in their promoters. At least in the case of E-cadherin (*CDH1* gene), snail1 has been demonstrated to recruit histone deacetylase complexes (HDAC1/2) and polycomb repressive complex 2 (PRC2) to E-boxes through the SNAG domain [133, 134]. In addition, the scaffold protein ajuba has also been related to the snail1 repressor mechanism by recruiting protein arginine methyltransferase 5 (PRMT5) to this same domain [299, 300]. Snail1 activity has also been correlated with high mRNA or protein (or both) of genes upregulated during EMT or tumour progression such as fibronectin [122, 138], vimentin [122, 136, 138], LEF-1, ZEB1 [138], ZEB2 [165], MMP2 [136], IL1 α , IL1 β , IL6, IL8, CXCL1, COX-2 [143], p21 [147], RhoB [142] or Bcl2 [146], not to mention the increase in the activity of general pathways mainly involved in cell cycle blockage and evasion of apoptosis [144, 147, 148].

The activator role of snail1 was already known in the early nineties, when studies on *Drosophila* embryo pointed at snail1, together with twist, as the inductor of the mesoderm [180]. Several studies correlate snail1 expression with increase of mRNA and/or protein levels of other genes [180, 301, 302]. In some cases, twist function was required for such activation, but in some others it was not. Conclusions were raised that defined snail1 but not twist as the mesoderm inductor at least in the anterior part of the ventral furrow during *Drosophila* development [301]. Despite the fact that nowadays the relationship of snail1 with increased activation of several genes is undeniable in a variety of systems (for further details see **Table D.1**), there is nearly no data about the mechanism through which this happens [303]*.

In the present work we tried to shed some light on such mechanism, confirming that snail1 is not only a direct repressor of gene transcription, but also a direct activator during the EMT process. Our results show that snail1 can directly modulate transcription through binding to promoter regions and modulate signaling pathways that promote gene activation. We based our study in two genes upregulated during

* During the preparation of this dissertation an article was published in which an activation mechanism for CES-1, the *C.elegans* snail1 homolog, was described.

the EMT process: *FN1* and *LEF1*. Both genes have been previously described to be activated upon snail1 expression and induction of EMT [122, 138]. We have demonstrated not only that in the cell lines used in this study both mRNA and protein levels of fibronectin and LEF-1 are upregulated upon snail1 expression (**Figure R.1**), but also that such upregulation takes place at transcriptional level (**Figure R.3**).

Snail family gene	Model	Effect	Genes		Ref
			Decrease	Increase	
snail1	Mouse keratinocytes, MDCK (dog), Human tumoural epithelial cells of diverse origin	EMT	E-cadherin (3 E-boxes)		[113]
	Colon carcinoma cells	EMT	E-cadherin (3 E-boxes)	Fibronectin (IF), Vimentin (IF)	[122]
	Colon carcinoma cells	EMT	Muc1 (2 E-boxes)	Fibronectin (RT), LEF-1 (RT, 1 E-box), ZEB1 (RT)	[138]
	Squamous cell carcinoma	invasion		MMP2 (reporter), vimentin	[136]
	HNSCC	enhanced ability to attract monocytes and to invade		IL1 α , IL1 β , IL6, IL8, CXCL1, COX-2 (RT)	[143]
	MDCK (dog), mouse keratinocytes, mouse/chick embryos	cell cycle blockage, resistance to cell death	Cyclin D2 (2 E-boxes)	p21 (WB), (PI3K & MAPK pathways)	[147]
	Epithelial cells	activation of β -catenin/TCF pathway	VDR (3 E-boxes)		[140]
	Epithelial cells of different origin	evasion of apoptosis	PTEN (1 E-box)		[148]
snail1/2	Breast carcinoma cell lines	invasion, evasion of apoptosis	BID, DFF40 (E-boxes)		[144]
snail2	Chick embryos	migration		RhoB (ISH)	[142]
	<i>Xenopus</i> embryos	evasion of apoptosis	Caspases (2, 3, 6, 7, 9, RT)	Bcl2 (RT)	[146]

Table D.1. Summary of modulation of gene expression reported after snail1/2 expression. MDCK, Madin-Darby canine kidney; EMT, Epithelial-mesenchymal transition; Muc-1, Mucin1; HNSCC, head and neck squamous cell carcinomas; CXCL1, Chemokine (C-X-C motif) ligand 1; p21, Cyclin-dependent kinase inhibitor 1A; PI3K, phosphatidylinositol 3-kinase; MAPK, Mitogen Activated Kinase; VDR, Vitamin D3 Receptor; PTEN, phosphatase and tensin homolog; RhoB, Ras homolog gene family, member B, Bcl2, B-cell lymphoma 2; IF, immunofluorescence; RT, retro-transcriptase PCR; WB, western blot; ISH, *in situ* hybridization.

LEF-1 is a member of the LEF/TCF family of transcription factors, originally identified as lymphoid-specific DNA binding protein [304, 305]. LEF-1 has been described to promote cell growth *via* its interaction with β -catenin [306-308], being fundamental in several developmental processes in mice such as formation of hair follicles, mammary glands, whiskers, the mesencephalic nucleus and teeth [309]. *LEF1* expression is highly controlled spatial and temporally during embryogenesis in a cell-specific pattern [282, 310, 311]; however, it is silenced or dramatically downregulated when cells reach a non-cycling, differentiated state [312]. *LEF1* expression has been demonstrated to be controlled at the transcriptional [218, 219, 282, 310, 312-315], post-transcriptional [312, 316] and post-translation [317] levels. In spite of this fine regulation, moderate to high levels of LEF-1 are frequently detected in tumours, even in cancerous cells from tissues that are normally negative for LEF-1 expression such as melanomas or colon cancer [312, 313]. The most striking case is that of colon, a tissue where LEF-1 cannot be detected in normal conditions but is aberrantly expressed in 80% of these cancers [316].

The LEF/TCF family of transcription factors is composed of four members: LEF-1, TCF-1, TCF-3 and TCF-4. All LEF/TCFs are downstream mediators of the Wnt signal transduction pathway, directly interacting with β -catenin to either activate (LEF-1, TCF-1 and TCF-4) or repress (TCF-3) transcription. LEF/TCFs possess a structure called High Mobility Group (HMG) that readily binds DNA in the absence of Wnt signal and causes a dramatic bending of it [318]. In addition, LEF/TCFs contain a context-dependent regulatory domain or CRD which mediates cooperative interactions with transcription factors and has been linked mainly in repression but also in activation. Thus, LEF/TCFs are basically context dependent regulators, cooperating with factors that regulate transcription dependently and independently of Wnt signaling [276]. LEF-1 can induce EMT directly when overexpressed in epithelial cells. LEF-1/ β -catenin [200] and LEF-1/(phospho)Smad2,4 mediated transcription have been described to participate in the LEF-1 mediated EMT [67, 68].

But LEF-1 is not only an effector of the Wnt pathway, it is also its target (and, by extension, of TGF β -Smads), generating a positive feedback on its regulation. Two promoters, named P1 and P2, have been described so far in *LEF1* (see **Figure D.1**) [276, 312, 313], and have been demonstrated to be activated by the Wnt/ β -catenin pathway, at least *in vitro* [219]. The promoter requirements for activation depend highly on the context in which it is activated, ranging from 110bp [218] to 5.7kb [311]. The promoter fragment we have been using for our study corresponds to P1 and is 2kb long, from -

527 to +1389. It has been described to be a TATA-less promoter [312], and several TSS have been described in several cell lines (one in Jurkat and HeLa using RNase protection experiments [312], four in HEK293 using primer extension [218]). Note that a third promoter named P3 was described [316] located inside the P1 region between TSS2 and TSS3 [218] with low activity, though it generates a full-length protein. P2 is a TATA promoter located at the edge between intron 2 and exon 3 and encodes for a truncated form of LEF-1 protein missing the β -catenin interacting domain and part of the CAD, thus acting as a dominant negative form [219]. The only promoter active in colon cancer cells is P1, giving rise to a 3.6kb mRNA [313].

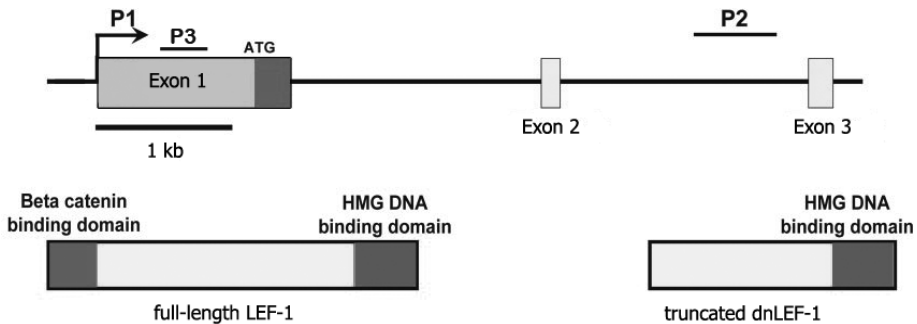


Figure D1. Schematic representation of the *LEF1* 5' region (modified from [313]). *LEF1* promoter 1 (P1) produces a 3.6kb mRNA encoding full-length LEF-1 protein with a β -catenin binding domain at the N terminus and a HMG DNA binding/binding domain near the C terminus. An undefined second promoter (P2) in the second intron produces a 2.2kb mRNA encoding a truncated polypeptide that lacks the β -catenin binding domain (dnLEF-1). A third promoter (P3) has been described to produce a 3.0kb mRNA.

Fibronectins (fibre=fiber + nectere=to bind, connect) are a class of high molecular weight glycoproteins that play a key role in cell-substrate contacts, controlling processes such as cell attachment and spreading, cell migration, morphology, differentiation and oncogenic transformation [319]. All of these are achieved by interaction of fibronectin with cell surface and extracellular materials [320]. Fibronectins have molecular weights between 220 and 270kDa [319, 320] and are found in the fibrillar component of the ECM. Variations in the basic fibronectin structure account for the difference between cellular and plasma fibronectins, though both types are heterodimers bound by disulfide bonds. Cellular fibronectins are insoluble multimers, synthesized locally in the tissue, while plasma fibronectins are soluble forms mainly synthesized in the liver [320-322].

The diverse forms of fibronectin (up to 20) seem to be generated by transcription of a single gene into a common precursor which undergoes alternative splicing [322-326]. Fibronectin is synthesized from a mRNA with a quite long 5'UTR (265 bp) and a 31-residue aminoacid extension not present in the mature form that seems to contain

both a signal peptide and a propeptide [327]. Fibronectin protein can be visualized as a series of globular domains that bind independently to a number of different molecules such as heparin, DNA, collagen, actin, as well as to the cell surface (through its receptors). Fibronectin interaction with the ECM is critically important because it is a way by which cells communicate with the extracellular environment and thus regulate growth and maintenance of normal tissue function [319]. The importance of the substratum in cell behaviour was demonstrated by Chou and collaborators in a study where they plated cells on a grooved surface and observed increase of about 2.5-fold in fibronectin mRNA compared to cells plated on a smooth surface [328].

High fibronectin levels are correlated with EMT and several stimuli have been described to upregulate fibronectin expression, among them TGF β [329-333], adenosine [334], glucocorticoid receptor [329], Interferon γ (IFN γ) [335], Wnt/Wg pathway [223], phorbol 12-myristate 13-acetate (PMA) [290, 336, 337], glucose [291], interleukin-18 (IL-18) [292] being the mediators as diverse as cyclic adenosine monophosphate (cAMP) [291, 329, 334, 338, 339], specificity protein 1 (Sp1) [340], Ha-ras [341], LEF/TCFs [223], phospholipase C (PLC) [331, 332], protein kinase C (PKC) [331, 332, 336, 342], p38 [331, 332], ERK [332], adaptor protein complex 1 (AP1) [291], NF- κ B [290-292, 343], early growth response protein 1 (Egr-1) [337] or PI3K/Akt [292]. Rat, mouse and human *FN1* promoters share extensive homology [344], and they have been studied quite indistinctively in several cell models which include cells from fibrosarcoma [329], granulosa [338], osteosarcoma [341], hepatoma [290, 343] and human glioblastoma [337] as well as human embryonic testicular germ cells [340], glomerular mesangial cells [332], human endothelial cells [291], lung epithelial cells [334] and fibroblasts of different origin [223, 292, 331, 335, 345] among others. In these models fibronectin has been described to be regulated at the transcriptional and post-transcriptional levels, differently even under the same stimulus. This observations state that the mechanisms that provoke increase of fibronectin are highly dependent on the cell type and context [53, 54, 58, 59, 63, 67, 69, 70, 72].

The *FN1* promoter we use in our experiments corresponds to sequence -341/+265, that includes a TATA box near the well defined TSS [327]. The -341/+265 promoter was used because it retains the same responsiveness to snail1 than longer promoters tested (up to -867bp, **Figure R.2**). According to several studies, it contains specific boxes for cAMP responsive element binding protein (CREB), NF- κ B, Sp1, Egr-1 and AP2 (**Figure D.2**) [290, 327, 337, 340, 344]. Our first studies, however, were directed to check motifs directly bound by snail1 (E-boxes) prior to delimitate what the minimal promoter responsive to snail1 was.

illustrate such phenomenon, the mRNA levels of endogenous snail1 (*Homo sapiens* snail1) in HT29 M6, RWP1 and SW480 snail1 and control clones are represented in **Figure D.3.A**. In HT26 M6 cells, stable expression of mmsnail1 causes repression of endogenous hssnail1. In RWP1 cells exogenous mmsnail1 has little repressive/activating effect on endogenous hssnail1, probably due to a balance between both mechanisms. In SW480 cells, cells with more mesenchymal phenotype than the ones mentioned before, the effect observed on hssnail1 upon mmsnail1 expression is activation.

Similarly to what we observed in *LEF1* promoter, Drs Sandra Peiró and María Escrivà also demonstrated that the repression of the -194/+59 *SNAIL1* promoter (with one E-box at -144/-139) was dependent on the presence of the E-box; however, activation of the same promoter was independent of the integrity of the E-box. **Figure D.3.B** shows a reporter experiment performed by transfecting the -194/+59 *SNAIL1* promoter into SW480 cells and cotransfecting either with snail1 or empty vector. Results reproduced what we observed for *LEF1* promoter in RWP1 cells (**Figure R.7**).

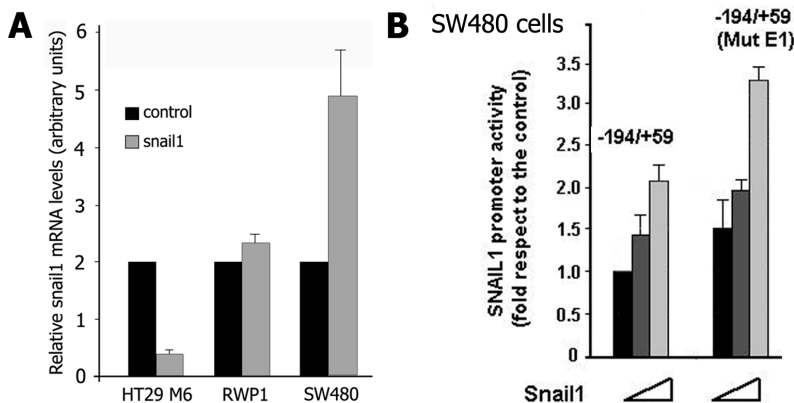


Figure D.3. Snail1 activates or represses its own promoter depending on cellular context. **A.** mRNA obtained from the cells specified was amplified with oligonucleotides for *Homo sapiens* snail1 (**E.P.13**) and HPRT used as internal control. Values shown are relative to mRNA levels of control cells. **B.** Snail1 induced stimulation of the -194/+59 *SNAIL1* promoter was determined by reporter assays in SW480 cells cotransfected with such promoter (in a luciferase vector) and increasing amounts of snail1. The figure shows the average +/- standard deviation of three experiments.

Surprisingly, and even though E-boxes were not acting as mediators, binding assays demonstrated that snail1 has the ability to bind to both *FN1* and *LEF1* promoters (**Figures R.8 and R9**) [347][§]. Indeed, *in vivo* binding of snail1 to *FN1* and *LEF1*

[§] ChIP-Seq experiments performed in the lab by Alba Millanes, Nicolás Herranz and Sandra Peiró also detect *in vivo* binding of snail1 to *FN1* and *LEF1* promoters.

promoters represents a new mechanism because it directly involves snail1 in transcriptional activation, demonstrating that snail1 can act as a coactivator in concert with, at least, a DNA binding partner. From these data, together with the observations regarding the E-boxes in *LEF1* and *SNAIL1* promoters, a dual function for snail1 (activator and repressor) is inferred depending on the cellular context and the availability of partners.

The characterization of the snail1 domains required for binding to promoters and activate transcription has not been studied in depth in this thesis. Yet, our studies demonstrate that the integrity of the SNAG domain, necessary for snail1 repression [113], is a requisite also for activation. Comparisons between the capacity of snail1-P2A and wild type snail1 to bind to the *CDH1* and *FN1* promoters (**Figure R.10**), however, demonstrate a different role for the SNAG domain in the snail1 mediated repression and activation mechanisms. Snail1-P2A, due to its intact DNA binding domain, retains the ability to directly bind to the *CDH1* promoter even when not repressing it because the mutation of the SNAG domain interferes with the recruitment of corepressors. However, snail1-P2A cannot bind to the *FN1* promoter, which we know that binds in an indirect manner, indicating a mechanism independent of the Zn finger DNA binding domain for such process.

Although the overall data suggest that snail1 requires the SNAG domain to bind a DNA-binding partner and achieve transcriptional activation, the mechanism lying underneath, as will be further discussed in subsequent sections, may be more complicated. We propose that repression by snail1 should take place prior to snail1 promoted activation. Since repression cannot take place without an intact SNAG domain, the lack of activation observed with snail1-P2A may be a secondary effect to its failure to repress. The simple fact that E-cadherin ectopic expression in snail1 clones (SW480) inhibits all traces of EMT stresses such possibility.

D.2 SNAIL1 REQUIRES β -CATENIN TO ACCOMPLISH ACTIVATION FROM THE *FN1* AND *LEF1* PROMOTERS

It has been mentioned previously that the repression of E-cadherin by snail1 and consequent downregulation of adherens junctions allows an increase in the cytotolic pool of β -catenin, subsequent nuclear translocation and gene activation. However, there seems to be a tight relationship between snail1 and β -catenin that is not restricted to the release of the second after the induction of the first. There is evidence from ours and other groups that β -catenin and snail1 do interact *in vitro* (results derived from experiments performed independently by Cristina Agustí** and Patricia Villagrasa) and *in vivo* [348].

Furthermore, snail1 is able to activate a synthetic promoter composed of TCF DNA binding sites (named TOP) in HEK293T (after cotransfection of β -catenin), SW480 (stable for snail1) and RWP1 (transiently transfected for snail1) cells [278, 348]. The interplay between both proteins goes even further, at the level of stability regulation, as both proteins have been described to be regulated by GSK3 β / β TRCP1 dependent degradation mechanism [57, 120]. In addition, in human breast cancer cells Wnt signaling promotes the upregulation of Axin2, which sequesters GSK3 β and increases both β -catenin and snail1 protein levels, thus leading to EMT [57]. Besides, snail1 exercises a positive feedback on Wnt signalling by binding to β -catenin and enhancing its transcriptional activity [348].

In addition to the binding of snail1 to *FN1* promoter, the ChIP experiments we performed with antibody against β -catenin (**Figure R.15**) as well as the results obtained with siRNA specific for β -catenin (**Figure R.13**) confirm the requirement and DNA binding of β -catenin in snail1 induced activation of *FN1* and *LEF1* promoters. Even though both snail1 and β -catenin bind to the *FN1* promoter, the efforts within the group^{††} to coimmunoprecipitate them *in vivo* were unsuccessful, what made us consider them as part of different complexes. Stemmer and collaborators have also described a mechanism of transcriptional cooperation between both proteins, however, they base that collaboration on their direct interaction [348].

** And collected in her PhD thesis: *Mecanisme d'activació de Fibronectina i LEF1 per Snail1 durant la transició epiteli-mesènquima*

†† Mainly carried out by Cristina Agustí

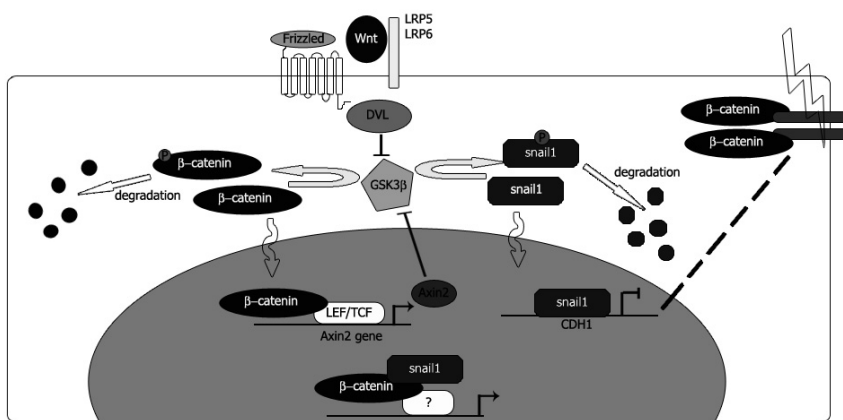


Figure D.4. Relationship between snail1 and β -catenin. Several interconnected processes take place (in an unknown time scale): 1) Snail1 represses E-cadherin; 2) β -catenin cytosolic pool is increased and, although part of the protein is degraded by GSK3 β , part of it can translocate to the nucleus; 3) β -catenin binds LEF/TCFs and activates Axin2 transcription; 4) Axin2 inhibits GSK3 β , what is translated into increase of snail1 and β -catenin protein levels; 5) snail1 cooperates with β -catenin in gene transcription, probably independently of TCFs [348].

Although *FN1* had been shown to be sensitive to the β -catenin-TCF/LEF complex in *Xenopus laevis* [223], no information about the human promoter had been described. The case of *LEF1* promoter was different: two boxes that were susceptible to TCF/LEF mediated activation had been identified in our sequence of study. From our results analysing mRNA levels and promoter activity in cells expressing the dominant negative Δ TCF4 (**Figure R.13**) as well as the activation upon snail1 expression of the promoters containing mutations in the TCF boxes (**Figures R.10** and **R.11**), we can conclude that, although TCF boxes may be involved in the basal activity of the promoters, they are certainly not mediating much of snail1 activation.

A third region of 110 bp (named WRE after Wnt Responsive Element) had also been isolated in *LEF1* promoter as responsive to β -catenin independently of TCF, though no DNA binding partner was identified [218]. This 110 bp region, located at +451/+560, has recently been suggested to have a TCF box [310], but our results when treating cells with Δ TCF, not only point at a TCF-independent mechanism but also, since a WRE deleted promoter was not activated upon snail1 expression (**Figure R.16**), that this region is required for snail1 responsiveness. From reporter experiments performed after fusion of the WRE to a minimal promoter, Filali and collaborators conclude that this 110 bp sequence is enough to mediate activation under Wnt3a stimulation *in vitro* [218] (though it does not seem to respond to it *in vivo* [282]). However, from similar experiments we performed for snail1, we conclude that, although this WRE is required,

there is need of another sequence of the *LEF1* promoter to accomplish activation by snail1 (**Figure R.24**).

However, while the WRE is enough to induce transcriptional activation of *LEF1* under Wnt3a stimulation *in vitro*, Filali et al also showed that in epithelial cells this sequence acted as a repressor of baseline transcription [218]. In another article from the same group, it is described that although the WRE influences *LEF1* promoter expression (during mammary gland and airway submucosal gland development *in vivo*), other sequences are also required for such activation [282]. Liu and colleagues, on the other hand, concluded (in a study performed on hair and vibrissa follicle development), that the WRE is an activator in mesenchymal cells and appears to act as a repressor in epithelial cells, indicating that additional sequences to the WRE are likely necessary for proper transcriptional regulation of the *LEF1* promoter [311]. From all this information gathered from the work by Engelhardt and collaborators, it is derived that *LEF1* promoter seems to be regulated by transcriptional modules differently regulated in epithelial and mesenchymal cells. The coordinated regulation of these modules may play an important role in LEF-1 function during development [282, 311, 313]. The results we got indicate that a similar phenomenon may be taking place in EMT: we have seen that the E-box in *LEF1* promoter is required for repression, WRE for activation and, at least, a third module to coordinate activation in collaboration with the WRE.

Given the involvement of β -catenin in the activation complex and the absence of TCF/LEF in it, we looked for alternatives. In her thesis, Cristina Agustí gathers experiments that point at the *SOX* family of transcription factors as possible mediators in this function [278]. *SOX* genes are a family transcription factors that, the same as the LEF/TCFs, contain a HMG domain. *SOX* genes are divided into ten subfamilies and a wide variety of functions have been attributed to them [349]. Both *sox7* and *sox9* have been reported to compete with LEF/TCFs for binding to β -catenin [193, 350]. *Sox7* has been described to have a dual function as activator and as modulator of the Wnt pathway [350], whereas *sox9* has been involved in chondrocyte differentiation through interaction with β -catenin [193].

The results of overexpressing *sox7* and *sox9* obtained by Cristina Agustí and summarized in **Figure D.5** suggest the possibility of a role for *sox7/9* in snail1-mediated activation. According to several articles published recently, *sox7/9*- β -catenin interaction would inhibit β -catenin transactivation and even promote its degradation rather than enhance its transcriptional activity [193, 351-353]. *Sox7* has been described

to act both as an activator and a repressor [350, 353], and has been mapped to a region classically linked to tumour suppressor genes. Furthermore, it has been described to block cell cycle, being downregulated in several cancers (among them colorectal) and to function as an independent checkpoint for β -catenin [351]. In conclusion, *sox7/9* have been associated with tumour suppression. Nevertheless, and taking into account the complex processes and networks involved in EMT, further research should be carried out to confirm which specific phenomenon is taking place between *sox7/9*, β -catenin and *snail1* during EMT.

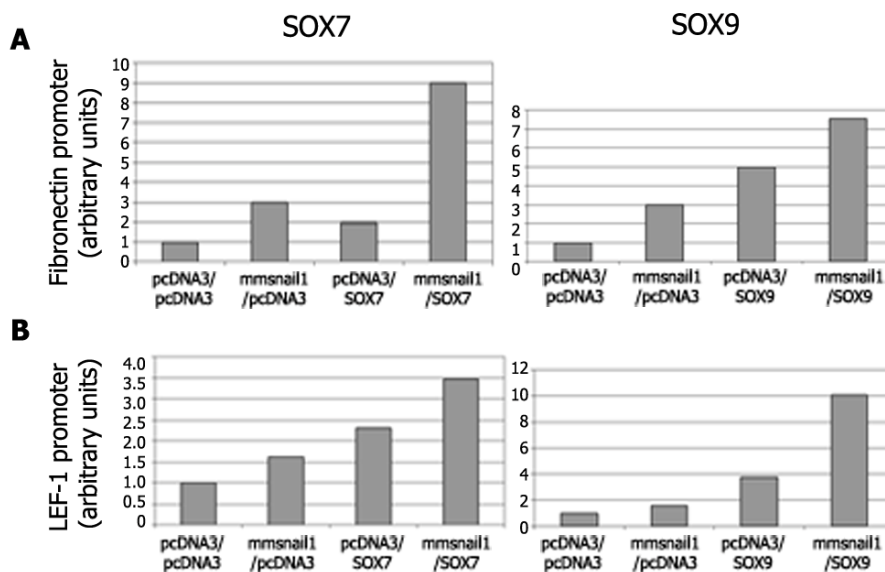


Figure D.5. Effect of *sox7* and *sox9* in *snail1* mediated activation.** **A.** Reporter experiments displayed illustrate that *sox7* enhances the activator effect of *snail1* on *FN1* promoter while the effect of *sox9* seems to be additive to the activation mediated by *snail1*. Reporter assays were performed in RWP1 cells by cotransfection with: (1) 5 ng of either *snail1* or empty pcDNA3; (2) 32 ng of either *sox7* or empty pcDNA3; (3) 100 ng of pXP2 -341/+265 *FN1* promoter or 150 ng of pGL3* -527/+1389 *LEF1* promoter; (4) 2 ng of pRL-SV-40 as transfection control. Results shown represent the mean of three independent experiments performed with triplicates. Standard deviation was not superior to 5 % in any case. **B.** Promoter assays show that the effect of *Sox7* on *snail1* activation of *LEF1* promoter seems to be additive while *Sox9* enhances the activator effect of *snail1* on it. Reporter assays were performed in RWP1 cells by cotransfection with: (1) 5 ng of either *snail1* or empty pcDNA3; (2) 32 ng of either *sox9* or empty pcDNA3; (3) 100 ng of pXP2 -341/+265 *FN1* promoter or 150 ng of pGL3* -527/+1389 *LEF1* promoter; (4) 2 ng of pRL-SV-40 as transfection control. Results shown represent the mean of three independent experiments performed with triplicates. Standard deviation was not superior to 5 % in any case.

Despite the details of how β -catenin binds to *snail1* activated promoters, the model proposed here in which *snail1* and β -catenin would somehow collaborate to

** Modified from the PhD thesis entitled *Mecanisme d'activació de Fibronectina i LEF1 per Snail1 durant la transició epitelial-mesènquima*, by Cristina Agustí.

activate transcription of certain genes is in line with the emerging hypothesis of CSC (cancer stem cells) as key for tumour formation and development described by Brabletz and colleagues [51]. In accordance to this model, at the early stages of tumourigenesis (see 1.2.3) stationary cancer stem cells (SCS) express nuclear β -catenin (aberrantly but still at low levels) which collaborates with LEF/TCFs to induce transcription of genes involved in self-renewal. However, regarding the model described by Brabletz and collaborators, SCS give rise to migrating cancer stem cells (MCS) which differ from the former in that they trigger EMT (maybe due to accumulation of mutations or extracellular signals at the invasive front). MCS also express higher levels of nuclear β -catenin than SCS, which promotes transcription of genes other than those involved in self-renewal. According to our observations, we suggest that induction of snail1 expression (and subsequent EMT) would cause larger accumulation of nuclear β -catenin. We think that it is possible that at such phase β -catenin would expand its usual transcriptional activity to promoters others than the “classical” ones, LEF/TCF-dependent, by interacting with other DNA-binding cofactors in a LEF/TCF independent manner.

D.3 NF-κB IS INVOLVED IN THE ACTIVATION OF *FN1* AND *LEF1* PROMOTERS INDUCED BY *SNAIL1*

The growing evidence about the involvement of NF-κB in EMT (see **I.4.6**) as well as reports describing the participation of NF-κB in *FN1* transcription [291, 292] suggested us the involvement of such proteins in snail1 mediated activation. At least three previous studies linked NF-κB with *FN1* gene activation, however, of the two NF-κB boxes identified, one has been associated with repression of *FN1* promoter rather than activation [290] and the other is located at -1180 of the rat *FN1* promoter [292], sequence not cloned in the promoter used for our studies (-341/+265). Our results, obtained by reporter, ChIP, BOPA and EMSA experiments (**Figures R.26, R.27 and R.29**), have identified a third active NF-κB box in the *FN1* promoter, located at +35/+48. Consistent with these results, Lee and colleagues had already recognized a region in the human *FN1* promoter located between +1 and +136 that was, at least in part, responsible for activation of the *FN1* promoter in hepatoma cells; however, no exact motif was identified [290].

Regarding *LEF1*, previous data exist linking its promoter activation to NF-κB; however, the responsive sequence is vaguely located at -14kbp, again, a region not included in our studies. Therefore, the results obtained by functional (reporter in **Figure R.26**) and binding (BOPA in **Figure R.27**) assays indicate the presence of a newly described active NF-κB box probably placed at +287/+295. We also performed BOPA experiments with the *SNAIL1* promoter (data not shown), which had been previously described to have a responsive NF-κB region between -194 and -125 [123]. Our results confirm that the p65/RelA subunit of NF-κB binds to that region of the *SNAIL1* promoter. With this promoter, the promoters we observed to be activated by snail1 in collaboration with NF-κB are a total of three, what might indicate a common mechanism for snail1 gene activation.

Not only do the results obtained by EMSA, ChIP and BOPA indicate that p65/RelA binds to *FN1* promoter and suggest a similar binding to *LEF1* and *SNAIL1* promoters, but also show that snail1 interacts with the *FN1* promoter in the same region as NF-κB. Thus, these data support the hypothesis that NF-κB mediates the demonstrated snail1 binding to *FN1* and *LEF1* promoters. However, in the EMSA experiments, two of the complexes observed are affected by the addition of specific antibody against snail1 (**Figure R.28**), and only one of them contains p65/RelA, what may indicate the

involvement of another protein in mediating DNA binding by snail1. ChIP, BOPA and EMSA experiments with SW480 clones (**Figures R.27, R.28 and R.29**) also demonstrate that forced E-cadherin expression disrupts the association of p65/RelA with DNA detected upon snail1 expression. In accordance with these observations, SW480 clones that express ectopic E-cadherin display much lower levels of fibronectin and LEF-1 mRNA (**Figure R.1**), even when snail1 is overexpressed. This fact strongly points at the requirement of adherens junctions downregulation as a prerequisite for NF- κ B binding to *FN1* and subsequent transcriptional activation. The observation that the snail1-P2A mutant, contrarily to wild type snail1, was unable to activate the synthetic NF- κ B promoter (*NF3*), reinforced the assumption that snail1-induced repression is required to achieve snail1 induced transcription in collaboration with NF- κ B (**Figure R.26.A**).

An inverse correlation between E-cadherin levels and NF- κ B activity has already been reported [106, 107, 266], although the mechanism involved in this effect had not been clarified. The results presented in this thesis, complemented with biochemical experiments performed in collaboration with Duñach's group, have recently been included in a publication in which we demonstrate that forced E-cadherin expression does not allow snail1-induced transcriptional activation (even when snail1 is overexpressed) because it retains p65/RelA in the adherens junctions [277]. In **Figure D.6.A** immunofluorescence of p65/RelA and β -catenin in SW480 snail1 and snail1/Ecadherin is displayed. A similar pattern is observed for both proteins. β -catenin, in green, is ubiquitously subcellularly distributed in snail1 cells, however, upon E-cadherin addition, it is retained at the membrane. p65/RelA (red) is detected in a diffused pattern in snail1 cells, however, in snail1/E-cadherin double transfectants, p65/RelA signal is mainly localized out of the nucleus, and a small pool can be observed colocalizing with E-cadherin at the membrane level (**Figure D.6.B**).

Nuclear fractioning of SW480 clones supported the result that p65/RelA was retained in the cytoplasm in E-cadherin clones while a pool of p65/RelA entered the nucleus in control and snail1 cells (**Figure D.6.C**). Immunoprecipitation assays confirmed what was inferred in the immunofluorescences: that p65/RelA interacted with members of the adherens junctions complex such as E-cadherin, β -catenin, α -catenin and 120-catenin in the presence of exogenous E-cadherin (**Figure D.6.D**). Therefore, snail1 induction in SW480 cells causes E-cadherin downregulation and subsequent contact disassembly, releasing the pool p65/reIA from the junctional complex and facilitating its function as transcriptional activator. The results given in this article provide evidence that NF- κ B, similarly to β -catenin, is regulated by E-cadherin-dependent immobilisation at the membrane. Although this interaction

explains the negative effect of E-cadherin on NF- κ B-dependent transcription, the possibility that E-cadherin also affects other factors required for the activity of this transcription factor cannot be excluded.

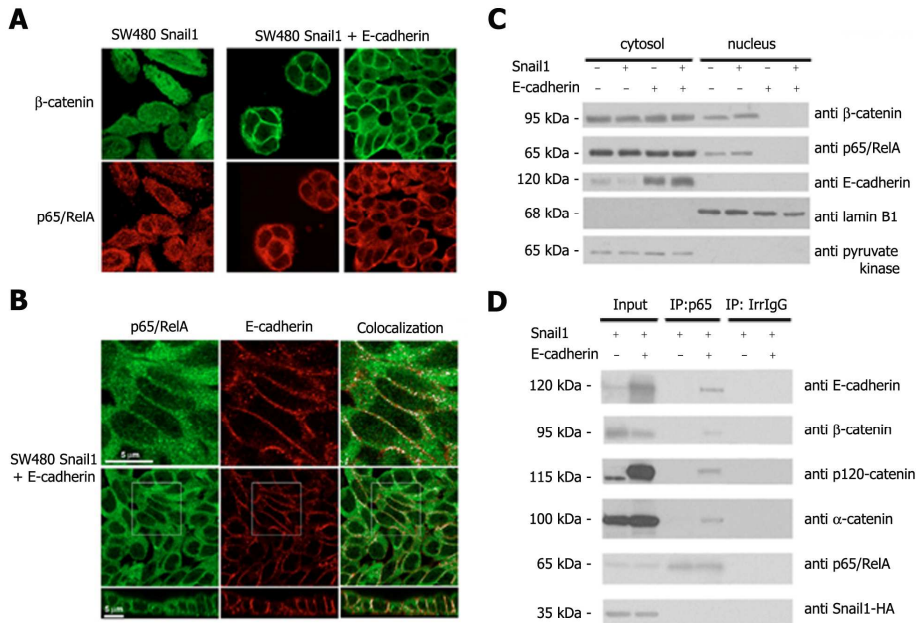


Figure D.6. NF- κ B subcellular localization is regulated similarly to β -catenin⁵⁵ (modified from [277]). **A.** Immunolocalization of p65 and β -catenin is affected by E-cadherin expression. Analysis of β -catenin (green) and p65/RelA (red) subcellular localization was carried out in SW480 snail1-stable transfectants and SW480 snail1/E-cadherin-stably transfected cells. E-cadherin-positive cells (right) were grown at equal (left) or lower (middle) cell density than E-cadherin negative cells in order to better visualize cell colonies. The analysis was performed by immunofluorescence using mouse antibody against β -catenin (BD Transduction Laboratories) and rabbit antibody against p65/RelA (Santa Cruz). No signal was obtained when the same analysis was performed in the absence of primary antibody. **B.** p65/RelA colocalizes with E-cadherin at the membrane. The subcellular distribution of p65/RelA (green) and E-cadherin (red) was determined by immunofluorescence in SW480 snail1/E-cadherin-stable transfectants cells as mentioned above, using specific mAbs against these two proteins (E-cadherin: BD Transduction Laboratories; p65/RelA, BD Transduction Laboratories). The upper row shows an amplified area selected from the panels shown below (boxed). An xz section is shown in the bottom row. **C.** β -catenin and p65/RelA are detected in the nuclear fraction in the absence of E-cadherin. Cytosol+membrane and nuclear fractions were prepared from SW480 cells and analysed by western blot. Lamin B1 was used as nuclear marker; pyruvate kinase was used as marker for the cytosolic fraction. **D.** NF- κ B co-immunoprecipitates with E-cadherin and β -catenin. The p65 subunit of NF- κ B was immunoprecipitated from whole-cell extracts of SW480 cells stably transfected with snail1-HA and E-cadherin. The associated proteins were analysed with specific mAbs against E-cadherin, and α -, β - and p120-catenin (all from BD Transduction Laboratories).

⁵⁵ Experiments performed by Dr. Cristina Agustí (A), Dr. Josep Baulida (A and B) and Dr. Guiomar Solanas (C and D)

The relationship between both NF- κ B and β -catenin pathways has already been demonstrated [129, 273-275]. Indeed, some studies point at β -catenin, together with GSK3 β , as a negative regulator of NF- κ B DNA-binding and transcription activity of several genes [129, 273]. Steinbrecher and collaborators, however, described that GSK3 β has the ability to positively regulate NF- κ B transactivation of some promoters such as IL-6 or monocyte chemoattractant protein 1 [274]. The work by Yun and collaborators [354] on the NF- κ B box at -14kbp of the *LEF1* promoter describes an activation mechanism that, in addition to NF- κ B recruitment, requires its interaction with the β -catenin/LEF-1 complex.

According to our co-immunoprecipitation data, NF- κ B transcriptional activity is mainly inhibited by the adherens junction-associated pool of β -catenin and not by the transcriptional nuclear pool. Our results showing that β -catenin and p65/RelA are both bound to the *FN1* promoter during gene activation are compatible with the hypothesis that the simultaneous activation of both pathways is required for the activation of specific genes during EMT [62]. Immunoprecipitation and immunocytochemistry experiments as well as cell fractioning suggest that the pool of NF- κ B bound to E-cadherin is much smaller than the pool bound to I κ B- α . However, since experiments performed with siRNA for E-cadherin (which does not alter the association of p65 with I κ B- α) still show increase in the nuclear pool of NF- κ B, the membrane pool of p65/RelA has a functional relevance [277]. Our results, thus, suggest that this membrane-associated pool is the one that is mobilised during EMT and is relevant for the expression of mesenchymal genes.

Further characterization of NF- κ B activation mechanism induced by snail1 has been performed in our group since several researchers pointed at poly (ADP-ribose) polymerase-1 (PARP-1) as a coactivator for NF- κ B [355-359]. Interestingly, we found out that, although PARP-1 enzymatic activity was not required (data not shown), PARP-1 protein is also involved in snail1 mediated gene activation^{***}. Several observations support the participation of PARP-1 in such mechanism. First, analysis of gene expression in knock-out mouse embryonic fibroblasts (MEF) for PARP-1 revealed lower fibronectin and LEF-1 and higher E-cadherin mRNA levels than in wild type MEFs (data not shown). In addition, EMSA assays performed with the +24/+53 *FN1* promoter probe, in which we had observed p65 and snail1 binding (**Figures R.28 and R.29**), displayed band shifting with specific antibody against PARP-1, indicating that PARP-1

^{***} Experiments mainly performed by Jelena Stanisavljevic

was in the complex formed by p65/RelA and snail1. Co-immunoprecipitation of the three proteins was also observed in several cell systems (both transfecting snail1-HA into HEK293T cells and with stable HT29 M6 snail1 clones). One last demonstration of the requirement of PARP-1 in the snail1/p65 complex to achieve transcriptional activation of the *FN1* promoter was provided by ChIP assays performed in the knock-out MEFs for PARP-1. These experiments performed by Jelena Stanisavljevic showed that in the absence of PARP-1 no specific complex with snail1 and p65/RelA was formed on the promoter. All these data suggest not only that PARP-1 is required for snail1-induced transcriptional activation of the *FN1* promoter, but also that PARP-1 binds to the DNA in the same region that snail1 and p65 do, probably acting as scaffolding protein for the formation of the activation complex.

PARP-1 is the founding member of the a gene family that contains at least 7 distinct proteins in humans [360] and is characterized by catalyzing poly(ADP-ribose)lation. PARP-1 mediates a wide range of physiological and pathophysiological processes such as maintenance of genomic integrity, inter and intracellular signalling, transcriptional regulation, cell differentiation and proliferation, energy metabolism and cell death [361]. PARP-1 is a highly conserved multifunctional enzyme (113kDa) consisting of three domains (Figure D.7).

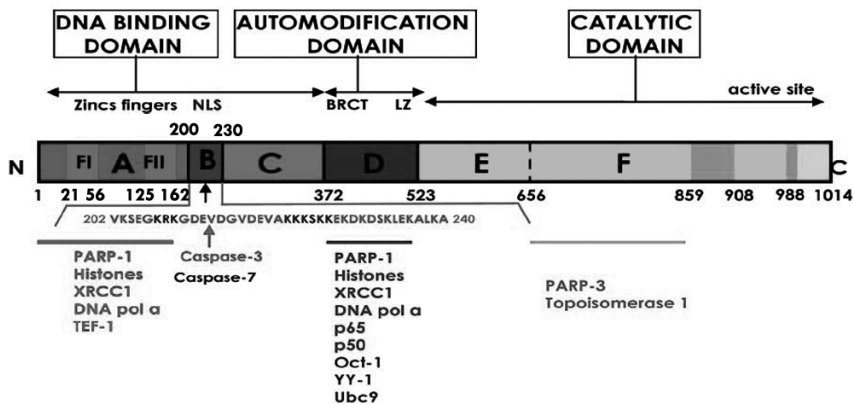


Figure D.7. Structural domains of human PARP-1 (modified from [362]). The three domains are displayed: (1) the amino-terminal region contains the DNA binding domain, with two zinc fingers, strictly conserved during evolution, and a bipartite NLS contains a caspase-3 and 7 cleavage site; (2) a central automodification domain, rich in glutamic acid residues (consistent with the fact that poly(ADP-ribose)lation occurs on such residues) and also containing a BRCT motif (present in many DNA damage repair and cell-cycle checkpoint proteins) and a Leucine Zipper motif (LZ); (3) a carboxi-terminal catalytic domain responsible for the nick-binding-dependent poly(ADP-ribose) synthesis [362-364]. Despite these domains, PARP-1 structure is often divided into 6 regions: A, DNA binding; B, NLS; C, D, automodification; E and F; the smallest fragment retaining catalytic activity. No information about domains C and E is known [360]. Globally, the structure and activities of PARP-1 suggest important roles for this in a variety of cell functions. The interactions of PARP domains with other proteins are shown.

Most of the physiological roles of PARP-1 are mediated by its capacity to bind DNA strand breaks and poly (ADP-ribose) polymerase activity; however, in the late nineties a new role for PARP-1 was described as involved in NF- κ B transcriptional activation. Although studies performed with leukemia cells indicate a negative regulation of PARP-1 in NF- κ B activation, data obtained with HeLa cells [365] and fibroblasts [357, 359] suggest a coactivator task for PARP-1 in NF- κ B activation. Several reports propose that the contradiction in PARP-1 effects on NF- κ B activity (repression versus activation) resides in the different stimuli and cell type. PARP-1 can directly interact with both subunits of NF- κ B (p65 and p50) *in vitro* and *in vivo*. Remarkably, neither the DNA binding nor the enzymatic activity of PARP-1 was required for full activation of NF- κ B in response to various stimuli *in vivo* [356]. PARP-1 and its ability to modulate the response through NF- κ B have also been associated with regulation of skin carcinogenesis [358].

The available data indicate that PARP-1 regulates transcription in perhaps as many as four ways: (i) as a modulator of chromatin structure by binding to nucleosomes, modifying histone proteins, or regulating the composition of chromatin, (ii) as an enhancer-binding factor that functions in a manner similar to classical sequence-specific DNA-binding activators or repressors, (iii) as a transcriptional coregulator that functions similarly to classical coactivators and corepressors, and (iv) as a component of transcriptional insulators [366]. Results obtained showed that PARP-1 already bound to the inactive *FN1* promoter (data not shown) would be in accordance with the hypothesis that PARP-1 is a modulator of chromatin architecture and transcriptional outcomes. Furthermore, there is evidence suggesting that, in activated genes, PARP-1 tends to interact with nucleosomes around TSS [367] where it would recruit the coactivator of NF- κ B p300/CBP to synergistically activate NF- κ B-dependent transcription. NF- κ B-dependent transactivation of PARP-1-dependent promoters not only requires the enzymatic activity of p300/CBP but also that PARP-1 itself is acetylated *in vivo* in response to inflammatory stimuli [368]. Thus, PARP-1 might facilitate, together with other structural/architectural positive cofactors (such as protein arginine methyltransferase 1, PRMT1)⁺⁺⁺, cooperative interactions between sequence-specific activators (as NF- κ B) and different coactivator complexes (such as p300/CBP); thereby providing an architectural function in stabilizing the pre-initiation complex [361, 363].

⁺⁺⁺ Note the different functional activity with PRMT5, which has been previously introduced as required for snail1 induced *CDH1* repression (see **D.1**).

Despite the putative role of PARP-1, we define a new collaborative mechanism between snail1 and NF- κ B proteins in the activation of mesenchymal gene expression. We hypothesize that an NF- κ B/snail1 complex may target specific transcription of mesenchymal genes in front transcription of other NF- κ B induced genes involved in inflammation, cell survival, cell differentiation or cell proliferation, which would still be activated in response to the inflammatory reaction surrounding the tumour [269]. In addition, our results also support previous reports indicating that NF- κ B can regulate *SNAIL1* expression at the transcriptional level [123, 271, 272, 369]. An article recently published by Wu and colleagues [370] states the relevance of the tumour environment in general and the inflammatory reaction in particular in the induction of EMT and enhancement of tumour cell migration and invasion. In the same work, they describe a new mechanism by which NF- κ B induction by the inflammatory cytokine TNF α , but not others (IL2, IL6 or IFN γ), increases snail1 protein stability through transcriptional activation of a protein (named CSN2) that disrupts the snail1-GSK3 β - β TrCP complex, thus preventing snail1 phosphorylation and ubiquitylation.

All these data suggest interconnection between NF- κ B and snail1 at different levels. NF- κ B induced in the inflammatory reaction at the tumour site would cause a positive effect on snail1 (1) at the transcriptional level, collaborating with it to activate the own snail1 transcription and (2) at the protein level, where NF- κ B would be capable of stabilizing snail1 as a means to increase the cellular pool. Snail1, at the same time, would collaborate in the increase of the nuclear pool of p65 by downregulating E-cadherin and, thus, disrupting the membrane docking of p65 to the adherens junctions. In addition, these two factors would work together with PARP-1, PRMT1 and p300 to activate transcription of mesenchymal genes such as *FN1* and *LEF1* and progress through the EMT process.

D.4 TFPC2c IS REQUIRED FOR THE SNAIL1-INDUCED TRANSCRIPTIONAL ACTIVATION OF *FN1* PROMOTER

Experiments directed to narrow the sequence responsive to snail1 in the *FN1* promoter provided us with a new transcription factor that seems to be required for snail1 mediated activation of the *FN1* promoter: TFPC2c. TFPC2c also receives other names like LSF, LBP1c and SEF1 as a consequence of independent identifications in viral and cellular promoters. However, it must not be confused with the also named CP2 protein, which binds CCAAT motifs and, although at first were thought to be the same protein, is not related at all with TFPC2c [293]. TFPC2c belongs to a highly conserved and ancient family which, based on sequence conservation, consists of two branches: the LSF/CP2 subfamily and the Grainyhead (GRH) subfamily (see **Figure D.8**).

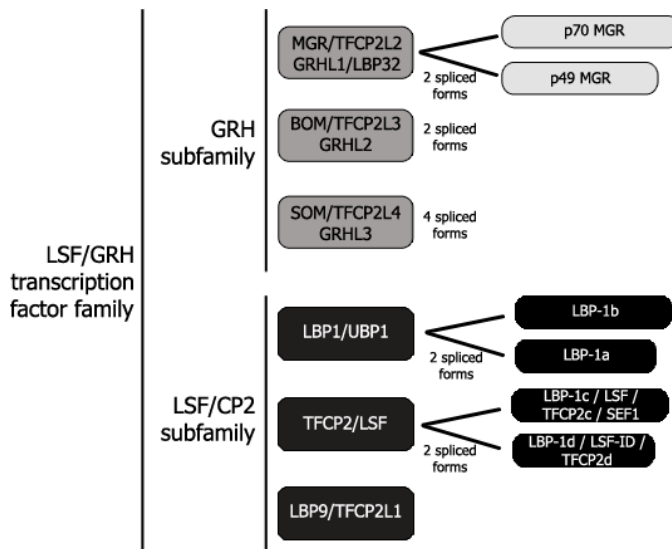


Figure D.8. Identified proteins in the mammalian LSF/GRH family. The GRH subfamily has a highly restricted pattern of expression and both DNA and oligomerization domains are very conserved with those of grainyhead (*Drosophila*). The LSF/CP2 subfamily members are ubiquitously expressed (except LBP9). This subfamily is composed of three members in mammals, which can suffer alternative splicing. Mouse homologs are NF2d9 for LBP1a, CP2 for TFPC2c and CRTR-1 for LBP9. In mammals, three to four members of each subfamily are represented in each genome, however, most other species contain a single gene of each subfamily (even in nematodes there is one representative of the GRH subfamily but none of the LSF/CP2). Neither LSF nor GRH genes are found in any sequenced genomes or EST databases from plants or unicellular organisms [293]. MGR: mammalian grainyhead; TFPC2L2: Transcription factor CP2 like protein 2; GRHL1: Grainyhead like protein 1; BOM: Brother of MGR; TFPC2L3: Transcription factor CP2 like protein 3; GRHL2: Grainyhead like protein 2; SOM: Sister of MGR; TFPC2L4: Transcription factor CP2 like protein 4; GRHL3: Grainyhead like protein 3; LBP: leader-binding protein; UBP1: Upstream region binding protein 1; LSF: Late simian virus 40 transcription factor; TFPC2: transcription factor CCAAT-binding protein 2; SEF1: Serum amyloid A3 enhancer factor 1; LSF-ID: LSF-internally deleted.

The general structure of the family consists of two domains: one involved in DNA binding and another in oligomerization (see **Figure D.9** for TFCP2c). The protein folding is highly similar to p53 and even the work of Kokoszynska and collaborators point at this protein family as highly likely to represent an ancestor of p53 [371]. What distinguishes the two subfamilies from each other is predominantly the oligomerization domain, being members of each subfamily able to interact with members of their same subfamily, but not with each other [372-375]. The distinct DNA-binding sites and inability to interact with each other imply that GRH and LSF family members target different sets of genes [293]. LBP1a/b and TFCP2c are mainly activators, while LBP9 acts as a repressor to the extent that it has been reported to suppress LBP1b activation [376]. The different behaviour seems to reside in the presence of the glutamine rich region in both LBP1a and TFCP2 that is missing in LBP9 [377].

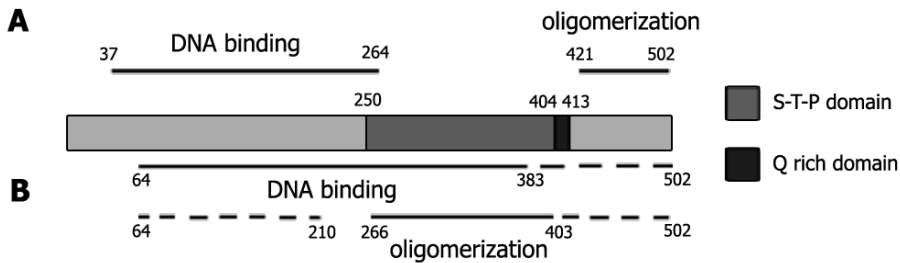


Figure D.9. Schematic representation of TFCP2c. **A.** *In silico* analysis of the TFCP2 family have elucidated the fold recognition and protein structure prediction, showing that the family adopts a DNA binding immunoglobulin fold (residues 37-264 in TFCP2c) homologous to the cell cycle regulator p53 core domain (though without zinc ion binding site), and that a novel type of ubiquitin-like domain and a sterile alpha motif (SAM) form the oligomerization modules (residues 421-502 in TFCP2c). The remaining internal segment was observed to be the most variable region among the two subfamilies [371]. **B.** Previous studies coordinating computational profiling and experimental analysis, however, differ in the functionality of those regions. According to this model, *in vivo* DNA binding activity requires a minimal region containing amino acids 64-383, though optimal binding requires additional C-terminal sequences between residues 383 and 502 (dashed lines). The core region required for LSF oligomerization *in vivo* was mapped between residues 266 and 403, although, again, additional regions are comprised between amino acids 64-210 and 403-502 (dashed lines [378]). In the middle the representation of the protein with two sequence important features is shown: a serine, threonine, proline rich domain (S-T-P domain) and a 10 glutamine rich region (Q rich domain) [377].

TFCP2c has been described to bind DNA through two directly repeated motifs either as tetramer [378, 379] or as dimer [294, 380, 381] in solution, however, it is predominantly found as a dimer [381]. TFCP2c interacts with cellular and viral promoters among which are the thymidylate synthase (TS) gene [382], murine α -globin [383-385], IL-4 [386], *c-fos* [297], ornithine decarboxylase (ODC) [297], chicken

Embryonic Stem 1 gene (cENS-1) [387], serum amyloid A3 [388], PAX6 [389] and human immunodeficiency virus (HIV) long terminal repeat (LTR) [375, 390-393]. TFCP2c can form homodimers [378, 379, 394], heterodimers with highly related proteins [375, 395] or heterodimers with unrelated proteins [379, 380, 386, 396, 397]. Although most articles agree that the consensus motif for TFCP2c binding has a six-base spacer that represents one turn helix [385], some researchers have also described that the spacer does not need to be conserved in length for TFCP2c binding [398].

Our results provide strong evidence that TFCP2c has a role in snail1 activation of the *FN1* promoter. The functional relevance of TFCP2c in such mechanism is established by the interference of the dominant negative form TFCP2c Q234L/K236E with wild type TFCP2c, what results in decrease of both fibronectin protein and mRNA levels (**Figure R.34**). Depletion of TFCP2c in HT29 M6 cells also point at the involvement of TFCP2c in snail1-induced increase of fibronectin (**Figure R.35**). Snail1 expression has also been observed to have several effects on TFCP2c. On one hand, snail1 changes TFCP2c subcellular localization, causing nuclear recruitment (**Figure R.37**); on the other, it induces TFCP2c phosphorylation (**Figure R.39**). The chronological order of these two processes has not been inferred in this work, however, we demonstrated that the overall result is TFCP2c binding to *FN1* promoter (**Figure R.33**). The data obtained in ChIP experiments are complimentary to evidence compiled in reporter and EMSA assays (**Figures R.18** and **R.21**) in which it was observed that a region at -341/-320 was required for snail1 induced *FN1* transcription. The location of several TFCP2c boxes in such region and the failure of a *FN1* promoter mutant for the boxes at -33/-330 and -326/-323 to be fully activated by snail1 make it a feasible DNA binding region for the transcription factor.

In EMSA experiments with the -341/-320 *FN1* probe, not only a complex is observed to be formed in snail1 expressing cells, but, again, a repressor seems to be released from the region where TFCP2c may bind upon snail1 expression. We do not know whether a repressor in that region is displaced by TFCP2c or there is another mechanism acting there. Tuckfield and collaborators describe that TFCP2c is able to repress transcription upon heterodimerizing with dinG (member of the repressors polycomb group of proteins (PRC1), but that excess of TFCP2c causes homodimer formation and displaces dinG, achieving activation [397]. When adapted to our results, we would expect more TFCP2c bound to *FN1* promoter in snail1 cells, but still some bound there in control cells. The ChIP experiments we performed in HT29 M6 cells indicate a binding of 1.3-fold in control cells with respect to the unspecific antibody, however, we cannot conclude whether such binding is significant (**Figure R.33.B**). To

investigate the participation of dinG as partner of TFCP2c in control cells, it would be necessary to analyze its specific binding to the *FN1* promoter performing ChIP assays with a specific antibody against dinG.

TFCP2c transcriptional activity has been described to be mainly regulated by subcellular localization [399] and phosphorylation [296, 297]. However, the observation that activation of TFCP2c upon snail1 did not correlate with higher but rather lower protein and mRNA levels (specially in HT29 M6 cells, **Figure R.36**) made us consider that snail1 may act at a third level of regulation of TFCP2c: transcription. The fact that in epithelial cells TFCP2c levels were decreased by snail1 while in cells with more mesenchymal phenotype they were increased was reminiscent of the dual behaviour observed for *LEF1* and *SNAIL1* promoters in response to snail1 (see **D.1**). These observations prompted us to analyze the *TFCP2* promoter, what unveiled an E-box sequence at -1230 bp, upstream to the translation start site and two NF- κ B boxes, one at -600 and the other at -300. *TFCP2* has been reported to have multiple TSS [400] and up to three different mRNAs isolated from HeLa, T and K562 cells [294, 377, 400] have been reported so far with more than 200 bp difference in length. The description of several TSS places the E-box between -700 bp and -500 bp and the NF- κ B boxes between -70 and +130 (box 1) and between +250 and +450 (box 2) from any of the three TSS.

In HT29 M6 cells, where we detect a clear decrease of the protein and mRNA levels of TFCP2c in snail1 cells, we have also observed that this decrease does not prevent the increase of snail1-induced TFCP2c phosphorylation, nuclear accumulation (or increase of the nuclear/cytosolic ratio of TFCP2c) and *FN1* promoter binding (**Figures R.39, R.37** and **R.33** respectively). Therefore, the pool of TFCP2c remaining in snail1 cells seems to be sufficient, after suffering snail1-induced modifications (phosphorylation, change of subcellular compartment), to mediate *FN1* activation. Our observations also indicate that snail1 may be modulating the increase of TFCP2c binding to the *FN1* promoter by increasing the pool of phosphorylated nuclear protein. TFCP2c has been described mainly as a nuclear factor [293, 295], but our studies suggest that it is distributed equally between both the cytosol and nucleus in HT29 M6 cells in the absence of snail1 (maybe with a reinforced signal along the nuclear membrane, **Figure R.37**). However, when snail1 expression is forced, the nuclear/cytosol ratio of TFCP2c increases (although, as mentioned, the total protein appears to decrease) and much less signal is detected in the cytosol.

Our observations are in agreement with what Kashour and collaborators describe in rat neuroblastoma B103 cells [399]. They detect TFCP2c in both the cytosol and the nucleus in basal conditions. However, upon stimulation of TFCP2c transcription, they observe that TFCP2c accumulates in the nucleus. Another article pointed at LBP-1b, which contains a NLS, as a cytosolic dimerization partner of TFCP2c that would allow nuclear localization of TFCP2c [401]. In accordance with these observations, thus, there is the possibility that snail1 does not provoke nuclear localization of TFCP2c by its direct modification, but by acting upon another protein that would act as nuclear transporter for TFCP2c (a possibility also considered by Kashour and colleagues [399]).

Concerning protein analysis of TFCP2c, we observed that, when the gel is resolved enough, the band developed in snail1 expressing cells corresponding to TFCP2c migrates slightly slower than the one in control cells (**Figures R.37 and R.39**). This effect is much evident in SW480 cells overexpressing snail1 when compared to cells overexpressing E-cadherin. TFCP2c has been described to migrate as three different bands in T lymphocytes [297] and NIH3T3 [296] when cells are growth-stimulated, corresponding to different phosphorylated states. According to our results, it is highly probable that these phenomena (phosphorylation and increase of DNA binding) are taking place in snail1 cells.

The kinases described to have the ability to phosphorylate TFCP2c in vitro are pp42/44 (ERK1/2) [296, 297], p38 [398], cyclinE/Cdk2, cyclin C/Cdk2, cyclinC/Cdk3 [298] and Akt [293, 399]. ERK, p38 and Akt kinases have been associated with snail1 induced EMT [147] and even ERK and Akt have been involved in *SNAIL1* promoter activation [123]. As mentioned, the work by Kashour and colleagues states a mechanism for TFCP2c activation that resembles ours in many aspects; though they describe the involvement of TFCP2c in the antiapoptotic effect of Alzheimer's amyloid precursor protein (APP). In their model, TFCP2c was expressed in both subcellular compartments (cytosol and nucleus) and translocated to the nucleus upon staurosporine (STS)-induced apoptosis, enhancing both DNA binding and transactivation of the TS promoter; the PI3K/Akt axis was responsible for TFCP2c activity (see **Figure D.10**). Consistent with this hypothesis, residue T344 in TFCP2c is highly susceptible of being phosphorylated by Akt. In fact, preliminary results performed in our lab with shRNA against Akt-1 and Akt-2 show that knockdown of Akt-2 strongly diminishes both protein and mRNA levels of fibronectin^{***}. Interestingly, Akt2 activation in ovarian carcinomas has been linked to aggressive clinical behavior and a loss of the

*** By a series of experiments performed by Patricia Villagrasa

histological features of epithelial differentiation [402]. The involvement of Akt in snail1-mediated activation of, at least, the *FN1* promoter, would be supported by the role fibronectin plays not only as a major constituent of the ECM but also as an apoptosis protector [403-405].

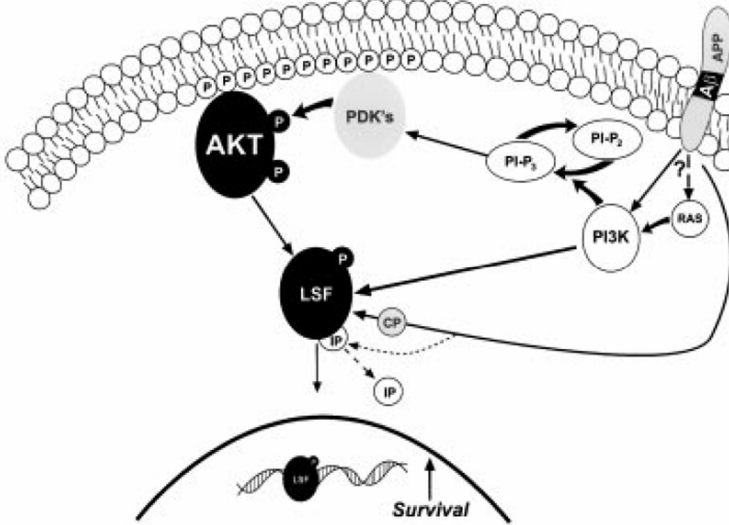


Figure D.10. PI 3-kinase/Akt links APP with TFCP2c/LSF in anti-apoptotic signaling [399]. STS treatment induced hAPPwt to activate TFCP2c via the PI 3-kinase/Akt pathway. Activated Akt may transiently associate with and phosphorylate TFCP2c to interact with nuclear chaperone proteins (CP), or Akt may phosphorylate an inhibitory protein (IP) to release TFCP2c.

Hansen and collaborators in their multiple studies of TFCP2c have isolated two major residues known to be phosphorylated in TFCP2c (none of them T344) after mitogenic stimulation (and subsequent MAPK pathway activation). They have described that in such context TFCP2c phosphorylation occurs on serine residues and that residue S291 plays a major role [297]. Hansen and colleagues isolated S291 as required but not enough to achieve DNA-binding to a consensus TFCP2c binding region (LSF-280 site within the SV40 late promoter) in T cells, hypothesizing the need of an additional factor which would be cell-specific [296, 297]. Similar results were obtained for NIH3T3 cells [296]. In their latest study, they show that ERK phosphorylation on S291 is followed by cyclinC/CDK phosphorylation on S309 [298]. Although they had previously demonstrated that TFCP2c was required for *TS* gene expression [382], phosphorylation on S291 and S309 does not enhance transactivation from the *TS* promoter but rather inhibits it. The explanation for these observations defined the two phosphorylation processes as a means to prevent a too early activation of the transcription of the gene (phosphorylations take place in early G₁


phase and dephosphorylation in late G₁ [298]). These results also suggest that phenomena other than phosphorylation on S291 and S309 are responsible for TFCP2c transactivation and activation of transcription from the *TS* gene.

Although the results obtained with specific phospho-antibodies seem to point at residues 291 and 309 as plausible candidates to be phosphorylated upon snail1 induction (**Figure R.39**), other phosphorylations, such as the previously mentioned T344, are possible, since the three bands in the migration pattern of TFCP2c are highly likely to represent more than two phosphorylated residues. The meaning of these two phosphorylations (S291 and S309), however, is not clear. We would expect it to be translated into increase in DNA-binding and transactivation, however, as mentioned, before, results in other cellular models, although support DNA binding, do not sustain the functional part.

In addition to these kinases, p38 does seem to be involved in TFCP2c binding to the RCS (repressor complex sequence) of the HIV LTR in HeLa cells [398]. However, the use of a MAPK specific inhibitor (PD98059) excluded p38 as responsible for TFCP2c mobility shifting in SV40 late promoter [296, 297], indicating the variability of processes involved in TFCP2c activation. The existence of a complex mechanism beneath likely explains the contradictory findings concerning TFCP2c transcriptional activity observed in the different experimental systems; the effect of a biological signal *in vivo* is probably to result from the integration of many of such opposing and synergizing pathways. Nevertheless, and even though the involvement of TFCP2c in snail1 mediated activation of *FN1* is proved, further experiments with specific kinase inhibitors must be performed to distinguish which pathway or pathways are mediating TFCP2c phosphorylation upon snail1 induction. In addition, point mutation on candidate residues would address the aminoacid or aminoacids responsible for such modification. It would also be interesting to decipher the mechanism by which TFCP2c enters the nucleus whether it is through interaction with LBP-1b or another protein [295] or if, as happens with β -catenin and NF- κ B, snail1 activates a pathway that releases TFCP2c from its cytosolic docking, or even if the sole TFCP2c modification (maybe phosphorylation) is enough to induce nuclear localization of the transcription factor.

TFCP2c had been previously described to have a role in the maintenance of cell pluripotency and stemness during chicken development. In this model, TFCP2c regulates the expression of chicken Embryonic Normal Stem (cENS) 1 gene (whose expression is much stronger in chicken stem cells than in differentiated cells) by

binding to its promoter through its consensus motif (located approximately at -300bp) and enhancing activation from it. Furthermore, when mapping the pattern of expression, it was discovered that it was alike for both cENS-1 and TFCP2c proteins [387]. The involvement of TFCP2c in maintenance of stemness and in EMT gene regulation, two cell processes linked to tumourigenesis, may suggest an undescribed role for TFCP2c in maintaining the cell pluripotency observed in tumoural cells and the establishment of CSC.



D.5 MODEL

It has been noted in the introduction that most cellular inputs that trigger EMT convey in an increase of snail1 transcription factor. Thus, taking expression of snail1 as a starting point and given the results in this study, we propose a model to explain gene activation of *FN1* promoter in during EMT (**Figure D.11**). As mentioned, the results presented here are mainly based on *FN1* promoter; however, *LEF1* promoter seems to be regulated in a similar fashion, suggesting that other NF- κ B-sensitive mesenchymal genes could be targeted likewise.

According to our results, in epithelial cells with mature adherens junctions, p65/RelA and β -catenin are stabilized in adherens junctions (1). Disruption of contacts by snail1-mediated E-cadherin repression (2) releases these signaling molecules to the cytosol and therefore enables their translocation to the nucleus. Disassembly of E-cadherin mediated contacts would be necessary, but not sufficient, for full mesenchymal gene expression, not only because before reaching the nucleus β -catenin and NF- κ B are modulated by additional mechanisms, but also because of snail1 participation in the activation complex.

Once in the nucleus, p65/RelA would bind to its box in *FN1* and *LEF1* promoters together with snail1 and PARP-1, recruit coactivators (such as p300) and promote transcription (3). At the same time, β -catenin translocation to the nucleus would also be translated into DNA binding through proteins other than LEF/TCFs in *FN1*, maybe a member of the SOX family or another unidentified protein and would collaborate in the activation of transcription (4). Simultaneous binding of the three EMT-related molecules (snail1, NF- κ B and β -catenin) to the promoters may activate transcription probably in a modular fashion and be selective for expression of mesenchymal genes.

In addition to the mechanism stated, promoters of mesenchymal genes containing E-boxes (or at least *LEF1* and *SNAIL1*) are also sensitive to a repressive regulation by snail1. Depending on the cellular context, and, particularly on E-cadherin levels, snail1 would cause either gene repression achieved by E-box binding (5) or gene activation, collaborating with proteins such as β -catenin or NF- κ B, this last one, as mentioned, facilitating snail1 indirect binding to DNA and the formation of an activation complex.

Other pathways such as MAPK or PI3K/Akt become active upon EMT induction (or as consequence of the same signals that promote snail1 expression and EMT). As a

result, TFCP2c would be activated by phosphorylation, probably on several residues, and nuclearly translocated (although we do not know the chronological order of such processes, 6). Once in the nucleus, TFCP2c would bind DNA, at least on the *FN1* promoter, upon release of a repressor (7) and collaborate with β -catenin and/or NF- κ B (though binding to a different region) to activate snail1-induced transcription.

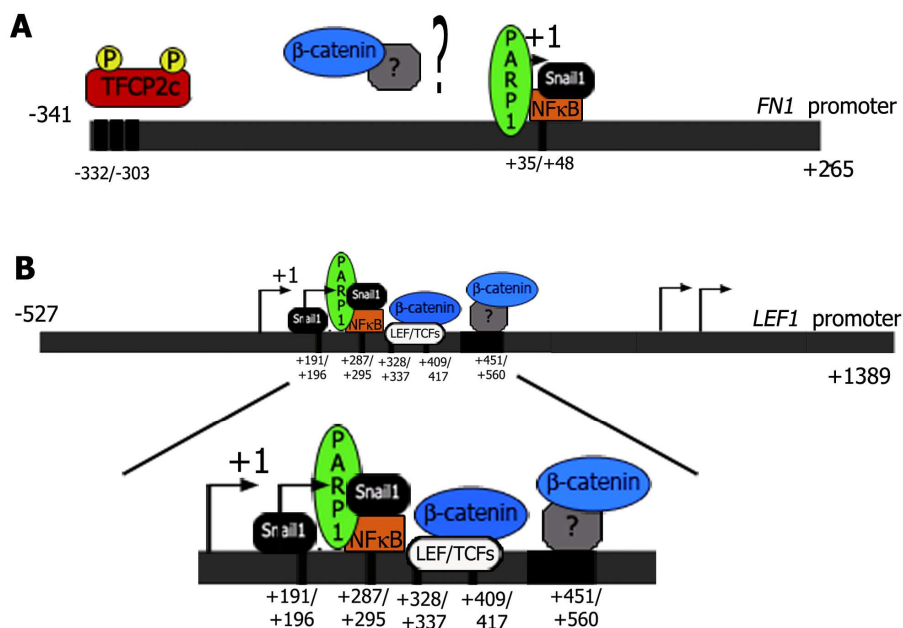


Figure D.11. Our model of gene activation induced by snail1. **A.** Schematic representation of the *FN1* promoter and the boxes identified as involved in snail1 mediated activation. Located at the region -332/-303 there are three putative boxes for TFCP2 and at +35/+48 a motif for NF- κ B binding. The proteins known to bind there are also represented. The sequence that mediates β -catenin binding remains unidentified. **B.** Schematic representation of the *LEF1* promoter and the boxes identified as involved in snail1-mediated activation. The four TSS are marked. At -191/-196 there is an E-box that can be bound by snail1 to mediate repression. Located at +287/+295 there is the NF- κ B box isolated in this study. The two LEF/TCF boxes are placed at +328/+337 and +409/+417, and the WRE at +450/+459. The proteins known to bind there are also represented. **C.** An epithelial cell displays adherens junction where E-cadherin maintains β -catenin and NF- κ B immobilized (1). The turnover of the junctions and occasional release of β -catenin results in its proteasomal degradation, preventing cytosolic and nuclear β -catenin accumulation. LEF/TCFs are bound to DNA but no transcription is active. *FN1* promoter also binds, at least, a repressor around -320bp. When EMT occurs (for example due to sufficient increase in snail1 protein levels caused by extracellular stimuli), E-cadherin is downregulated (2), junctions disassembled and both β -catenin and NF- κ B are released from their membrane docking. The cytosolic pool of β -catenin that avoids the degradation mechanisms (maybe due to mutations in the degradation pathway, which are frequently found in cancer cells) enters the nucleus and activates transcription both LEF/TCF dependently and/or independently (4). Similarly, NF- κ B, also released from the junctions, can translocate to the nucleus and activate transcription together with snail1 and PARP-1 from *FN1* and *LEF1* promoters (3). Snail1 can also bind to E-boxes of activated promoters and repress transcription, playing a dual repressor/activator role on them (5). Snail1 induced EMT also causes phosphorylation of TFCP2c by an unknown kinase and nuclear accumulation (6). Active TFCP2c binds to *FN1* promoter and collaborates to activate transcription (7).



CONCLUSIONS

CONCLUSIONS

1. In cultured epithelial cells snail1 expression induces phenotypic changes that are accompanied by an increase of *FN1* and *LEF1* gene expression. Forced E-cadherin expression blocks the action of snail1.
2. Snail1 activates transcription of *FN1* and *LEF1* promoters through indirect DNA binding to sequences other than E-boxes. The SNAG domain is required for this activation and for snail1 binding to the *FN1* promoter.
3. β -catenin is required for snail1-induced transcriptional activation of *FN1* and *LEF1* promoters. Snail1 expression induces *in vivo* binding of β -catenin to the *FN1* promoter in a TCF-independent manner.
4. The -341/-323 *FN1* promoter sequence and the +451+560 *LEF1* promoter region are required but not sufficient for transcriptional activation induced by snail1.
5. Snail1 promotes NF- κ B activity, an increase of the nuclear fraction of p65/RelA and *in vivo* binding of this NF- κ B subunit to a consensus binding sequence in *FN1* promoter located at +35/+48.
6. Snail1 binds to the +35/+48 NF- κ B box of *FN1* promoter indirectly. E-cadherin retains p65/RelA out of the nucleus and prevents NF- κ B and snail1 binding to the *FN1* promoter.
7. TFCP2c binds to the *FN1* promoter in snail1 expressing cells and is required for the snail1-induced transcriptional activity of this promoter. Snail1 causes nuclear accumulation and phosphorylation of TFCP2c.

EXPERIMENTAL PROCEDURES

E.P.1 CELL CULTURE

All cells were grown in Dulbecco's modified Eagle's medium (DMEM, Invitrogen) except for LS174T, which were grown in Roswell Park Memorial Institute (RPMI) 1640 medium (Invitrogen). Media were supplemented with glucose 4.5 g/L (Life Technologies), glutamine 2 mM, penicillin 56 U/ml, streptomycin 56 µg/L and 10 % fetal bovine serum (FBS; GIBCO). Cells were maintained at 37°C in a humid atmosphere containing 5 % CO₂ and 95 % air.

Cell line	Origin	Characteristics
HT29 M6	Human colon adenocarcinoma	Epithelial morphology. High levels of E-cadherin and tight cell contacts. Form compact colonies.
LS174T	Human colon adenocarcinoma	Epithelial morphology. Trypsinized variant of LS180 cells. Cells grow in islands and tend to pile on top of each other. Present a truncated allele of E-cadherin.
RWP1	Human pancreatic carcinoma	Epithelial morphology. Well-formed intercellular junctions.
SW480	Human colon adenocarcinoma	Intermediate morphology. At low confluence present low E-cadherin levels, phenotype reverted at high confluence. Truncated APC, β -catenin/TCF pathway highly active.
NIH3T3	Mouse embryonic fibroblasts	Mesenchymal morphology. Do not express E-cadherin.

Table E.P.I. Cell lines used during the development of this study and some of their characteristics.

HT29 M6 cells are a subpopulation of HT29 cells selected with metotrexate 10⁻⁶M that present mucosecretor phenotype. Stable HT29 M6 clones for mmsnail1-haemagglutinin (HA) were generated [406] and maintained in our laboratory. Expression of mmsnail1 in these clones is knocked down upon addition of doxycycline to the medium (2 µg/ml). Stable expression of snail1 is conserved with the addition of the antibiotics G418 (500 µg/ml) and hygromycin (200 µg/ml) to the culture medium.

Generation of LS174T cell clones with doxycycline inducible siRNA for β -catenin and doxycycline inducible Δ TCF4, kindly provided by Dr.H.Clevers (Hubrecht Institute for Developmental Biology and Stem Cell Research, Utrecht, The Netherlands), have been described elsewhere [227, 280]. Snail1-HA LS174T cells were generated by

Francisco Sánchez-Aguilera in our lab by transfecting pIRES-Snail1-eGFP or backbone plasmid into LS174T control cells with LipofectAMINE Plus kit from Invitrogen. A pool of GFP positive cells selected by fluorescence-activated cell sorter (FACS) was used in the experiments. Stable clones for snail1-HA were generated by Ferran Pons transfecting pIRES-snail1-neo or backbone plasmid into both LS174T clones and control cells with LipofectAMINE Plus kit from Invitrogen. Transfected cells were selected in medium containing G418 (300 $\mu\text{g}/\text{ml}$), and individual clones were isolated and grown under standard conditions [277]. Characterization of these cells can be observed in **Figure E.P.1**.

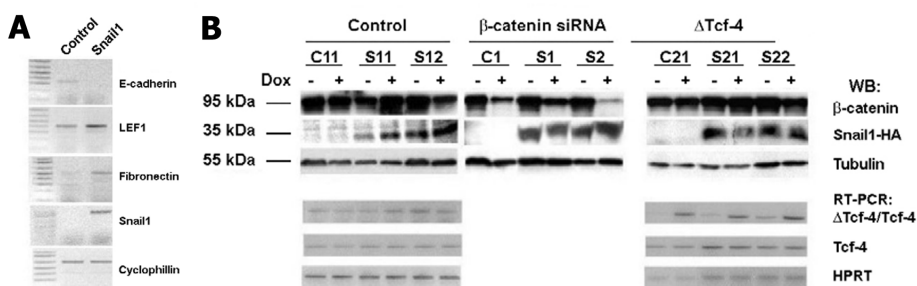


Figure E.P.1. Characterization of LS174T snail1 clones **A.** Snail1 expression induces mRNA levels of mesenchymal genes in LS174T control cells. mRNA was extracted from a pool of green LS174T control or Snail1 cells. Indicated genes were amplified by semiquantitative RT-PCR. **B.** Inducible repression of β -catenin and expression of Δ TCF4 in LS-174T clones. Total-cell protein extracts or RNAs were obtained from clones expressing snail1 (clones S) or controls (clones C). Doxycycline (1 $\mu\text{g}/\text{ml}$) was added for 6 days prior to the preparation of the extracts as indicated. β -catenin and snail1 expression were analysed by western blot with specific mAbs. Anti- α -tubulin was used as a loading control. Endogenous full-length TCF4 mRNA and exogenous Δ TCF4 plus endogenous TCF4 mRNAs were also analysed by RT-PCR. As a control, HPRT levels were determined.

Stable RWP1 clones were obtained after transfection with pIRES, pIRES-mmsnail1-HA or pIRES-mmsnail1-P2A-HA using LipofectAMINE reagent (Invitrogen). 48 hours after transfection cells were selected with G418 (500 $\mu\text{g}/\text{ml}$) and clones isolated. Expression of HA tag was confirmed by western blot.

Stable clones with SW480 cells, kindly provided by Dr. Alberto Muñoz (Instituto de Investigaciones Biomédicas "Alberto Sols," Consejo Superior de Investigaciones Científicas–Universidad Autónoma de Madrid, Madrid, Spain), were performed in two steps. Generation of SW480-ADH control and snail1-HA cells has been previously described [140]. These cells are sorted by an Epics Altra HSS (Beckman-Coulter) to select GFP-positive cells. For E-cadherin transfectants, SW480-ADH were transfected

with E-cadherin cDNA in the eukaryotic vector pBATEM2 (kindly provided by M. Takeichi, Kyoto University, Kyoto, Japan) [407]. Stable transfectants were obtained after selection with 2 mg/ml G418 and screened by western blot and immunofluorescence. The clones with higher E-cadherin expression were selected for subsequent experiments.

To obtain SW480 double transfectants, SW480-ADH cells previously transfected with E-cadherin were retrovirally transduced with murine snail1 cDNA tagged at the 3' end with the sequence encoding HA into the pRV-IRES-GFP retroviral vector (E-cadh-snail1-HA cells) or with the empty pRV-IRES-GFP vector (E-cadh cells). Retroviral infection was performed as described elsewhere [346]. Transduced GFP-positive cells were sorted by an Epics Altra HSS (Beckman-Coulter) and the pool of infected cells was used for further studies. As a routine, cells were sorted every 5-10 passages to eliminate the subpopulation of cells negative for GFP or GFP-snail1.

E.P. 2 DNA CONSTRUCTS

A summary of the constructs and vectors detailed here can be found in the annex (A.1)

Unless otherwise specified, a general cloning protocol was used to perform the constructions detailed here:

- (i) **Production of the linear insert** (a linear piece of the desired DNA sequence was obtained either from PCR or cutting a piece out of an already existing vector)
- (ii) **Cutting the insert (if needed) and target vector with appropriate endonucleases**
- (iii) **Ligating the linearized vector and insert together**
- (iv) **Transformation of the completed vector and screening** (in the DH5 α strain of *E. coli*)

All linearized vectors were dephosphorylated using calf intestine phosphatase (CIP) from New England Biolabs (NEB) for one hour at 37°C and ligation was performed with T4 ligase (NEB) either one hour at room temperature (for cohesive ends) or o/n on melting ice (blunt edges). Positive DNAs were confirmed by sequencing. For PCR fragments cloned blunt, phosphorylation was performed with T4 kinase and *Forward* buffer (Invitrogen) for fifteen minutes at room temperature. If fill-in was needed, *Klenow fragment* (NEB) was the enzyme used, fifteen minutes at room temperature. When needed, DNA was purified either from solution or agarose gel (0.5, 1 or 2 % depending on the size of the DNA) using the GFX PCR DNA and Gel Band Purification kit (Amersham Biosciences).

E.P.2.1 mmsnail1 constructs

E.P.2.1.i pcDNA3/pIRESneo-mmsnail1/P2A-HA

mmsnail1 in pcDNA3 and pIRESneo had already been cloned in our laboratory by Dr. Eduard Batlle; the process is described in [113]. cDNA from mmsnail1 was obtained by selective snail1 amplification from mRNA obtained from NIH3T3 cells. RT-PCR was performed using specific oligonucleotides obtained from the sequence published in GenBank (NM_011427) and cloned in 1992 in Thomas Gridley laboratory. The sense primer included a BamHI site, a *Kozak* sequence after the BamHI site and prior to the ATG initiation codon to improve translation. For the antisense oligonucleotide, the stop codon was eliminated and an EcoRV site used to keep the reading frame and the first Tyrosine of the haemagglutinin peptide (see **Table E.P.2**). The recipient vector (pcDNA3/pIRESneo) already had the HA tag cloned EcoRV/NotI.

Mutant mmsnail1-P2A was constructed on pcDNA3-mmsnail1-HA in our laboratory by Dr Eduard Batlle using the Quickchange Site Directed Mutagenesis Kit (Stratagene) as described in [113]. Primers used are stated in **Table E.P.2**. Cloning in pIRESneo was performed isolating mmsnail1-P2A from pcDNA3 using EcoICRI and NotI sites. pIRESneo was digested with EcoRV/NotI.

cDNA	Sense oligonucleotide (5'-3')	Antisense oligonucleotide (5'-3')
mmsnail1	CCGGAT <u>CCACC</u> ATG CCGCGCTCCTTCC TGG	CCGGATATCCGCGAGGGCCTCCGGAGCA
mmsnail1-P2A	GGCGGATCCACC <u>CCATG</u> G CGCGCTC CTTCCTGG	CCAGGAAGGAGCGCG CCAT <u>G</u> GGTGGATCC GCC

Table E.P.II. Oligonucleotides used for mmsnail1 and mmsnail1-P2A. Kozak sequence is underlined, initiation codon in bold, and mutation introduced in italic bold.

E.P.2.1.ii RSVneo-mmsnail1-HA

mmsnail1-HA cloned into pRSVneo was generated in our laboratory by Dr. Josep Baulida. A 0.9 Kb fragment was isolated from pcDNA3-mmsnail1-HA using HindIII and NotI digestion enzymes; vector was digested with XhoI. Cohesive ends were filled in and turned blunt prior to cloning.

E.P.2.1.iii pGEX-mmsnail1-HA

mmsnail1-HA had been previously cloned in our lab in pGEX-6P2 vector (Pharmacia) using BamHI/NotI digestion sites [113]. This vector was used to express mmsnail1 protein fused to GST in bacteria and subsequent purification for further assays.

E.P.2.1.vi pEGFP-mmsnail1-HA

Cloning of mmsnail1-HA in pEGFP-C1 was performed as described in [130].

E.P.2.2 VP16-TCF4/Rel-VP16

VP16-TCF4 was constructed by Dr. Isabel Puig by inserting the VP16 activating domain with a Kozak sequence just upstream of the initiation codon of TCF-4 [125]. Rel-VP16 was generated in our laboratory by Dr. David Domínguez. cDNA corresponding to VP16 was obtained from a construct already existing in our laboratory (VP16-Snail1, [113]) and fused in frame with the Rel domain of p65 (subunit of NF-κB). This chimeric cDNA was cloned into pcDNA3.

E.P.2.3 Luciferase reporter vector

The luciferase reporter vector used in most of the experiments of this study was pGL3 basic (promega) unless otherwise specified. Note that a putative snail1 binding site within the plasmid was mutated to eliminate background, subsequently naming the resulting vector pGL3*. pXP2 luciferase vector, courtesy of Dr. Manuel Fresno (Centro de Biología Molecular, CSIC-UAM, Madrid, Spain), was also used in some cases.

E.P.2.3.i pXP2

In order to clone the -341/+370 *FN1* promoter in pXP2, pGL3* -341/+370 *FN1* promoter (described in [130]) was first digested with *Mlu*I and filled in. A second digestion with *Xho*I was carried out and DNA obtained sliced from 1 % agarose gels. pXP2 was cut open by sequential digestion with *Sma*I and *Xho*I. *FN1* promoters -867/+265, -606/+265 and -341/+265 were PCR amplified (-867/+265, -606/+265 from genomic HT29 M6 DNA, 341/+265 from pGL3*-341/+370 *FN1*) with specific oligonucleotides (Table E.P.3) and high-fidelity *Pfx* polymerase (Invitrogen). Amplicons obtained were sliced from 1 % agarose gels and cloned into pXP2 cut open with *Sma*I.

Comparison of activity in basal conditions of the -341/+265 and -341/+370 *FN1* promoters (this last one with the prefibronectin sequence) in reporter assays made us choose the shorter sequence in front of the longer (previously used in our laboratory) since the prefibronectin coding sequence reduced the basal luciferase activity (Figure E.P.2).

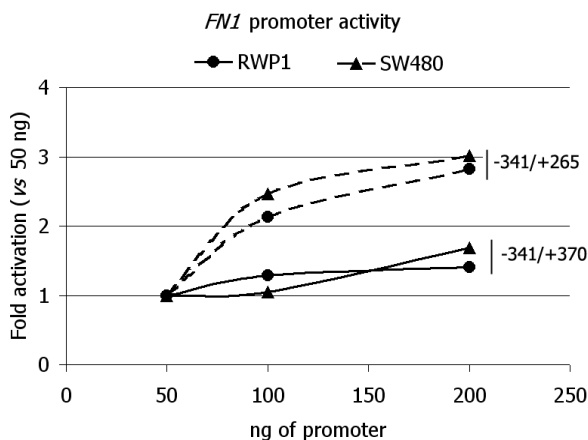


Figure E.P.2. The Prefibronectin sequence interferes with the *FN1* promoter activity. Reporter assays were performed transfecting RWP1 or SW480 cells with the indicated amount of pXP2 containing either -341/+370 (solid line) or -341/+265 (dashed line) *FN1* promoter. Luciferase activity was analyzed as explained in E.P.4. Values are referred to the activity of 50 ng of promoter.

E.P.2.3.ii pGL3*

- *FN1* promoters

Cloning of the -341/+370 *FN1* promoter in pGL3* has already been reported in [130]. The -867/+265 and -606/+265 promoters were obtained after selective PCR amplification from HT29 M6 genomic DNA with specific oligonucleotides and *Pfx* polymerase (Table E.P.3). The -341/+265 *FN1* promoter was amplified from the -341/+370 fragment also with *Pfx* polymerase (see Table E.P.3 for oligonucleotides). In the three cases the sense primer contained the restriction site for *MluI* and promoters were cloned digesting both vector and promoter with *MluI* and vector with *SmaI*. Except for the -341/+72 fragment, promoters were obtained by PCR amplification with specific oligonucleotides (Table E.P.3) and *Pfx* polymerase. The -341/+72 shortened *FN1* promoter was achieved digesting the -341/+370 *FN1* promoter with *PstI*-*XhoI* and ligating the resulting DNA. All the rest of truncated promoters were cloned using the *SmaI* restriction site in the pGL3* vector.

<i>FN1</i> promoter	Sense oligonucleotide (5'-3')	Antisense oligonucleotide (5'-3')
-867/+265	CCCCACGCGTCCCAGGAAAGGAAGGC	GTTGAGACGGTGGGGAGAG
-606/+265	CCCCACGCGTCCCAGTCAGTACCCTTTAG	GTTGAGACGGTGGGGAGAG
-341/+265	CCCCACGCGTACACAAGTCCAGCCACTCCC	GTTGAGACGGTGGGGAGAG
-322/+265	C TTTCTCCCAGCC	GTTGAGACGGTGGGGAGAG
-278/+265	GCTTCCCATCCCTTCCCCCA	GTTGAGACGGTGGGGAGAG
-236/+265	CCCAGTCTGGCGGGCCATCAGCATCTCTT TTGTTGCTGCGAACCACAGT	GTTGAGACGGTGGGGAGAG
-192/+265	CCCACAGTCCCCCGTG	GTTGAGACGGTGGGGAGAG
-36/+265	TACCGTCCCATATAAGCCCCGG	GTTGAGACGGTGGGGAGAG

Table E.P.III. Sense and antisense primers used to amplify the specified *FN1* promoters.

TCF, p300, NF- κ B and TFCP2c motif mutants of the *FN1* promoter were obtained from pGL3*-341/+265 *FN1* promoter according to the QuickChange™ side-directed mutagenesis protocol (STRATAGENE). Oligonucleotides used are specified in Table E.P.4. Mutations were confirmed by DNA sequencing.

Mutant	Oligonucleotide (5'-3')	
TCF [223]	Sense	TTCCCCCATCCCCTAA CAAGGGAGAGG ACCGCAAAGAAACC
	Antisense	GGTTTCCTTTGCGGTCTCT CCCTT GTTAGGGGATGGGGGAA
p300 [289]	Sense	CACGCGTACACAAGTCC ACCC CCCCCTTCTCCAGCC
	Antisense	GGCTGGGAGGAAAGGG GGGGG TGGACTTGTGTACGCGTG
NF-κB [408]	Sense	CTGCACAGGGGGAGGAGAG AGATCTGG AGGCGGAGCGGG
	Antisense	CCCCTCGCGCT CCAGAT TCTCTCTCTCCCTGTGCAG
TFCP2c (boxes 1&2)	Sense	GCTCTTACGCGTACACAAG GAATTCCGATAT CTTCTCCAGCCG
	Antisense	CGGCTGGGAGGAAAG ATATCGGAATTC CTTGTGTACGCGTAAGAGC

Table E.P.IV. Sense and antisense oligonucleotides used to amplify the specified *FN1* promoter mutants where the mutated bases are indicated (bold). In the case of NF-κB mutation, a BglII site was introduced. For the mutation of box number 1 of TFPC2c an EcoRI site was introduced; for box number 2 the site introduced was for EcoRV. References indicate the origin of the mutations introduced.

Reporter assays performed in RWP1 wild type cells upon cotransfection with VP16-TFC4 and the -341/+265 *FN1* promoters to confirm the loss of responsiveness of the TCF-box mutant to TCF showed that neither the mutant nor the wild type promoter were sensitive to TCF binding mediated transcription^{§§§§§§}. Loss of responsiveness of the NF-κB-box mutant of the -341/+265 *FN1* promoter to NF-κB binding mediated transcription was checked in reporter assays upon cotransfection with Rel-VP16 in SW480 wild type cells (**Figure E.P.3**).

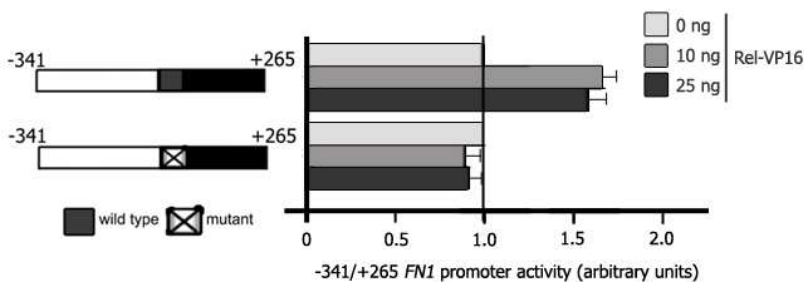


Figure E.P.3. The NF-κB-box *FN1* promoter mutant is not sensitive to Rel-VP16 in reporter assays. 500 ng of wild type or the NF-κB-box mutant *FN1* promoters cloned in pGL3* were cotransfected with the indicated amounts of Rel-VP16 in SW480 wild type cells. Luciferase activity was analyzed as explained in **E.P.4**. Values are referred to activity of the promoters when cotransfected with empty pcDNA3 (0 ng Rel-VP16), taken as 1 (vertical line).

^{§§§§§§} Assays performed by Cristina Agustí and collected in her PhD thesis entitled *Mecanisme d'activació de Fibronectina i LEF1 per Snail1 durant la transició epiteli-mesènquima*

- *LEF1* promoters

Generation of pGL3* luciferase reporter vector containing -527/+1389 *LEF1* promoter was performed by Francisco Sánchez-Aguilera as described in [130] (see **Table E.P.5** for primers). The E-box, TCF, and p300 mutants of *LEF1* promoter were obtained from the pGL3*-527/+1389 *LEF1* promoter following a QuickChange™ side-directed mutagenesis protocol (STRATAGENE) with specific primers shown in **Table E.P.5**. Double mutant for TCF boxes was obtained by mutation of the +406 TCF box on the promoter already containing the mutation of the +330 TCF box. Deletion of the Wnt responsive element (WRE) was performed PCR-amplifying the two fragments at each side of the element (-527/+450 and +561/+1389) independently with *Pfx* polymerase. A third PCR was carried out to join the two fragments obtained. Mutations were confirmed by DNA sequencing.

Mutant	Oligonucleotide (5'-3')	
-527/+1389	Sense	ATGCGGTACCCCTGTCTCCAAGAGCG
	Antisense	TGGCGCAGAGTTCCGG
Ebox [113]	Sense	GCAGTGGGAGGGCGCAGCCGCT AACCTAC GGGGCAGGGCGCGGAG
	Antisense	CTCCGCGCCCTGCCCCGTAGGTTAGCGGCTGCGCTCCCACTGC
TCF (+330) [223]	Sense	CAAGGGGCGCAGCT CGGAGCG TTGACAGAGCTGGCCG
	Antisense	CGGCCAGTCTGTCAAC GCTCCG AGCTGCGCCCTTG
TCF (+406) [223]	Sense	CTCGAGCCGGG ACCCTG ACGGGTCGG ACTGAGTGTG
	Antisense	CACACTAGTCCG ACCCGTCA GGGGTCCCGGCTCGAG
ΔWRE (+450/+559)	Sense	GTGTGTGTGTCGGCTCGAGCTACTTCTTTCTTCCCTCC
	Antisense	<u>GGAGGGGAAGAGAAAGAGAAGTAGCTCGAGCCGACACACAC</u>
p300 [289]	Sense	GAGGCCCCCGCT CTGCCCC CGAGACTCCGC
	Antisense	GCGGAGTCTCGGGG GGGCAG AGCGGGGGCCTC
NF-κB [408]	Sense	CGCGGCCAAGCTCG AAGGATCGG TCCCCCTCGGCCG
	Antisense	CGGCCGAGGGGAG CCGATCCTT CGAGCTTGCCCGCG

Table E.P.V. Sense and antisense oligonucleotides used to amplify the specified *LEF1* promoter mutants where the mutated bases are indicated (bold). For the WRE, the underlined sequences were used to anneal the two fragments (-527/+450 and +561/+1389) of the DNA. References indicate the origin of the mutations introduced. KpnI restriction site is in italics.

Reporter assays performed in RWP1 wild type cells upon cotransfection of each mutated promoter with VP16-TFC4 confirmed the progressive loss of responsiveness

of the TCF-box mutants to TCF binding mediated transcription (**Figure E.P.4.A**). Loss of responsiveness of the NF- κ B-box mutant of the -527/+1389 *LEF1* promoter to NF- κ B binding mediated transcription was checked in reporter assays upon cotransfection with Rel-VP16 in SW480 wild type cells (**Figure E.P.4.B**).

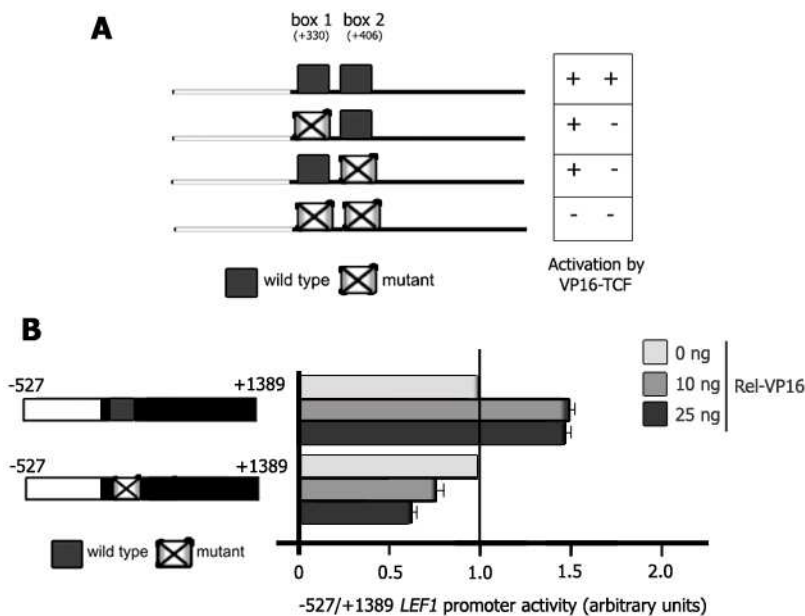


Figure E.P.4. Loss of responsiveness to specific transcription factors of the different mutant promoters were confirmed in reporter assays. A. Table that states the different response to VP16-TCF of the three TCF-box mutants of the -467/+1329 *LEF1* promoters and the wild type promoter upon cotransfection in RWP1 cells. **B.** The NF- κ B-box *LEF1* promoter mutant is not sensitive to Rel-VP16 in reporter assays. 250 ng of wild type or the NF- κ B-box mutant promoters cloned in pGL3* were cotransfected with the indicated amounts of Rel-VP16 in SW480 wild type cells. Luciferase activity was analyzed as explained in **E.P.4**. Values are referred to activity of the promoters when cotransfected with empty pcDNA3 (0 ng Rel-VP16), taken as 1 (vertical line).

E.P.2.3.iii pGL3* TK

This vector was obtained from Dr. Eduard Batlle's laboratory (IRB, Barcelona). It carries the minimal promoter of thymidine kinase (*TK*), cloned at the BglIII site of pGL3*. The -341/-185 *FN1* promoter was obtained through PCR amplification with Pfx polymerase of the -341/+265 *FN1* promoter using specific oligonucleotides (sense: 5' - CCCCACGCGTACACAAGTCCAGCCACTCCC - 3', antisense: 5' - ACTGTGGGTTCCGACGCG - 3'). Vector was cut open with SmaI.

The WRE of *LEF1* promoter was amplified by PCR with Pfx polymerase using the specific oligonucleotides 5' - CTTACGCGTCCGGGCAGAGGCATTT - 3' (sense) and 5' -

GATCTCGAGTTGCCAAGAATAAAGTTTTTGCC – 3' (antisense) on the -527/+1389 LEF1 promoter (used as template). It was cloned in MluI and XhoI sites.

E.P.2.3.iv NF3

The NF- κ B-sensitive plasmid *NF3*, which contains three binding sequences for this transcriptional factor upstream from a luciferase reporter gene, was kindly provided by Dr. Manuel Fresno (Centro de Biología Molecular, CSIC-UAM, Madrid, Spain).

E.P.2.4 TFCP2c constructs

E.P.2.4.i pcDNA3.1-TFCP2c-myc-His

cDNA corresponding to TFCP2c (NM_005653) mRNA was amplified by RT-PCR using 250 ng of RNA from RWP1 cells and specific primers (**Table E.P.6**). The sense oligonucleotide also included a *Kozak* (underlined) sequence after the BamHI site and prior ATG initiation codon (blod) to improve translation. For the antisense primer, the stop codon was eliminated. It was cloned blunt using the EcoRV site in the vector (isoform C). Expression of the tag was confirmed by western blot.

E.P.2.4.ii pcDNA3.1-TFCP2d-myc-His

Two independent PCRs were performed with pcDNA3.1-TFCP2c-myc-His as template, *Pfx* polymerase and specific primers to amplify sequences 1-564 and 717-1506 (**Table E.P.6**). A third PCR was performed to join the two parts of the cDNA. TFCP2d was cloned using the BamHI site in the sense primer and vector was cut open with BamHI and EcoRV sites. Expression of the tag was confirmed by western blot.

E.P.2.4.iii pBABE-TFCP2c-myc-His

cDNA corresponding to TFCP2c was obtained from pcDNA3.1-TFCP2c-myc-His digesting first with BamHI, filling in, and posterior digestion with PmeI. pBABE was cut open with EcoRI. Expression of the tag was confirmed by western blot.

E.P.2.4.vi pBABE-TFCP2c Q234L/K236E-myc-His

Specific sense and antisense primers (**Table E.P.6**) were used on the pBABE-TFCP2c-myc-His construct to generate the TFCP2c Q234L/K236E mutant in pBABE following a QuickChange™ side-directed mutagenesis protocol (STRATAGENE). Mutation was confirmed by DNA sequencing. Expression of the tag was confirmed by western blot.

Amplicon	Oligonucleotide (5'-3')	
TFCP2c	Sense	CGCGGAT <u>CCACCAT</u> GG CCTGGGCTCTGAAGC
	Antisense	GCCGCGGCCGCTTCAGTATGATTGATAGCTATCATTGG
1-564	Sense	CGCGGATCCACCATGGCCTGGGCTCTGAAGC
	Antisense	GCTTTCTGTCTGCACCTTTGGG <u>CTGAATAAACACAGATGCCTCTTTGC</u>
717-1506	Sense	<u>GCAAAGAGGACATCTGTGTTTATT</u> CAGCCCAAAGGTGCAGACAGAAAGC
	Antisense	GCCGCGGCCGCTTCAGTATGATTGATAGCTATCATTGG
TFCP2c Q234L/K236E	Sense	CGGCCAGCTGCCTGATC GAAG TTTTCAAGCCCAAAGG
	Antisense	CCTTTGGGCTTGAAA ACTTC GATCAGGCAGCTGGCCG

Table E.P.VI. Primers used to amplify the different TFCP2 constructs. For TFCP2c note the *Kozac* sequence, underlined, and the initiation codon, in bold. In addition, a BamHI site (in italics) is observed, although it was not used for the cloning. The antisense primer contains a NotI site (in italics), but it was not used either. The underlined sequences were used to anneal the two fragments of DNA amplified independently to clone TFCP2d. Mutations introduced to produce the TFCP2c Q234L/K236E are shown in bold.

E.P.2.5 pLKO

shRNAs for TFCP2c cloned into pLKO were obtained from MISSION (Sigma) with the reference numbers TRCN0000019824, TRCN0000019825, TRCN0000019826, TRCN0000019827, TRCN0000019828.

Solutions

Luria-Bertani (LB)

10 g/L tryptone
5 g/L yeast extract
10 g/L NaCl

LB-agar

LB
1.5 % agar (w/v)

Terrific Broth (TB)

12 g/L tryptone
24g/L yeast extract
720 mM K₂HPO₄
170 mM KH₂PO₄
4 % glycerol

Antibiotics

Ampicillin: 0.05 mg/ml
Kanamycin: 0.05 mg/ml

TAE

40 mM Tris pH 7.6
9.4 mM acetic acid
1 mM EDTA

Sample buffer for DNA (10x)

16.7 mM Tris-HCl pH 7.5
83.3 mM EDTA
16.7 Ficoll 400
0.6 % orange green

E.P.3 RNA STABILIZATION

LS174T cells stable for snail1 and control cells were seeded in 10-mm-diameter plates and grown until 70-90 % confluence. Actinomycin D was added at 5 µg/ml concentration and cells lysed for RNA extraction 4, 8 and 16 hours after the addition of the drug. A sample was taken without addition of actinomycin D as control. RNA was extracted with *Gene Elute™ Mammalian Total RNA Miniprep Kit* (Sigma-Aldrich) and quantified using a quartz cuvette and Cary 50 UV-Vis spectrophotometer (Varian). 300 ng of total RNA was used to perform quantitative PCR with specific primers (**Table E.P.7**) in *QuantiTect SYBR Green RT-PCR* (QIAGEN) in ABI PRISM 7900HT (Applied Biosystems). Hypoxanthine-guanine phosphoribosyltransferase (HPRT) was used as a control for qRT-PCR.

Amplicon	Primers	
	Sense (5'-3')	Antisense (5'-3')
HPRT	GGCCAGACTTTGTTGGATTTG	TGCGCTCATCTTAGGCTTTGT
Fibronectin	AGCAAGCCCGTTGTTATG	GCTCCACTGTTGACCCATCTG
LEF-1	CGAAGAGGAAGGCGATTTAG	GTCTGGCCACCTCGTGTC

Table E.P.VII. Pairs of primers used for quantitative RT-PCR after actinomycin D treatment.

E.P.4 REPORTER EXPERIMENTS

Cells were trypsinized between 60% and 80% of confluence seeded in 24-well culture plates at a density of 1×10^5 (HT29 M6), 8×10^4 (RWP1) or 6×10^4 (SW480) cells per well and transfected after 24 hours. Transfections were performed with *LipofectAMINE Plus* (Life Technologies) according to manufacturer's instructions. Cotransfection was performed with 1 ng of simian virus 40-Renilla luciferase plasmid as control for transfection efficiency. The activities of Firefly and Renilla were measured using the Dual Luciferase Reporter Assay System (Promega) 48 h after transfection with an FB 12 luminometer (Berthold Detection Systems, Pforzheim, Germany). Unless otherwise specified, luciferase activity was normalized by Renilla luciferase activity and empty reporter vector. Triplicates were systematically included, and experiments were repeated at least three times (represented by +/- standard deviation) unless otherwise specified.

E.P.5 GST FUSION PROTEIN PURIFICATION

For protein purification, an overnight 20 ml culture of bacteria (*E. Coli* BL21 or DH5 α strains) carrying pGEX-mmsnail1-HA was grown in Luria-Bertani (LB), diluted in a 180 ml culture and grown for 2 hours approximately until O.D._{600nm} was between 0.3 and 0.7. IPTG was added at final concentration of 0.1 M and culture grown for two more hours. Cells were centrifuged for 10 minutes at 4000 xg, 4°C and resuspended in cold STE buffer, 0.1 mg/ml lysozyme and 1.5 % sarkosyl. Sonication was performed (5x 10 seconds, 35 % amplitude) Triton X-100 added at 1% final concentration and lysates incubated 30 minutes at 4°C and agitation. Lysates were centrifuged for 20 minutes at 20000 xg and 4°C and GST-mmsnail1-HA recovered through affinity chromatography with Glutathion-Sepharose 4B beads (Amersham). After 10x beads volume washes with cold phosphate-buffered saline (PBS), beads were washed once with elution buffer. Next, protein was released using elution buffer and 100 mM reduced glutathione in elution buffer. If required, this step was repeated up to two or three times. Protein was dialyzed o/n against dialysis buffer. If protein was stored (-20/-80 °C) glycerol was added at a final concentration of 50 %.

Efficiency of the process was tested by loading samples obtained during the purification in a polyacrylamide gel and Coomassie blue staining. Protein concentration was determined by comparison in a polyacrylamide gel (SDS-PAGE) with a bovine serum albumin (BSA) patron after Coomassie blue staining.

Buffers and solutions

LB/TB (E.P.2)

Ampicillin 0.05 mg/ml

IPTG 0.1 M

STE

10 mM Tris pH 8.0

100 mM NaCl

1 mM EDTA

Sarkosyl 1.5 %

Lysozyme 0.1 mg/ml

PBS

136.9 mM NaCl

2.7 mM KCl

10.14 mM Na₂HPO₄

1.76 mM KH₂PO₄ pH 7.3

Elution buffer

100 mM Tris-HCl pH 8.0

120 mM NaCl

10 % glycerol

0.1% Triton X-100

5 mM DTT

(100 mM reduced glutathione)

Dialysis buffer

25 mM Tris pH 8.0

1 mM EDTA

120 mM NaCl

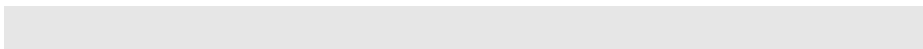
1 mM DTT

Coomassie blue staining

0.1 % (w/v) Coomassie blue

20 % (v/v) MeOH

10 % (v/v) Glacial acetic acid

SDS-PAGE (E.P.10)

E.P.6 BIOTINYLATED OLIGONUCLEOTIDE PULL-DOWN ASSAY (BOPA)

PCR was performed using as template pGL3* and the corresponding promoter (except for *CDH1*) with specific oligonucleotides (see **Table E.P.8**) tagged with biotin in the 5' end (sense primer only) and high-fidelity *Pfx* polymerase (Invitrogen).

	Promoter	Template	Sense primer (5'-3')	Antisense primer (5'-3')
FN1	-341/+265	pGL3* -341/+265 <i>FN1</i>	TACACAAGTCCAGCCACTCCC	GTTGAGACGGTGGGGAGAG
	-341/-37		TACACAAGTCCAGCCACTCCC	CCAGAGGGGCGGGAGG
	-36/+265		TACCGTCCCATATAAGCCCCGG	GTTGAGACGGTGGGGAGAG
LEF1	-527/+1389	pGL3* -527/+1389 <i>LEF1</i>	CTTGTCTCCAAAGAGCG	TGGCGCAGAGTCCGG
	-527/+1389 E-box mut	pGL3* -527/+1389 E box mut <i>LEF1</i>	CTTGTCTCCAAAGAGCG	TGGCGCAGAGTCCGG
CDH1	-92/-64	-	GGCTGAGGGTTCACCTGCC CCACAGCC	GGCTGTGGCGGCAGGTGAAC CCTCAGCCC
	-92/-64 E- box mut	-	GGCTGAGGGT TAACCT ACCG CCACAGCC	GGCTGTGGCGG GAAGGT AAA CCCTCAGCCC

Table E.P.VIII. Sense and antisense primers used to amplify the specified probes for BOPA assays. In the case of the *CDH1* promoter, probe was obtained annealing the primers as described for EMSA (**E.P.8**). Mutations are shown in bold. All sense primers were labelled with biotin at the 5' end.

PCR products were loaded in 1 % agarose gels and purified using GFX PCR DNA and Gel Band Purification Kit (Amersham). DNA was quantified using either a quartz cuvette and Cary 50 UV-Vis spectrophotometer (Varian, **Figure R.6, R.25**) or Thermo Scientific NanoDrop™ 1000 Spectrophotometer (**Figure R.8, R.27**) and loaded in a gel at equal amounts to confirm quantification.

With recombinant protein (Figure R.6)

Fibronectin promoter

Recombinant GST-mmsnail1-HA protein (10 ng) was incubated overnight at 4°C with 200 ng of *FN1* promoter probe (-341/+265) in binding buffer and agitation. 20 µl of total volume of streptavidin conjugated beads (Roche) blocked with 1 % bovine serum albumin (BSA) for 1 hour at room temperature (RT) were added to each sample

and incubated for 10 minutes at RT and agitation. Biotinylated streptavidin-conjugated probes were pulled-down centrifuging for 5 minutes at maximum speed, supernatant discarded and beads washed three times with washing buffer for 10 minutes. Beads were resuspended in 20 µl of sample buffer for proteins 1X concentrated (**E.P.10**) and incubated 5 minutes at 95°C. Protein was loaded in a 10 % polyacrylamide gel (SDS-PAGE) and transferred to a nitrocellulose membrane (Protran). Western blot was performed with rat antibody against HA (Roche).

LEF1 promoter*

GST or recombinant GST-mmsnail1-HA protein (100 ng) were incubated overnight at 4°C with 4 µg of wild type or mutated biotinylated LEF1 promoter probe (-467/+1329) in binding buffer and agitation. 5 µl of total streptavidin conjugated magnetic beads (New England Biolabs, NEB) were added to each sample and incubated for 10 minutes at 4°C and agitation. Biotinylated streptavidin-conjugated probes were pulled-down using a magnet (Promega); supernatant was discarded and beads washed. Beads were resuspended in 25 µl of sample buffer for proteins 1X concentrated and incubated for 5 minutes at 95°C. Protein was loaded in a 12 % polyacrylamide gel (SDS-PAGE) and transferred to a nitrocellulose membrane (Protran). Western blot was performed with antibody against GST (Pharmacia).

With total cell extracts (Figure R.25)

Control or snail1-HA stable SW480 cells were seeded in 150-mm-diameter plates and grown for 48 hours. Cells were then washed twice with phosphate-buffered saline (PBS), scrapped, and lysis buffer added. Lysates were incubated at 4°C for 30 minutes and then pelleted for 5 minutes at 14,000 rpm. 250 ng of DNA were incubated with 300 µg of protein in binding buffer.

10 µl of total streptavidin-conjugated magnetic beads (NEB, blocked overnight in PBS - 3% BSA) were added to each sample and incubated for 10 minutes at 4°C and agitation. Magnetic beads were pulled-down with a magnet (Promega) and washed three times. Protein was analysed in 15 % SDS-PAGE and western blot with antibody against HA.

* Experiment already presented in the PhD thesis entitled *Mecanisme d'activació de Fibronectina i LEF1 per Snail1 durant la transició epiteli-mesènquima*, by Cristina Agustí

With nuclear cell extracts (Figure R.8, R.29)

Nuclear extracts of snail1-HA or snail1-HA/E-cadherin stable SW480 cells were prepared as detailed in **E.P.10**. 250 µg of extract was preincubated with binding buffer and 15 µl of effective streptavidin-combined magnetic beads (New England Biolabs, NEB) for 3 hours at 4°C.

Samples were then incubated in a Dynal MPC®-S Magnet (Invitrogen) and supernatant recovered, storing 10 % of the volume as input (4°C). 250 ng of DNA probe was added to each sample and incubated overnight (~16 hours) at 4°C and agitation. 15 µl of effective streptavidin-conjugated magnetic beads (NEB) were added to each tube and samples incubated for 10 minutes at 4°C and agitation. Biotinylated probes were pulled-down with the streptavidin-combined magnetic beads and the unbound fraction was recovered (10 %). Three washes of 10 minutes each were performed at 4°C and agitation with the same buffer used for extracting the nuclear fraction. The remaining beads were resuspended in 15 µl of sample buffer for proteins 1X concentrated.

Samples were incubated at 95°C for 5 minutes. Protein was loaded in a 10 % polyacrylamide gel (SDS-PAGE) and transferred to a nitrocellulose membrane (Protran). Western blot was performed with rabbit antibody against HA (Sigma) or p65 (Santa Cruz, SC-372).

Buffers

PBS (E.P.5)

Washing buffer

Recombinant protein

FN1

Binding buffer

20 mM HEPES pH 7.6
150 mM KCl
3 mM MgCl₂
10 % glycerol
0.3 mg/ml BSA
0.5% Nonidet P-40
0.2 % Triton X-100
20 µg poly dl-dC

50 mM Tris pH 8.0
150 mM NaCl
1 % Triton X-100
0.5 % NaDoc
0.1 % SDS
5 µM ZnCl₂

LEF1

20 mM Tris pH 7.5
1 mM EDTA
300 mM NaCl

Total cell extracts

Lysis buffer

- 50 mM Tris pH 8.0
- 150 mM NaCl
- 1 % Triton X-100
- 0.5 % NaDoc
- 0.1 % SDS
- 5 μ M ZnCl₂
- Protease and phosphatase inhibitors

Binding buffer (BB)

- 20 mM HEPES pH 7.6
- 150 mM KCl
- 3 mM MgCl₂
- 10 % glycerol
- 0.3 mg/ml BSA
- 0.2 mM ZnSO
- 10 μ g of poly dl-dC
- 1 mM DTT
- Protease and phosphatase inhibitors

Washing buffer

- 50 mM Tris pH 8.0
- 150 mM NaCl
- 1 % Triton X-100
- 0.5 % NaDoc
- 0.1 % SDS
- 5 μ M ZnCl₂
- Protease and phosphatase inhibitors

Nuclear cell extracts

Cytoplasmic extraction buffer (E.P.10)

Nuclear extraction buffer (E.P.10)

Binding buffer

(total cell extracts BB)

Washing buffer

(nuclear extraction buffer)

SDS-PAGE (E.P.10)

E.P.7 CHROMATIN IMMUNOPRECIPITATION (ChIP)

Cells seeded in 150-mm-diameter plates were washed twice with phosphate-buffered saline (PBS) pre-warmed at 37°C and cross-linked with 1% formaldehyde for 10 minutes at 30°C in DMEM. Reaction was stopped by adding 250 µl of glycylglycine 2.5 M (0.125 M final concentration) and incubating for 2 more minutes. Cells were washed twice with cold PBS and 1 ml of Soft Lysis Buffer was added to the plates on ice. After scrapping, lysates were incubated for 10 minutes on ice and centrifuged for 15 minutes at 3000 rpm. Supernatant was discarded, pellet resuspended in SDS lysis buffer and sonicated to generate fragments of DNA from 200 to 1000 bp (40 % amplitude in Branson DIGITAL Sonifier® UNIT Model S-450D sonicator, **Table E.P.9**). Lysates were incubated for 20 minutes on ice and centrifuged at maximum speed for 10 minutes.

Cell line	Sonication pulses
HT29 M6	10 x 10 seconds
RWP1	10 x 10 seconds
SW480	5 x 10 seconds

Table E.P.IX. Sonication pulses in Branson DIGITAL Sonifier® UNIT Model S-450D sonicator.

Protein concentration was determined by Lowry and the desired amount of protein per immunoprecipitation (IP) was diluted in Dilution Buffer. Pre-clearing was performed to reduce background with mouse IgG (Dako) and salmon sperm-BSA (bovine serum albumin) blocked protein G (Upstate) for 3 hours at 4°C and agitation. Samples were then centrifuged at 2000 rpm input was stored and samples for IP divided and incubated either with specific antibody or irrelevant antibody of the same species (**Table E.P.10**) overnight at 4°C and agitation.

Antibody against	Species	Commercial	Dilution
HA	Rat/rabbit	Roche/Sigma	1:100
snail1 (hybridoma supernatant)	Mouse	-	1:30
Unspecific	Mouse	Sigma	1 ng/µl
p65/Rel A (sc-372)	Rabbit	Santa Cruz	1 ng/µl
TFCP2c (ab42973)	Rabbit	Abcam	10 ng/µl
Unspecific	Rabbit	DAKO	Same ng as the specific IgG

Table E.P.X. Antibodies used for ChIP analysis, their origin and assay dilution.

Blocked beads were added to each sample and incubated for one more hour at 4°C. Five washes were performed in MoBiTec columns with each Low Salt Buffer, High Salt Buffer, LiCl Buffer and TE Buffer (see below). Samples were eluted after centrifuging the columns to eliminate all traces of buffer (2 minutes, 2000 rpm) and incubating the remaining beads with Elution buffer at 37°C for 30 minutes. DNA was recovered by centrifugation (5 minutes, 2000 rpm).

Decrosslinking was performed incubating samples at 65°C overnight. After 2-4 hours digestion with proteinase K DNA was purified by the GFX PCR DNA and Gel Band Purification kit (Amersham Biosciences). DNA fragments were analyzed using quantitative PCR (Table E.P.9).

	Promoter amplified	Figure	Primers	
			Sense (5'-3')	Antisense (5'-3')
FN1	-1958/-1870	R.9.B, C; R.10; R.33	TCCTTCCCCCAGAATCAATGAA	GGGAAGCCGAGTGTTCCTCC
	Exogenous (+247/luc)	R.9.A; R.10.E; 15.B; R.33A	GTTGAGACGGTGGGGGAGA	GGTGGCTTACCAACAGTACCG
	+116/+265	R.9.B, C; R.10.E; R.15.A, C;	CGTCCCCTTCCCCACC	GTTGAGACGGTGGGGGAGA
	-375/-320	R.29.C; R.33.B	GGGAAGGGGGAGCGTCTTG	AAGGGAGTGGCTGGACTTGT
Pol II	-126/-63	R.9.A; R.15.C	GCTTTTTCTCCCAACTCG	TAGGTGCTCAGACCTCGTCA
CDH1 [134]	-178/+72	R.10. E	ACTCCAGGCTAGAGGGTCAC	GCCCGACCCGACCGCACCCG

Table E.P.XI. Primers used to analyze the promoters by quantitative PCR. Note that to amplify exogenous promoter the antisense primer anneal with the pGL3* sequence 3' to the cloned promoter (luciferase gene). Pol II: polymerase II

Exogenous promoter (Figure R.9.A, R.10.E R.15.B, R.33.A)

3.5x10⁶ RWP1 cells were plated in 150 mm dishes and 5 µg of pGL3*-341/+265 FN1 promoter transfected with LipofectAMINE®-PLUS reagent (Invitrogen) according to manufacturer's instructions. 48 hours after transfection cells were treated following the protocol described. The amount of protein used per IP was 100 µg unless otherwise specified.

Endogenous promoter (Figure R.9.B, C, R.10.E, R.15.A, C, R.29.C, R.33.B)

Cells were plated in 150 mm dishes according to the cell line needed. The amount of protein used per IP was 250 µg or 500 µg.

Cell line	Number of cells	Days seeded before extraction
HT29 M6	15x10 ⁶	1-2
RWP1	10x10 ⁶	1-2
SW480	3x10 ⁶	4-5

Table E.P.XII. Number of cells seeded and days in plate to ensure formation of junctions before performing the assay.

Buffers and solutions

PBS (E.P.5)

DMEM 0 % FBS

2.5 M glycine

Proteinase K

Soft lysis buffer

50 mM Tris pH 8.0

2 mM EDTA

0.1 % Nonidet P-40

10 % glycerol

Protease and phosphatase inhibitors

SDS lysis buffer

1% SDS

10 mM EDTA

50 mM Tris pH 8.0

Dilution buffer

0.001% SDS

1.1% Triton X-100

16.7 mM Tris pH 8.0

2 mM EDTA

2 mM EGTA

167 mM NaCl

Low Salt buffer

0.1 % SDS

1 % Triton X-100

2 mM EDTA

20 mM Tris pH 8.0

150 mM NaCl

High Salt buffer

0.1 % SDS

1 % Triton X-100

2 mM EDTA

20 mM Tris pH 8.0

500 mM NaCl

LiCl buffer

250 mM LiCl

1 % Nonidet P-40

1 % Sodium deoxycholate

1 mM EDTA

10 mM Tris pH 8.0

Elution buffer

100 mM Na₂CO₃

1% SDS

E.P.8 ELECTROPHORETIC MOBILITY SHIFT ASSAY (EMSA)

Cells seeded in 150-mm-diameter plates were washed twice with cold phosphate-buffered saline (PBS) and centrifuged for 5-10 minutes at 1000 rpm. Pellet was resuspended softly with two volumes of buffer 1 and incubated on ice for 10 minutes. After a 10 minute centrifugation at 5000 rpm (4°C) cytosol was isolated in the supernatant. Pellet was then resuspended with the same volume of buffer 2 (see below), incubated on ice for twenty minutes and centrifuged at 5000 rpm for 30 minutes (4°C). The supernatant, containing the nuclear fraction, was dialyzed o/n against 1L of buffer 3 (4°C). Samples were quantified by Bradford and stored at -80°C.

Probe	Oligonucleotides	
	Sense (5'-3')	Antisense (5'-3')
<i>FN1</i> -339/-320	ACAAGTCCAGCCACTCCCTT	AAGGGAGTGGCTGGACTTGT
<i>FN1</i> -322/-309	CTTTCCTCCCAGCC	GGCTGGGAGGAAAG
<i>FN1</i> -341/-301	ACACAAGTCCAGCCACTCCCTTCTCCC AGCCGATTCCCAT	ATGGGAACGGCTGGGAGGAAAGGGAGT GGCTGGACTTGTGT
<i>FN1</i> +24/+53	GGGGGAGGAGAGGGAACCCAGGCGCGAG	CTCGCGCTGGGGTCCCTCTCTCCCCC

Table E.P.XIII. ³²P labelled probes used in EMSA experiments.

Sense and antisense oligonucleotides of the probes (Table E.P.13) were annealed in TEN buffer for 10 minutes at 70°C and allowed to cool until they reached room temperature (about three hours or o/n). Probe was then labelled with gamma ³²P using T4 polynucleotide kinase (Invitrogen) according to manufacturer's instructions. Excess of unincorporated radioactive ATP was removed with the use of *Microspin TM G-25 columns* (Amersham Pharmacia Biotech Inc). One microliter was used for cpm quantification.

Cell extracts

EMSA reaction was carried out with the smallest possible volume (usually 10-20 µl) according to the components needed. 10µg of nuclear extract or the indicated amount of recombinant protein (Figure R.22) were incubated with 100,000 cpm of ³²P labelled probe in binding buffer for 30 minutes on ice. When competition was performed the stated amount of cold probe (Table E.P.14) was added to the reaction.

When antibody (**Table E.P.15**) was used the binding reaction was supplemented with the indicated amounts of irrelevant or specific antibody and incubated for 15 minutes prior to the addition of the radiolabelled probe.

Probe to compete	Sense oligonucleotide (5'-3')	Wt	Mutated	Figure
FN1 -341/-301	ACACAAGTCCAGCCACTCCCTTTCTCCAGCCGATTCCCAT	X		R.21
	ACACAAGTCCAGCCACTCCCTT	X		R.31
	<u>GTG</u> CAAGTCCAGCCACTCCCTT		X	R.31
	ACAT <u>GCG</u> CTCAGCCACTCCCTT		X	R.31
	ACACA <u>AAAA</u> CAGCCACTCCCTT		X	R.31
	ACACAAGTCTTTCCACTCCCTT		X (TFCP2c)	R.31
	ACACAAGTCCAGTTGCTCCCTT		X	R.31
	ACACAAGTCCAGCCAG <u>GGG</u> CCTT		X (TFCP2c)	R.31
	ACACAAGTCCAGCCACTCGGGG		X	R.31
FN1 +24/+53	AGTTGAGGGGACTTTCCAGGC *	X		R.28
	AGTTGAGGAGATCTG <u>G</u> CCAGGC *		X (NF-κB)	R.28

Table E.P.XIV. Probes used to compete EMSA experiments. Mutations are underlined. The asterisks indicate probes not annealing the *FN1* promoter sequence itself but consensus NF-κB motif [409].

Antibody	Commercial
Mouse unspecific	Sigma
Rabbit unspecific	DAKO
snail1 (hybridoma purified)	-
β-catenin	BD Transduction Laboratories
p65 (sc-372)	Santa Cruz

Table E.P.XV. Antibodies used in EMSA and their origin

A non-denaturing TBE-polyacrylamide gel was prepared and left polymerizing o/n at 4°C. Prerunning was performed for at least one hour prior to loading the gel (100 V). Samples were loaded in the gel and an additional lane was left for loading buffer. Gel was run at constant voltage (125 V), dried and exposed to an autoradiography.

Buffers and solutions

Buffer 1

10 mM Hepes pH 7.6
1.5 mM Cl_2Mg
10 mM KCl
0.5 % Nonidet P-40
0.5 mM DTT
Protease and phosphatase inhibitors

Buffer 2

20 mM Hepes pH 7.6
1.5 mM Cl_2Mg
840 mM KCl
0.5 mM DTT
0.2 mM EDTA
25 % glycerol
Protease and phosphatase inhibitors

Buffer 3

20 mM Hepes pH 7.6
100 mM KCl
0.5 mM DTT
0.2 mM EDTA
20 % glycerol

Binding buffer (for nuclear extracts)

20 mM HEPES pH 7.6
150 mM KCl
3 mM MgCl_2
10 % glycerol
0.3 mg/ml BSA
0.2 mM ZnSO_4
10 μg of poly dl-dC
Protease and phosphatase inhibitors
1mM DTT

Binding buffer (for recombinant protein)

20 mM HEPES pH 7.9
100 mM KCl
3 mM MgCl_2
4 % Ficoll 400
0.1 % Nonidet P-40
1.5 mM ZnCl_2
0.5 mg/ml BSA
10 μg of poly dl-dC
1 mM DTT
Protease and phosphatase inhibitors

TEN buffer

10 mM Tris pH 7.5
50 mM NaCl
1 mM EDTA

Loading buffer

20 % Ficoll 400
0.1 mM EDTA
1 % SDS
0.25 % Bromophenol blue
0.25 % Cyanol xylene

TBE (10x)

1 M Tris
1 M Boric acid
10 mM EDTA pH 8.0

Non-denaturing TBE-polyacrylamide gel

0.5X TBE
8 % polyacrylamide (37.5.1
acrylamide/biscarylamide)
0.02 % APS
0.0012 % TEMED

E.P.9 TRANSFECTION/INFECTION

Cell type	Plate	Number of cells
HT29 M6	6 well plate	5×10^5
	100 mm \emptyset	1×10^6
RWP1	6 well plate	5×10^5
	100 cm \emptyset	1×10^6
	150 mm \emptyset	1×10^7
SW480	150 mm \emptyset	1×10^7

Table E.P.XVI. Conditions in which cells were plated for transfection/infection

E.P.9.1 Transfection

Cells were seeded according to the cell type and plate (see **table E.P.16**) and 24 hours later transfection was performed using either LipofectAMINE®-PLUS reagent (Invitrogen) according to manufacturer's instructions or polyethylenimine polymer (PEI).

For PEI, a mixture was performed with NaCl, DNA and, ultimately, PEI (see **table E.P.17**), incubated 15 minutes at room temperature and added drop-wise to the target cells. 24-48 hours later, cells were analysed.

Plate	DNA amount (max)	NaCl (final volume, μ l)	PEI (μ l)
6 well plate	2 μ g	200	10
100 cm \emptyset	15 μ g	1560	78
150 mm \emptyset	33 μ g	3320	166

Table E.P.XVII. Conditions for PEI transfection.

E.P.9.2 Infection

Retrovirus

The cell line used for retrovirus production was HEK-293 Phoenix Gag-pol cells (derivatives of the Human Embryonic Kidney cell line 293), which stably express HIV-1 *Gag* and *Pol* gene products [410]. Cells were plated in flasks and grown to 90-

110 % confluence. For transfection, a mix containing NaCl, DNA (20 % pCMV-VSV-G, coding for the viral envelope, and 80 % pBABE or pBABE-TFCP2c Q234L/K236E-myc) and PEI polymer, was vortexed and incubated for 15 minutes at room temperature. The mixture was added to 293 cells drop-wise and, after 24 hours, the medium changed to concentrate the virus (see **table EP.18**). After 24 more hours fresh medium was added to 293 cells and the former was filtered, added 8 µg/ml polybrene and used to replace the medium of the target cells. A second infection was carried out 24 hours after the first and 293 cells discarded. One day after the second infection cell were either lysed or selected with puromycin (2µg/ml).

293 Gag-pol cell flask	Concentration medium (ml)
6 well plate	2
100 cm ø	8
T-75	12
T-150	24

Table E.P.XVIII. Concentration medium according to cell flask

Lentivirus

Lentiviruses were used for expressing shRNAs for TFCP2c. The cell line used for virus production was HEK-293T. The process carried out was basically the same as for retrovirus; the DNAs transfected were: pLKOsh (50 %), pCMV-VSV-G (10 %), pMDLg/pRRE (30 %) and pRSV rev (10%), these last two for virus packing. Five shRNAs for TFCP2c were infected as a mix or an irrelevant shRNA (Sigma) as control.

Thymidine (20 µM) was added to the medium of target cells to avoid apoptosis caused by TFCP2c knockdown [382].

Solutions

- 1 mg/ml PEI pH 7.35
- 150 mM NaCl
- 8 µg/ml polybrene (1000x)

E.P.10 PROTEIN EXTRACTION AND ANALYSIS

Total protein extraction buffer (1% SDS)

Total cell extracts were prepared by homogenising cells in SDS buffer after two washes with PBS. After passing cells through a 20-gauge syringe, extracts were centrifuged at 20,000 g for 5 minutes. Protein concentration from supernatants was determined by Lowry.

Nuclear/cytosol extraction

Cells were washed twice with PBS and scrapped in 500 μ l of cytoplasmic extraction buffer (buffer A). After 10 minutes of incubation on ice, Triton X-100 was added 1/30 to the extract and the samples vortexed for 30 seconds. After one minute centrifugation, the supernatant, containing the cytosolic fraction, was recovered and treated as explained in (i). Nuclei, in the pellet, were treated as detailed in (ii)

(i) Buffer B was added at 1.1 times the volume of the cytosolic fraction and the mix incubated for 30 minutes in agitation; then it was centrifuged at maximum speed for 30 minutes and pellets discarded.

(ii) Pellet containing the nuclei was washed three times in the buffer for cytosolic extraction to eliminate contamination and then resuspended in 100 μ l of nuclear extraction buffer (buffer C). Samples were incubated at 4°C for 30 minutes in agitation and then centrifuged at maximum speed for 15 minutes. The supernatant contained the nuclear fraction.

Analysis by western blot

Protein was loaded in sodium dodecyl sulfate polyacrylamide gel electrophoresis (SDS-PAGE) at different percentages and gels were run in TGS buffer. Proteins were transferred to a nitrocellulose membrane (Protran), between one and two hours and a half depending on the MW of the protein using transfer buffer (TB).

Membranes were blocked with 5 % non-fat milk in TBS-t for one hour. Primary antibody was added to fresh blocking solution or prepared in 3 % bovine serum albumin(BSA)-TBS-t (see **Table E.P.19** for dilutions) and incubated either one hour at room temperature (RT) or o/n at 4°C. After three ten minutes washes with TBS-t-milk, secondary antibody peroxidase-combined (HRP) was incubated (in the same solution) for forty-five minutes at RT. Two more ten minutes washes were performed with TBS-t and one last with TBS prior to developing.

Recognizes	Species	Commercial	Code	Dilution	Protein		Gel		Transfer time (400 mA)	Type of extracts	
					Identity	Amount	PAM %	Width			Kit
annexin	rabbit		-	1:2000	annexin	5 µg	10/7.5	0.75 mm	Mp3 (Biorad)	90 min	Total
pyruvate kinase	goat	Chemicon	AB1235	1:10000	pyruvate kinase	5 µg	10	1.50 mm	Mp3 (Biorad)	90 min	Total/cytosol
lamin B1	rabbit	Abcam	ab16048	1:2000	lamin B1	5 µg	10/7.5	1.50 mm	Mp3 (Biorad)	90 min	Nucleus
E-cadherin	mouse	BD Transduction Laboratories	610182	1:2500	E-cadherin	5 µg	7.5	1.50 mm	Mp3 (Biorad)	120 min	Total
HA	rat	Roche	1867431	1:1000	small HA	Min 20 µg	10/15	1.50 mm	Mp3 (Biorad))	90 min	Total/nucleus
fibronectin	rabbit	Sigma	H6908	1:2000	fibronectin	5 µg	7.5	0.75 mm	Mp3 (Biorad)	120 min	Total
LEF-1	rabbit	Cell signaling	A0245	1:2000	LEF-1	Min 40 µg	10/7.5	1.50 mm	Mp3 (Biorad)	90 min	Nucleus
TFCP2c	rabbit	Abcam	ab42973	1:2000	TFCP2c	Min 40 µg	7.5	1.50 mm	Mp3 (Biorad)	90 min	Total/Nucleus
TFCP2c	rabbit	Abcam	ab42973	1:2000	TFCP2c	Min 40 µg	7.5	1.50 mm	Protein Xi (Biorad)	300 min (800 mA)	Nucleus
myc	mouse	(hybridoma)	-	1:100	TFCP2c-myc	Min 20 µg	7.5	1.50 mm	Mp3 (Biorad)	90 min	Total/nucleus

Table E.P.XIX. Proteins analyzed and details for western blot. PAM: polyacrylamide; Min: minimum; Mp 3: miniprotein 3

Membranes were developed using substrate for HRP *Enhanced ChemiLuminescence*, *ECL*, either incubating PIERCE® ECL Western Blotting substrate for one minute or Supersignal® West Dura Extended Duration substrate. Membranes were exposed on Agfa-Curix autoradiographic films.

Solutions

1 % SDS buffer

1% SDS
10 mM EDTA
50 mM Tris pH 8.0

Citoplasmic extraction buffer (A)

10 mM HEPES pH 7.8
1.5 mM MgCl₂
10 mM KCl
0.5 mM DTT

Buffer B

0.3 M HEPES pH 7.8
1.4 M KCl
30 mM MgCl₂

Nuclear extraction buffer (C)

20 mM HEPES pH 7.8
25 % glycerol
0.42 M NaCl
1.5 mM MgCl₂
0.2 mM EDTA
0.5 mM DTT

Ponceau

0.5 % Ponceau (w/v)
1 % Glacial acetic acid

SDS-PAGE recipe (Table E.P.20)

TGS

25 mM Tris OH pH8.3
192 mM glycine
5 % SDS

Transfer buffer

50 mM Tris OH
386 mM glycine
0.1 % SDS

Sample buffer for proteins (Laemmli, 1X)

60 mM Tris-HCl pH 6.8
2% SDS
5 % β-mercaptoethanol
0.005 % Bromophenol blue
5 % glycerol

TBS

25 mM Tris-HCl pH 7.5
137 mM NaCl

TBS-t

TBS
0.1 % tween

Protease inhibitors

10 µg/ml aprotinin
1 mM leupeptin
2 mM pepablock
10 µg/ml pepstatin

Phosphatase inhibitors

1 mM b-glycerol phosphate
10 mM sodium fluoride phosphatase (NaF)
2 mM sodium orthovanadate (NaOV)

	Resolving			Stacking
% polyacrylamide	7.5	10	15	4
H ₂ O	5.5 ml	4.9 ml	3.6 ml	6 ml
Tris-HCl 1.5 M pH 8.8	2.5 ml			-
Tris-HCl 0.5 M pH 6.8	-			2.5 ml
10 % SDS	100 µl			
Acrylamide/bisacrylamide (37.5:1)	1.9 ml	2.5 ml	3.8 ml	1.4 ml
10 % APS	40 µl			
TEMED	20 µl			
Final volume	10 ml			

Table E.P.XX. Reagents used to prepare polyacrylamide gels.

E.P.11 COMPUTATIONAL TOOLS

Sequence alignment was performed using either Clustal w algorithm [175] or the application of Basic Local Alignment Search Tool (BLAST) to compare two known sequences (bl2seq) [411].

- Clustal w web page: <http://www.ebi.ac.uk/Tools/clustalw2/index.html>
- BLAST two sequences web page: <http://www.bork.embl.de/blast2gene/>

The scanning of promoter sequences for transcription factor motives were performed with two online programs that use the TRANSFAC database [412]:

- TFSEARCH (Searching Transcription Factor Binding Sites):
<http://www.cbrc.jp/research/db/TFSEARCH.html>
- TESS: (Transcription Element Search System):
<http://www.cbil.upenn.edu/cgi-bin/tess/tess>

E.P.12 IMMUNOFLUORESCENCE

Cells were grown on ethanol sterilized glass coverslips for at least 48 hours. After two washes with phosphate-buffered saline (PBS), 4 % paraformaldehyde (PFA) was added for fixing and incubated for ten minutes at room temperature (RT). After two more washes with PBS, coverslips were incubated with 50 mM NH₄Cl/PBS for five minutes RT to neutralize fluorescence emitted by PFA. Permeabilization was performed with 0.2 % Triton X-100, five minutes at RT.

Blocking was carried out for 1 h with PBS containing 3 % bovine serum albumin (BSA). Primary antibody was diluted in the same blocking solution and incubated for 1 more hour. After five washes with blocking solution secondary antibody was incubated for 45 minutes at RT. Once the antibody was removed, three washes with blocking solution and two with PBS alone were performed. In **Table E.P.21** there is a summary of the antibodies used.

If nuclear counterstaining was performed, coverslips were incubated for one minute with a solution prepared at 5 µg/ml of propidium iodide and 100 µg/ml RNase. Two more washes with PBS were performed and one last with water prior to mounting either with Mowiol 4.88 or fluoromont G.

Finally, fluorescence was viewed through a Leica TCS-SP2 confocal microscope.

Primary antibody		Secondary antibody		Figure
	dilution		dilution	
β-catenin (BD Transduction Laboratories)	5 µg/ml	anti mouse IgG TRITC (DAKO)	1:50	R.14
TFCP2c (Abcam)	20 µg/ml	anti rabbit IgG 488 (Alexa)	1:500	R.37.A

Table E.P.XXI. Antibodies and conditions for immunofluorescence.

Solutions

PBS (E.P.5)	5 µg/ml propidium iodide
4 % PFA	100 µg/ml RNase
50 mM NH ₄ Cl/PBS	Mowiol 4.88
Triton X-100	fluoromont G
PBS/3 % BSA	

E.P.13 RT-PCR

RNA was extracted with *Gene Elute™ Mammalian Total RNA Miniprep Kit* (Sigma-Aldrich) and quantified using either a quartz cuvette and Cary 50 UV-Vis spectrophotometer (Varian) or Thermo Scientific NanoDrop™ 1000 Spectrophotometer. For semiquantitative analysis 250 ng of RNA were used for reaction. For quantitative analysis 100 ng of the cDNA obtained with Transcriptor First Strand cDNA Synthesis Kit (Roche) from 1 µg of RNA was used. Products from both semiquantitative RT-PCR and quantitative PCR were loaded in 2% agarose gels to check that fragment size was that expected.

Amplicon	Primers		PCR conditions	
	Sense (5'-3')	Antisense (5'-3')	Temp (°C)	Cycles
HPRT	GGCCAGACCTTTGTTGGATTTG	GGCCAGACCTTTGTTGGATTTG	55-60	28
pumilio	CGGTCGTCTGAGGATTAATAA	CGTACGTGAGGCCGTGAATAA	58	-
mmsna11	GCGCCGGTCGTCTTCTCGTC	CTTCGGCGAC TGGGGGTCT	55-60	28-30
hssna11	TTCCAAGCAGCCCTACGACCAAG	GCCTTTCCCACTGTCTCATC	58	28-35
E-cadherin	GAAAGCATTGCACATACAC	ATTGGGGCTTGTGTGTCATTC	55-60	24-27
fibronectin	AGCAAGCCCGTTGTTATG	AGCAAGCCCGTTGTTATG	55-60	26-30
LEF1	CGAAAGAGGAAAGCGATTAG	GTCTGGCCACCTCGTGTGTC	55	35-40
TFCP2c	TTCTGTGGGACCCCTGC	CTATTGTACTCGGATGACACCC	55-60	26-32
TFCP2d	TTCTGTGGGACCCCTGC	TGCACCTTTGGCTGATATAAC	60	35-40

Table E.P.XXII. Primers and conditions for RT-PCR analysis

E.P.14 CELL ELECTROPORATION (AMAXA)

In **Figure R.14**, electroporation of LS174T cells was performed with Cell Line Nucleofector® kit (Amata GmbH). 3×10^6 cells were trypsinized and centrifuged at 200xg for ten minutes. After completely discarding supernatant, cells were resuspended in Nucleofector® Solution V. Cell suspension was mixed with 4 µg of pEGFP-snail1-HA and electroporated in the Nucleofector® device according to program T-20. 500 µl of pre-warmed culture medium were added to the cuvette to transfer cells to a 24 well plate (approx. 125,000 cells per well).

REFERENCES

1. Lodish H, Berk A, Zipursky SL, Matsudaira P, Baltimore D, Darnell J: *Molecular cell biology*. 4th edn. New York: W. H. Freeman; 2000.
2. Evan G, Littlewood T: **A matter of life and cell death**. *Science* 1998, **281**:1317-1322.
3. Kinzler KW, Vogelstein B: **ONCOGENESIS: Landscaping the Cancer Terrain**. *Science* 1998, **280**:1036-1037.
4. Hanahan D, Weinberg RA: **The hallmarks of cancer**. *Cell* 2000, **100**:57-70.
5. Christiansen JJ, Rajasekaran AK: **Reassessing epithelial to mesenchymal transition as a prerequisite for carcinoma invasion and metastasis**. *Cancer Res* 2006, **66**:8319-8326.
6. Gotzmann J, Mikula M, Eger A, Schulte-Hermann R, Foisner R, Beug H, Mikulits W: **Molecular aspects of epithelial cell plasticity: implications for local tumor invasion and metastasis**. *Mutat Res* 2004, **566**:9-20.
7. Farquhar MG, Palade GE: **Junctional complexes in various epithelia**. *J Cell Biol* 1963, **17**:375-412.
8. Thiery JP: **Epithelial-mesenchymal transitions in development and pathologies**. *Curr Opin Cell Biol* 2003, **15**:740-746.
9. Boyer B, Thiery JP: **Epithelium-mesenchyme interconversion as example of epithelial plasticity**. *Apmis* 1993, **101**:257-268.
10. Hay ED: **An overview of epithelio-mesenchymal transformation**. *Acta Anat (Basel)* 1995, **154**:8-20.
11. Savagner P: **Leaving the neighborhood: molecular mechanisms involved during epithelial-mesenchymal transition**. *Bioessays* 2001, **23**:912-923.
12. Yang J, Weinberg RA: **Epithelial-mesenchymal transition: at the crossroads of development and tumor metastasis**. *Dev Cell* 2008, **14**:818-829.
13. Boyer B, Valles AM, Edme N: **Induction and regulation of epithelial-mesenchymal transitions**. *Biochem Pharmacol* 2000, **60**:1091-1099.
14. Burdsal CA, Damsky CH, Pedersen RA: **The role of E-cadherin and integrins in mesoderm differentiation and migration at the mammalian primitive streak**. *Development* 1993, **118**:829-844.
15. Nieto MA: **The early steps of neural crest development**. *Mech Dev* 2001, **105**:27-35.
16. Bissell MJ, Radisky D: **Putting tumours in context**. *Nat Rev Cancer* 2001, **1**:46-54.
17. Martin P: **Wound healing--aiming for perfect skin regeneration**. *Science* 1997, **276**:75-81.
18. Thiery JP, Chopin D: **Epithelial cell plasticity in development and tumor progression**. *Cancer Metastasis Rev* 1999, **18**:31-42.
19. Adams CL, Nelson WJ: **Cytomechanics of cadherin-mediated cell-cell adhesion**. *Curr Opin Cell Biol* 1998, **10**:572-577.
20. Garrod D, Chidgey M, North A: **Desmosomes: differentiation, development, dynamics and disease**. *Curr Opin Cell Biol* 1996, **8**:670-678.

21. Ahmed S, Nawshad A: **Complexity in interpretation of embryonic epithelial-mesenchymal transition in response to transforming growth factor-beta signaling.** *Cells Tissues Organs* 2007, **185**:131-145.
22. Li S, Guan JL, Chien S: **Biochemistry and biomechanics of cell motility.** *Annu Rev Biomed Eng* 2005, **7**:105-150.
23. LaGamba D, Nawshad A, Hay ED: **Microarray analysis of gene expression during epithelial-mesenchymal transformation.** *Dev Dyn* 2005, **234**:132-142.
24. **UNC School of medicine, Embryo images online** [http://www.med.unc.edu/embryo_images/unit-bdyfm/bdyfm_https/bdyfmtoc.htm]
25. Duband JL, Monier F, Delannet M, Newgreen D: **Epithelium-mesenchyme transition during neural crest development.** *Acta Anat (Basel)* 1995, **154**:63-78.
26. Huang X, Saint-Jeannet JP: **Induction of the neural crest and the opportunities of life on the edge.** *Dev Biol* 2004, **275**:1-11.
27. Tucker GC, Duband JL, Dufour S, Thiery JP: **Cell-adhesion and substrate-adhesion molecules: their instructive roles in neural crest cell migration.** *Development* 1988, **103 Suppl**:81-94.
28. Lee JM, Dedhar S, Kalluri R, Thompson EW: **The epithelial-mesenchymal transition: new insights in signaling, development, and disease.** *J Cell Biol* 2006, **172**:973-981.
29. Duband JL, Thiery JP: **Distribution of laminin and collagens during avian neural crest development.** *Development* 1987, **101**:461-478.
30. Nichols DH: **Neural crest formation in the head of the mouse embryo as observed using a new histological technique.** *J Embryol Exp Morphol* 1981, **64**:105-120.
31. Fitchett JE, Hay ED: **Medial edge epithelium transforms to mesenchyme after embryonic palatal shelves fuse.** *Dev Biol* 1989, **131**:455-474.
32. Stainier DY: **Zebrafish genetics and vertebrate heart formation.** *Nat Rev Genet* 2001, **2**:39-48.
33. Griffith CM, Hay ED: **Epithelial-mesenchymal transformation during palatal fusion: carboxyfluorescein traces cells at light and electron microscopic levels.** *Development* 1992, **116**:1087-1099.
34. Schafer M, Werner S: **Cancer as an overhealing wound: an old hypothesis revisited.** *Nat Rev Mol Cell Biol* 2008, **9**:628-638.
35. Davies JA: **Mesenchyme to epithelium transition during development of the mammalian kidney tubule.** *Acta Anat (Basel)* 1996, **156**:187-201.
36. Allan GJ, Beattie J, Flint DJ: **Epithelial injury induces an innate repair mechanism linked to cellular senescence and fibrosis involving IGF-binding protein-5.** *J Endocrinol* 2008, **199**:155-164.
37. Kalluri R, Neilson EG: **Epithelial-mesenchymal transition and its implications for fibrosis.** *J Clin Invest* 2003, **112**:1776-1784.
38. Neilson EG: **Setting a trap for tissue fibrosis.** *Nat Med* 2005, **11**:373-374.
39. Iwano M, Plieth D, Danoff TM, Xue C, Okada H, Neilson EG: **Evidence that fibroblasts derive from epithelium during tissue fibrosis.** *J Clin Invest* 2002, **110**:341-350.

40. Willis BC, Liebler JM, Luby-Phelps K, Nicholson AG, Crandall ED, du Bois RM, Borok Z: **Induction of epithelial-mesenchymal transition in alveolar epithelial cells by transforming growth factor-beta1: potential role in idiopathic pulmonary fibrosis.** *Am J Pathol* 2005, **166**:1321-1332.
41. Yao HW, Xie QM, Chen JQ, Deng YM, Tang HF: **TGF-beta1 induces alveolar epithelial to mesenchymal transition in vitro.** *Life Sci* 2004, **76**:29-37.
42. Thiery JP: **Epithelial-mesenchymal transitions in tumour progression.** *Nat Rev Cancer* 2002, **2**:442-454.
43. Tarin D, Thompson EW, Newgreen DF: **The fallacy of epithelial mesenchymal transition in neoplasia.** *Cancer Res* 2005, **65**:5996-6000; discussion 6000-5991.
44. Reya T, Morrison SJ, Clarke MF, Weissman IL: **Stem cells, cancer, and cancer stem cells.** *Nature* 2001, **414**:105-111.
45. Bonnet D, Dick JE: **Human acute myeloid leukemia is organized as a hierarchy that originates from a primitive hematopoietic cell.** *Nat Med* 1997, **3**:730-737.
46. Al-Hajj M, Wicha MS, Benito-Hernandez A, Morrison SJ, Clarke MF: **Prospective identification of tumorigenic breast cancer cells.** *Proc Natl Acad Sci U S A* 2003, **100**:3983-3988.
47. Mani SA, Guo W, Liao MJ, Eaton EN, Ayyanan A, Zhou AY, Brooks M, Reinhard F, Zhang CC, Shipitsin M, et al: **The epithelial-mesenchymal transition generates cells with properties of stem cells.** *Cell* 2008, **133**:704-715.
48. O'Brien CA, Pollett A, Gallinger S, Dick JE: **A human colon cancer cell capable of initiating tumour growth in immunodeficient mice.** *Nature* 2007, **445**:106-110.
49. Ricci-Vitiani L, Lombardi DG, Pilozzi E, Biffoni M, Todaro M, Peschle C, De Maria R: **Identification and expansion of human colon-cancer-initiating cells.** *Nature* 2007, **445**:111-115.
50. Singh SK, Hawkins C, Clarke ID, Squire JA, Bayani J, Hide T, Henkelman RM, Cusimano MD, Dirks PB: **Identification of human brain tumour initiating cells.** *Nature* 2004, **432**:396-401.
51. Brabletz T, Jung A, Spaderna S, Hlubek F, Kirchner T: **Opinion: migrating cancer stem cells - an integrated concept of malignant tumour progression.** *Nat Rev Cancer* 2005, **5**:744-749.
52. Heppner GH: **Tumor heterogeneity.** *Cancer Res* 1984, **44**:2259-2265.
53. Fidler IJ, Kripke ML: **Metastasis results from preexisting variant cells within a malignant tumor.** *Science* 1977, **197**:893-895.
54. Fidler IJ, Hart IR: **Biological diversity in metastatic neoplasms: origins and implications.** *Science* 1982, **217**:998-1003.
55. Nowell PC: **Mechanisms of tumor progression.** *Cancer Res* 1986, **46**:2203-2207.
56. Fialkow PJ: **Clonal origin of human tumors.** *Biochim Biophys Acta* 1976, **458**:283-321.
57. Yook JI, Li XY, Ota I, Hu C, Kim HS, Kim NH, Cha SY, Ryu JK, Choi YJ, Kim J, et al: **A Wnt-Axin2-GSK3beta cascade regulates Snail1 activity in breast cancer cells.** *Nat Cell Biol* 2006, **8**:1398-1406.

58. Hollier BG, Evans K, Mani SA: **The epithelial-to-mesenchymal transition and cancer stem cells: a coalition against cancer therapies.** *J Mammary Gland Biol Neoplasia* 2009, **14**:29-43.
59. Li X, Lewis MT, Huang J, Gutierrez C, Osborne CK, Wu MF, Hilsenbeck SG, Pavlick A, Zhang X, Chamness GC, et al: **Intrinsic resistance of tumorigenic breast cancer cells to chemotherapy.** *J Natl Cancer Inst* 2008, **100**:672-679.
60. Sabbah M, Emami S, Redeuilh G, Julien S, Prevost G, Zimber A, Ouelaa R, Bracke M, De Wever O, Gaspach C: **Molecular signature and therapeutic perspective of the epithelial-to-mesenchymal transitions in epithelial cancers.** *Drug Resist Updat* 2008, **11**:123-151.
61. Jones RJ, Matsui WH, Smith BD: **Cancer stem cells: are we missing the target?** *J Natl Cancer Inst* 2004, **96**:583-585.
62. Huber MA, Kraut N, Beug H: **Molecular requirements for epithelial-mesenchymal transition during tumor progression.** *Curr Opin Cell Biol* 2005, **17**:548-558.
63. Martínez Arias A: **Epithelial mesenchymal interactions in cancer and development.** *Cell* 2001, **105**:425-431.
64. Massague J: **TGF-beta signal transduction.** *Annu Rev Biochem* 1998, **67**:753-791.
65. Massague J: **How cells read TGF-beta signals.** *Nat Rev Mol Cell Biol* 2000, **1**:169-178.
66. Willis BC, Borok Z: **TGF-beta-induced EMT: mechanisms and implications for fibrotic lung disease.** *Am J Physiol Lung Cell Mol Physiol* 2007, **293**:L525-534.
67. Nawshad A, Hay ED: **TGFbeta3 signaling activates transcription of the LEF1 gene to induce epithelial mesenchymal transformation during mouse palate development.** *J Cell Biol* 2003, **163**:1291-1301.
68. Nawshad A, Medici D, Liu CC, Hay ED: **TGFbeta3 inhibits E-cadherin gene expression in palate medial-edge epithelial cells through a Smad2-Smad4-LEF1 transcription complex.** *J Cell Sci* 2007, **120**:1646-1653.
69. Zavadil J, Cermak L, Soto-Nieves N, Bottlinger EP: **Integration of TGF-beta/Smad and Jagged1/Notch signalling in epithelial-to-mesenchymal transition.** *Embo J* 2004, **23**:1155-1165.
70. Zavadil J, Bottlinger EP: **TGF-beta and epithelial-to-mesenchymal transitions.** *Oncogene* 2005, **24**:5764-5774.
71. Siegel PM, Massague J: **Cytostatic and apoptotic actions of TGF-beta in homeostasis and cancer.** *Nat Rev Cancer* 2003, **3**:807-821.
72. Wodarz A, Nusse R: **Mechanisms of Wnt signaling in development.** *Annu Rev Cell Dev Biol* 1998, **14**:59-88.
73. Eisenmann DM: **Wnt signaling.** *WormBook* 2005:1-17.
74. Lu W, Yamamoto V, Ortega B, Baltimore D: **Mammalian Ryk is a Wnt coreceptor required for stimulation of neurite outgrowth.** *Cell* 2004, **119**:97-108.
75. Bienz M, Clevers H: **Linking colorectal cancer to Wnt signaling.** *Cell* 2000, **103**:311 - 320.
76. Polakis P, Hart M, Rubinfeld B: **Defects in the regulation of beta-catenin in colorectal cancer.** *Adv Exp Med Biol* 1999, **470**:23-32.

77. Huang D, Du X: **Crosstalk between tumor cells and microenvironment via Wnt pathway in colorectal cancer dissemination.** *World J Gastroenterol* 2008, **14**:1823-1827.
78. Katoh M, Katoh M: **WNT signaling pathway and stem cell signaling network.** *Clin Cancer Res* 2007, **13**:4042-4045.
79. Lu X, Borchers AG, Jolicoeur C, Rayburn H, Baker JC, Tessier-Lavigne M: **PTK7/CCK-4 is a novel regulator of planar cell polarity in vertebrates.** *Nature* 2004, **430**:93-98.
80. Oishi I, Suzuki H, Onishi N, Takada R, Kani S, Ohkawara B, Koshida I, Suzuki K, Yamada G, Schwabe GC, et al: **The receptor tyrosine kinase Ror2 is involved in non-canonical Wnt5a/JNK signalling pathway.** *Genes Cells* 2003, **8**:645-654.
81. Boutros M, Paricio N, Strutt DI, Mlodzik M: **Dishevelled activates JNK and discriminates between JNK pathways in planar polarity and wingless signaling.** *Cell* 1998, **94**:109-118.
82. Tao W, Pennica D, Xu L, Kalejta RF, Levine AJ: **Wrch-1, a novel member of the Rho gene family that is regulated by Wnt-1.** *Genes Dev* 2001, **15**:1796-1807.
83. Greenwald I: **LIN-12/Notch signaling: lessons from worms and flies.** *Genes Dev* 1998, **12**:1751-1762.
84. Radtke F, Raj K: **The role of Notch in tumorigenesis: oncogene or tumour suppressor?** *Nat Rev Cancer* 2003, **3**:756-767.
85. Timmerman LA, Grego-Bessa J, Raya A, Bertran E, Perez-Pomares JM, Diez J, Aranda S, Palomo S, McCormick F, Izpisua-Belmonte JC, de la Pompa JL: **Notch promotes epithelial-mesenchymal transition during cardiac development and oncogenic transformation.** *Genes Dev* 2004, **18**:99-115.
86. Endo Y, Osumi N, Wakamatsu Y: **Bimodal functions of Notch-mediated signaling are involved in neural crest formation during avian ectoderm development.** *Development* 2002, **129**:863-873.
87. Grego-Bessa J, Diez J, Timmerman L, de la Pompa JL: **Notch and epithelial-mesenchyme transition in development and tumor progression: another turn of the screw.** *Cell Cycle* 2004, **3**:718-721.
88. Gridley T: **Notch signaling during vascular development.** *Proc Natl Acad Sci U S A* 2001, **98**:5377-5378.
89. Pourquie O: **Segmentation of the paraxial mesoderm and vertebrate somitogenesis.** *Curr Top Dev Biol* 2000, **47**:81-105.
90. Ramaswamy S, Ross KN, Lander ES, Golub TR: **A molecular signature of metastasis in primary solid tumors.** *Nat Genet* 2003, **33**:49-54.
91. Pasca di Magliano M, Hebrok M: **Hedgehog signalling in cancer formation and maintenance.** *Nat Rev Cancer* 2003, **3**:903-911.
92. Wu Y, Zhou BP: **New insights of epithelial-mesenchymal transition in cancer metastasis.** *Acta Biochim Biophys Sin (Shanghai)* 2008, **40**:643-650.
93. Zhou BP, Hung MC: **Wnt, hedgehog and snail: sister pathways that control by GSK-3beta and beta-Trcp in the regulation of metastasis.** *Cell Cycle* 2005, **4**:772-776.

94. Thayer SP, di Magliano MP, Heiser PW, Nielsen CM, Roberts DJ, Lauwers GY, Qi YP, Gysin S, Fernandez-del Castillo C, Yajnik V, et al: **Hedgehog is an early and late mediator of pancreatic cancer tumorigenesis.** *Nature* 2003, **425**:851-856.
95. Ruiz i Altaba A, Sanchez P, Dahmane N: **Gli and hedgehog in cancer: tumours, embryos and stem cells.** *Nat Rev Cancer* 2002, **2**:361-372.
96. Watkins DN, Berman DM, Burkholder SG, Wang B, Beachy PA, Baylin SB: **Hedgehog signalling within airway epithelial progenitors and in small-cell lung cancer.** *Nature* 2003, **422**:313-317.
97. Berman DM, Karhadkar SS, Hallahan AR, Pritchard JI, Eberhart CG, Watkins DN, Chen JK, Cooper MK, Taipale J, Olson JM, Beachy PA: **Medulloblastoma growth inhibition by hedgehog pathway blockade.** *Science* 2002, **297**:1559-1561.
98. Katoh Y, Katoh M: **Hedgehog signaling, epithelial-to-mesenchymal transition and miRNA (review).** *Int J Mol Med* 2008, **22**:271-275.
99. Kemler R: **From cadherins to catenins: cytoplasmic protein interactions and regulation of cell adhesion.** *Trends Genet* 1993, **9**:317-321.
100. Takeichi M: **Morphogenetic roles of classic cadherins.** *Curr Opin Cell Biol* 1995, **7**:619-627.
101. Tepass U, Truong K, Godt D, Ikura M, Peifer M: **Cadherins in embryonic and neural morphogenesis.** *Nat Rev Mol Cell Biol* 2000, **1**:91-100.
102. Thiery JP, Sleeman JP: **Complex networks orchestrate epithelial-mesenchymal transitions.** *Nat Rev Mol Cell Biol* 2006, **7**:131-142.
103. Ara T, Deyama Y, Yoshimura Y, Higashino F, Shindoh M, Matsumoto A, Fukuda H: **Membrane type 1-matrix metalloproteinase expression is regulated by E-cadherin through the suppression of mitogen-activated protein kinase cascade.** *Cancer Lett* 2000, **157**:115-121.
104. Noren NK, Arthur WT, Burridge K: **Cadherin engagement inhibits RhoA via p190RhoGAP.** *J Biol Chem* 2003, **278**:13615-13618.
105. Wu H, Liang YL, Li Z, Jin J, Zhang W, Duan L, Zha X: **Positive expression of E-cadherin suppresses cell adhesion to fibronectin via reduction of alpha5beta1 integrin in human breast carcinoma cells.** *J Cancer Res Clin Oncol* 2006, **132**:795-803.
106. Kuphal S, Bosserhoff AK: **Influence of the cytoplasmic domain of E-cadherin on endogenous N-cadherin expression in malignant melanoma.** *Oncogene* 2006, **25**:248-259.
107. Kuphal S, Poser I, Jobin C, Hellerbrand C, Bosserhoff AK: **Loss of E-cadherin leads to upregulation of NFkappaB activity in malignant melanoma.** *Oncogene* 2004, **23**:8509-8519.
108. Wells A, Yates C, Shepard CR: **E-cadherin as an indicator of mesenchymal to epithelial reverting transitions during the metastatic seeding of disseminated carcinomas.** *Clin Exp Metastasis* 2008, **25**:621-628.
109. Peinado H, Portillo F, Cano A: **Transcriptional regulation of cadherins during development and carcinogenesis.** *Int J Dev Biol* 2004, **48**:365-375.
110. Giroldi LA, Bringuier PP, de Weijert M, Jansen C, van Bokhoven A, Schalken JA: **Role of E boxes in the repression of E-cadherin expression.** *Biochem Biophys Res Commun* 1997, **241**:453-458.

111. Hennig G, Behrens J, Truss M, Frisch S, Reichmann E, Birchmeier W: **Progression of carcinoma cells is associated with alterations in chromatin structure and factor binding at the E-cadherin promoter in vivo.** *Oncogene* 1995, **11**:475-484.
112. Behrens J, Lowrick O, Klein-Hitpass L, Birchmeier W: **The E-cadherin promoter: functional analysis of a G.C-rich region and an epithelial cell-specific palindromic regulatory element.** *Proc Natl Acad Sci U S A* 1991, **88**:11495-11499.
113. Batlle E, Sancho E, Franci C, Dominguez D, Monfar M, Baulida J, Garcia De Herreros A: **The transcription factor snail is a repressor of E-cadherin gene expression in epithelial tumour cells.** *Nat Cell Biol* 2000, **2**:84-89.
114. Kataoka H, Murayama T, Yokode M, Mori S, Sano H, Ozaki H, Yokota Y, Nishikawa S, Kita T: **A novel snail-related transcription factor Smuc regulates basic helix-loop-helix transcription factor activities via specific E-box motifs.** *Nucleic Acids Res* 2000, **28**:626-633.
115. Manzanares M, Blanco MJ, Nieto MA: **Snail3 orthologues in vertebrates: divergent members of the Snail zinc-finger gene family.** *Dev Genes Evol* 2004, **214**:47-53.
116. Knight RD, Shimeld SM: **Identification of conserved C2H2 zinc-finger gene families in the Bilateria.** *Genome Biol* 2001, **2**:RESEARCH0016.
117. Mauhin V, Lutz Y, Dennefeld C, Alberga A: **Definition of the DNA-binding site repertoire for the Drosophila transcription factor SNAIL.** *Nucleic Acids Res* 1993, **21**:3951-3957.
118. Manzanares M, Locascio A, Nieto MA: **The increasing complexity of the Snail gene superfamily in metazoan evolution.** *Trends Genet* 2001, **17**:178-181.
119. Barrallo-Gimeno A, Nieto MA: **The Snail genes as inducers of cell movement and survival: implications in development and cancer.** *Development* 2005, **132**:3151-3161.
120. Zhou BP, Deng J, Xia W, Xu J, Li YM, Gunduz M, Hung MC: **Dual regulation of Snail by GSK-3beta-mediated phosphorylation in control of epithelial-mesenchymal transition.** *Nat Cell Biol* 2004, **6**:931-940.
121. Yang Z, Rayala S, Nguyen D, Vadlamudi RK, Chen S, Kumar R: **Pak1 phosphorylation of snail, a master regulator of epithelial-to-mesenchyme transition, modulates snail's subcellular localization and functions.** *Cancer Res* 2005, **65**:3179-3184.
122. Cano A, Perez-Moreno MA, Rodrigo I, Locascio A, Blanco MJ, del Barrio MG, Portillo F, Nieto MA: **The transcription factor snail controls epithelial-mesenchymal transitions by repressing E-cadherin expression.** *Nat Cell Biol* 2000, **2**:76-83.
123. Barbera MJ, Puig I, Dominguez D, Julien-Grille S, Guaita-Esteruelas S, Peiro S, Baulida J, Franci C, Dedhar S, Larue L, Garcia de Herreros A: **Regulation of Snail transcription during epithelial to mesenchymal transition of tumor cells.** *Oncogene* 2004, **23**:7345-7354.
124. Peinado H, Quintanilla M, Cano A: **Transforming growth factor beta-1 induces snail transcription factor in epithelial cell lines: mechanisms for epithelial mesenchymal transitions.** *J Biol Chem* 2003, **278**:21113-21123.
125. Tan C, Costello P, Sanghera J, Dominguez D, Baulida J, de Herreros AG, Dedhar S: **Inhibition of integrin linked kinase (ILK) suppresses beta-catenin-Lef/Tcf-dependent transcription and expression of the E-cadherin repressor, snail, in APC-/- human colon carcinoma cells.** *Oncogene* 2001, **20**:133-140.

126. Oda H, Tsukita S, Takeichi M: **Dynamic behavior of the cadherin-based cell-cell adhesion system during *Drosophila* gastrulation.** *Dev Biol* 1998, **203**:435-450.
127. Sefton M, Sanchez S, Nieto MA: **Conserved and divergent roles for members of the Snail family of transcription factors in the chick and mouse embryo.** *Development* 1998, **125**:3111-3121.
128. Nieto MA, Sargent MG, Wilkinson DG, Cooke J: **Control of cell behavior during vertebrate development by Slug, a zinc finger gene.** *Science* 1994, **264**:835-839.
129. Deng J, Xia W, Miller SA, Wen Y, Wang HY, Hung MC: **Crossregulation of NF-kappaB by the APC/GSK-3beta/beta-catenin pathway.** *Mol Carcinog* 2004, **39**:139-146.
130. Dominguez D, Montserrat-Sentis B, Virgos-Soler A, Guaita S, Grueso J, Porta M, Puig I, Baulida J, Franci C, Garcia de Herreros A: **Phosphorylation regulates the subcellular location and activity of the snail transcriptional repressor.** *Mol Cell Biol* 2003, **23**:5078-5089.
131. Peinado H, Del Carmen Iglesias-de la Cruz M, Olmeda D, Csiszar K, Fong KS, Vega S, Nieto MA, Cano A, Portillo F: **A molecular role for lysyl oxidase-like 2 enzyme in snail regulation and tumor progression.** *Embo J* 2005, **24**:3446-3458.
132. Peinado H, Portillo F, Cano A: **Switching on-off Snail: LOXL2 versus GSK3beta.** *Cell Cycle* 2005, **4**:1749-1752.
133. Peinado H, Ballestar E, Esteller M, Cano A: **Snail mediates E-cadherin repression by the recruitment of the Sin3A/histone deacetylase 1 (HDAC1)/HDAC2 complex.** *Mol Cell Biol* 2004, **24**:306-319.
134. Herranz N, Pasini D, Diaz VM, Franci C, Gutierrez A, Dave N, Escriva M, Hernandez-Munoz I, Di Croce L, Helin K, et al: **Polycomb complex 2 is required for E-cadherin repression by the Snail1 transcription factor.** *Mol Cell Biol* 2008, **28**:4772-4781.
135. Jiao W, Miyazaki K, Kitajima Y: **Inverse correlation between E-cadherin and Snail expression in hepatocellular carcinoma cell lines in vitro and in vivo.** *Br J Cancer* 2002, **86**:98-101.
136. Yokoyama K, Kamata N, Fujimoto R, Tsutsumi S, Tomonari M, Taki M, Hosokawa H, Nagayama M: **Increased invasion and matrix metalloproteinase-2 expression by Snail-induced mesenchymal transition in squamous cell carcinomas.** *Int J Oncol* 2003, **22**:891-898.
137. Poser I, Dominguez D, de Herreros AG, Varnai A, Buettner R, Bosserhoff AK: **Loss of E-cadherin expression in melanoma cells involves up-regulation of the transcriptional repressor Snail.** *J Biol Chem* 2001, **276**:24661-24666.
138. Guaita S, Puig I, Franci C, Garrido M, Dominguez D, Batlle E, Sancho E, Dedhar S, De Herreros AG, Baulida J: **Snail induction of epithelial to mesenchymal transition in tumor cells is accompanied by MUC1 repression and ZEB1 expression.** *J Biol Chem* 2002, **277**:39209-39216.
139. Ikenouchi J, Matsuda M, Furuse M, Tsukita S: **Regulation of tight junctions during the epithelium-mesenchyme transition: direct repression of the gene expression of claudins/occludin by Snail.** *J Cell Sci* 2003, **116**:1959-1967.
140. Palmer HG, Larrriba MJ, Garcia JM, Ordonez-Moran P, Pena C, Peiro S, Puig I, Rodriguez R, de la Fuente R, Bernad A, et al: **The transcription factor SNAIL represses vitamin D receptor expression and responsiveness in human colon cancer.** *Nat Med* 2004, **10**:917-919.

141. Carver EA, Jiang R, Lan Y, Oram KF, Gridley T: **The Mouse Snail Gene Encodes a Key Regulator of the Epithelial-Mesenchymal Transition.** *Mol Cell Biol* 2001, **21**:8184-8188.
142. del Barrio MG, Nieto MA: **Overexpression of Snail family members highlights their ability to promote chick neural crest formation.** *Development* 2002, **129**:1583-1593.
143. Lyons JG, Patel V, Roue NC, Fok SY, Soon LL, Halliday GM, Gutkind JS: **Snail up-regulates proinflammatory mediators and inhibits differentiation in oral keratinocytes.** *Cancer Res* 2008, **68**:4525-4530.
144. Kajita M, McClinic KN, Wade PA: **Aberrant expression of the transcription factors snail and slug alters the response to genotoxic stress.** *Mol Cell Biol* 2004, **24**:7559-7566.
145. Lee SH, Lee SJ, Jung YS, Xu Y, Kang HS, Ha NC, Park BJ: **Blocking of p53-Snail binding, promoted by oncogenic K-Ras, recovers p53 expression and function.** *Neoplasia* 2009, **11**:22-31, 26p following 31.
146. Tribulo C, Aybar MJ, Sanchez SS, Mayor R: **A balance between the anti-apoptotic activity of Slug and the apoptotic activity of msx1 is required for the proper development of the neural crest.** *Dev Biol* 2004, **275**:325-342.
147. Vega S, Morales AV, Ocana OH, Valdes F, Fabregat I, Nieto MA: **Snail blocks the cell cycle and confers resistance to cell death.** *Genes Dev* 2004, **18**:1131-1143.
148. Escriva M, Peiro S, Herranz N, Villagrasa P, Dave N, Montserrat-Sentis B, Murray SA, Franci C, Gridley T, Virtanen I, Garcia de Herreros A: **Repression of PTEN phosphatase by Snail1 transcriptional factor during gamma radiation-induced apoptosis.** *Mol Cell Biol* 2008, **28**:1528-1540.
149. Nieto MA: **The snail superfamily of zinc-finger transcription factors.** *Nat Rev Mol Cell Biol* 2002, **3**:155-166.
150. Linker C, Bronner-Fraser M, Mayor R: **Relationship between gene expression domains of Xsnail, Xslug, and Xtwist and cell movement in the prospective neural crest of Xenopus.** *Dev Biol* 2000, **224**:215-225.
151. Bolos V, Peinado H, Perez-Moreno MA, Fraga MF, Esteller M, Cano A: **The transcription factor Slug represses E-cadherin expression and induces epithelial to mesenchymal transitions: a comparison with Snail and E47 repressors.** *J Cell Sci* 2003, **116**:499-511.
152. Savagner P, Yamada KM, Thiery JP: **The zinc-finger protein slug causes desmosome dissociation, an initial and necessary step for growth factor-induced epithelial-mesenchymal transition.** *J Cell Biol* 1997, **137**:1403-1419.
153. Wu WS, Heinrichs S, Xu D, Garrison SP, Zambetti GP, Adams JM, Look AT: **Slug antagonizes p53-mediated apoptosis of hematopoietic progenitors by repressing puma.** *Cell* 2005, **123**:641-653.
154. Lai ZC, Fortini ME, Rubin GM: **The embryonic expression patterns of zfh-1 and zfh-2, two Drosophila genes encoding novel zinc-finger homeodomain proteins.** *Mech Dev* 1991, **34**:123-134.
155. Fortini ME, Lai ZC, Rubin GM: **The Drosophila zfh-1 and zfh-2 genes encode novel proteins containing both zinc-finger and homeodomain motifs.** *Mech Dev* 1991, **34**:113-122.

156. Funahashi J, Sekido R, Murai K, Kamachi Y, Kondoh H: **Delta-crystallin enhancer binding protein delta EF1 is a zinc finger-homeodomain protein implicated in postgastrulation embryogenesis.** *Development* 1993, **119**:433-446.
157. Sekido R, Murai K, Kamachi Y, Kondoh H: **Two mechanisms in the action of repressor deltaEF1: binding site competition with an activator and active repression.** *Genes Cells* 1997, **2**:771-783.
158. Postigo AA, Dean DC: **Differential expression and function of members of the zfh-1 family of zinc finger/homeodomain repressors.** *Proc Natl Acad Sci U S A* 2000, **97**:6391-6396.
159. Van de Putte T, Maruhashi M, Francis A, Nelles L, Kondoh H, Huylebroeck D, Higashi Y: **Mice lacking ZFH1B, the gene that codes for Smad-interacting protein-1, reveal a role for multiple neural crest cell defects in the etiology of Hirschsprung disease-mental retardation syndrome.** *Am J Hum Genet* 2003, **72**:465-470.
160. Lai Z, Fortini ME, Rubin GM: **The embryonic expression patterns of zfh-1 and zfh-2, two Drosophila genes encoding novel zinc-finger homeodomain proteins.** *Mechanisms of Development* 1991, **34**:123-134.
161. Grootclaes ML, Frisch SM: **Evidence for a function of CtBP in epithelial gene regulation and anoikis.** *Oncogene* 2000, **19**:3823-3828.
162. Eger A, Aigner K, Sonderegger S, Dampier B, Oehler S, Schreiber M, Bex G, Cano A, Beug H, Foisner R: **DeltaEF1 is a transcriptional repressor of E-cadherin and regulates epithelial plasticity in breast cancer cells.** *Oncogene* 2005, **24**:2375-2385.
163. Comijn J, Bex G, Vermassen P, Verschueren K, van Grunsven L, Bruyneel E, Mareel M, Huylebroeck D, van Roy F: **The two-handed E box binding zinc finger protein SIP1 downregulates E-cadherin and induces invasion.** *Mol Cell* 2001, **7**:1267-1278.
164. Vandewalle C, Comijn J, De Craene B, Vermassen P, Bruyneel E, Andersen H, Tulchinsky E, Van Roy F, Bex G: **SIP1/ZEB2 induces EMT by repressing genes of different epithelial cell-cell junctions.** *Nucleic Acids Res* 2005, **33**:6566-6578.
165. Beltran M, Puig I, Pena C, Garcia JM, Alvarez AB, Pena R, Bonilla F, de Herreros AG: **A natural antisense transcript regulates Zeb2/Sip1 gene expression during Snail1-induced epithelial-mesenchymal transition.** *Genes Dev* 2008, **22**:756-769.
166. Ellenberger T, Fass D, Arnaud M, Harrison SC: **Crystal structure of transcription factor E47: E-box recognition by a basic region helix-loop-helix dimer.** *Genes Dev* 1994, **8**:970-980.
167. Massari ME, Murre C: **Helix-loop-helix proteins: regulators of transcription in eucaryotic organisms.** *Mol Cell Biol* 2000, **20**:429-440.
168. Sun XH, Baltimore D: **An inhibitory domain of E12 transcription factor prevents DNA binding in E12 homodimers but not in E12 heterodimers.** *Cell* 1991, **64**:459-470.
169. Engel I, Murre C: **Transcription factors in hematopoiesis.** *Curr Opin Genet Dev* 1999, **9**:575-579.
170. Lee JE: **Basic helix-loop-helix genes in neural development.** *Curr Opin Neurobiol* 1997, **7**:13-20.
171. Olson EN, Klein WH: **bHLH factors in muscle development: dead lines and commitments, what to leave in and what to leave out.** *Genes Dev* 1994, **8**:1-8.

172. Perk J, Iavarone A, Benezra R: **Id family of helix-loop-helix proteins in cancer.** *Nat Rev Cancer* 2005, **5**:603-614.
173. Ruzinova MB, Benezra R: **Id proteins in development, cell cycle and cancer.** *Trends Cell Biol* 2003, **13**:410-418.
174. Peinado H, Olmeda D, Cano A: **Snail, Zeb and bHLH factors in tumour progression: an alliance against the epithelial phenotype?** *Nat Rev Cancer* 2007, **7**:415-428.
175. Thompson JD, Higgins DG, Gibson TJ: **CLUSTAL W: improving the sensitivity of progressive multiple sequence alignment through sequence weighting, position-specific gap penalties and weight matrix choice.** *Nucleic Acids Res* 1994, **22**:4673-4680.
176. Slattery C, Ryan MP, McMorrow T: **E2A proteins: regulators of cell phenotype in normal physiology and disease.** *Int J Biochem Cell Biol* 2008, **40**:1431-1436.
177. Kondo M, Cubillo E, Tobiume K, Shirakihara T, Fukuda N, Suzuki H, Shimizu K, Takehara K, Cano A, Saitoh M, Miyazono K: **A role for Id in the regulation of TGF-beta-induced epithelial-mesenchymal transdifferentiation.** *Cell Death Differ* 2004, **11**:1092-1101.
178. Perez-Moreno MA, Locascio A, Rodrigo I, Dhondt G, Portillo F, Nieto MA, Cano A: **A new role for E12/E47 in the repression of E-cadherin expression and epithelial-mesenchymal transitions.** *J Biol Chem* 2001, **276**:27424-27431.
179. Slattery C, McMorrow T, Ryan MP: **Overexpression of E2A proteins induces epithelial-mesenchymal transition in human renal proximal tubular epithelial cells suggesting a potential role in renal fibrosis.** *FEBS Lett* 2006, **580**:4021-4030.
180. Leptin M: **twist and snail as positive and negative regulators during Drosophila mesoderm development.** *Genes Dev* 1991, **5**:1568-1576.
181. Yang J, Mani SA, Donaher JL, Ramaswamy S, Itzykson RA, Come C, Savagner P, Gitelman I, Richardson A, Weinberg RA: **Twist, a master regulator of morphogenesis, plays an essential role in tumor metastasis.** *Cell* 2004, **117**:927-939.
182. McCreath PD, Turck CW, Gumbiner B: **A homolog of the armadillo protein in Drosophila (plakoglobin) associated with E-cadherin.** *Science* 1991, **254**:1359-1361.
183. Schneider S, Steinbeisser H, Warga RM, Hausen P: **Beta-catenin translocation into nuclei demarcates the dorsalizing centers in frog and fish embryos.** *Mech Dev* 1996, **57**:191-198.
184. Yost C, Torres M, Miller JR, Huang E, Kimelman D, Moon RT: **The axis-inducing activity, stability, and subcellular distribution of beta-catenin is regulated in Xenopus embryos by glycogen synthase kinase 3.** *Genes Dev* 1996, **10**:1443-1454.
185. Larabell CA, Torres M, Rowning BA, Yost C, Miller JR, Wu M, Kimelman D, Moon RT: **Establishment of the dorso-ventral axis in Xenopus embryos is presaged by early asymmetries in beta-catenin that are modulated by the Wnt signaling pathway.** *J Cell Biol* 1997, **136**:1123-1136.
186. Brannon M, Gomperts M, Sumoy L, Moon RT, Kimelman D: **A beta-catenin/XTcf-3 complex binds to the siamois promoter to regulate dorsal axis specification in Xenopus.** *Genes Dev* 1997, **11**:2359-2370.
187. Peifer M, McCreath PD, Green KJ, Wieschaus E, Gumbiner BM: **The vertebrate adhesive junction proteins beta-catenin and plakoglobin and the Drosophila segment polarity gene armadillo form a multigene family with similar properties.** *J Cell Biol* 1992, **118**:681-691.

188. Huber AH, Nelson WJ, Weis WI: **Three-dimensional structure of the armadillo repeat region of beta-catenin.** *Cell* 1997, **90**:871-882.
189. Xu W, Kimelman D: **Mechanistic insights from structural studies of beta-catenin and its binding partners.** *J Cell Sci* 2007, **120**:3337-3344.
190. Aberle H, Butz S, Stappert J, Weissig H, Kemler R, Hoschuetzky H: **Assembly of the cadherin-catenin complex in vitro with recombinant proteins.** *J Cell Sci* 1994, **107**:3655-3663.
191. Hecht A, Litterst CM, Huber O, Kemler R: **Functional characterization of multiple transactivating elements in beta-catenin, some of which interact with the TATA-binding protein in vitro.** *J Biol Chem* 1999, **274**:18017-18025.
192. Zorn AM, Barish GD, Williams BO, Lavender P, Klymkowsky MW, Varmus HE: **Regulation of Wnt signaling by Sox proteins: XSox17 alpha/beta and XSox3 physically interact with beta-catenin.** *Mol Cell* 1999, **4**:487-498.
193. Akiyama H, Lyons JP, Mori-Akiyama Y, Yang X, Zhang R, Zhang Z, Deng JM, Taketo MM, Nakamura T, Behringer RR, et al: **Interactions between Sox9 and beta-catenin control chondrocyte differentiation.** *Genes Dev* 2004, **18**:1072-1087.
194. Nishita M, Hashimoto MK, Ogata S, Laurent MN, Ueno N, Shibuya H, Cho KW: **Interaction between Wnt and TGF-beta signalling pathways during formation of Spemann's organizer.** *Nature* 2000, **403**:781-785.
195. Castano J, Raurell I, Piedra JA, Miravet S, Dunach M, Garcia de Herreros A: **Beta-catenin N- and C-terminal tails modulate the coordinated binding of adherens junction proteins to beta-catenin.** *J Biol Chem* 2002, **277**:31541-31550.
196. Piedra J, Martinez D, Castano J, Miravet S, Dunach M, de Herreros AG: **Regulation of beta-catenin structure and activity by tyrosine phosphorylation.** *J Biol Chem* 2001, **276**:20436-20443.
197. Solanas G, Miravet S, Casagolda D, Castano J, Raurell I, Corrionero A, de Herreros AG, Dunach M: **beta-Catenin and plakoglobin N- and C-tails determine ligand specificity.** *J Biol Chem* 2004, **279**:49849-49856.
198. Hatsell S, Rowlands T, Hiremath M, Cowin P: **Beta-catenin and Tcfs in mammary development and cancer.** *J Mammary Gland Biol Neoplasia* 2003, **8**:145-158.
199. **BTR | Image library** [<http://www.york.ac.uk/res/btr/imagelibrary.html>]
200. Kim K, Lu Z, Hay ED: **Direct evidence for a role of beta-catenin/LEF-1 signaling pathway in induction of EMT.** *Cell Biol Int* 2002, **26**:463-476.
201. Brabletz T, Hlubek F, Spaderna S, Schmalhofer O, Hiendlmeyer E, Jung A, Kirchner T: **Invasion and metastasis in colorectal cancer: epithelial-mesenchymal transition, mesenchymal-epithelial transition, stem cells and beta-catenin.** *Cells Tissues Organs* 2005, **179**:56-65.
202. Eger A, Stockinger A, Schaffhauser B, Beug H, Foisner R: **Epithelial mesenchymal transition by c-Fos estrogen receptor activation involves nuclear translocation of beta-catenin and upregulation of beta-catenin/lymphoid enhancer binding factor-1 transcriptional activity.** *J Cell Biol* 2000, **148**:173-188.
203. Morali OG, Delmas V, Moore R, Jeanney C, Thiery JP, Larue L: **IGF-II induces rapid beta-catenin relocation to the nucleus during epithelium to mesenchyme transition.** *Oncogene* 2001, **20**:4942-4950.

204. Novak A, Hsu SC, Leung-Hagesteijn C, Radeva G, Papkoff J, Montesano R, Roskelley C, Grosschedl R, Dedhar S: **Cell adhesion and the integrin-linked kinase regulate the LEF-1 and beta-catenin signaling pathways.** *Proc Natl Acad Sci U S A* 1998, **95**:4374-4379.
205. He T-C, Sparks AB, Rago C, Hermeking H, Zawel L, da Costa LT, Morin PJ, Vogelstein B, Kinzler KW: **Identification of c-MYC as a Target of the APC Pathway.** *Science* 1998, **281**:1509-1512.
206. Roose J, Huls G, Beest Mv, Moerer P, Horn Kvd, Goldschmeding R, Logtenberg T, Clevers H: **Synergy Between Tumor Suppressor APC and the -Catenin-Tcf4 Target Tcf1.** *Science* 1999, **285**:1923-1926.
207. Mann B, Gelos M, Siedow A, Hanski ML, Gratchev A, Ilyas M, Bodmer WF, Moyer MP, Riecken EO, Buhr HJ, Hanski C: **Target genes of β -catenin/T cell-factor/lymphoid-enhancer-factor signaling in human colorectal carcinomas.** *Proceedings of the National Academy of Sciences of the United States of America* 1999, **96**:1603-1608.
208. Zhang X, Gaspard JP, Chung DC: **Regulation of Vascular Endothelial Growth Factor by the Wnt and K-ras Pathways in Colonic Neoplasia.** *Cancer Res* 2001, **61**:6050-6054.
209. Blache P, van de Wetering M, Duluc I, Domon C, Berta P, Freund J-N, Clevers H, Jay P: **SOX9 is an intestine crypt transcription factor, is regulated by the Wnt pathway, and represses the CDX2 and MUC2 genes.** *J Cell Biol* 2004, **166**:37-47.
210. Hill TP, Später D, Taketo MM, Birchmeier W, Hartmann C: **Canonical Wnt/ β -Catenin Signaling Prevents Osteoblasts from Differentiating into Chondrocytes.** 2005, **8**:727-738.
211. Day TF, Guo X, Garrett-Beal L, Yang Y: **Wnt/ β -Catenin Signaling in Mesenchymal Progenitors Controls Osteoblast and Chondrocyte Differentiation during Vertebrate Skeletogenesis.** 2005, **8**:739-750.
212. Yano F, Kugimiya F, Ohba S, Ikeda T, Chikuda H, Ogasawara T, Ogata N, Takato T, Nakamura K, Kawaguchi H, Chung UI: **The canonical Wnt signaling pathway promotes chondrocyte differentiation in a Sox9-dependent manner.** *Biochem Biophys Res Commun* 2005, **333**:1300-1308.
213. Kim J-S, Crooks H, Dracheva T, Nishanian TG, Singh B, Jen J, Waldman T: **Oncogenic β -Catenin Is Required for Bone Morphogenetic Protein 4 Expression in Human Cancer Cells.** *Cancer Res* 2002, **62**:2744-2748.
214. Yan D, Wiesmann M, Rohan M, Chan V, Jefferson AB, Guo L, Sakamoto D, Caothien RH, Fuller JH, Reinhard C, et al: **Elevated expression of axin2 and hnk4 mRNA provides evidence that Wnt/ β -catenin signaling is activated in human colon tumors.** *Proceedings of the National Academy of Sciences of the United States of America* 2001, **98**:14973-14978.
215. Lustig B, Jerchow B, Sachs M, Weiler S, Pietsch T, Karsten U, van de Wetering M, Clevers H, Schlag PM, Birchmeier W, Behrens J: **Negative Feedback Loop of Wnt Signaling through Upregulation of Conductin/Axin2 in Colorectal and Liver Tumors.** *Mol Cell Biol* 2002, **22**:1184-1193.
216. Jho E-h, Zhang T, Domon C, Joo C-K, Freund J-N, Costantini F: **Wnt/ β -Catenin/Tcf Signaling Induces the Transcription of Axin2, a Negative Regulator of the Signaling Pathway.** *Mol Cell Biol* 2002, **22**:1172-1183.
217. Batlle E, Henderson JT, Beghtel H, van den Born MMW, Sancho E, Huls G, Meeldijk J, Robertson J, van de Wetering M, Pawson T, Clevers H: **Beta-Catenin and TCF Mediate**

Cell Positioning in the Intestinal Epithelium by Controlling the Expression of EphB/EphrinB. 2002, **111**:251-263.

218. Filali M, Cheng N, Abbott D, Leontiev V, Engelhardt JF: **Wnt-3A/beta-catenin signaling induces transcription from the LEF-1 promoter.** *J Biol Chem* 2002, **277**:33398-33410.
219. Hovanes K, Li TW, Munguia JE, Truong T, Milovanovic T, Lawrence Marsh J, Holcombe RF, Waterman ML: **Beta-catenin-sensitive isoforms of lymphoid enhancer factor-1 are selectively expressed in colon cancer.** *Nat Genet* 2001, **28**:53-57.
220. Brabletz T, Jung A, Dag S, Hlubek F, Kirchner T: **beta-catenin regulates the expression of the matrix metalloproteinase-7 in human colorectal cancer.** *Am J Pathol* 1999, **155**:1033-1038.
221. Crawford HC, Fingleton BM, Rudolph-Owen LA, Goss KJ, Rubinfeld B, Polakis P, Matrisian LM: **The metalloproteinase matrilysin is a target of beta-catenin transactivation in intestinal tumors.** *Oncogene* 1999, **18**:2883-2891.
222. ten Berge D, Koole W, Fuerer C, Fish M, Eroglu E, Nusse R: **Wnt Signaling Mediates Self-Organization and Axis Formation in Embryoid Bodies.** *Cell Stem Cell* 2008, **3**:508-518.
223. Gradl D, Kuhl M, Wedlich D: **The Wnt/Wg signal transducer beta-catenin controls fibronectin expression.** *Mol Cell Biol* 1999, **19**:5576-5587.
224. Rockman SP, Currie SA, Ciavarella M, Vincan E, Dow C, Thomas RJ, Phillips WA: **Id2 is a target of the beta-catenin/T cell factor pathway in colon carcinoma.** *J Biol Chem* 2001, **276**:45113 - 45119.
225. Willert J, Epping M, Pollack JR, Brown PO, Nusse R: **A transcriptional response to Wnt protein in human embryonic carcinoma cells.** *BMC Dev Biol* 2002, **2**:8.
226. **List of target genes of Wnt/beta-catenin signaling**
[<http://www.stanford.edu/~rnusse/pathways/targets.html>]
227. van de Wetering M, Sancho E, Verweij C, de Lau W, Oving I, Hurlstone A, van der Horn K, Battle E, Coudreuse D, Haramis AP, et al: **The beta-catenin/TCF-4 complex imposes a crypt progenitor phenotype on colorectal cancer cells.** *Cell* 2002, **111**:241-250.
228. Bjerknes M, Cheng H: **Clonal analysis of mouse intestinal epithelial progenitors.** *Gastroenterology* 1999, **116**:7-14.
229. Hermiston ML, Green RP, Gordon JI: **Chimeric-transgenic mice represent a powerful tool for studying how the proliferation and differentiation programs of intestinal epithelial cell lineages are regulated.** *Proc Natl Acad Sci U S A* 1993, **90**:8866-8870.
230. Roth KA, Hermiston ML, Gordon JI: **Use of transgenic mice to infer the biological properties of small intestinal stem cells and to examine the lineage relationships of their descendants.** *Proc Natl Acad Sci U S A* 1991, **88**:9407-9411.
231. Novelli M, Cossu A, Oukrif D, Quaglia A, Lakhani S, Poulsom R, Sasieni P, Carta P, Contini M, Pasca A, et al: **X-inactivation patch size in human female tissue confounds the assessment of tumor clonality.** *Proc Natl Acad Sci U S A* 2003, **100**:3311-3314.
232. Kirchner T, Brabletz T: **Patterning and nuclear beta-catenin expression in the colonic adenoma-carcinoma sequence. Analogies with embryonic gastrulation.** *Am J Pathol* 2000, **157**:1113-1121.

233. Brabletz T, Jung A, Hermann K, Gunther K, Hohenberger W, Kirchner T: **Nuclear overexpression of the oncoprotein beta-catenin in colorectal cancer is localized predominantly at the invasion front.** *Pathol Res Pract* 1998, **194**:701-704.
234. Brabletz S, Schmalhofer O, Brabletz T: **Gastrointestinal stem cells in development and cancer.** *J Pathol* 2009, **217**:307-317.
235. Fukuchi T, Sakamoto M, Tsuda H, Maruyama K, Nozawa S, Hirohashi S: **Beta-catenin mutation in carcinoma of the uterine endometrium.** *Cancer Res* 1998, **58**:3526-3528.
236. Michaelson JS, Leder P: **beta-catenin is a downstream effector of Wnt-mediated tumorigenesis in the mammary gland.** *Oncogene* 2001, **20**:5093-5099.
237. Chesire DR, Ewing CM, Gage WR, Isaacs WB: **In vitro evidence for complex modes of nuclear beta-catenin signaling during prostate growth and tumorigenesis.** *Oncogene* 2002, **21**:2679-2694.
238. Karin M, Yamamoto Y, Wang QM: **The IKK NF-kappa B system: a treasure trove for drug development.** *Nat Rev Drug Discov* 2004, **3**:17-26.
239. Ghosh S, May MJ, Kopp EB: **NF-kappa B and Rel proteins: evolutionarily conserved mediators of immune responses.** *Annu Rev Immunol* 1998, **16**:225-260.
240. Ghosh S, Karin M: **Missing pieces in the NF-kappaB puzzle.** *Cell* 2002, **109 Suppl**:S81-96.
241. Collart MA, Baeuerle P, Vassalli P: **Regulation of tumor necrosis factor alpha transcription in macrophages: involvement of four kappa B-like motifs and of constitutive and inducible forms of NF-kappa B.** *Mol Cell Biol* 1990, **10**:1498-1506.
242. Pan ZK, Zuraw BL, Lung CC, Prossnitz ER, Browning DD, Ye RD: **Bradykinin stimulates NF-kappaB activation and interleukin 1beta gene expression in cultured human fibroblasts.** *J Clin Invest* 1996, **98**:2042-2049.
243. Plummer SM, Holloway KA, Manson MM, Munks RJ, Kaptein A, Farrow S, Howells L: **Inhibition of cyclo-oxygenase 2 expression in colon cells by the chemopreventive agent curcumin involves inhibition of NF-kappaB activation via the NIK/IKK signalling complex.** *Oncogene* 1999, **18**:6013-6020.
244. Park SK, Lin HL, Murphy S: **Nitric oxide regulates nitric oxide synthase-2 gene expression by inhibiting NF-kappaB binding to DNA.** *Biochem J* 1997, **322 (Pt 2)**:609-613.
245. Mengshol JA, Vincenti MP, Coon CI, Barchowsky A, Brinckerhoff CE: **Interleukin-1 induction of collagenase 3 (matrix metalloproteinase 13) gene expression in chondrocytes requires p38, c-Jun N-terminal kinase, and nuclear factor kappaB: differential regulation of collagenase 1 and collagenase 3.** *Arthritis Rheum* 2000, **43**:801-811.
246. Ricca A, Biroccio A, Del Bufalo D, Mackay AR, Santoni A, Cippitelli M: **bcl-2 overexpression enhances NF-kappaB activity and induces mmp-9 transcription in human MCF7(ADR) breast-cancer cells.** *Int J Cancer* 2000, **86**:188-196.
247. Kim H, Koh G: **Lipopolysaccharide activates matrix metalloproteinase-2 in endothelial cells through an NF-kappaB-dependent pathway.** *Biochem Biophys Res Commun* 2000, **269**:401-405.
248. Bond M, Baker AH, Newby AC: **Nuclear factor kappaB activity is essential for matrix metalloproteinase-1 and -3 upregulation in rabbit dermal fibroblasts.** *Biochem Biophys Res Commun* 1999, **264**:561-567.

249. Niederberger E, Geisslinger G: **The IKK-NF- κ B pathway: a source for novel molecular drug targets in pain therapy?** *FASEB J* 2008, **22**:3432-3442.
250. Duh EJ, Maury WJ, Folks TM, Fauci AS, Rabson AB: **Tumor necrosis factor alpha activates human immunodeficiency virus type 1 through induction of nuclear factor binding to the NF- κ B sites in the long terminal repeat.** *Proc Natl Acad Sci USA* 1989, **86**:5974-5978.
251. Israel A, Le Bail O, Hatat D, Piette J, Kieran M, Logeat F, Wallach D, Fellous M, Kourilsky P: **TNF stimulates expression of mouse MHC class I genes by inducing an NF κ B-like enhancer binding activity which displaces constitutive factors.** *Embo J* 1989, **8**:3793-3800.
252. Hohmann HP, Remy R, Poschl B, van Loon AP: **Tumor necrosis factors-alpha and -beta bind to the same two types of tumor necrosis factor receptors and maximally activate the transcription factor NF- κ B at low receptor occupancy and within minutes after receptor binding.** *J Biol Chem* 1990, **265**:15183-15188.
253. Grilli M, Goffi F, Memo M, Spano P: **Interleukin-1beta and Glutamate Activate the NF- κ B/Rel Binding Site from the Regulatory Region of the Amyloid Precursor Protein Gene in Primary Neuronal Cultures.** *J Biol Chem* 1996, **271**:15002-15007.
254. Claudio E, Brown K, Park S, Wang H, Siebenlist U: **BAFF-induced NEMO-independent processing of NF- κ B2 in maturing B cells.** *Nat Immunol* 2002, **3**:958-965.
255. Coope HJ, Atkinson PG, Huhse B, Belich M, Janzen J, Holman MJ, Klaus GG, Johnston LH, Ley SC: **CD40 regulates the processing of NF- κ B2 p100 to p52.** *Embo J* 2002, **21**:5375-5385.
256. Muller JR, Siebenlist U: **Lymphotoxin beta Receptor Induces Sequential Activation of Distinct NF- κ B Factors via Separate Signaling Pathways.** *J Biol Chem* 2003, **278**:12006-12012.
257. Brach MA, Hass R, Sherman ML, Gunji H, Weichselbaum R, Kufe D: **Ionizing radiation induces expression and binding activity of the nuclear factor kappa B.** *J Clin Invest* 1991, **88**:691-695.
258. Lee HW, Ahn DH, Crawley SC, Li JD, Gum JR, Jr., Basbaum CB, Fan NQ, Szymkowski DE, Han SY, Lee BH, et al: **Phorbol 12-myristate 13-acetate up-regulates the transcription of MUC2 intestinal mucin via Ras, ERK, and NF- κ B.** *J Biol Chem* 2002, **277**:32624-32631.
259. Li Y, Mak G, Franza BR, Jr.: **In vitro study of functional involvement of Sp1, NF- κ B/Rel, and AP1 in phorbol 12-myristate 13-acetate-mediated HIV-1 long terminal repeat activation.** *J Biol Chem* 1994, **269**:30616-30619.
260. Kato T, Jr., Delhase M, Hoffmann A, Karin M: **CK2 Is a C-Terminal I κ B Kinase Responsible for NF- κ B Activation during the UV Response.** *Mol Cell* 2003, **12**:829-839.
261. Shimada T, Kawai T, Takeda K, Matsumoto M, Inoue J, Tatsumi Y, Kanamaru A, Akira S: **IKK-i, a novel lipopolysaccharide-inducible kinase that is related to I κ B kinases.** *Int Immunol* 1999, **11**:1357-1362.
262. Peters RT, Maniatis T: **A new family of IKK-related kinases may function as I κ B kinase kinases.** *Biochim Biophys Acta* 2001, **1471**:M57-62.
263. Basseres DS, Baldwin AS: **Nuclear factor- κ B and inhibitor of κ B kinase pathways in oncogenic initiation and progression.** *Oncogene* 2006, **25**:6817-6830.

264. Radisky DC, Bissell MJ: **NF-kappaB links oestrogen receptor signalling and EMT.** *Nat Cell Biol* 2007, **9**:361-363.
265. Chua HL, Bhat-Nakshatri P, Clare SE, Morimiya A, Badve S, Nakshatri H: **NF-kappaB represses E-cadherin expression and enhances epithelial to mesenchymal transition of mammary epithelial cells: potential involvement of ZEB-1 and ZEB-2.** *Oncogene* 2007, **26**:711-724.
266. Huber MA, Azoitei N, Baumann B, Grunert S, Sommer A, Pehamberger H, Kraut N, Beug H, Wirth T: **NF-kappaB is essential for epithelial-mesenchymal transition and metastasis in a model of breast cancer progression.** *J Clin Invest* 2004, **114**:569-581.
267. Min C, Eddy SF, Sherr DH, Sonenshein GE: **NF-kappaB and epithelial to mesenchymal transition of cancer.** *J Cell Biochem* 2008, **104**:733-744.
268. Huber MA, Beug H, Wirth T: **Epithelial-mesenchymal transition: NF-kappaB takes center stage.** *Cell Cycle* 2004, **3**:1477-1480.
269. Karin M, Greten FR: **NF-kappaB: linking inflammation and immunity to cancer development and progression.** *Nat Rev Immunol* 2005, **5**:749-759.
270. Jiang J, Kosman D, Ip YT, Levine M: **The dorsal morphogen gradient regulates the mesoderm determinant twist in early Drosophila embryos.** *Genes Dev* 1991, **5**:1881-1891.
271. Bachelder RE, Yoon SO, Franci C, de Herreros AG, Mercurio AM: **Glycogen synthase kinase-3 is an endogenous inhibitor of Snail transcription: implications for the epithelial-mesenchymal transition.** *J Cell Biol* 2005, **168**:29-33.
272. Kim HJ, Litzenger BC, Cui X, Delgado DA, Grabner BC, Lin X, Lewis MT, Gottardis MM, Wong TW, Attar RM, et al: **Constitutively active type I insulin-like growth factor receptor causes transformation and xenograft growth of immortalized mammary epithelial cells and is accompanied by an epithelial-to-mesenchymal transition mediated by NF-kappaB and snail.** *Mol Cell Biol* 2007, **27**:3165-3175.
273. Deng J, Miller SA, Wang HY, Xia W, Wen Y, Zhou BP, Li Y, Lin SY, Hung MC: **beta-catenin interacts with and inhibits NF-kappa B in human colon and breast cancer.** *Cancer Cell* 2002, **2**:323-334.
274. Steinbrecher KA, Wilson W, III, Cogswell PC, Baldwin AS: **Glycogen Synthase Kinase 3{beta} Functions To Specify Gene-Specific, NF-{kappa}B-Dependent Transcription.** *Mol Cell Biol* 2005, **25**:8444-8455.
275. Lamberti C, Lin K-M, Yamamoto Y, Verma U, Verma IM, Byers S, Gaynor RB: **Regulation of beta -Catenin Function by the Ikappa B Kinases.** *J Biol Chem* 2001, **276**:42276-42286.
276. Arce L, Yokoyama NN, Waterman ML: **Diversity of LEF/TCF action in development and disease.** *Oncogene* 2006, **25**:7492-7504.
277. Solanas G, Porta-de-la-Riva M, Agusti C, Casagolda D, Sanchez-Aguilera F, Larriba MJ, Pons F, Peiro S, Escriva M, Munoz A, et al: **E-cadherin controls beta-catenin and NF-kappaB transcriptional activity in mesenchymal gene expression.** *J Cell Sci* 2008, **121**:2224-2234.
278. Agustí Benito C: **Mecanisme d'activació de fibronectina i LEF1 per Snail1 durant la transició epili-mesènquima.** Universitat Pompeu Fabra, Departament de Ciències de la Salut i de la Vida; 2007.

279. van de Wetering M, Cavallo R, Dooijes D, van Beest M, van Es J, Loureiro J, Ypma A, Hursh D, Jones T, Bejsovec A, et al: **Armadillo coactivates transcription driven by the product of the *Drosophila* segment polarity gene dTCF.** *Cell* 1997, **88**:789-799.
280. van de Wetering M, Oving I, Muncan V, Pon Fong MT, Brantjes H, van Leenen D, Holstege FC, Brummelkamp TR, Agami R, Clevers H: **Specific inhibition of gene expression using a stably integrated, inducible small-interfering-RNA vector.** *EMBO Rep* 2003, **4**:609-615.
281. Asally M, Yoneda Y: **Beta-catenin can act as a nuclear import receptor for its partner transcription factor, lymphocyte enhancer factor-1 (Ief-1).** *Exp Cell Res* 2005, **308**:357-363.
282. Driskell RR, Liu X, Luo M, Filali M, Zhou W, Abbott D, Cheng N, Moothart C, Sigmund CD, Engelhardt JF: **Wnt-responsive element controls Lef-1 promoter expression during submucosal gland morphogenesis.** *Am J Physiol Lung Cell Mol Physiol* 2004, **287**:L752-763.
283. Ogryzko VV, Schiltz RL, Russanova V, Howard BH, Nakatani Y: **The transcriptional coactivators p300 and CBP are histone acetyltransferases.** *Cell* 1996, **87**:953-959.
284. Arany Z, Sellers WR, Livingston DM, Eckner R: **E1A-associated p300 and CREB-associated CBP belong to a conserved family of coactivators.** *Cell* 1994, **77**:799-800.
285. Kamei Y, Xu L, Heinzel T, Torchia J, Kurokawa R, Gloss B, Lin SC, Heyman RA, Rose DW, Glass CK, Rosenfeld MG: **A CBP integrator complex mediates transcriptional activation and AP-1 inhibition by nuclear receptors.** *Cell* 1996, **85**:403-414.
286. Kundu TK, Palhan VB, Wang Z, An W, Cole PA, Roeder RG: **Activator-dependent transcription from chromatin in vitro involving targeted histone acetylation by p300.** *Mol Cell* 2000, **6**:551-561.
287. Schiltz RL, Mizzen CA, Vassilev A, Cook RG, Allis CD, Nakatani Y: **Overlapping but distinct patterns of histone acetylation by the human coactivators p300 and PCAF within nucleosomal substrates.** *J Biol Chem* 1999, **274**:1189-1192.
288. Suhara W, Yoneyama M, Kitabayashi I, Fujita T: **Direct involvement of CREB-binding protein/p300 in sequence-specific DNA binding of virus-activated interferon regulatory factor-3 holocomplex.** *J Biol Chem* 2002, **277**:22304-22313.
289. Rikitake Y, Moran E: **DNA-binding properties of the E1A-associated 300-kilodalton protein.** *Mol Cell Biol* 1992, **12**:2826-2836.
290. Lee BH, Kim MS, Rhew JH, Park RW, de Crombrughe B, Kim IS: **Transcriptional regulation of fibronectin gene by phorbol myristate acetate in hepatoma cells: a negative role for NF-kappaB.** *J Cell Biochem* 2000, **76**:437-451.
291. Chen S, Mukherjee S, Chakraborty C, Chakrabarti S: **High glucose-induced, endothelin-dependent fibronectin synthesis is mediated via NF-kappa B and AP-1.** *Am J Physiol Cell Physiol* 2003, **284**:C263-272.
292. Reddy VS, Harskamp RE, van Ginkel MW, Calhoon J, Baisden CE, Kim IS, Valente AJ, Chandrasekar B: **Interleukin-18 stimulates fibronectin expression in primary human cardiac fibroblasts via PI3K-Akt-dependent NF-kappaB activation.** *J Cell Physiol* 2008, **215**:697-707.
293. Veljkovic J, Hansen U: **Lineage-specific and ubiquitous biological roles of the mammalian transcription factor LSF.** *Gene* 2004, **343**:23-40.

294. Shirra MK, Zhu Q, Huang HC, Pallas D, Hansen U: **One exon of the human LSF gene includes conserved regions involved in novel DNA-binding and dimerization motifs.** *Mol Cell Biol* 1994, **14**:5076-5087.
295. Zambrano N, Minopoli G, de Candia P, Russo T: **The Fe65 adaptor protein interacts through its PID1 domain with the transcription factor CP2/LSF/LBP1.** *J Biol Chem* 1998, **273**:20128-20133.
296. Pagon Z, Volker J, Cooper GM, Hansen U: **Mammalian transcription factor LSF is a target of ERK signaling.** *J Cell Biochem* 2003, **89**:733-746.
297. Volker JL, Rameh LE, Zhu Q, DeCaprio J, Hansen U: **Mitogenic stimulation of resting T cells causes rapid phosphorylation of the transcription factor LSF and increased DNA-binding activity.** *Genes Dev* 1997, **11**:1435-1446.
298. Saxena UH, Powell CM, Fecko JK, Cacioppo R, Chou HS, Cooper GM, Hansen U: **Phosphorylation by cyclin C/cyclin-dependent kinase 2 following mitogenic stimulation of murine fibroblasts inhibits transcriptional activity of LSF during G1 progression.** *Mol Cell Biol* 2009, **29**:2335-2345.
299. Hou Z, Peng H, Ayyanathan K, Yan KP, Langer EM, Longmore GD, Rauscher FJ, 3rd: **The LIM protein AJUBA recruits protein arginine methyltransferase 5 to mediate SNAIL-dependent transcriptional repression.** *Mol Cell Biol* 2008, **28**:3198-3207.
300. Langer EM, Feng Y, Zhaoyuan H, Rauscher FJ, 3rd, Kroll KL, Longmore GD: **Ajuba LIM proteins are snail/slug corepressors required for neural crest development in Xenopus.** *Dev Cell* 2008, **14**:424-436.
301. Casal J, Leptin M: **Identification of novel genes in Drosophila reveals the complex regulation of early gene activity in the mesoderm.** *Proc Natl Acad Sci U S A* 1996, **93**:10327-10332.
302. Shishido E, Higashijima S, Emori Y, Saigo K: **Two FGF-receptor homologues of Drosophila: one is expressed in mesodermal primordium in early embryos.** *Development* 1993, **117**:751-761.
303. Reece-Hoyes JS, Deplancke B, Barrasa MI, Hatzold J, Smit RB, Arda HE, Pope PA, Gaudet J, Conradt B, Walhout AJ: **The C. elegans Snail homolog CES-1 can activate gene expression in vivo and share targets with bHLH transcription factors.** *Nucleic Acids Res* 2009.
304. Travis A, Amsterdam A, Belanger C, Grosschedl R: **LEF-1, a gene encoding a lymphoid-specific protein with an HMG domain, regulates T-cell receptor alpha enhancer function [corrected].** *Genes Dev* 1991, **5**:880-894.
305. Waterman ML, Fischer WH, Jones KA: **A thymus-specific member of the HMG protein family regulates the human T cell receptor C alpha enhancer.** *Genes Dev* 1991, **5**:656-669.
306. Hsu SC, Galceran J, Grosschedl R: **Modulation of transcriptional regulation by LEF-1 in response to Wnt-1 signaling and association with beta-catenin.** *Mol Cell Biol* 1998, **18**:4807-4818.
307. Behrens J, von Kries JP, Kuhl M, Bruhn L, Wedlich D, Grosschedl R, Birchmeier W: **Functional interaction of beta-catenin with the transcription factor LEF-1.** *Nature* 1996, **382**:638-642.
308. Huber O, Korn R, McLaughlin J, Ohsugi M, Herrmann BG, Kemler R: **Nuclear localization of beta-catenin by interaction with transcription factor LEF-1.** *Mech Dev* 1996, **59**:3-10.

309. van Genderen C, Okamura RM, Farinas I, Quo RG, Parslow TG, Bruhn L, Grosschedl R: **Development of several organs that require inductive epithelial-mesenchymal interactions is impaired in LEF-1-deficient mice.** *Genes Dev* 1994, **8**:2691 - 2703.
310. Driskell RR, Goodheart M, Neff T, Liu X, Luo M, Moothart C, Sigmund CD, Hosokawa R, Chai Y, Engelhardt JF: **Wnt3a regulates Lef-1 expression during airway submucosal gland morphogenesis.** *Dev Biol* 2007, **305**:90-102.
311. Liu X, Driskell RR, Luo M, Abbott D, Filali M, Cheng N, Sigmund CD, Engelhardt JF: **Characterization of Lef-1 promoter segments that facilitate inductive developmental expression in skin.** *J Invest Dermatol* 2004, **123**:264-274.
312. Hovanes K, Li TW, Waterman ML: **The human LEF-1 gene contains a promoter preferentially active in lymphocytes and encodes multiple isoforms derived from alternative splicing.** *Nucleic Acids Res* 2000, **28**:1994-2003.
313. Li TW, Ting JH, Yokoyama NN, Bernstein A, van de Wetering M, Waterman ML: **Wnt activation and alternative promoter repression of LEF1 in colon cancer.** *Mol Cell Biol* 2006, **26**:5284-5299.
314. Vadlamudi U, Espinoza HM, Ganga M, Martin DM, Liu X, Engelhardt JF, Amendt BA: **PITX2, beta-catenin and LEF-1 interact to synergistically regulate the LEF-1 promoter.** *J Cell Sci* 2005, **118**:1129-1137.
315. Amen M, Liu X, Vadlamudi U, Elizondo G, Diamond E, Engelhardt JF, Amendt BA: **PITX2 and beta-catenin interactions regulate Lef-1 isoform expression.** *Mol Cell Biol* 2007, **27**:7560-7573.
316. Jimenez J, Jang GM, Semler BL, Waterman ML: **An internal ribosome entry site mediates translation of lymphoid enhancer factor-1.** *Rna* 2005, **11**:1385-1399.
317. Sachdev S, Bruhn L, Sieber H, Pichler A, Melchior F, Grosschedl R: **PIASy, a nuclear matrix-associated SUMO E3 ligase, represses LEF1 activity by sequestration into nuclear bodies.** *Genes Dev* 2001, **15**:3088-3103.
318. Giese K, Kingsley C, Kirshner JR, Grosschedl R: **Assembly and function of a TCR alpha enhancer complex is dependent on LEF-1-induced DNA bending and multiple protein-protein interactions.** *Genes Dev* 1995, **9**:995-1008.
319. Yamada KM: **Cell surface interactions with extracellular materials.** *Annu Rev Biochem* 1983, **52**:761-799.
320. Kornblihtt AR, Umezawa K, Vibe-Pedersen K, Baralle FE: **Primary structure of human fibronectin: differential splicing may generate at least 10 polypeptides from a single gene.** *Embo J* 1985, **4**:1755-1759.
321. Weber KT, Brilla CG: **Pathological hypertrophy and cardiac interstitium. Fibrosis and renin-angiotensin-aldosterone system.** *Circulation* 1991, **83**:1849-1865.
322. Vibe-Pedersen K, Kornblihtt AR, Baralle FE: **Expression of a human alpha-globin/fibronectin gene hybrid generates two mRNAs by alternative splicing.** *Embo J* 1984, **3**:2511-2516.
323. Hynes RO, Schwarzbauer JE, Tamkun JW: **Fibronectin: a versatile gene for a versatile protein.** *Ciba Found Symp* 1984, **108**:75-92.
324. Kornblihtt AR, Vibe-Pedersen K, Baralle FE: **Isolation and characterization of cDNA clones for human and bovine fibronectins.** *Proc Natl Acad Sci U S A* 1983, **80**:3218-3222.

325. Schwarzbauer JE, Tamkun JW, Lemischka IR, Hynes RO: **Three different fibronectin mRNAs arise by alternative splicing within the coding region.** *Cell* 1983, **35**:421-431.
326. Tamkun JW, Schwarzbauer JE, Hynes RO: **A single rat fibronectin gene generates three different mRNAs by alternative splicing of a complex exon.** *Proc Natl Acad Sci USA* 1984, **81**:5140-5144.
327. Dean DC, Bowlus CL, Bourgeois S: **Cloning and analysis of the promoter region of the human fibronectin gene.** *Proc Natl Acad Sci USA* 1987, **84**:1876-1880.
328. Chou L, Firth JD, Uitto VJ, Brunette DM: **Substratum surface topography alters cell shape and regulates fibronectin mRNA level, mRNA stability, secretion and assembly in human fibroblasts.** *J Cell Sci* 1995, **108 (Pt 4)**:1563-1573.
329. Dean DC, Newby RF, Bourgeois S: **Regulation of fibronectin biosynthesis by dexamethasone, transforming growth factor beta, and cAMP in human cell lines.** *J Cell Biol* 1988, **106**:2159-2170.
330. Wrana JL, Overall CM, Sodek J: **Regulation of the expression of a secreted acidic protein rich in cysteine (SPARC) in human fibroblasts by transforming growth factor beta. Comparison of transcriptional and post-transcriptional control with fibronectin and type I collagen.** *Eur J Biochem* 1991, **197**:519-528.
331. Kucich U, Rosenbloom JC, Shen G, Abrams WR, Hamilton AD, Sebt SM, Rosenbloom J: **TGF-beta1 stimulation of fibronectin transcription in cultured human lung fibroblasts requires active geranylgeranyl transferase I, phosphatidylcholine-specific phospholipase C, protein kinase C-delta, and p38, but not erk1/erk2.** *Arch Biochem Biophys* 2000, **374**:313-324.
332. Uchiyama-Tanaka Y, Matsubara H, Mori Y, Kosaki A, Kishimoto N, Amano K, Higashiyama S, Iwasaka T: **Involvement of HB-EGF and EGF receptor transactivation in TGF-beta-mediated fibronectin expression in mesangial cells.** *Kidney Int* 2002, **62**:799-808.
333. Hocevar BA, Brown TL, Howe PH: **TGF-beta induces fibronectin synthesis through a c-Jun N-terminal kinase-dependent, Smad4-independent pathway.** *Embo J* 1999, **18**:1345-1356.
334. Roman J, Rivera HN, Roser-Page S, Sitaraman SV, Ritzenthaler JD: **Adenosine induces fibronectin expression in lung epithelial cells: implications for airway remodeling.** *Am J Physiol Lung Cell Mol Physiol* 2006, **290**:L317-325.
335. Diaz A, Jimenez SA: **Interferon-gamma regulates collagen and fibronectin gene expression by transcriptional and post-transcriptional mechanisms.** *Int J Biochem Cell Biol* 1997, **29**:251-260.
336. Lee BH, Park RW, Choi JY, Ryoo HM, Sohn KY, Kim IS: **Stimulation of fibronectin synthesis through the protein kinase C signalling pathway in normal and transformed human lung fibroblasts.** *Biochem Mol Biol Int* 1996, **39**:895-904.
337. Liu C, Yao J, Mercola D, Adamson E: **The transcription factor EGR-1 directly transactivates the fibronectin gene and enhances attachment of human glioblastoma cell line U251.** *J Biol Chem* 2000, **275**:20315-20323.
338. Bernath VA, Muro AF, Vitullo AD, Bley MA, Baranao JL, Kornblihtt AR: **Cyclic AMP inhibits fibronectin gene expression in a newly developed granulosa cell line by a mechanism that suppresses cAMP-responsive element-dependent transcriptional activation.** *J Biol Chem* 1990, **265**:18219-18226.

339. Miao S, Suri PK, Shu-Ling L, Abraham A, Cook N, Milos P, Zern MA: **Role of the cyclic AMP response element in rat fibronectin gene expression.** *Hepatology* 1993, **17**:882-890.
340. Suzuki M, Oda E, Nakajima T, Sekiya S, Oda K: **Induction of Sp1 in differentiating human embryonal carcinoma cells triggers transcription of the fibronectin gene.** *Mol Cell Biol* 1998, **18**:3010-3020.
341. Chandler LA, Ehretsmann CP, Bourgeois S: **A novel mechanism of Ha-ras oncogene action: regulation of fibronectin mRNA levels by a nuclear posttranscriptional event.** *Mol Cell Biol* 1994, **14**:3085-3093.
342. Mimura Y, Ihn H, Jinnin M, Asano Y, Yamane K, Tamaki K: **Epidermal growth factor induces fibronectin expression in human dermal fibroblasts via protein kinase C delta signaling pathway.** *J Invest Dermatol* 2004, **122**:1390-1398.
343. Norton PA, Reis HM, Prince S, Larkin J, Pan J, Liu J, Gong Q, Zhu M, Feitelson MA: **Activation of fibronectin gene expression by hepatitis B virus x antigen.** *J Viral Hepat* 2004, **11**:332-341.
344. Kornblihtt AR, Pesce CG, Alonso CR, Cramer P, Srebrow A, Werbajh S, Muro AF: **The fibronectin gene as a model for splicing and transcription studies.** *Faseb J* 1996, **10**:248-257.
345. Eckes B, Mauch C, Huppe G, Krieg T: **Differential regulation of transcription and transcript stability of pro-alpha 1(I) collagen and fibronectin in activated fibroblasts derived from patients with systemic scleroderma.** *Biochem J* 1996, **315** (Pt 2):549-554.
346. Peiro S, Escriva M, Puig I, Barbera MJ, Dave N, Herranz N, Larriba MJ, Takkunen M, Franci C, Munoz A, et al: **Snail1 transcriptional repressor binds to its own promoter and controls its expression.** *Nucleic Acids Res* 2006, **34**:2077-2084.
347. Millanes A, Herranz N, Peiro S: **Unpublished results.**
348. Stemmer V, de Craene B, Berx G, Behrens J: **Snail promotes Wnt target gene expression and interacts with beta-catenin.** *Oncogene* 2008, **27**:5075-5080.
349. Guth SI, Wegner M: **Having it both ways: Sox protein function between conservation and innovation.** *Cell Mol Life Sci* 2008, **65**:3000-3018.
350. Takash W, Canizares J, Bonneaud N, Poulat F, Mattei MG, Jay P, Berta P: **SOX7 transcription factor: sequence, chromosomal localisation, expression, transactivation and interference with Wnt signalling.** *Nucleic Acids Res* 2001, **29**:4274-4283.
351. Guo L, Zhong D, Lau S, Liu X, Dong XY, Sun X, Yang VW, Vertino PM, Moreno CS, Varma V, et al: **Sox7 Is an independent checkpoint for beta-catenin function in prostate and colon epithelial cells.** *Mol Cancer Res* 2008, **6**:1421-1430.
352. Topol L, Chen W, Song H, Day TF, Yang Y: **Sox9 inhibits Wnt signaling by promoting beta-catenin phosphorylation in the nucleus.** *J Biol Chem* 2009, **284**:3323-3333.
353. Zhang Y, Huang S, Dong W, Li L, Feng Y, Pan L, Han Z, Wang X, Ren G, Su D, et al: **SOX7, down-regulated in colorectal cancer, induces apoptosis and inhibits proliferation of colorectal cancer cells.** *Cancer Lett* 2009, **277**:29-37.
354. Yun K, Choi YD, Nam JH, Park Z, Im SH: **NF-kappaB regulates Lef1 gene expression in chondrocytes.** *Biochem Biophys Res Commun* 2007, **357**:589-595.

355. Chiarugi A, Moskowitz MA: **Poly(ADP-ribose) polymerase-1 activity promotes NF-kappaB-driven transcription and microglial activation: implication for neurodegenerative disorders.** *J Neurochem* 2003, **85**:306-317.
356. Hassa PO, Covic M, Hasan S, Imhof R, Hottiger MO: **The enzymatic and DNA binding activity of PARP-1 are not required for NF-kappa B coactivator function.** *J Biol Chem* 2001, **276**:45588-45597.
357. Hassa PO, Hottiger MO: **A role of poly (ADP-ribose) polymerase in NF-kappaB transcriptional activation.** *Biol Chem* 1999, **380**:953-959.
358. Martin-Oliva D, O'Valle F, Munoz-Gamez JA, Valenzuela MT, Nunez MI, Aguilar M, Ruiz de Almodovar JM, Garcia del Moral R, Oliver FJ: **Crosstalk between PARP-1 and NF-kappaB modulates the promotion of skin neoplasia.** *Oncogene* 2004, **23**:5275-5283.
359. Oliver FJ, Menissier-de Murcia J, Nacci C, Decker P, Andriantsitohaina R, Muller S, de la Rubia G, Stoclet JC, de Murcia G: **Resistance to endotoxic shock as a consequence of defective NF-kappaB activation in poly (ADP-ribose) polymerase-1 deficient mice.** *Embo J* 1999, **18**:4446-4454.
360. Ame JC, Spenlehauer C, de Murcia G: **The PARP superfamily.** *Bioessays* 2004, **26**:882-893.
361. Hassa PO, Hottiger MO: **The diverse biological roles of mammalian PARPS, a small but powerful family of poly-ADP-ribose polymerases.** *Front Biosci* 2008, **13**:3046-3082.
362. Aguilar-Quesada R, Munoz-Gamez JA, Martin-Oliva D, Peralta-Leal A, Quiles-Perez R, Rodriguez-Vargas JM, Ruiz de Almodovar M, Conde C, Ruiz-Extremera A, Oliver FJ: **Modulation of transcription by PARP-1: consequences in carcinogenesis and inflammation.** *Curr Med Chem* 2007, **14**:1179-1187.
363. Hassa PO, Hottiger MO: **The functional role of poly(ADP-ribose)polymerase 1 as novel coactivator of NF-kappaB in inflammatory disorders.** *Cell Mol Life Sci* 2002, **59**:1534-1553.
364. Shall S, de Murcia G: **Poly(ADP-ribose) polymerase-1: what have we learned from the deficient mouse model?** *Mutat Res* 2000, **460**:1-15.
365. Chang WJ, Alvarez-Gonzalez R: **The sequence-specific DNA binding of NF-kappa B is reversibly regulated by the automodification reaction of poly (ADP-ribose) polymerase 1.** *J Biol Chem* 2001, **276**:47664-47670.
366. Kraus WL: **Transcriptional control by PARP-1: chromatin modulation, enhancer-binding, coregulation, and insulation.** *Curr Opin Cell Biol* 2008, **20**:294-302.
367. Krishnakumar R, Gamble MJ, Frizzell KM, Berrocal JG, Kininis M, Kraus WL: **Reciprocal binding of PARP-1 and histone H1 at promoters specifies transcriptional outcomes.** *Science* 2008, **319**:819-821.
368. Hassa PO, Buerki C, Lombardi C, Imhof R, Hottiger MO: **Transcriptional coactivation of nuclear factor-kappaB-dependent gene expression by p300 is regulated by poly(ADP)-ribose polymerase-1.** *J Biol Chem* 2003, **278**:45145-45153.
369. Julien S, Puig I, Caretti E, Bonaventure J, Nelles L, van Roy F, Dargemont C, de Herreros AG, Bellacosa A, Larue L: **Activation of NF-kappaB by Akt upregulates Snail expression and induces epithelium mesenchyme transition.** *Oncogene* 2007, **26**:7445-7456.

370. Wu Y, Deng J, Rychahou PG, Qiu S, Evers BM, Zhou BP: **Stabilization of snail by NF-kappaB is required for inflammation-induced cell migration and invasion.** *Cancer Cell* 2009, **15**:416-428.
371. Kokoszynska K, Ostrowski J, Rychlewski L, Wyrwicz LS: **The fold recognition of CP2 transcription factors gives new insights into the function and evolution of tumor suppressor protein p53.** *Cell Cycle* 2008, **7**:2907-2915.
372. Ting SB, Wilanowski T, Cerruti L, Zhao LL, Cunningham JM, Jane SM: **The identification and characterization of human Sister-of-Mammalian Grainyhead (SOM) expands the grainyhead-like family of developmental transcription factors.** *Biochem J* 2003, **370**:953-962.
373. Uv AE, Thompson CR, Bray SJ: **The Drosophila tissue-specific factor Grainyhead contains novel DNA-binding and dimerization domains which are conserved in the human protein CP2.** *Mol Cell Biol* 1994, **14**:4020-4031.
374. Wilanowski T, Tuckfield A, Cerruti L, O'Connell S, Saint R, Parekh V, Tao J, Cunningham JM, Jane SM: **A highly conserved novel family of mammalian developmental transcription factors related to Drosophila grainyhead.** *Mech Dev* 2002, **114**:37-50.
375. Yoon JB, Li G, Roeder RG: **Characterization of a family of related cellular transcription factors which can modulate human immunodeficiency virus type 1 transcription in vitro.** *Mol Cell Biol* 1994, **14**:1776-1785.
376. Huang N, Miller WL: **Cloning of factors related to HIV-inducible LBP proteins that regulate steroidogenic factor-1-independent human placental transcription of the cholesterol side-chain cleavage enzyme, P450scc.** *J Biol Chem* 2000, **275**:2852-2858.
377. Lim LC, Swendeman SL, Sheffery M: **Molecular cloning of the alpha-globin transcription factor CP2.** *Mol Cell Biol* 1992, **12**:828-835.
378. Shirra MK, Hansen U: **LSF and NTF-1 share a conserved DNA recognition motif yet require different oligomerization states to form a stable protein-DNA complex.** *J Biol Chem* 1998, **273**:19260-19268.
379. Murata T, Nitta M, Yasuda K: **Transcription factor CP2 is essential for lens-specific expression of the chicken alphaA-crystallin gene.** *Genes Cells* 1998, **3**:443-457.
380. Jane SM, Nienhuis AW, Cunningham JM: **Hemoglobin switching in man and chicken is mediated by a heteromeric complex between the ubiquitous transcription factor CP2 and a developmentally specific protein.** *Embo J* 1995, **14**:97-105.
381. Zhong F, Swendeman SL, Popik W, Pitha PM, Sheffery M: **Evidence that levels of the dimeric cellular transcription factor CP2 play little role in the activation of the HIV-1 long terminal repeat in vivo or following superinfection with herpes simplex virus type 1.** *J Biol Chem* 1994, **269**:21269-21276.
382. Powell CM, Rudge TL, Zhu Q, Johnson LF, Hansen U: **Inhibition of the mammalian transcription factor LSF induces S-phase-dependent apoptosis by downregulating thymidylate synthase expression.** *Embo J* 2000, **19**:4665-4675.
383. Kim CG, Barnhart KM, Sheffery M: **Purification of multiple erythroid cell proteins that bind the promoter of the alpha-globin gene.** *Mol Cell Biol* 1988, **8**:4270-4281.
384. Barnhart KM, Kim CG, Banerji SS, Sheffery M: **Identification and characterization of multiple erythroid cell proteins that interact with the promoter of the murine alpha-globin gene.** *Mol Cell Biol* 1988, **8**:3215-3226.

385. Lim LC, Fang L, Swendeman SL, Sheffery M: **Characterization of the molecularly cloned murine alpha-globin transcription factor CP2.** *J Biol Chem* 1993, **268**:18008-18017.
386. Casolaro V, Keane-Myers AM, Swendeman SL, Steindler C, Zhong F, Sheffery M, Georas SN, Ono SJ: **Identification and characterization of a critical CP2-binding element in the human interleukin-4 promoter.** *J Biol Chem* 2000, **275**:36605-36611.
387. Acloque H, Mey A, Birot AM, Gruffat H, Pain B, Samarut J: **Transcription factor cCP2 controls gene expression in chicken embryonic stem cells.** *Nucleic Acids Res* 2004, **32**:2259-2271.
388. Bing Z, Reddy SA, Ren Y, Qin J, Liao WS: **Purification and characterization of the serum amyloid A3 enhancer factor.** *J Biol Chem* 1999, **274**:24649-24656.
389. Zheng JB, Zhou YH, Maity T, Liao WS, Saunders GF: **Activation of the human PAX6 gene through the exon 1 enhancer by transcription factors SEF and Sp1.** *Nucleic Acids Res* 2001, **29**:4070-4078.
390. Jones KA, Luciw PA, Duchange N: **Structural arrangements of transcription control domains within the 5'-untranslated leader regions of the HIV-1 and HIV-2 promoters.** *Genes Dev* 1988, **2**:1101-1114.
391. Kato H, Horikoshi M, Roeder RG: **Repression of HIV-1 transcription by a cellular protein.** *Science* 1991, **251**:1476-1479.
392. Malim MH, Fenrick R, Ballard DW, Hauber J, Bohnlein E, Cullen BR: **Functional characterization of a complex protein-DNA-binding domain located within the human immunodeficiency virus type 1 long terminal repeat leader region.** *J Virol* 1989, **63**:3213-3219.
393. Wu FK, Garcia JA, Harrich D, Gaynor RB: **Purification of the human immunodeficiency virus type 1 enhancer and TAR binding proteins EBP-1 and UBP-1.** *Embo J* 1988, **7**:2117-2130.
394. Huang HC, Sundseth R, Hansen U: **Transcription factor LSF binds two variant bipartite sites within the SV40 late promoter.** *Genes Dev* 1990, **4**:287-298.
395. Sueyoshi T, Kobayashi R, Nishio K, Aida K, Moore R, Wada T, Handa H, Negishi M: **A nuclear factor (NF2d9) that binds to the male-specific P450 (Cyp 2d-9) gene in mouse liver.** *Mol Cell Biol* 1995, **15**:4158-4166.
396. Zhou W, Clouston DR, Wang X, Cerruti L, Cunningham JM, Jane SM: **Induction of human fetal globin gene expression by a novel erythroid factor, NF-E4.** *Mol Cell Biol* 2000, **20**:7662-7672.
397. Tuckfield A, Clouston DR, Wilanowski TM, Zhao LL, Cunningham JM, Jane SM: **Binding of the RING polycomb proteins to specific target genes in complex with the grainyhead-like family of developmental transcription factors.** *Mol Cell Biol* 2002, **22**:1936-1946.
398. Ylisastigui L, Kaur R, Johnson H, Volker J, He G, Hansen U, Margolis D: **Mitogen-activated protein kinases regulate LSF occupancy at the human immunodeficiency virus type 1 promoter.** *J Virol* 2005, **79**:5952-5962.
399. Kashour T, Burton T, Dibrov A, Amara FM: **Late Simian virus 40 transcription factor is a target of the phosphoinositide 3-kinase/Akt pathway in anti-apoptotic Alzheimer's amyloid precursor protein signalling.** *Biochem J* 2003, **370**:1063-1075.

400. Swendeman SL, Spielholz C, Jenkins NA, Gilbert DJ, Copeland NG, Sheffery M: **Characterization of the genomic structure, chromosomal location, promoter, and development expression of the alpha-globin transcription factor CP2.** *J Biol Chem* 1994, **269**:11663-11671.
401. Sato F, Yasumoto K, Kimura K, Numayama-Tsuruta K, Sogawa K: **Heterodimerization with LBP-1b is necessary for nuclear localization of LBP-1a and LBP-1c.** *Genes Cells* 2005, **10**:861-870.
402. Bellacosa A, de Feo D, Godwin AK, Bell DW, Cheng JQ, Altomare DA, Wan M, Dubeau L, Scambia G, Masciullo V, et al: **Molecular alterations of the AKT2 oncogene in ovarian and breast carcinomas.** *Int J Cancer* 1995, **64**:280-285.
403. Xing H, Cao Y, Weng D, Tao W, Song X, Wang W, Meng L, Xu G, Zhou J, Wang S, Ma D: **Fibronectin-mediated activation of Akt2 protects human ovarian and breast cancer cells from docetaxel-induced apoptosis via inhibition of the p38 pathway.** *Apoptosis* 2008, **13**:213-223.
404. Edderkaoui M, Hong P, Lee JK, Pandol SJ, Gukovskaya AS: **Insulin-like growth factor-I receptor mediates the prosurvival effect of fibronectin.** *J Biol Chem* 2007, **282**:26646-26655.
405. Gao L, Zhang Y, Qiu W, Xu W, Feng X, Ren J, Jiang X, Wang H, Zhao D, Wang Y: **Effects of PI3-k/Akt short hairpin RNA on proliferation, fibronectin production and synthesis of thrombospondin-1 and transforming growth factor-beta1 in glomerular mesangial cells induced by sublytic C5b-9 complexes.** *Cell Prolif* 2009, **42**:83-93.
406. Lesuffleur T, Barbat A, Dussaulx E, Zweibaum A: **Growth adaptation to methotrexate of HT-29 human colon carcinoma cells is associated with their ability to differentiate into columnar absorptive and mucus-secreting cells.** *Cancer Res* 1990, **50**:6334-6343.
407. Nose A, Nagafuchi A, Takeichi M: **Expressed recombinant cadherins mediate cell sorting in model systems.** *Cell* 1988, **54**:993-1001.
408. Udalova IA, Knight JC, Vidal V, Nedospasov SA, Kwiatkowski D: **Complex NF-kappaB interactions at the distal tumor necrosis factor promoter region in human monocytes.** *J Biol Chem* 1998, **273**:21178-21186.
409. Huang C, Bi E, Hu Y, Deng W, Tian Z, Dong C, Hu Y, Sun B: **A novel NF-kappaB binding site controls human granzyme B gene transcription.** *J Immunol* 2006, **176**:4173-4181.
410. Chin-Tien Wang J-JLH-YLB-SH: **A human cell line constitutively expressing HIV-1 <I>Gag</I> and <I>Gag-Pol</I> gene products.** *Journal of Medical Virology* 1999, **57**:17-24.
411. Suyama M, Torrents D, Bork P: **BLAST2GENE: a comprehensive conversion of BLAST output into independent genes and gene fragments.** *Bioinformatics* 2004, **20**:1968-1970.
412. Wingender E, Dietze P, Karas H, Knuppel R: **TRANSFAC: a database on transcription factors and their DNA binding sites.** *Nucleic Acids Res* 1996, **24**:238-241.

ANNEX

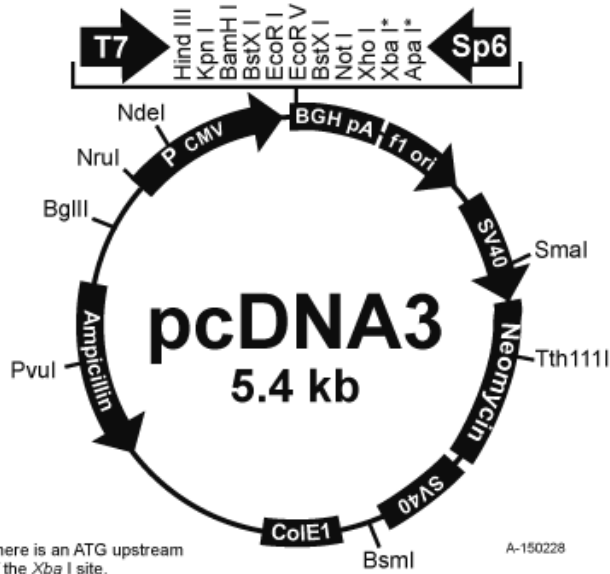
A.1 VECTORS

A.1.1 Eukaryotic expression vectors

pcDNA3

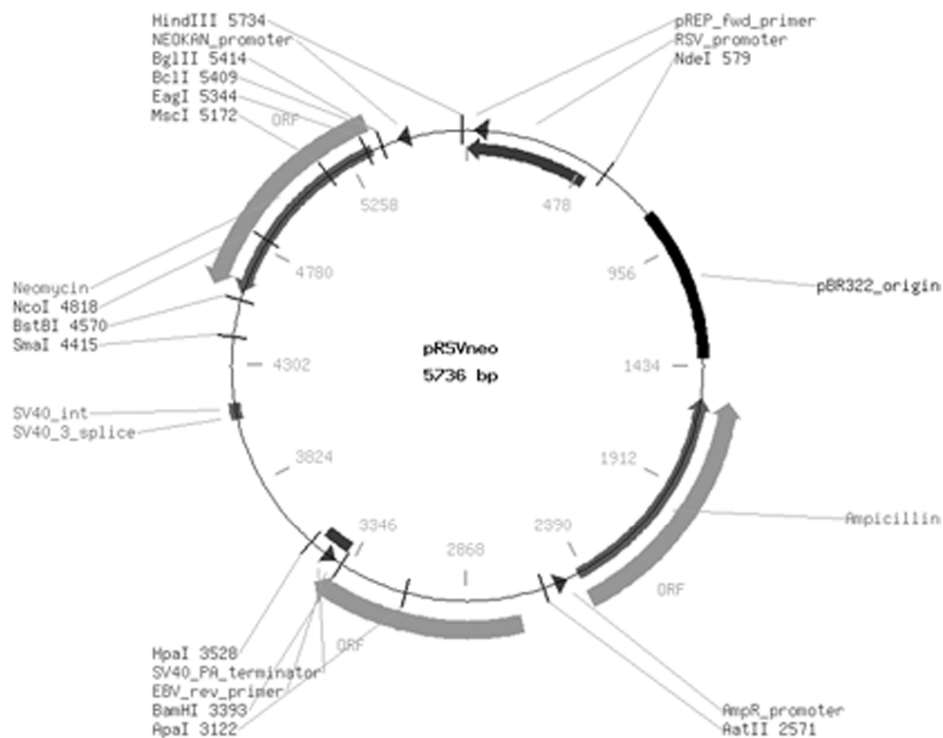
Comments for pcDNA3:
5446 nucleotides

CMV promoter: bases 209-863
T7 promoter: bases 864-882
Polylinker: bases 889-994
Sp6 promoter: bases 999-1016
BGH poly A: bases 1018-1249
SV40 promoter: bases 1790-2115
SV40 origin of replication: bases 1984-2069
Neomycin ORF: bases 2151-2945
SV40 poly A: bases 3000-3372
ColE1 origin: bases 3632-4305
Ampicillin ORF: bases 4450-5310

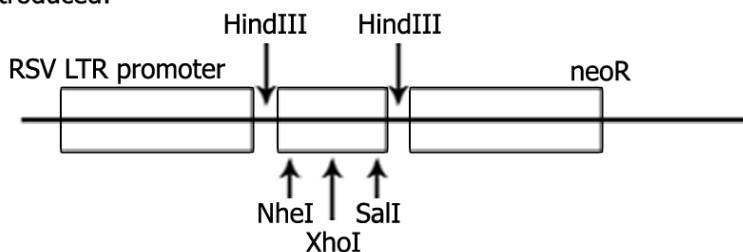


Insert	Origin	Cloned
mmsnail1-HA	selective snail1 amplification from mRNA obtained from NIH3T3 cells	BamHI/NotI
mmsnail1-P2A-HA	PCR amplification from pcDNA3-mmsnail1-HA	BamHI/NotI
VP16-TCF4		
VP16-Rel	Rel domain: pcDNA3-p65 VP16 : VP16-snail1	

pRSV



MCS introduced:



Insert	Origin	Cloned
mmsnail1-HA	pcDNA3-mmsnail1-HA	HindIII /NotI (i) XhoI (v)

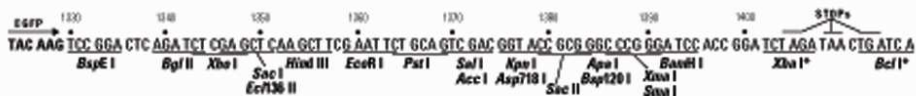
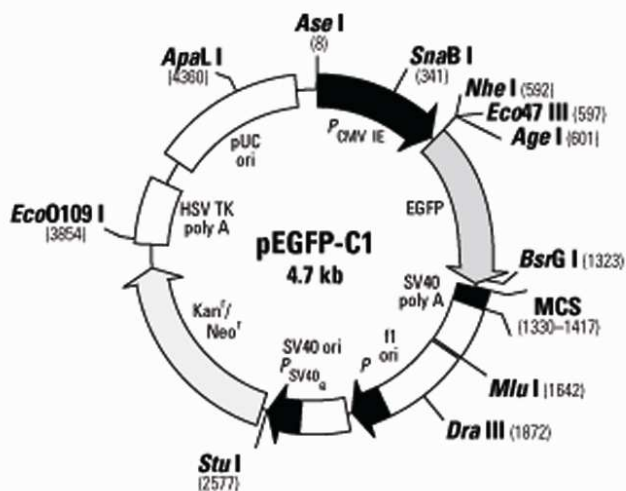
pEGFP

pEGFP-C1 Vector Information

GenBank Accession #: U55763

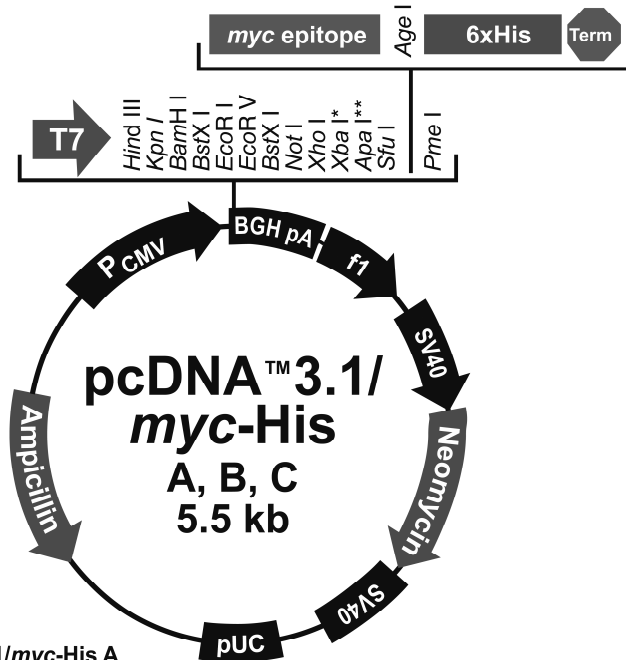
PT3028-5

Catalog #6084-1



Insert	Origin	Cloned
mmsnail1-HA	pcDNA3-mmsnail1-HA	

pcDNA3.1



**Comments for pcDNATM 3.1/myc-His A
5493 nucleotides**

- CMV promoter: bases 209-863
- T7 promoter/priming site: bases 863-882
- Multiple cloning site: bases 902-999
- myc epitope: bases 997-1026
- Polyhistidine tag: bases 1042-1059
- BGH reverse priming site: bases 1082-1099
- BGH polyadenylation signal: bases 1081-1295
- f1 origin of replication: bases 1358-1771
- SV40 promoter and origin: bases 1836-2160
- Neomycin resistance gene: bases 2196-2990
- SV40 polyadenylation signal: bases 3166-3296
- pUC origin: bases 3679-4352
- Ampicillin resistance gene: bases 4497-5357 (complementary strand)

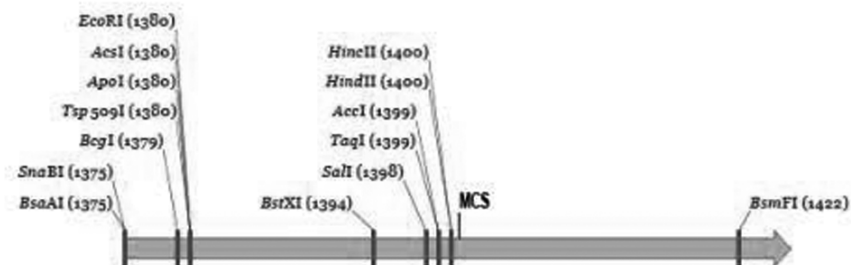
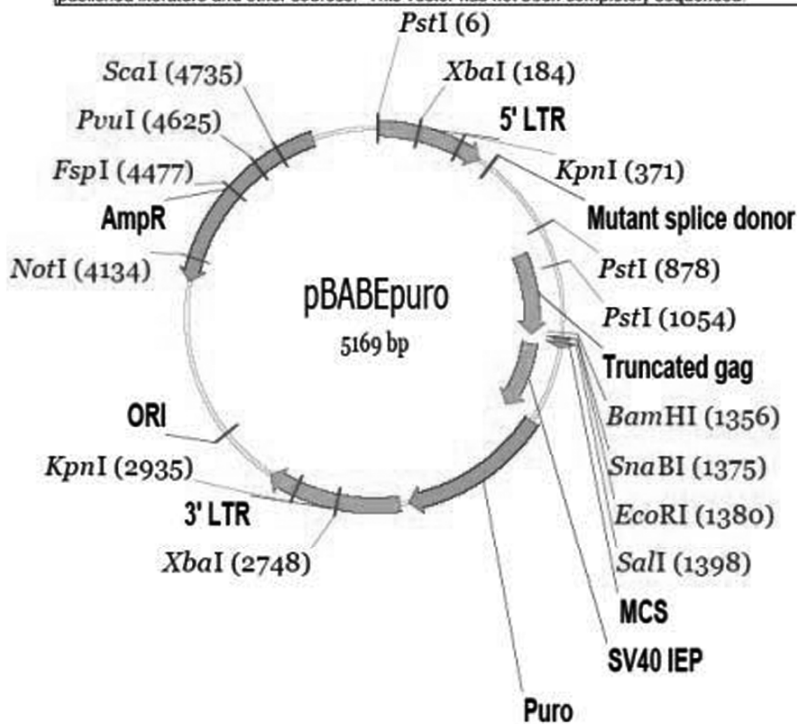
* There is a unique *BstE* II site, but no *Xba* I or *Apa* I sites in version C.

** There is a unique *Sac* II site between the *Apa* I site and the *Sfu* I site in version B only.

Insert	Origin	Cloned
TFCP2c/LSF	selective TFCP2c amplification from mRNA obtained from RWP1 cells	EcoRV (site lost after cloning)
TFCP2d/LSF-ID	PCR amplification from TFCP2c	BamHI/EcoRV

pBABE

pBABEpuro
 Note: The following document has been compiled from information in sequence databases, published literature and other sources. This vector has not been completely sequenced.



Fragment of pBABEpuro
 51 bp (molecule 5169 bp)

Insert	Origin	Cloned
TFCP2c/LSF	pcDNA3.1-TFCP2c	EcoRI
TFCP2d/LSF-ID	pcDNA3.1-TFCP2d	EcoRI
TFCP2cQ234L/K236E	PCR amplification from pBABE-TFCP2c	EcoRI

A.1.2 Prokaryotic expression vector

pGEX

pGEX-6P-1 (27-4597-01)

PreScission™ Protease

Leu Glu Val Leu Phe Gln⁺Gly Pro Leu Gly Ser Pro Glu Phe Pro Gly Arg Leu Glu Arg Pro His
 CTG GAA GTT CTG TTC CAG GGG CCC CTG GGA TCC CCG GAA TTC CCG GGT CGA CTC GAG CGG CCG CAT
 BamH I EcoR I Sma I Sal I Xho I Not I

pGEX-6P-2 (27-4598-01)

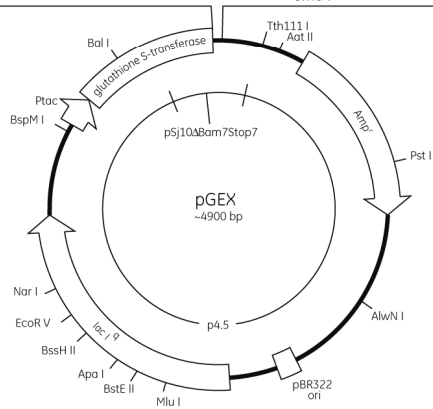
PreScission™ Protease

Leu Glu Val Leu Phe Gln⁺Gly Pro Leu Gly Ser Pro Gly Ile Pro Gly Ser Thr Arg Ala Ala Ala Ser
 CTG GAA GTT CTG TTC CAG GGG CCC CTG GGA TCC CCA GGA ATT CCC GGG TCG ACT CGA GCG GCC GCA TCG
 BamH I EcoR I Sma I Sal I Xho I Not I

pGEX-6P-3 (27-4599-01)

PreScission™ Protease

Leu Glu Val Leu Phe Gln⁺Gly Pro Leu Gly Ser Pro Asn Ser Arg Val Asp Ser Ser Gly Arg
 CTG GAA GTT CTG TTC CAG GGG CCC CTG GGA TCC CCG AAT TCC CGG GTC GAC TCG AGC GGC CGC
 BamH I EcoR I Sma I Sal I Xho I Not I



Insert	Origin	Cloned
mmsnail1-HA	pcDNA3-mmsnail1-HA	BamHI/XhoI

A.1.3 Luciferase reporter vector

pGL3

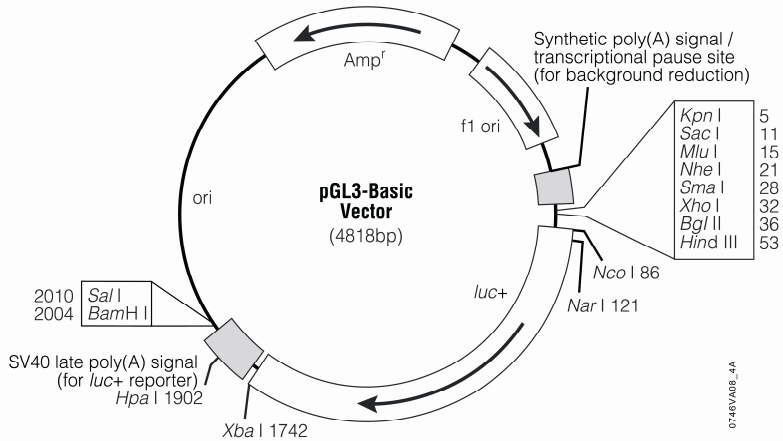


Figure 1. pGL3-Basic Vector circle map. Additional description: *luc+*, cDNA encoding the modified firefly luciferase; *Amp^r*, gene conferring ampicillin resistance in *E. coli*; *f1 ori*, origin of replication derived from filamentous phage; *ori*, origin of replication in *E. coli*. Arrows within *luc+* and the *Amp^r* gene indicate the direction of transcription; the arrow in the *f1 ori* indicates the direction of ssDNA strand synthesis.

pGL3-Basic Vector Sequence Reference Points:

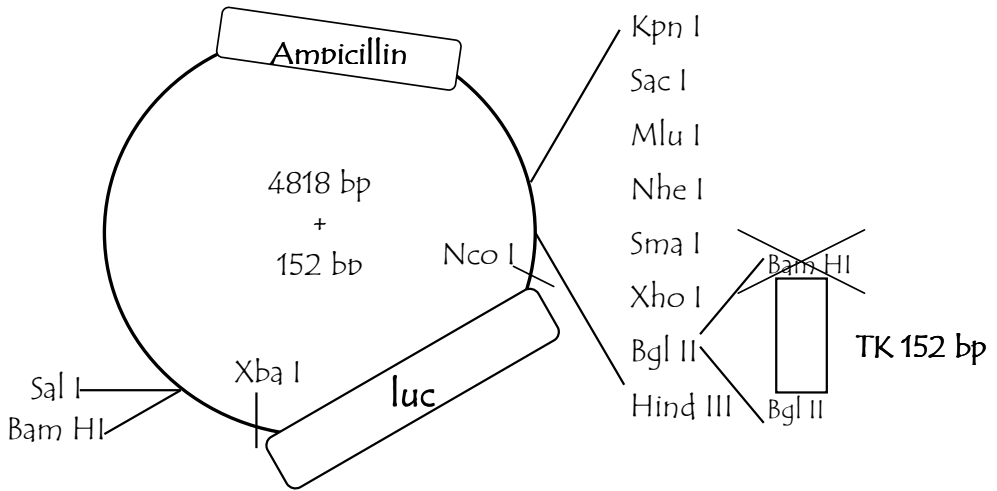
SV40 Promoter	(none)
SV40 Enhancer	(none)
Multiple cloning region	1–58
Luciferase gene (<i>luc+</i>)	88–1740
GLprimer2 binding site	89–111
SV40 late poly(A) signal	1772–1993
RVprimer4 binding site	2080–2061
<i>ColE</i> 1-derived plasmid replication origin	2318
β -lactamase gene (<i>Amp^r</i>)	3080–3940
<i>f1</i> origin	4072–4527
Synthetic poly(A) signal	4658–4811
RVprimer3 binding site	4760–4779

Insert	Origin	Cloned
-341/+370 <i>FN1</i>	selective <i>FN1</i> amplification from HT29 genomic DNA	MluI/XhoI
-867/+265 <i>FN1</i>	selective <i>FN1</i> amplification from HT29 genomic DNA	MluI/SmaI (site lost)
-606/+265 <i>FN1</i>	selective <i>FN1</i> amplification from HT29 genomic DNA	MluI/SmaI (site lost)
-341/+265 <i>FN1</i>	PCR amplification from -341/+370 <i>FN1</i>	MluI/SmaI (site lost)

-322/+265 <i>FN1</i>	PCR amplification from -341/+265 <i>FN1</i>	SmaI (site lost)
-278/+265 <i>FN1</i>	PCR amplification from -341/+265 <i>FN1</i>	SmaI (site lost)
-236/+265 <i>FN1</i>	PCR amplification from -341/+265 <i>FN1</i>	SmaI (site lost)
-192/+265 <i>FN1</i>	PCR amplification from -341/+265 <i>FN1</i>	SmaI (site lost)
-36/+265 <i>FN1</i>	PCR amplification from -341/+265 <i>FN1</i>	SmaI (site lost)
-341/+72 <i>FN1</i>	-341/+265 <i>FN1</i>	MluI/XhoI (site lost)
-341/+265 <i>FN1</i> mut LEF/TCF, p300, NF-κB, TFCP2c (boxes 1&2)	PCR amplification -341/+265 <i>FN1</i>	MluI/SmaI (site lost)
-527/+1389 <i>LEF1</i>	selective <i>LEF1</i> amplification from HT29 genomic DNA	KpnI/SmaI (site lost)
-527/+1389 <i>LEF1</i> mut LEF/TCF, WRE, p300, NF-κB	PCR amplification from -527/+1389 <i>LEF1</i>	KpnI/SmaI (site lost)

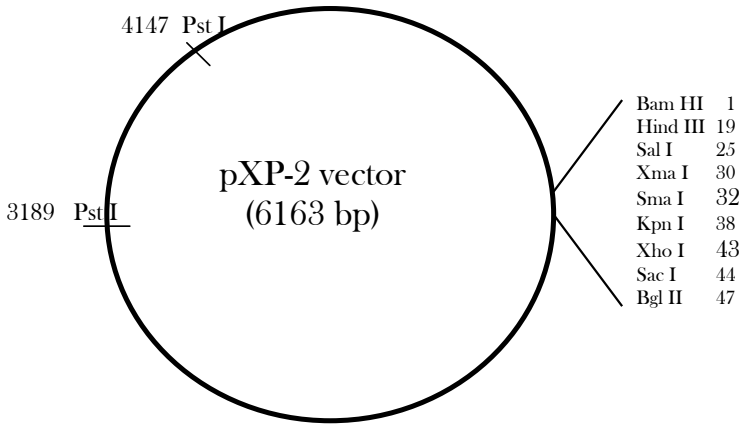
pGL3-TK

pGL3* TK aprox. 4970



Insert	Origin	Cloned
-341/-185 <i>FN1</i>	PCR amplification from pGL3*-341/-210 <i>FN1</i>	<i>Sma</i> I (siteslost)
+451+560 <i>LEF1</i>	PCR amplification from pGL3* -527/+1389 <i>LEF1</i>	<i>Mlu</i> I/ <i>Xho</i> I

pXP2



Bam HI
Hind III
Sal I
Sma I
Kpn I
Xho I

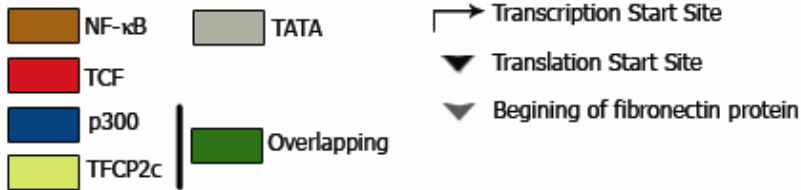
GGATCCAAGCTCAGATCCAAGCTTGTTCGACCCGGGTACCGAGCTCGAGATCTGAGCTTGGCA
 CCTAGGTTTCGAGTCTAGGTTTCGAACAGCTGGGCCCATGGCTCGAGCTCTAGACTCGAACCGT

Xma I
Sac I
Bgl II

Insert	Origin	Cloned
-341/+370 <i>FN1</i>	pGL3* -341/+370	SmaI (site lost) /XhoI
-867/+265 <i>FN1</i>	selective <i>FN1</i> amplification from HT29 genomic DNA	SmaI (site lost, but additional MluI site 5' the insert)
-606/+265 <i>FN1</i>	selective <i>FN1</i> amplification from HT29 genomic DNA	SmaI (site lost, but additional MluI site 5' the insert)
-341/+265 <i>FN1</i>	PCR amplification from pGL3* -341/+370	SmaI (site lost, but additional MluI site 5' the insert)

A.2 FN1 PROMOTER

-341 acacaagtccaaccaactcctttctccagccgcttcccatcccttccccatccct -282
 -281 aaaaagtttgatgacgcgcaaaggaaaccgaaaaaaagtgtcttgccccagtcctggcg -223
 -222 ggccatcagcatctcttttgctcgtgcgaacccacagtcccccgtagcgtcacccgga -164
 -163 gcccgggccaatcgggcgcgggtcggtgcggcgggcgggcgggcggggtgggggtgg -105
 -104 ggcgggcggggacagcccgggggtctctctcccccgcgccccggggcctccagaggg -46
 -45 gcgggagggaccgtccatataagccccggctcccgcgctccgacgcccgcgcggct +14
 +14 gtgctgcacagggggaggagaggaaccccaggcgcgagcgggaagaggggacctgcag +72
 +73 ccacaactctctggtcctctgcatccctctgtccctccaccgctcccttccccacc +131
 +132 ctctggccccacctctctggaggcgacaacccccgggaggcattagaagggatttttc +189
 +190 ccgcagttgogaaggggaagcaaacttggtggcaactgcctcccggcggggctctct +248
 +249 cccccaccgtctcaacatgcttaggggtccggggccccgggctgctgctgctggccgtcc +307
 +308 tgtgctggggacagcgggtgccctccacgggagcctcgaagagcaagagggcaggctcag +367
 +368 caaatgggtcagccccagtcccccgggtggctgtcagtcgaaagcaagcgtgagtactgacc +426
 +427 gcggg +431

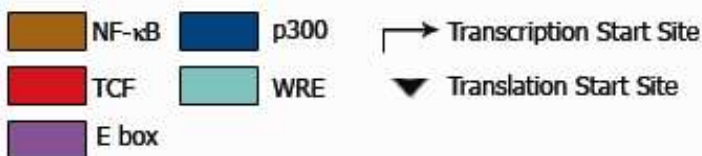


A.3 LEF1 PROMOTER

```

-527 cccttgtctccaaagagcgtgtgtgatattatattcgggaaagctacaactctcttt -467
-468 tccttgtcctctctgttctctcttaaatagttgagcaatgtctgttatattttccctttt -408
-409 cctttttttctcagtcocagattcccgctctccccactgtcagagcatctatcaatgt -349
-350 ggtgtccatcacagcggcagcggettctcttttcatcttctccctctgccagagccag -290
-291 ggagggagagtgaggagcgtcaaggaggtaggggagagactggcagaggaaaaggagtg -231
-232 ggtgggtggggccaagtaaatagatacttagatgatgaagtcaagccactgaggcaat -172
-173 gtttcttgtcagtttcaacggggcaaacgctgcctttcgggtgggttataagcagcgccc -113
-114 ggtccttctctctctcgccaagtgcctgatccttccctccaggcgcgcgcacacac -54
-55 cacactcacacacccccaaaaccaagactcgtcctacaggatctgggaaaaagaaaagaa +4
+5 aaaaaagccctcaatcaccacctctctctcgcgactccccctcacccccgcctcccc +63
+64 tccagcggggcagccaaggagagctagaggcgggggaggggagaggagaagcgcagc +122
+123 caagtgggtagcttttcagcgcgggcgaggcgcgggaggaggagaagcagtggggagggc +181
+182 gcagccgctcacactgcggggcagggcgcggaggagggaccgggctgcgcgctctcggg +240
+241 ccgaggaaccaggaacgcgccggagcctgcacgcggccaagctcggggctccctcc +299
+300 cctcggccgggcgaactcaaggggcgcagcctttgctttcacagagctggccggcgga +358
+359 ggctgtcagagcggcgagccggcgagccaggctgagaaactcgagccggaaacaaagg +417
+418 gggtcggactcagtggtgtgtcggctcgagctcggggcagagccatttggggccggagg +476
+477 cccccgctgccccgagactcgcagtgccctccactcggagtcctccgcgcttg +535
+536 cgggcaaaaacttttatcttggcaaacttctctttctcttccctctctcctcgggcccc +594
+595 catcttctgtcctcctcctctctctctagcagattaaatgagcctcgagaagaaaaaccga +653
+654 agcgaaggggaagaaaaataagaagatctaaaacggacatctccagcgtgggtggtcct +712
+713 ttttctttttcttttttccccaccttcaggaagtggaagcttctgttatctctctgatcc +771
+772 ttgcacctctctttggggcaaacggggccctctcgcacagatccccctctctttctcgg +830
+831 aaaacaaactactaagtcggcatcggggtaactacagtgagaggggttccgcggaga +889
+890 cgcgcgcgggaccctcctctgcaacttggggaggcgtgctccctccagaaccggcgtt +948
+949 ctccgcgcaaaatcccggcagcgggggtcgcgggggtggcgcgggggcagcctcgtc +1007
+1008 tagcgcgcgcgcgcagacgccccggagtcgccagctaccgcagccctcgcgcgccag +1066
+1067 tgcccttcggcctcgggggggggcgctcgtcggctccgcgaagcgggaaagcgcgg +1125
+1126 cggcgcgggattcggggcgcgggcagctgctcggctgccggccggcggcccccgcg +1184
+1185 ctgcgccgcccgcttcgccccgctgtcctgtgcaacgaacccttccaactctccttcc +1243
+1244 ctccccacccttgagttaccctctgtcttctcctgctgttgccgggggtgctcccacag +1302
+1303 cggagcggagattacagagccgcgggatgcccacaactctcggaggaggtggcggcgg +1361
+1362 cgggggggaccgggaactctgcgccacg +1389

```



A.4 ARTICLE

- Solanas G*, **Porta-de-la-Riva M***, Agustí C, Casagolda D, Sánchez-Aguilera F, Larriba MJ, Pons F, Peiró S, Escrivà M, Muñoz A, Duñach M, García de Herreros A, Baulida J: *E-cadherin controls β -catenin and NF- κ B transcriptional activity in mesenchymal gene expression*. *J Cell Sci* 2008. **121**, 2224-2234

Solanas G, Porta-de-la-Riva M, Agustí C, Casagolda D, Sánchez-Aguilera F, Larriba MJ, et al.

[*E-cadherin controls beta-catenin and NF-kappaB transcriptional activity in mesenchymal gene expression.*](#)

J Cell Sci. 2008 Jul 1;121(Pt13):2224-34.



